The regulation of the cAMP signalling pathway in the human pathogenic fungus *Paracoccidioides brasiliensis*

Thamarai kannan Janganan, M.Sc.

Submitted for the Degree of Doctor of Philosophy

School of Biological and Biomedical Sciences

Centre for Infectious Diseases

University of Durham

September 2008

Declaration of Originality

I, Thamarai Kannan Janganan, declare that this thesis is my own work and no part of this thesis has been submitted for other qualifications to this or any other University or any educational institution. Information retrieved from the published work of others have been acknowledged and listed in the references.

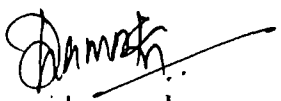

Thamarai kannan Janganan

September 2008

Acknowledgement

I thank whole heartedly my supervisors Prof Adrian Walmsley and Dr. Ines Borges-Walmsley, School of Biological sciences, University of Durham UK, for providing me with an opportunity and supervision to carry out this research. My gratitude to my research supervisors goes beyond what words could justify because their help in correcting my thesis and training me to appreciate the nuances of molecular biology techniques. They have been kind and endearing and helped me in more ways than one to make this endeavour a success.

My special thanks to Diane Hart and Simon Padbury for their technical support. I also thank Dr. Daliang Chen and Dr. Gongyou Chen for providing the constructs for two-hybrid assays and *P. brasiliensis* library.

I would like to thank Dr. Paul Yeo, Dr. Gary Sharples and Dr. Paul Denny for their valuable suggestions. I also thank my colleagues in the lab for valuable discussion and working in a sociable environment.

I thank God, my God father, my parents and my wife for being what I am today.

Finally I thank the Bank of Baroda, RJPM, Tamil nadu, India, for providing the loan for supporting my studies.

Publications arising from this thesis

Chen, D., Janganan, T.K., Chen, G., Marques, E.R., Kress, M.R., Goldman, G.H., Walmsley, A.R., and Borges-Walmsley, M.I. (2007) The cAMP pathway is important for controlling the morphological switch to the pathogenic yeast form of *Paracoccidioides brasiliensis*. Mol Microbiol 65: 761-779.

Janganan T K, Chen D, Chen G, Marques E R, Marcia, Goldman G H, Walmsley, A. R., and Borges-Walmsley M. I. (2008) A role for the Gβ protein in attenuating the activity of protein kinase A from the human pathogenic fungus *Paracoccidioides brasiliensis*. Submitted to Molecular Microbiology.

ABSTRACT

Paracoccioides brasiliensis (Pb) is the causative agent of the disease Paracoccioidomycosis (PCM), which is one of the most prevalent systemic mycoses in Latin Amercia (Borges-Walmsley *et al.*, 2002). *P. brasiliensis* is a thermally dimorphic fungus which undergoes morphological changes from a mycelial form at 26°C (environment) to a pathogenic yeast form at 37°C (human body) after inhalation of spores/conidia into the lungs of a human host (Nemecek *et al.*, 2006). The cAMP pathway controls this morphological transformation in several fungi (Borges-Walmsley and Walmsley, 2000; Kronstad *et al.*, 1998).

G proteins are guanine-nucleotide (GDP or GTP) binding proteins that are generally associated with the cytoplasmic side of the plasma membrane. They receive signals from G protein-coupled receptors (GPCR). Adenylyl cyclase acts downstream of these G proteins. Gα subunits are required to regulate the activity of adenylyl cyclase (AC), which controls the level of cellular cAMP (Ivey and Hoffman, 2005). Protein Kinase A (PKA), which is activated by cAMP, is required for morphogenesis and virulence (Durrenberger *et al.*, 1998; Sonneborn *et al.*, 2000).

The cAMP pathway in *P. brasiliensis* is poorly understood. However, recently the genes encoding a number of the components of the cAMP pathway have been cloned in our lab: these include the genes encoding three Gα proteins, Gpa1-3, a Gβ protein, Gpb1; a Gγ protein, Gpg1; Ras; adenylyl cyclase, Cyr1; and the catalytic subunit of PKA, Tpk2. Two-hybrid analyses confirmed that Gpa1 and Gpg1 interact with Gpb1. These data indicate the formation of a Gαβγ trimer complex. A GST pull-down assay confirmed that Gpa1 and Gpb1 interacted with the N-terminus of adenylyl cyclase. Our hypothesis is that Gpa1 and Gpb1 modulate the activity of the AC/Tpk2 signalling pathway. Consistent with this hypothesis, we found changes in intracellular cAMP levels during the mycelium to yeast transformation that correlated with changing transcript levels of the signalling genes (Chen *et al.*, 2007).

We have established that Tpk2 interacts with the N-terminus of adenylyl cyclase, the G protein β subunit Gpb1 and with the co-repressor Tup1 by both two-hybrid and GST pull-down analyses. This suggests that Tpk2 activity is required for feedback regulation of adenylyl cyclase to reduce cAMP levels. *P. brasiliensis* Tpk2-C-terminal 226-583-GFP and Tpk2 full length (FL) complemented the growth defect of a *S. cerevisiae tpk2* temperature sensitive mutant strain SGY446 and induced the formation of pseudohyphae in the *S. cerevisiae tpk2* mutant diploid strain XPY5**a**/α. Tpk2 C-terminus has been over expressed in *E. coli* and *in vitro* PKA activity was measured. On the other hand we have also analysed the second catalytic subunit Tpk1, which failed to induce pseudohyphae in *S. cerevisiae tpk2* mutant strain and is localised to the cytoplasm.

Interestingly, the Pb Gβ subunit Gpb1 inhibited the development of pseudohyphae in *TPK2* FL transformed yeast cells. Tpk2 C-terminus and Tpk2 FL co-transformed with Gpb-GFP were localized in the nucleus. Our hypothesis is that Gpb1 down regulates the activity of Tpk2, because Gpb1 binds to the catalytic C-terminal domain of Tpk2.

Abbreviations

AC	Adenylyl cyclase
cAMP	Cyclic Adenosine Monophosphate
CAP	Cyclase Associated Protein
DAPI	4',6-diamidino-2-phenylindole
DTH	Delayed T-cel Hypersensitivity
GAP	GTPase-Activating Protein
GEF	Guanine Nucleotide Exchange Factor
GFP	Green Fluorecence Protein
GPI	Glycosyl-Phosphatidyl-Inositol
GPCR	G protein-Coupled Receptor
HSP	Heat Shock Protein
IPTG	Isoprophyl-1-thio-β-D-Galacoside
KRH	Kelch Repeat Homologue
MAPK	Mitogen Activated Protein Kinase
MW	Molecular Weight
OD	Optical Density
Pb	*Paracoccidioides brasiliensis*
PCM	Paracoccidioidomycosis
PCR	Polymerase Chain Reaction
PKA	Protein Kinase A
PVDF	Polyvinylidene Fluoride
RPM	Rotation Per Minute
SH3	Src Homology 3
TAE	Tris Acetate EDTA
TE	Tris EDTA
Ts	Temperature Sensitive
α-X-Gal	5-Bromo-4-chloro-3-indoxyl-alpha-D-galactopyranoside
X-Gal	5-bromo-4-chloro-3-indolyl-b-D-galactopyranoside
URA	Uracil

Contents

LIST OF FIGURES AND TABLES

CHAPTER ONE

INTRODUCTION

1.1 *Paracoccidioides brasiliensis*: Introduction

Fungal infections cause many life threatening diseases in humans such as pneumonia, septicaemia, systemic and skin infections. *Paracoccidioides brasiliensis* is the etiological agent of the disease Paracoccidioidomycosis (PCM). *P. brasiliensis* is part of the group of Ascomycetes fungi, which are the main causes of systemic mycoses. PCM is endemic in South and Central America and is often referred to as South American Blastomysis (Ajello and Polonelli, 1985; Azambuja *et al.*, 1981; Borges-Walmsley *et al.*, 2002; Brummer *et al.*, 1993; San-Blas *et al.*, 2002). *P. brasiliensis* is a thermally dimorphic fungi, which can undergo a morphological change from a saprobic filamentous mycelial form at 26°C (environment) to a pathogenic multi-budding yeast form at 37°C (human body). The mycelial form produces conidia that act as infectious propagules that persist in the environment and enter the human host by inhalation. In the lungs, the conidia transform into the yeast form which is pathogenic. PCM is gender biased with the infection more common in males than females, because the female hormone oestrogen inhibits the transition of conidia to the yeast form (Borges-Walmsley *et al.*, 2002; Hogan *et al.*, 1996).

When conidia reach the distal portions of the human lungs they transform into the yeast form by growing on the lung parenchyma cells and progressively cause the disease to develop. Conidia from the lungs subsequently disseminate to other parts of the body forming secondary lesions in adrenal glands, lymph nodes, mucous membranes and in the skin (Borges-Walmsley *et al.*, 2002; Brummer *et al.*, 1993). In endemic regions about 10% of the population are infected by PCM (Borges-Walmsley *et al.*, 2002). Initially the infection is asymptomatic and there is a dormancy period that can range from 4 months to many decades. Ketoconazole, amphotericin B and itraconazole are currently used as the drugs of choice for PCM (Ajello and Polonelli, 1985; Borges-Walmsley *et al.*, 2002; Lortholary *et al.*, 1999).

1.2 Clinical manifestations

1.2.1 Juvenile type Paracoccidioidomycosis

Paracoccidioidomycosis is characterised by several clinical forms that arise after infection of the lungs; an acute or sub-acute form referred to as the juvenile type and a chronic form found mainly in adults. The juvenile type PCM can take weeks or months to progress to the severe disease and it causes high mortality due to reticuloendothelial system (lymph nodes, liver, spleen and bone marrow) organ hypertrophy and bone marrow dysfunction. It is often misdiagnosed as lympho proliferative disorder. The lymph node hypertrophy sometimes leads to bowel obstruction and an acute abdominal syndrome. The biopsy examination shows a large number of yeast cells and no formation of granulomas. This type is very common in children and young adults, who have a depressed cell-mediated immune response (Borges-Walmsley *et al.*, 2002; Brummer *et al.*, 1993).

1.2.2 Adult type Paracoccidioidomycosis

The adult type PCM has a long latency period ranging from months to several years before the onset of disease symptoms and occurs in 90% of infected adult males. The main symptoms are cough, shortness of breath, fever, weight loss and anorexia. Unlike juvenile type PCM, the adult type infection is localised in the pulmonary system (known as unifocal phase) and in later stages is disseminated to other organs and systems (this is known as multifocal, chronic phase). A case study of 352 patients revealed lesions in lungs (76.7 %), mucous membrane (63.0%), skin (41%), lymph node (47%), spleen, liver, abdominal and other tissues (less than 20%) (Brummer *et al.*, 1993). A few cases have also been noticed with PCM in ocular, central nervous system, bone destruction and vascular system pathology. A rare case has been noticed with thyroid impairment. The adult type PCM has some resemblance to tuberculosis and so it is often misdiagnosed as tuberculosis. Therefore the adult type is chronic and slow, with granuloma formation dependent upon the patient's health condition (Borges-Walmsley *et al.*, 2002; Brummer *et al.*,

1993; San-Blas *et al.*, 2002). Two other clinical forms that have been reported recently are meningitis and pseudotumoral, which are more dangerous than the previously reported juvenile and adult forms (Elias *et al.*, 2005). A laryngeal paracoccidioidomycosis has also recently been observed in which lesions were found in buccal pharynx mucosa and also in the liver and gastrointestinal tract (Tristano and Diaz, 2007).

1.3 Host interaction

P. brasiliensis is responsible for invasive systemic mycosis; the yeast form initially adheres to the epithelial cells by forming a narrow tube like structure, which contacts the surface of the epithelial cells before invasion. The entire yeast cell invades the host cell cytoplasm. The host-parasite interaction happens after 30 minutes of contact and the yeast starts multiplying between 5 and 24 hours later. This invasion of *P. brasiliensis* into the host epithelial cells enables the fungus to escape from phagocytosis. *P. brasiliensis* gp43 is a major antigen and virulence factor. An inhibition assay was performed with a mixture of anti-gp43 serum and a pool of sera from the PCM patients, which demonstrated that the anti-gp43 serum inhibited the binding of *P. brasiliensis* to host cells (Hanna *et al.*, 2000).

Immunocompromised individuals are more susceptible to PCM. PCM is common in males, with an infection rate 13 times higher in males than in females because the female hormone inhibits the transition. This has been demonstrated in a mouse model (Aristizabal *et al.*, 1998; Borges-Walmsley *et al.*, 2002). An *in vitro* analysis also shows that the female hormone oestrogen inhibits the morphological transition of conidium to yeast (Salazar *et al.*, 1988). Skin test data for PCM cases in the endemic area revealed that both sexes have equal exposure to the fungus and disease develops equally in both sexes before puberty (Hogan *et al.*, 1996).

It has been shown that a receptor-like protein present in the cytoplasm of *P. brasiliensis* binds specifically to oestrogen (Loose *et al.*, 1983). An *in vitro* assay demonstrates that the oestrogen analogue 17β-estradiol inhibits the transition of

conidia to yeast form, however 17β-estradiol has no effect on the reverse (yeast to mycelial) transformation (Restrepo *et al.*, 1984; Stevens, 1989).

1.4 Immunology

The P. brasiliensis yeast form resists destruction by human peripheral blood polymorphonuclear leucocytes (PMN), but the fungal cell wall is damaged by PMN during co-culture with the PMN. However PMN showed fungistatic activity against *P. brasiliensis* (Kurita *et al.*, 1999). The cytokine interferon (IFN) plays an important role in the host defence. Human IFN-γ treated PMN show higher antifungal activity than untreated PMN, which indicates that IFN-γ enhances the activity of PMN. The yeast form has a higher rate of multiplication in the absence of PMN (Borges-Walmsley *et al.*, 2002; Kurita *et al.*, 1999). In a murine model study, resident peritoneal macrophages can phagocyte but cannot kill *P. brasiliensis*; however recombinant IFN-γ treated macrophages can kill the *P. brasiliensis* yeast cells and at the same time activated macrophages show less phagocytosis (Brummer *et al.*, 1988b). In a similar way, the pulmonary macrophages recovered after 24 hours from IFN-γ injected mice show higher percentage of killing *P. brasiliensis* and *Blastomyces dermatitidis* than macrophages from control mice (Brummer *et al.*, 1988a). *P. brasiliensis* yeast form is ingested by pulmonary macrophages (PuM) and the ingested yeast grows as an intracellular pathogen inside the PuM. An enhanced growth was observed after 72 hours of co-culturing the *P. brasiliensis* yeast cells with PuM (Brummer *et al.*, 1989).

Interferon (IFN-γ) and tumour necrosis factor (TNF-α) both exert a natural defence against the infection. INF-γ activates *P. brasiliensis* infected macrophages to produce TNF-α, which in turn facilitates the formation of granulomas. It has been shown that IFN-γ and TNF-α receptor p55 knockout mice infected with the yeast form of *P. brasiliensis* succumbed to infection by the 16th day but wild-type mice succumbed by the 90th day. An examination of the p55 receptor knockout mice infected with *P. brasiliensis* showed that they contained a higher infection load of the yeast form with no granuloma formation. IFN-γ and TNF-α knockout mice also

showed less nitric oxide (NO) production. These experiments demonstrate that both IFN-γ and TNF-α have a role in the host resistance and controlling the infection by the production of NO and controlling granuloma formation (Borges-Walmsley *et al.*, 2002; Souto *et al.*, 2000).

In contrast, prostaglandins have a negative role in the host defence by mediating immunosuppression. Prostaglandins are produced by COX-2 (in the cyclo-oxygenase pathway), which down-regulates (interleukin) IL-2 production during the early phase of *P. brasiliensis* infection. This whole mechanism is mediated by IL-4 and IL-10, because inhibition of COX-2 also lowered IL-4 and IL-10 production (Borges-Walmsley *et al.*, 2002; Michelin *et al.*, 2002; Soares *et al.*, 2001).

P. brasiliensis produces a serine–thiol protease which can cleave laminin, fibronectin and other components of the basement membrane of the extracellular matrix. This cleavage is the primary stage for the fungal invasion (Borges-Walmsley *et al.*, 2002; Puccia *et al.*, 1998). Recently it was found that *P. brasiliensis* has the ability to synthesis chondroitinase and hyaluronidase from the substrates chondroitin sulphate type A and sodium hyaluronate, respectively. Hyaluronidase and chondroitinase are the major virulence factors which facilitate the depolymerisation of the connecting tissues by cleaving the hyaluronic acid and chondroitin sulphate; which favour the microbes to penetrate and disseminate into the host cells (de Assis *et al.*, 2003).

It has been shown that gp43 is an important antigen, which is a secretery glycoprotein (Vicentini *et al.*, 1994). *In vitro* and *in vivo* studies confirm the binding of gp43 to laminin, a glycoprotein present in the basement membrane (extracellular matrix). The binding of the gp43 antigen laminin increases the invasion and dissemination of the yeast form to other organs and tissues. *P. brasiliensis* yeast cells coated laminin injected into hamster testicles showed higher virulence and more granulomatous disease (Vicentini *et al.*, 1994).

Melanin production has been correlated with the virulence in human pathogenic fungi (Franzen *et al.*, 2008). Both the *P. brasiliensis* mycelial and yeast forms can produce the melanin pigment in the presence of L-3,4-dihydroyphenylalanine (L-DOPA); which has been demonstrated by immunofluorescence with antibodies against the melanin cross-reacting with pigmented yeast, conidia and other fungal particles. Anti-melanin antibodies have also been shown to react with tissue particles extracted from the *P. brasiliensis* infected mice. This indicates that *P. brasiliensis* can produce melanin both *in vivo* and *in vitro* (Gomez *et al.*, 2001). Recent studies indicate that melanin pigmented yeast cells are poorly phagocytosed by the macrophages even in the presence of complement (da Silva *et al.*, 2006). Moreover, melaninization also interferes with the binding of cell wall components to the lectin receptor of peritoneal and alveolar macrophages, which eventually protect the yeast cells from phagocytosis. A 'killing assay' demonstrated that melanised cells are less susceptible to antifungal drugs such as amphotericin B, ketoconazole, fluconazole, itraconazole and sulfamethoxazole (da Silva *et al.*, 2006). Consistent with these findings from *P. brasiliensis*, melanin production was also observed in both *in vivo* and *in vitro* in *Histoplasma capsulatum* and *Cryptococcus neoformans* and the melanised cells were less susceptible to amphotericin B and caspofungin (van Duin *et al.*, 2002).

1.5 Epidemiology

Paracoccidioidomycosis (PCM), a common systemic mycosis is restricted to certain countries in Latin America such as Brazil, Venezuela, Ecuador, Mexico Argentina and Colombia. PCM is a major health problem in Brazil. A few cases have also been reported in non-endemic areas such as Italy, arising in immigrants (Ajello and Polonelli, 1985; Borges-Walmsley *et al.*, 2002; Brummer *et al.*, 1993; San-Blas *et al.*, 2002). The ecological niche of *P. brasiliensis* is still not well defined, but it is thought to be present in the soil of warm and humid areas near (tropical and subtropical) forests. *P. brasiliensis* is a dimorphic fungus for which conidia from the humid area enters into the lungs of a human and develops the pathogenic yeast form (Azambuja *et al.*, 1981; Hogan *et al.*, 1996).

PCM is frequently diagnosed in adults aged between 30 and 60 years but it is limited in children (3%) and young adults (10%). Indeed, skin tests in endemic areas have revealed a low reactivity in children and young adults (Brummer *et al.*, 1993). In most endemic regions the infection ratio (males: females) with regard to sex is about 13:1, but a higher ratio of about 150:1 was observed in Argentina, Ecuador and Columbia. About 70% of the patients were originally agriculturists, which are frequently brought into contact with soils or vegetative matter. A few cases have also been reported for people who have had less contact with agriculture. Indians are rarely infected by Paracoccidioidomycosis; most infected cases are white people. A severe form of PCM was observed among immigrants moving to the endemic area. PCM is not a contagious disease (Brummer *et al.*, 1993).

1.6 Dimorphism

There are six phylogenetically related Ascomycetes fungi that are found in the environment; *Blastomyces dermatitis*, *Histoplasma capsulatum*, *Coccidioides immitis*, *Paracoccidioides brasiliensis*, *Sporothrix schenkii* and *Penicillium marneffei*. These fungi are known as dimorphic fungi, because they are able to switch from a non-pathogenic mycelial form to a pathogenic yeast form; and strains that are unable to undergo this transformation are avirulent (Borges-Walmsley and Walmsley, 2000; Chen *et al.*, 2007; Nemecek *et al.*, 2006). Dimorphism is controlled by various signalling pathways in fungi and necessary for pathogenesis (Madhani and Fink, 1998). In *P. brasiliensis* temperature plays a major role in the transition from the non-pathogenic mycelial form to the pathogenic yeast form (San-Blas *et al.*, 2002), whereas in *Candida albicans*, the transition from yeast to hyphae (germ tube) involves complex stimulation (i.e. serum requirement) (Borges-Walmsley *et al.*, 2002).

Figure 1.6.1Electron microscopic study of mycelial to yeast transformation in *P. brasiliensis*

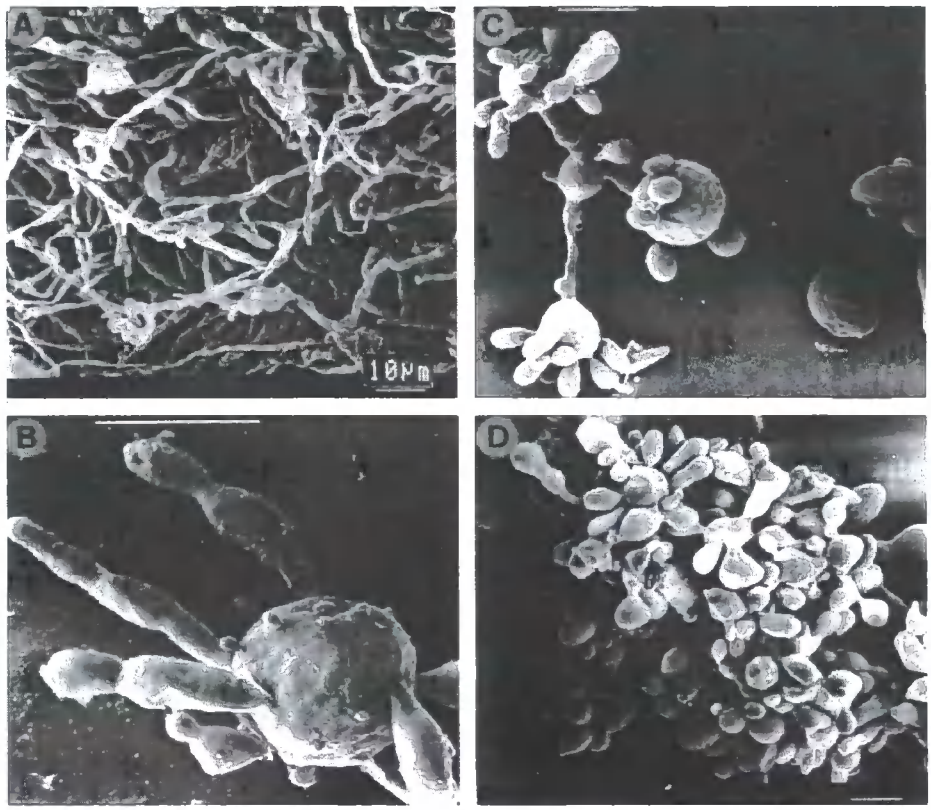

Picture reproduced from the reference (da Silva *et al.*, 1999).

A. Mycelial cells grown at 26°C.
B. Mycelial cells grown at 36°C for 11 days.
C. Mycelial cells grown at 36°C for 15 days.
D. Yeast cells grown at 36°C.

The mycelial-to-yeast morphological transition is characterised by the initial increase in the diameter of the hyphae, leading to cracking of the outer layer and thickening of the inner layer of the cell wall. During this transformation stage, most of the hyphae die and only intra-hyphae remain. At a later stage, a few of the interseptal regions detach as round yeast cells. The reverse transition from yeast to mycelium has shown that the yeast cells elongate and produce enlarged buds with intra-yeast-hyphae. Subsequently in the second stage, the enlarged buds reduce their

diameter and undergo cytoplasmic compartmentalization and finally form a mycelial structure (Restrepo *et al.*, 1993).

The yeast form cell wall contains alkali-soluble α-1,3-glucan, this is not present in the cell wall of the mycelial form. The yeast cells found in host tissues form a characteristic ''Pilot's wheel'' structure (Hogan *et al.*, 1996). The yeast form cell wall has two layers and is thicker than the mycelial cell wall, which is 200-600 nm in width. The outer periphery has short thick fibrils of α-1,3-glucan (100 nm length) in aggregates of 200-250 nm bundles. The inner cell wall layer is thicker than the outer cell wall layer. An electron microscopic study has revealed that the yeast form has a spherical or oval shape with globular blastoconidia. Repeated sub-culturing of *P. brasiliensis* cells for many years revealed various phenotypes such as mixture of spherical, catenular, pseudohyphae, and bottle-shaped cells. The yeast form produces soft, wrinkled and cream coloured colonies in a period of 10 to 15 days of incubation (Restrepo *et al.*, 1993).

A change in cell wall composition was observed during the morphological transition. The cell walls of *P. brasiliensis* and *Blastomyces dermatitidis* have a similar composition of lipids, chitin, glucan and proteins. Chitin, a polysaccharide fibrillar material, is present in both fungi in both forms. However, the yeast form of both fungi have a larger proportion of chitin (37- 48%) than the mycelial form (7-18%), but the yeast form has less proteins (7-14%) compared with the mycelial form (24 to 41%) (Kanetsuna *et al.*, 1969). The yeast form of both fungi have α-1,3-glucan and the mycelial form have β-1,3-glucan. The fibrillar nature of this glucan contributes to the shape of the fungi and these polysaccharides help to protect the fungus against the host defence mechanism (San-Blas and San-Blas, 1977). During the mycelial to yeast transition, the mycelial form produce a thick cell wall with multiple nuclei (Carbonell, 1969).

P. brasiliensis yeast cell possess α-1,3-glucan and lowering the content of this molecule correlates with a reduction in virulence however, some mutant avirulent strains seem to retain the same amount of α-1,3-glucan as the wild-type.

Therefore, a correlation between the α-1,3-glucan content and virulence is indirect. When a virulent *P. brasiliensis* was grown for an extended period of time *in vitro*, eventually the α-1,3-glucan level in the cell wall was lowered; the cell wall became thinner and the strain lost its virulence in an animal model study. α-1,3-glucan is present in the outer peripheral area of the cell wall, which is thought to be a protective layer against the host defence system (Hogan *et al.*, 1996).

β-1,3-glucan acts as an immunomodulator and there is direct evidence of a correlation between β-1,3-glucan and virulence from various animal model studies. Intraperitoneal injection of purified β-1,3-glucan and cell fractions with β-1,3-glucan induces tumour necrosis factor (TNF). This indicates that β-1,3-glucan and other cell wall components modulate the host cytokines and inflammatory response in the host cells (Hogan *et al.*, 1996).

1.7 Laboratory Diagnosis

A laboratory diagnosis process can be used for a definitive diagnosis of PCM. The process includes visualization, isolation and identification of pathogens from clinical specimens. A skin test (Delayed Type Hypersensitivity reaction (DTH)) and other immunological tests have also been employed in diagnosis. The usual clinical specimen collected is sputum; other specimens collected are bronchoalveolar lavage fluids, crusts, tissue or material from the granulomatous lesions or material from ulcers, pus from lymph nodes, cerebrospinal fluid and biopsy tissue. Direct examination of clinical specimens by wet preparation is the quickest way to detect the presence of fungal bodies (KOH, Immunofluorescence and Calco-fluor) (Brummer *et al.*, 1993).

The isolation of this fungus from sputum specimen is a challenging process, because the sputum has more contaminating resident flora. The addition of antibacterial and mold inhibitors to plates improved the yield of the fungus. Using these additives, direct microscopy has become more frequently used, because the fungi culturing process takes 20 to 30 days. *P. brasiliensis* was first isolated by Lutz

in 1908 on sabouraud agar and he described this fungus as like white mouse hair. In *P. brasiliensis*, a temperature shift from 26°C to 37°C facilitates fast growing yeast cells that form cream coloured colonies; whilst microscopic examination of the yeast cells revealed a globose with multiple budding. The mother cells are about 60 μm in diameter, but the size of the daughter cells may vary from 2-30 μm in diameter. The multibudding yeast cells are a unique characteristic of *P. brasiliensis* (pilot's wheel). A microscopic analysis of the mycelial form of *P. brasiliensis* shows branched hyphae measuring 3 to 4 μm in diameter with an intercalary chlamydospore 15 to 30 μm in diameter (Brummer *et al.*, 1993).

The production of specific antibodies was observed in all PCM patients and a high titre was detected in patients with disseminated infection. A high sensitive immunodiffusion test was developed for the diagnosis of PCM using the *P. brasiliensis* gp43 antigen that is responsible for the DTH in patients (McGowan and Buckley, 1985). An immunoblotting technique was developed in order to detect the gp43 antigen from PCM patient's sera (Mendes-Giannini *et al.*, 1989). Camargo *et al.* developed a capture-Enzyme Immuno Assay (EIA) using the monoclonal antibodies raised against gp43 antigen in mouse, which detects anti-gp43 IgG in the PCM patients serum at high sensitivity (Camargo *et al.*, 1994). In addition, a PCR based diagnosis was developed (for sputum sample) by designing specific primers for the *GP43* gene (Gomes *et al.*, 2000).

1.8 Treatment

Paracoccidioidomycosis was thought to be an incurable disease until 1940. Relapse is the major problem in treating PCM. Initially sulfonamides (sulfamidopyridine) and subsequently its derivatives (sulfadiazine) were used. A combination of trimethoperim and sulphonamides is recommended for the patient with sulphadiazine resistant strains, because sulfonamides are inexpensive and have low toxicity. PCM in combination with AIDS has been observed with a mortality rate as high as 30%. Early diagnosis and treatment with amphotericin B followed by trimethoprim-

sulfamethoxazole has been found to be effective for PCM (Brummer *et al.*, 1993; Goldani and Sugar, 1995).

Systemic mycosis is a major health problem in developing countries, which involves long term treatment; this is the main reason for emergence of drug resistance. A review by Lortholary recommends amphotericin as the drug of choice for immunocompetent and immunocompromised patients; however, 20-30% of cases treated with amphotericin B have relapsed and 60% of cases have been in remission. Ketoconazole was shown to be an effective drug in 80-90% of cases, with a recommended dose of 200-400 mg/day for 6-12 months. Sequelae are frequently observed in many pulmonary infections, so it is a challenging problem for clinicians (Lortholary *et al.*, 1999). Itraconazole is also an effective drug, with a dosage of 100 mg/day for 6 months. Several effective strategies have been implicated to over come drug resistance in fungi; increasing antifungal dosage, new delivery methods, using combination of drugs, removing sequestered lesions by surgery and investigating new antifungal agents (Kontoyiannis and Lewis, 2002).

1.9 Genetic studies

Fungal diseases pose a serious and a major health problem (with high rate of mortality) around the world. PCM is an endemic disease in Latin American countries. There is evidence that the temperature modulates the transition of *P. brasiliensis* that its pathogenesis is based on the morphological transition to the yeast form (Borges-Walmsley and Walmsley, 2000; Brummer *et al.*, 1993; San-Blas *et al.*, 2002). The study of this disease at a molecular level has been neglected for many decades for various reasons, and only a limited number of papers have been published. Consequently, the mechanism of pathogenesis and morphological transition from mycelial to pathogenic yeast form is poorly understood in *P. brasiliensis*. It has been shown that cAMP modulates the morphological switch in several human and plant pathogenic fungi (Durrenberger *et al.*, 1998). In the present work we sought to study the components of the cyclic AMP pathway in *P. brasiliensis* by characterizing the

genes involving in the morphological change as a means to find the potential drug targets.

1.10 Components of cAMP/PKA pathway: G Proteins

The guanine-nucleotide binding proteins known as G proteins play a vital role in various cell signalling processes in eukaryotes. The first step in the G protein signalling cascade is the binding of specific ligands (hormones; glucose or any fermentable sugars; glycoproteins; growth factors; etc) to the seven-transmembrane helix G protein-coupled receptors (GPCR). In general, G proteins are activated when they interact with a G protein-coupled receptor and they then transmit signals to downstream effectors such as adenylyl cyclase, protein kinases, phospholipases Cβ, cGMP and phosphodiesterases. The downstream effectors further regulate intracellular levels of second messengers, such as cAMP, diacylglycerol, inositol triphosphate, cGMP, sodium, potassium, calcium ions and arachidonic acid. G proteins function as a heterotrimeric complex composed of Gα, Gβ, Gγ subunits; which are activated when GTP binds to and replaces bound GDP. The activated GTP-bound Gα dissociates from the G$\beta\gamma$ dimer. The signalling process is mediated by Gα-GTP, G$\beta\gamma$ dimer or both. The signal is terminated by hydrolysis of GTP and reassociation of this heterotrimeric complex. More than 20 different Gα subunits have been identified in mammalian systems and these are classified under 4 main groups: G_s, G_i, G_q and G_{12} (Dohlman, 2002; Sprang, 1997).

Fungi possess 2 to 4 Gα subunits, but they have only one Gβ and Gγ subunit (forming a dimer, G$\beta\gamma$). This suggests that some Gα subunits either act independently or the G$\beta\gamma$ dimer associates with more than one Gα protein (Pryciak and Huntress, 1998). G protein signalling regulates several important processes including cell growth, morphogenesis, development, virulence and transcriptional activation through the cAMP/PKA and MAPK pathways (Hoffman, 2005; Tamaki, 2007).

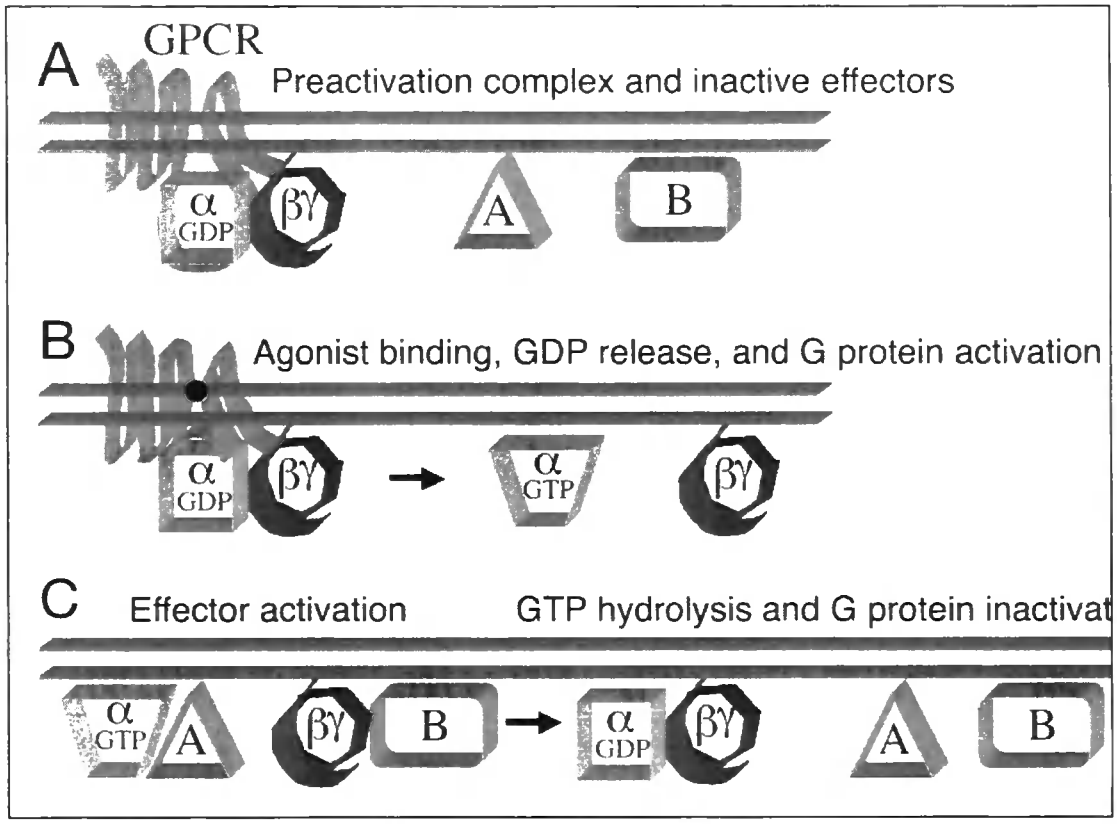

Figure 1.10.1 G protein activation and inactivation cycle (Hoffman, 2005).

A. G proteins exist as an inactive heterotrimer in the absence of a ligand and GDP bound to Gα. This complex is bound to a G protein-coupled receptor. A and B are downstream effectors shown separately.
B. Nucleotide exchange in the Gα-subunit; GDP is replaced by abundant GTP, causing a conformational change in Gα, which then dissociates from the Gβγ dimer.
C. The GTP bound Gα and Gβγ can both activate downstream effectors independently and after the completion of the signalling process the Gα hydrolyses the GTP, binding the resulting GDP; finally Gαβγ is re-formed as an inactive heterotrimer.

Gα subunits have intrinsic GTP hydrolysis activity. This activity is necessary for the cycling of the G protein signalling. RGS (Regulator of G protein Signalling) proteins also called GAPs (GTPase accelerating proteins) activate the GTP hydrolysis of G proteins and thereby terminate or desensitize the signalling by Gα and Gβγ subunits. About 20 different RGS proteins have been identified (De Vries and Gist Farquhar, 1999; De Vries *et al.*, 2000).

It has been known for a long time that G protein signals are transmitted from the plasma membrane to intracellular effectors. Recent studies have demonstrated that G proteins signals may also start from intracellular compartments, independent of cell surface receptors or G protein-coupled receptors, via accessory proteins. These accessory proteins help the G proteins to reach the right environment and for the formation of the functional complex. The RGS family (Regulator of G protein signalling) proteins are one of the main families of accessory proteins. Initially it was thought that RGS proteins are GTPase accelerating proteins that facilitate signal termination, but recently it was found that they can also directly regulate G protein signalling in the absence of the G protein-coupled receptor in three ways, which is shown in figure 1.10.2 (Sato *et al.*, 2006; Slessareva and Dohlman, 2006).

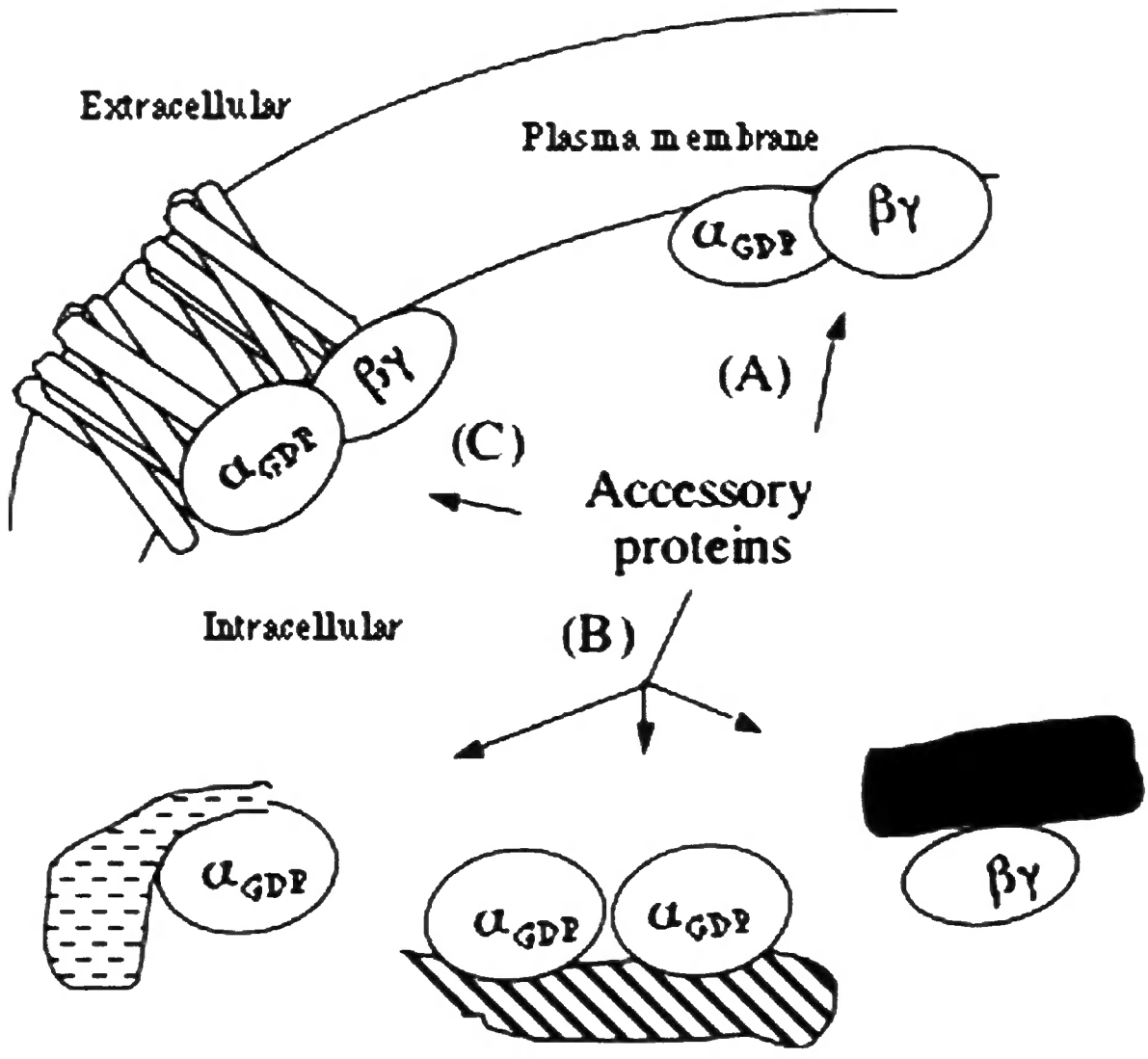

Figure 1.10.2 Role of accessory proteins in G protein signalling. A: Accessory proteins regulate the membrane bound G proteins independent of the G protein-coupled receptor. B: Dissociated G proteins bind to alternative binding partners; other G proteins. This complex may be present in intracellular compartments (Golgi) or the plasma membrane. C: Accessory proteins may also regulate G proteins which have been activated by receptors (Sato *et al.*, 2006).

1.11 G protein signalling in *S. cerevisiae* and *Schizosaccharomyces pombe*

Saccharomyces cerevisiae has two Gα subunits namely Gpa1 and Gpa2; Gpa1 is involved in Mitogen-Activated Protein Kinase (MAPK) pathway in response to pheromones and Gpa2 is involved in cAMP signalling pathway in response to glucose. The diploid strain of *S. cerevisiae* undergoes a morphological transition from yeast to pseudohyphal growth under nitrogen starvation/low nitrogen conditions via Gpa2; *gpa2* mutants are defective for formation of pseudohyphae. Early studies established that the cAMP pathway in *S. cerevisiae* is Ras dependent; later it was shown that the Gα subunit Gpa2 and Ras are both positive regulators of the cAMP pathway, regulating intracellular cAMP levels by activating adenylyl cyclase. Activation of adenylyl cyclase by Gpa2 is by glucose detection whereas that of Ras is by intracellular acidification. Recent studies show that Ras is responsible for triggering the cAMP pathway independent of Gpr1 and Gpa2 in glucose signalling. Gpa1 negatively regulates the MAPK pathway on pheromone stimulation (Hoffman, 2005; Kubler *et al.*, 1997; Lorenz and Heitman, 1997).

The *GPR1* gene has been identified that encodes a G protein-coupled receptor. This receptor senses the glucose level and interacts with Gpa2 and is responsible for the glucose-dependent increase in intracellular cAMP levels. Gpa2 forms a complex with the Gβ mimic Krh1 (Batlle *et al.*, 2003; Peeters *et al.*, 2006). Ras2 functions in parallel with Gpa2; *gpa2* or *ras2* or both deletion mutants show severe growth defects (Tamaki, 2007). GTP-bound Gpa2 can interact with adenylyl cyclase (Peeters *et al.*, 2006). In the pheromone response pathway Gpa1 forms a heterotrimer with Ste4 (Gβ) and Ste18 (Gγ) (Rocha *et al.*, 2001). After dissociation of Gpa1-GTP, the Gβγ dimer remains attached to the membrane and activates the pheromone response pathway by recruiting Ste5 (scaffold protein) and Ste20 p21-activated kinase (Hoffman, 2005; Pryciak and Huntress, 1998).

Schizosaccharomyces pombe possesses two 2 Gα proteins. Gpa1 is essential for mating and sporulation but is not required for vegetative growth. A Gpa1 deletion is not lethal in *S. pombe* but in *S. cerevisiae* Gpa1 has the opposite function, with a

negative role in the pheromone pathway and its deletion is lethal (Obara *et al.*, 1991). The G protein-coupled receptor Git3 acts in a similar manner to Gpr1 of *S. cerevisiae*, which senses glucose levels and triggers the cAMP pathway. The Gα protein Gpa2 forms a heterotrimer with Gβ Git5 and Gγ Gi11. Both Gpa2 and Git5 can activate adenylyl cyclase to stimulate the cAMP pathway, but Ras1 is not involved in the cAMP pathway. A putative G protein-coupled receptor Stm1 interacts with Gpa2, but it is not involved in glucose signalling (Hoffman, 2005; Landry *et al.*, 2000; Landry and Hoffman, 2001). Adenylyl cyclase is directly activated by the Gα protein Gpa2; Gpa2 interacts with the N-terminal region of adenylyl cyclase and the interaction is strengthen in the presence of GTP (Ivey and Hoffman, 2005; Ogihara *et al.*, 2004).

1.12 Adenylyl cyclase and associated proteins

cAMP (3', 5'cyclic adenosine monophosphate) is an important second messenger molecule which modulate several signal transduction processes in eukaryotic cells. Adenylyl cyclase (AC) is the central component of the cAMP pathway. In *S. cerevisiae* the gene encoding for adenylyl cyclase is *CYR1* (also named as *CDC*35), which is activated and inactivated by G proteins. Adenylyl cyclase catalyses the synthesis of cAMP from ATP and in turn cAMP binds to the cAMP-dependent protein kinase regulatory subunit. Cell viability requires a basal cAMP level, therefore deletion of adenylyl cyclase is lethal (Tamaki, 2007). *S. cerevisiae* Cyr1 has 2026 amino acids and the catalytic domain lies in the C-terminal 400 amino acids (Kataoka *et al.*, 1985). *S. cerevisiae* Cyr1 is anchored to the peripheral membrane but its activity was also observed in the cytoplasmic fractions. Although 0.5 % NaCl can remove the membrane-bound Cyr1, part of the enzyme is still bound on the membrane and a Western blot has detected adenylyl cylcase in both fractions. The leucine-rich repeats are evidently essential for membrane binding since a protein derivative in which they were deleted protein was only present in the soluble fraction (Mitts *et al.*, 1990). It has been demonstrated that a mutation in AC K1876M failed to respond to the exogenous addition of glucose/intracellular acidification, however the cells maintained a basal intracellular cAMP level (Vanhalewyn *et al.*, 1999).

Pde1 and Pde2 (low/high affinity PDEases) are the two major phosphodiesterases that regulate intracellular cAMP levels by feedback inhibition. PDEases hydrolyse cAMP to AMP. Pde1 has been shown to be phosphorylated by PKA during elevated cAMP levels in cells or in cells stimulated by the addition of glucose. A *pde1* mutant shows a threefold increase in intracellular cAMP levels but *pde2* has no effect. No cAMP signal is seen in a *pde1/pde2* double mutant (Ma *et al.*, 1999).

Ras is a small G protein with intrinsic GTP hydrolysis activity. GTP-bound Ras is active whereas GDP-bound Ras is inactive. Ras1 and Ras2 proteins are the major activators of adenylyl cyclase upon glucose stimulation in the cAMP pathway. Simultaneous deletion of *RAS1* and *RAS2* seem to be lethal to the cells (Tamaki, 2007). An *in vitro* experiment confirmed that adenylyl cyclase is activated by purified Ras protein from either yeast or humans. Yeast strains lacking Ras function behave similar to adenylyl cyclase mutant strains (Broek *et al.*, 1985; Toda *et al.*, 1985). Ras proteins require post-translational modifications such as farnesylation and palmitoylation. Farnesylated Ras has higher affinity for adenylyl cyclase than the unmodified form and palmitoylation is necessary for efficient membrane binding (Kuroda *et al.*, 1993).

The activity of adenylyl cyclase on the membrane is dependent upon its association with the cyclase associated protein (CAP). It has been shown that the C-terminal of Cyr1 interacts with the N-terminal region of CAP. Adenylyl cyclase in *CAP* deletion mutant is not activated by Ras2. In addition, the following phenotypes are observed: sensitive to temperature, swollen cell and a growth defect on rich medium. This shows that Ras activation of adenylyl cyclase requires CAP association (Field *et al.*, 1990; Shima *et al.*, 2000). Ira1 and Ira2 are two major proteins (GAPs; GTPase activating proteins) that down-regulate Ras signalling by activating GTP hydrolysis by Ras. An *ira1* and *ira2* deletion strains are constitutively activated by the cAMP pathway and are hyperfilamentous (Borges-Walmsley and Walmsley, 2000). Overexpressed Ras1 and Ras2 proteins in a *ira1*

mutant cell are found with GTP-bound rather than as the GDP-bound form (Tanaka *et al.*, 1990a; Tanaka *et al.*, 1990b). Ira1 forms a complex with adenylyl cyclase, which facilitates the binding of adenylyl cyclase to the membrane. An *IRA1* disrupted mutant strain has 90% adenylyl cyclase activity in the soluble fraction; whilst the wild-type has 20% activity in the soluble fraction and 80% activity in the membrane fraction. Antibodies to Ira1 have been shown to inhibit the membrane binding of adenylyl cyclase (antibodies blocked Ira1 binding site on adenylyl cyclase). Ira1-antibodies detected Ira1 in the membrane fraction but not in the cytoplasmic fractions. Ira1 and adenylyl cyclase form a large complex that also includes CAP and Ras (Mitts *et al.*, 1991).

On the other hand Ras is positively activated by guanine-nucleotide exchange factors (GEFs), namely Cdc25 and Sdc25. The catalytic activity of Cdc25 has been demonstrated by an *in vitro* assay that shows Cdc25 promotes guanine-nucleotide exchange (GDP-GTP) on Ras proteins (Jones *et al.*, 1991). Cdc25p has two major domains: an α-domain and a β-domain. The α-domain is responsible for the transient increase in cAMP and the β-domain is involved in the feed back control loop of cAMP. It was shown that an α-domain deletion mutant does not respond to the glucose stimulated rise in cAMP and a β-domain deletion is lethal (Munder and Kuntzel, 1989). The N-terminus of Cdc25 (65-134) incorporates a SH3 domain, which interacts with the C-terminal region of adenylyl cyclase (see fig.1.12.1) (Mintzer and Field, 1999).

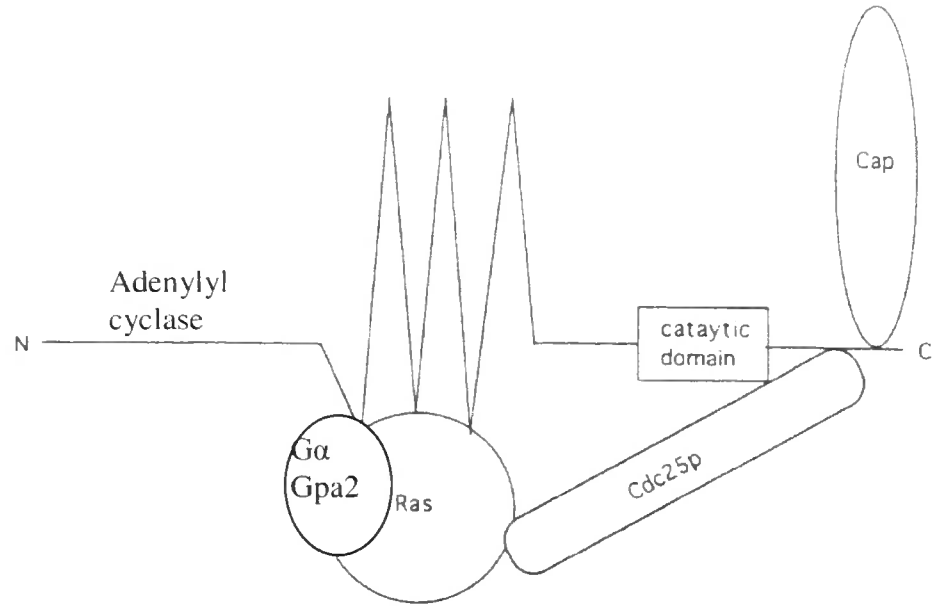

Figure 1.12.1 Adenylyl cyclase and its associated protein complex. Ras interacts with the N-terminus of adenylyl cyclase that incorporates the Ras association domain (RAD). The Gα protein Gpa2 also binds to the RAD. The cyclase associated protein (CAP) and Cdc25 both associate with the C-terminus of adenylyl cyclase. Cdc25 directly activates Ras. Figure slightly modified from reference (Mintzer and Field, 1999).

It has been demonstrated that Cdc25 relocalises adenylyl cyclase activity to the membrane in the absence of Ras. This finding suggests that there is cross talk between Cdc25 and Cdc35 without Ras proteins (Engelberg *et al.*, 1990). Further studies indicate that Ras signalling forms a large complex which includes adenylyl cyclase, cyclase associated protein, Cdc25 and Ira1 but how the Cdc25/Ras/cAMP pathway transduce the signal is still unclear.

An adenylyl cyclase encoding gene *spCYR1* has been identified in *S. pombe*, which encodes a protein of 1692 amino acids. *spCYR1* complements the *S. cerevisiae CYR1* temperature sensitive mutant strain T50-3A and is a membrane bound protein. It has been confirmed that the C-terminal is the functional domain and it is not activated by the addition of purified Ras protein (Yamawaki-Kataoka *et al.*, 1989).

1.13 cAMP-dependent Protein Kinase A

cAMP-dependent PKA is a well characterised large kinase enzyme that is found to be a primary target for the second messenger cAMP. Phosphorylation plays a vital role in connecting several eukaryotic signalling networks that are required for mating, cell division, differentiation and cell death. In *S. cerevisiae*, Ras2 and Gpa2 activate adenylyl cyclase in parallel to increase intracellular cAMP levels. The transient increase in cAMP activates the cAMP-dependent PKA. The inactive form of the PKA holoenzyme is a tetramer consisting of two catalytic subunits (*TPK*) and two regulatory subunits (*BCY1*). PKA is activated by binding of cAMP to its regulatory subunits which causes the dissociation of active catalytic subunits; the released catalytic subunits phosphorylate (transfer of phosphate from ATP to protein substrate) transcription factors and other proteins required for various cellular processes such as filamentous or pseudohyphal growth and also for metabolic control and stress resistance in fungi. It has recently been suggested that PKA is a potential drug target (Borges-Walmsley and Walmsley, 2000; Taylor *et al.*, 2008; Thevelein and de Winde, 1999) in pathogenic fungi.

1.14 Dimorphism in *S. cerevisiae*

The cAMP-PKA pathway controls morphogenesis in several fungi. Diploid strains of *S. cerevisiae* (MLY61**a**/α) undergo a dimorphic transition from a yeast form to a pseudohyphal form under low nitrogen conditions and in the presence of glucose. This is characterised by changes in the cell morphology from oval to elongated cells. The pseudohyphae are induced *in vitro* in SLAD (Synthetic Low Ammonium Dextrose) agar medium with 50 to 500 μM ammonium sulphate. *In vitro*, the cells invade the agar surface by pseudohyphae. The cells can produce more pseudohyphae at the lowest ammonium concentration of 50 μM. During pseudohyphal growth the yeast cell switches from bipolar budding to unipolar budding and the resulting mother cell forms an elongated chain of daughter buds which remain attached to the

mother cell. This growth is called pseudohyphae. The *gpr1* (G Protein-coupled receptor), *gpa2* and *tpk2* (cAMP-dependent Protein kinase A catalytic subunit) mutants are defective for formation of pseudohyphae (Borges-Walmsley and Walmsley, 2000; Pan and Heitman, 1999; Tamaki, 2007).

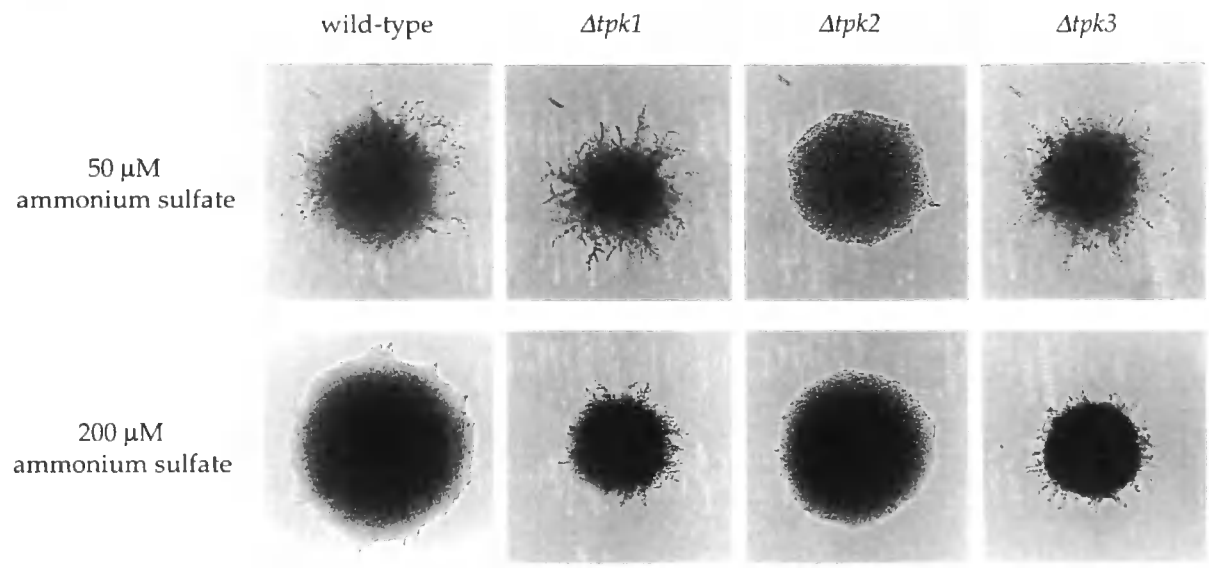

Figure 1.14.1 Pseudohyphal growth of diploid *S. cerevisiae* wild type MLY61**a**/α and *tpk1-3* mutants on low nitrogen medium (SLAD agar with 50 μM -200 μM ammonium sulphate) incubated at 30°C for 3 days: Δ*tpk1*/Δ*tpk1* (XPY4**a**/α) and Δ*tpk3*/Δ*tpk3* (XPY6**a**/α) produce enhanced filamentation and Δ*tpk2*/Δ*tpk2* (XPY5**a**/α) is defective for pseudohyphae (Pan and Heitman, 1999).

The nitrogen sensing component phosphatidylinosital-specific phospholipase C (Plc1) has been shown to form a complex with Gpr1 and Gpa2. This complex is required for pseudohyphal growth. Plc1 catalyses the hydrolysis of the substrate membrane phospholipid phoshatidylinositol 4, 5 biphosphate (PPI2) to inositol 1,4,5-triphosphate and diacylglycerol. The yeast two-hybrid and co-immunoprecipitation assays confirmed the interaction of Plc1 with Gpr1, independent of Gpa2 but Gpa2 and Gpr1 interaction depends on the presence of Plc1. The *plc1* or *gpr1* deletion mutants are defective for pseudohyphal growth (Ansari *et al.*, 1999; Tisi *et al.*, 2002). The kelch-repeat Gβ mimic proteins Gpb1/Krh2 and Gpb2/Krh1 have been identified recently. The *KRH1* and *KRH2* deletion mutants

show enhanced filamentation and invasive growth (Batlle *et al.*, 2003; Tamaki, 2007).

S. cerevisiae haploid cells undergo invasive growth rather than pseudohyphal growth (see figures. 1.14.1 and 1.14.2). This invasive growth takes place typically in rich medium. During the haploid invasive growth the cells invade the agar, which cannot be removed by washing. A gene encoding the cell surface flocullin *FLO11* was identified that is homologous to *STA* genes (novel cell surface flocullin gene). It was shown that Flo11 is required for both formation of diploid pseudohyphae and haploid invasive growth. The *FLO11* deletion mutant neither forms pseudohyphae nor has an invasive phenotype. A Flo11-GFP fusion localizes in the periphery of the cells. The N-terminus of Flo11 has a signal sequence and the C-terminus is similar to GPI-anchored serine/threonine cell wall proteins. Flo11 has a flocculating activity, in which yeast cells aggregate in a calcium-dependent manner (non sexual process). The promoter of *FLO11* has consensus binding sites for the transcription factors Ste12 and Tec1. There are no *FLO11* transcripts observed in *Ste12* deletion strains, in addition *Ste12* deleted mutants failed to invade agar (Colombo *et al.*, 1998; Lo and Dranginis, 1996).

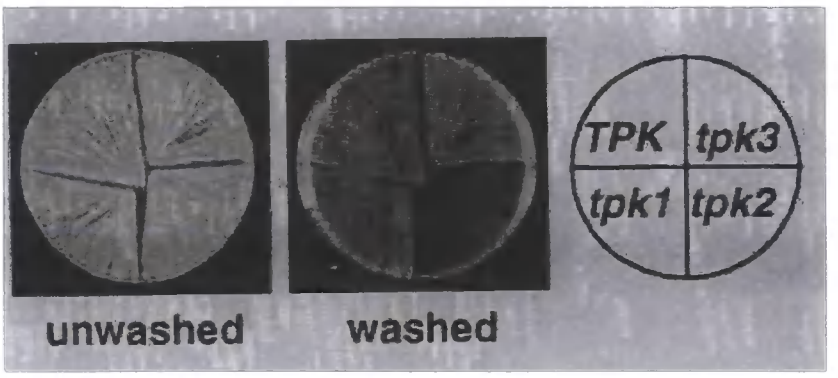

Figure 1.14.2 *S. cerevisiae* haploid invasive growth: wild type 10560-23C (Tpk^+), LRY629 (Δ*tpk3*), LRY594 (Δ*tpk2*) and LRY517 (Δ*tpk1*) were streaked on yeast extract dextrose agar, incubated at 30°C for 3 days and further incubated at room temperature for 2 days. The plate was photographed (unwashed) and the plate was gently washed with deionised water and photographed again (washed). This demonstrates that the *tpk2* mutant failed to produce invasive growth (Robertson and Fink, 1998).

S. cerevisiae has three PKA catalytic subunits Tpk1-3. At least one is essential for normal growth of the cell. Tpk1 and Tpk3 have more identity (about 88 %), but Tpk2 is distinct from other two (Pan and Heitman, 1999). A diploid *tpk2/tpk2* mutant strain is totally defective for pseudohyphae on SLAD agar whereas a *tpk3/tpk3* mutant strain has a hyperfilamentous phenotype. This behaviour is also apparent in haploid strains as well; a *tpk2* haploid mutant is unable to invade rich medium whilst *tpk3* mutant is hyperinvasive. On the other hand *tpk1* diploid and haploid mutants exhibit no change in phenotype (see figure 1.14.1 and 1.14.2). The two-hybrid assay demonstrated that Tpk2 interacts only with Sfl1, a transcriptional repressor and indicates that Sfl1 is downstream of Tpk2 and upstream of Flo11. The *SFL1* deletion mutant displays hyperinvasive and hyperfilamentous phenotypes in haploid and diploid strains, respectively (Toda *et al.*, 1987). Further studies demonstrate that the regulatory subunit *BCY1* mutants are hyperfilamentous while Tpk1 and Tpk3 have a negative role and Tpk2 has a positive role in filamentation (Pan and Heitman, 1999).

An *in vitro* assay demonstrates that Sfl1 and Flo8 (activator) both are phosphorylated directly by Tpk2. However Flo8 and Sfl1 have antagonistic functions on *FLO11* expression. Tpk2, Sfl1 and Flo8 bind to a common area of the *FLO11* promoter over a 250 base pair region. Phosphorylation activity of Tpk2 on Sfl1 and Flo8 inhibits and activates binding on *FLO11* promoter, respectively. Therefore Sfl1 acts as a negative regulator of pseudohyphal growth and Flo8 acts as positive regulator of pseudohyphal growth by allowing the transcription of *FLO11* (see fig. 1.14.3) (Pan and Heitman, 2002). The *FLO11* transcripts are dramatically decreased in a *flo8* deletion strain (Rupp *et al.*, 1999).

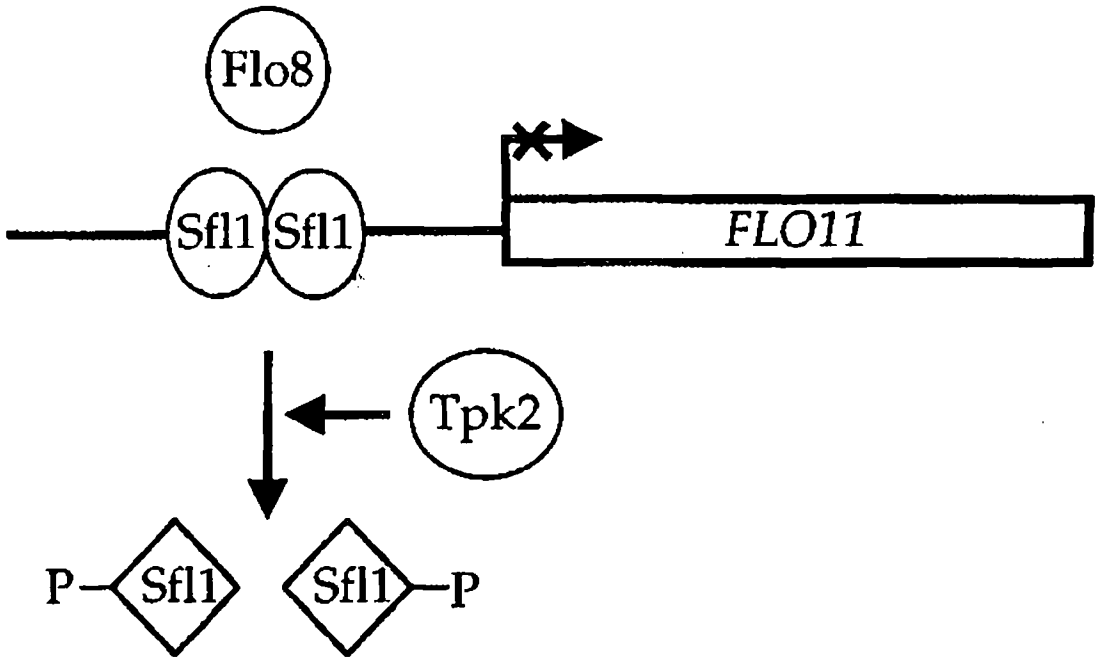

Figure 1.14.3 Tpk2 controls the assembly of Sfl1 and Flo8 transcription factors on the *FLO11* promoter. The binding of Sfl1 on the *FLO11* promoter represses *FLO11* expression and the binding of Flo8 on the *FLO11* promoter activates the expression of *FLO11* (Pan and Heitman, 2002).

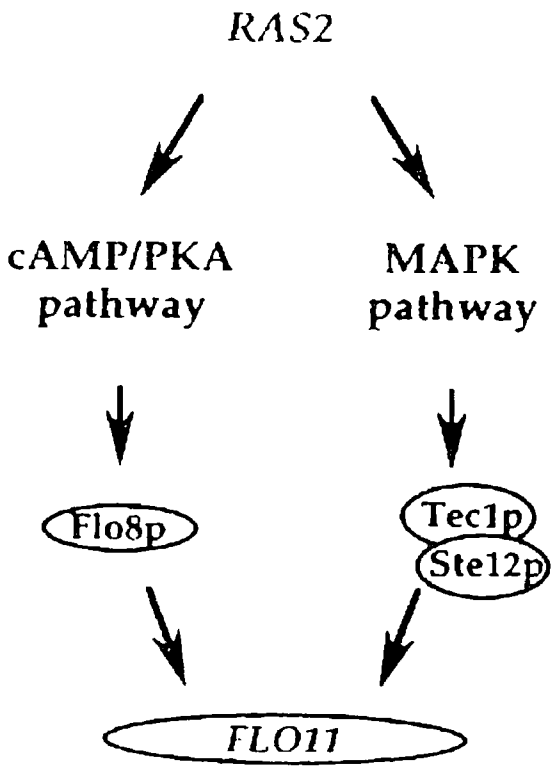

Figure 1.14.4 The merging of the cAMP and MAPK Pathways. cAMP and MAP kinase pathways induce invasive and pseudohyphal growth by activating a common area of the *FLO11* promoter. Tec1 and Ste12 are necessary to induce Flo11 in the MAPK pathway. Flo8 is required to induce Flo11 in the cAMP/PKA pathway (Rupp *et al.*, 1999).

In *S. cerevisiae,* Flo11 is involved in cell-cell adhesion and cell-surface adhesion (aggregation of cells). Flo11 is responsible for the characteristic mat formation and filamentous growth on solid medium. A *flo11*Δ mutant cannot form mat or pseudohyphae. Flo11 increases the hydrophobicity that is required for cell adhesion and biofilm formation. In the Σ1278b parental strain background, haploid forms more mat than tetraploid and demonstrates that the increase in ploidy decrease the mat formation. These findings indicate that Flo11 is required for biofilm formation (Reynolds and Fink, 2001). The human fungal pathogen *C. albicans* produces a biofilm: a strain with yeast form produces a thinner layer of biofilm than the hyphal form. The biofilms produced by yeast form weakly adheres to the surface

and can be washed away easily. The surface of the biofilm seems to have various layers of hyphal forms of *C. albicans* (O'Toole *et al.*, 2000).

Ammonium permeases have been shown to be involved in nitrogen sensing and ammonium transport. Three ammonium permeases have been identified in *S. cerevisiae*, namely Mep1-3. At least one Mep isoform is necessary for yeast to grow on nitrogen limiting media, but pseudohyphal growth requires Mep2. Mep2 is present upstream of Gpa2, but there is no direct evidence for the interaction of Mep2 and Gap2 (Lorenz and Heitman, 1998). Similarly, *C. albicans* has ammonium permeases Mep1 and Mep2; one of which is required to grow on nitrogen limiting medium. However Mep2 is necessary for the transition of yeast to filamentous growth (Biswas and Morschhauser, 2005).

It has recently been shown that sucrose can induce pseudohyphae with Gpr1, cAMP-dependent PKA and Snf1 kinase pathway on rich nitrogen medium and even in the ammonium permease mutant *mep2Δ/ mep2Δ* cells. Gpr1 also acts as a strong receptor for maltose; maltose induces pseudohyphae under nitrogen starvation but not under nitrogen rich medium (Van de Velde and Thevelein, 2008). Snf1 is a serine/threonine protein kinase essential for relieving the genes repressed by glucose. Snf1 forms a complex with Snf4 with the help of bridging protein (Brp; Sip1/2 or Gal83) in the absence or under low glucose (see fig. 1.14.5) (Jiang and Carlson, 1997), then activates the genes necessary for the utilization of alternative carbon sources such as sucrose. Snf4 has a similar structure and function to Sfl1, which is also required for the expression of glucose repressed genes (Gancedo, 1998; Hedbacker and Carlson, 2008).

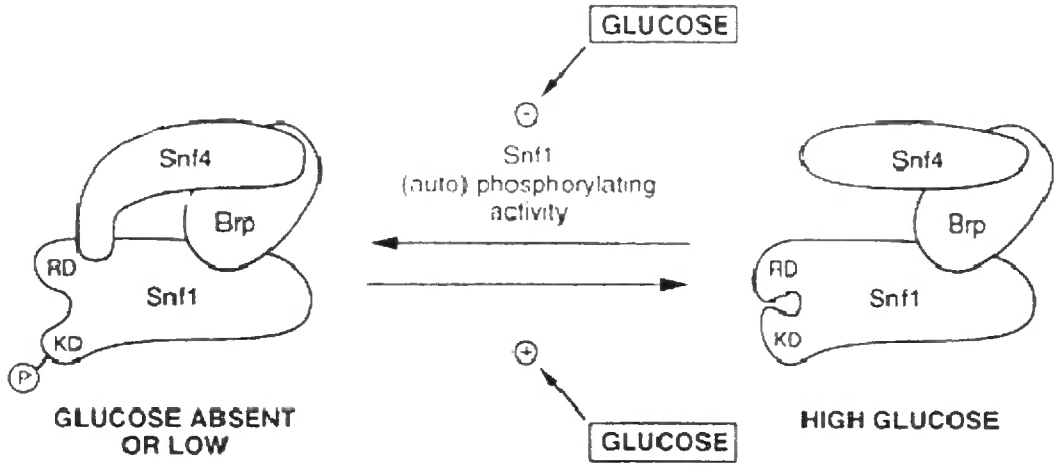

Figure 1.14.5 Regulation of Snf1 and Snf4 complex by glucose and interaction between Snf1 and Snf4. Snf1 and Snf4 are linked by bridging proteins Brp/ Gal83/Sip1/Sip2. The Glucose level mediates the association of the Snf1 regulatory and catalytic subunits by phosphorylation activity. When glucose is high, the Snf1 regulatory subunit binds to its catalytic subunit in order to inhibit the kinase activity, whereas in low levels of glucose the inhibition is released by binding of Snf4 to Snf1's regulatory subunit (figure slightly modified from (Gancedo, 1998; Jiang and Carlson, 1997).

1.15 G Protein mimics Krh1/2 down-regulate pseudohyphal and invasive growth

In *S. cerevisiae,* the G protein Gpa2 is involved in the cAMP/PKA pathway. It has recently demonstrated that the Gpb mimic protein Krh1 interacts with Gpa2 and Krh1/2 are downstream of Gpa2 (Batlle *et al.*, 2003; Peeters *et al.*, 2006). The expression of the cell surface flocullin *FLO11* was analysed in various mutant backgrounds in the wild-type haploid strain (SKY763): a *gpa2*Δ haploid mutant displays ninefold lower expression levels than wild-type cells; *KRH1* and *KRH2* single or double deletion mutants show three to fourfold higher expression levels than wild-type cells and a *krh1*Δ *krh2*Δ *gpa2*Δ triple mutant has increased expression over the *gpa2* single mutant. It has been suggested that deletion of *KRH1/2* resulted

in stimulation of signalling pathways leading to high level expression of *FLO11* (Batlle *et al.*, 2003). The expression level of *FLO11* corresponds to the level of pseudohyphal and invasive growth in diploid and haploids strains, respectively. The agar invasion assay on solid medium demonstrates that *krh1*Δ, *krh2*Δ and *krh1*Δ *krh2*Δ double mutants show enhanced invasive growth than the wild-type; in particular the double mutants are hyperinvasive compared to other mutants, whilst *gpa2*Δ mutant does not invade significantly. The *flo11*Δ single mutant and the *krh1*Δ *krh2*Δ *flo11*Δ triple mutant also failed to invade. The *krh1*Δ/*krh2*Δ mutant shows a different macroscopic phenotype; cells form patches that are similar to biofilms. These findings suggest that *krh1*Δ/*krh2*Δ mutant (deletion activates the pathway) with high level expression of Flo11 contribute to biofilm formation and demonstrate that Krh1 and Krh2 down-regulate the signalling pathway (Batlle *et al.*, 2003).

A potential downstream target of Krh1/2 is the PKA catalytic subunit Tpk2. In another experiment the *FLO11* mRNA was analysed in *tpk2* mutant. *FLO11* mRNA was not detectable in the *tpk2*Δ single mutant and *krh1*Δ *krh2*Δ *tpk2*Δ triple mutant; however, the wild-type strain has a basal level of *FLO11*. In addition, the *krh1/krh2* mutation leads to higher sensitivity to heat shock and lower sporulation efficiency, therefore the cells grow continuously, which is indicative of activation of the cAMP/PKA signalling pathway.

The *krh1* and *krh2* mutants show a hyperfilamentous phenotype with a high PKA activity. However, deletion of *gpa2* causes a defect in pseudohyphae formation and lower PKA activity. In addition to the above findings, the *krh1* and *krh2* mutants exhibit a lower accumulation of the reserve carbohydrates trehalose and glycogen and lower expression of *HSP12*. An *in vitro* GST-pull down demonstrated that Krh1 binds to Tpk1-3 and the PKA holoenzyme complex (Tpk1 and Bcy1 co-expressed) in order to down-regulate its activity. Krh1 binds to the PKA catalytic subunits and this binding enhances the association between PKA regulatory and catalytic subunits, because a weaker interaction among catalytic and regulatory subunits is observed in the absence of Krh1 *in vivo*. It has also been shown that Krh1 has same effect on mammalian PKA: the interaction between mouse catalytic subunit Cα with its

regulatory subunit I is reduced in the absence of Krh1 (Batlle *et al.*, 2003; Lu and Hirsch, 2005; Peeters *et al.*, 2006).

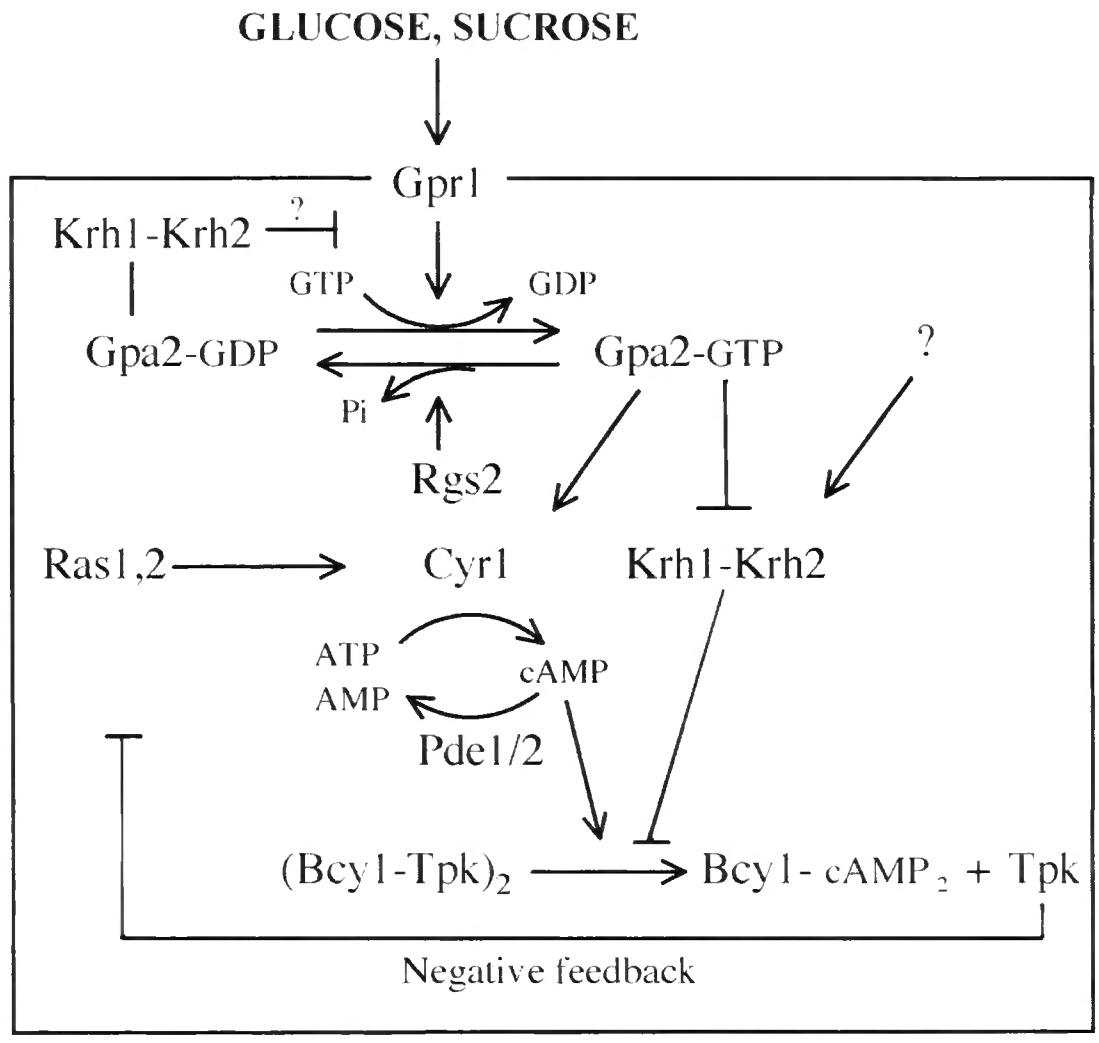

Figure 1.15.1 Gpa2 and Krh1 signalling pathway. Activated Gpa2 regulates PKA in two different mechanisms: the classical direct activation of adenylyl cyclase and inhibition of Krh1/2 dependent down regulation of PKA. Krh1 is downstream of Gpa2 which bypasses the activity of adenylyl cyclase and enhances the association between PKA regulatory and catalytic subunit subunits (Peeters *et al.*, 2006).

The inhibition of PKA activity by Krh1 has not been demonstrated *in vitro* using purified Krh1. Krh1 is not a canonical Gpb partner for Gpa2. Gpa2 is involved in two different pathways: it directly activates adenylyl cyclase in a classical cAMP pathway and in the other pathway it dissociates from the kelch repeat Gpb mimics Krh1/2, which bypasses the requirement of adenylyl cyclase by directly regulating

PKA by Krh1/2 interacting with its catalytic subunits. It has been suggested from the above finding that the Krh1 and Krh2 proteins down-regulate the PKA activity (Batlle *et al.*, 2003; Lu and Hirsch, 2005; Peeters *et al.*, 2006).

1.16.1 Comparison between cAMP/ PKA and MAP kinase pathways

In general, cAMP-protein kinase A and MAP kinase pathways are involved in pseudohyphal/invasive growth, but they are stimulated by different external cues. Interestingly, both kinases have dual roles in filamentous growth. The cAMP/PKA pathway is stimulated by low nitrogen with different carbon sources e.g. glucose and sucrose. The PKA catalytic subunit Tpk2 has a positive effect, whilst the other catalytic subunits, Tpk1 and Tpk3, exhibit a negative role in filamentation (Pan and Heitman, 1999; Robertson and Fink, 1998). Consistent with this, the MAP kinase Kss1 has two functions; phosphorylated Kss1 stimulates pseudohyphal growth and unphosphorylated (unactivated) Kss1 has a negative role in filamentation. Ste7 is an upstream component of Kss1, which phosphorylates Kss1 and activates it. Phosphorylated Kss1 relieves the repression on the Ste12/Tec1 heterodimer and allows *FLO11* transcription that is necessary for filamentation, whereas unphosphorylated Kss1 binds to the repressors Dig1/2 and this complex binds to Ste12/Tec1 in order to inhibit *FLO11* transcription (see figure 1.16.1.1 and 1.16.1.2) (Cook *et al.*, 1997; Madhani *et al.*, 1997; Pan and Heitman, 2002). Similarly, in the cAMP/PKA pathway, Flo8 and Sfl1 are phosphorylated by Tpk2. Flo8 has a role in activation and Sfl1 has a role in repression of *FLO11* transcription. The binding of activator and repressor on the *FLO11* promoter is controlled by Tpk2 (see fig. 1.16.1) (Pan and Heitman, 2002). Flo11 is responsible for filamentous growth and it is the point of convergence point for both the cAMP and MAP kinase pathways (see fig. 1.14.4) (Rupp *et al.*, 1999).

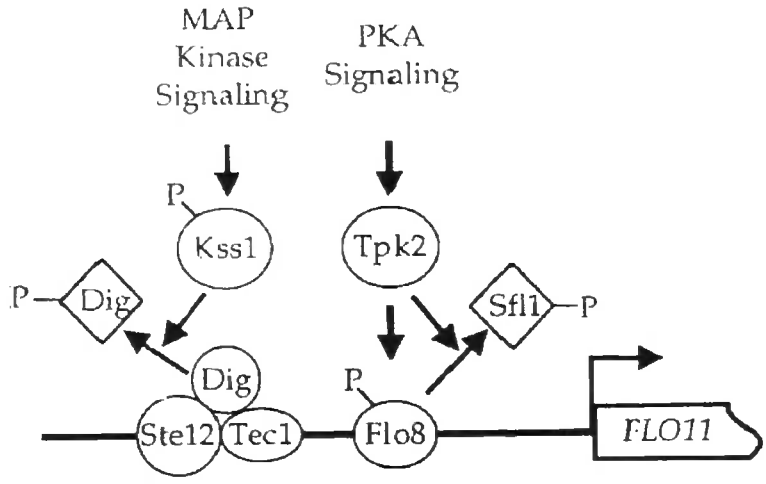

Figure 1.16.1.1 Control of *FLO11* transcription. Kss1 activates the Ste12 and Tec1 complex and inhibits the repressor Dig binding on the *FLO11* promoter. Tpk2 activates Flo8 and prevents the repressor Sfl1 from binding the *FLO11* promoter for the expression of *FLO11* (Pan and Heitman, 2002).

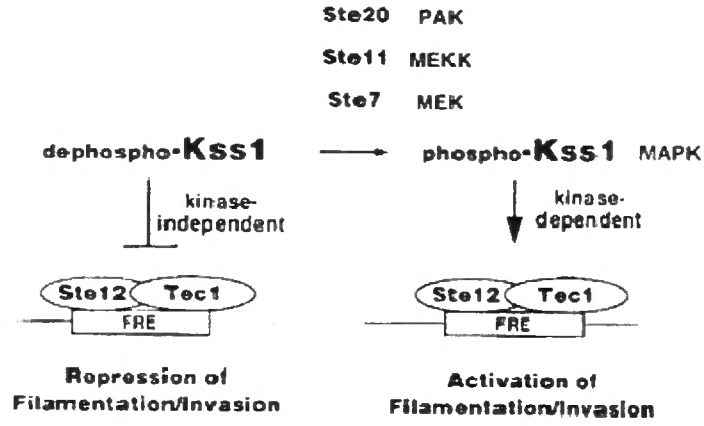

Figure 1.16.1.2 Kss1 showing antagonistic function. Dephosphorylated Kss1 represses transcription and phosphorylated Kss1 activates *FLO11* expression (Madhani *et al.*, 1997).

1.17 Summary of cAMP pathway in *S. cerevisiae*

Initially it was thought that *S. cerevisiae* glucose/cAMP pathway is a Ras-dependent pathway. Ras is positively activated by Cdc25 and Sdc35 and down-regulated by Ira1/2. Activated Ras associates with adenylyl cyclase and the CAP complex. Recent research has focused more on the glucose/cAMP pathway mediated by the G protein-coupled receptor Gpr1 (GPCR). Gpr1 is coupled with the G protein Gpa2 on stimulation by a fermentable carbon source and in the presence of Plc1 (Hoffman, 2005; Toda *et al.*, 1985). The C-terminal of Gpr1 interacts with Gpa2 and it has been shown that Gpr1-GFP concentrates at the plasma membrane. Gpa2 interacts with the Gpb mimics kelch repeat proteins Gpb2/Krh1 and Gpb1/Krh2 and Gγ Gpg1. However, Gpb2/Krh1 and Gpb1/Krh2 do not function as canonical Gpb proteins (Harashima and Heitman, 2002; Tamaki, 2007), because Gpr1 and Gpa2 are positive regulators and Krh1/2 are negative regulators of pseudohyphal and invasive growth. A *krh1/2* deletion has no effect on the association of Gpr1 and Gpa2. Therefore Krh1 is referred to as a pseudostructural inhibitor of G protein signalling (Hoffman, 2005; Ivey and Hoffman, 2002).

It was recently demonstrated that activated Gpa2 stimulates adenylyl cyclase activity (Peeters *et al.*, 2006). The Ras and Gpa2 pathways independently activate adenylyl cyclase; however, whilst Ras stimulated adenylyl cyclase activity is essential for cell viability, Gpa2 is not. The downstream component of adenylyl cyclase is cAMP-dependent PKA. The three isoforms of PKA have various roles in pseudohyphal or invasive growth (Robertson and Fink, 1998). When cAMP is depleted, or PKA is inactivated, the cells cannot proliferate and completely enter into the G0 stationary phase. In contrast with this, cells having high PKA activity have reduced sporulation, whilst those with low PKA activity constitutively sporulate (Thevelein and de Winde, 1999). Pde1 has been shown to be involved in the feed back inhibition of cAMP by hydrolysing cAMP to AMP. The PKA catalytic subunit Tpk2 phosphorylates the transcriptional activator Flo8 and transcriptional repressor Sfl1. Finally, activation and binding of Flo8 to the *FLO11* promoter stimulates the

dimorphic differentiation in both haploid and diploid strains (Pan and Heitman, 2002; Rupp *et al.*, 1999; Tamaki, 2007).

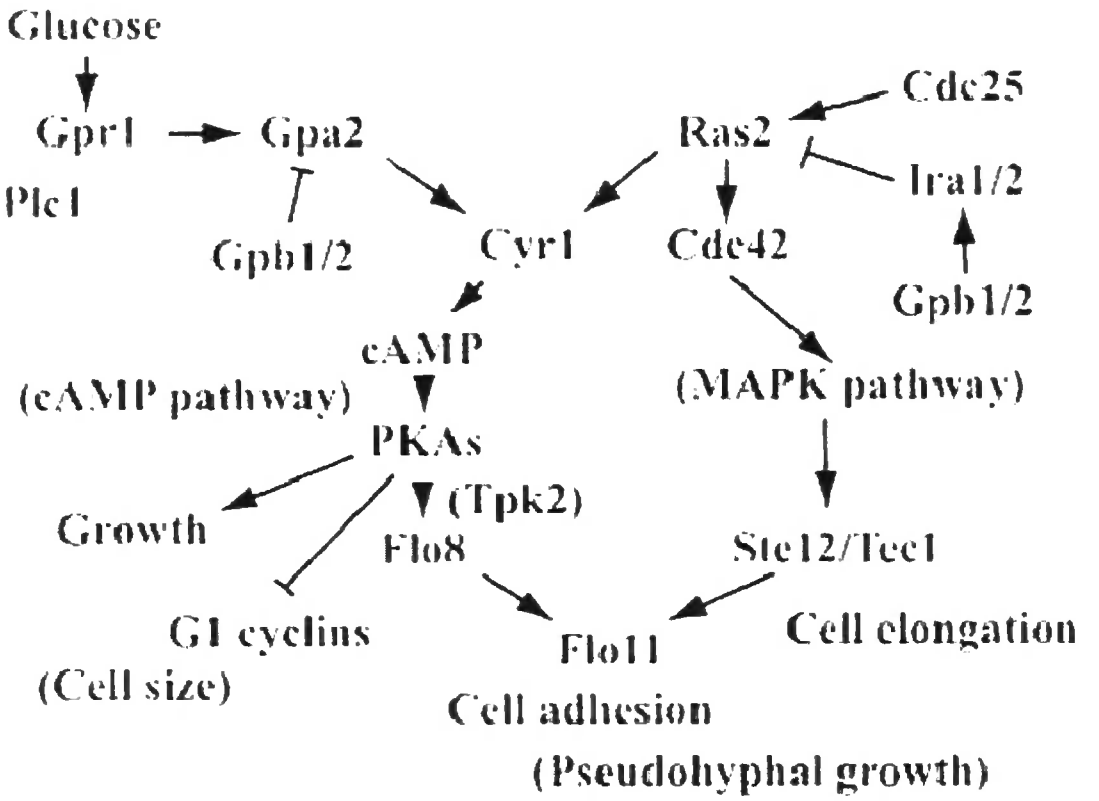

Figure 1.17.1 *S. cerevisiae* glucose-cAMP/PKA pathway is parallel to the MAPK pathway. On glucose activation Gpr1 is coupled to Gpa2 in the presence of Plc1. Activated Gpa2 stimulates adenylyl cyclase, which syntheses cAMP. The intracellular rise in cAMP activates PKA then PKA catalytic subunit Tpk2 phosphorylates Flo8, which is a transcriptional activator of *FLO11* transcription. Flo11 is responsible for pseudohyphal and invasive growth. PKA also regulates the cell size and cell division. cAMP/PKA and MAPK pathways converge at *FLO11* (Tamaki, 2007).

1.18 cAMP/PKA pathway in *S. pombe*

In *S. pombe*, the glucose/cAMP pathway is regulated by nine *git* (glucose insensitive transcription) genes. Glucose is sensed by a seven transmembrane helix G protein-coupled receptor Git3. The downstream component of Git3 is Gpa2 (Git8), which associates with Gβ (Git 5) and Gγ (Git11). Git1, Git7 and Git10 have been identified and they function independent of the G protein Gpa2. They are found to be essential for stabilizing the signalling complex. Adenylyl cyclase (Git2) is activated by Gpa2 but not Ras. In addition, adenylyl cyclase is not required for cell viability. To date, no RGS protein connected with cAMP/PKA pathway has been identified, but one RGS protein Rgs1 is involved in the pheromone pathway (Hoffman, 2005). The components of the cAMP/PKA pathway are similar to those in *S. cerevisiae*. However, recently Git1 has been identified and shown to interact with adenylyl cyclase Git2, which is distinct from the conserved components of cAMP pathway. In addition, a *git1*Δ mutant displays defective cAMP signalling but the cells are viable (Kao *et al.*, 2006). The PKA regulatory subunit *CGS1* and catalytic subunits *PKA1* have also been identified and shown to be involved in the glucose cAMP/PKA pathway (Hoffman, 2005). The cAMP pathways in *S. cerevisiae* and *S. pombe* provide new insights to explore the cAMP pathway in pathogenic fungi.

1.19 cAMP pathways in pathogenic fungi

1.19.1 cAMP pathway in *C. albicans*

Candidosis is caused by *C. albicans*, one of the most important human opportunistic systemic mycoses (Odds, 1987). *C. albicans* is a dimorphic fungus that can undergo a reversible morphogenesis. The transition is characterised by the conversion of unicellular yeast to a chain of distinct daughter cells in a filamentous form (pseudohyphal/hyphal), which usually do not become detached from the mother cells. Mutants unable to undergo this transition are avirulent (Brown and Gow, 1999; Lo *et al.*, 1997; Merson-Davies and Odds, 1989). The important factors inducing the transformation are temperature, neutral pH (stress) and oxygen limitation; apart from these stimuli, *in vitro* nitrogen starvation can also induce hyphal growth. A higher

degree of germ tube induction has been observed in serum or when it contact with macrophages (Brown and Gow, 1999). Exogenous cAMP and the cAMP analogue N_6, O_2'-dibutyryl cAMP induce the transition from yeast to mycelial form. During the morphological transition, the intracellular and extracellular cAMP levels increase and the increase in intracellular cAMP levels correlates with the level of germ tube formation (Sabie and Gadd, 1992).

A number of the components of the cAMP/PKA pathway such as the homologue of Ras *RAS2*, adenylyl cyclase *CYR1*, G protein α-subunits *CAG1* and Gpa2 homologue *CAG99* (Brown and Gow, 1999), PKA catalytic subunit *TPK1* and *TPK2* (Cloutier *et al.*, 2003) have been identified. The transcription factors Efg1 (*S. cerevisiae* Phd1 homologue) and Cph1 (*S. cerevisiae* Ste12 homologue) have been identified and mutation of these shown to cause a defect for growth and avirulence (in a mouse model) (Lo *et al.*, 1997). The G protein-coupled receptor Gpr1 is upstream of Gpa2 both of which have a role in the glucose-cAMP/PKA pathway. It was demonstrated that Gpr1 interacts with Gpa2 (Maidan *et al.*, 2005). Deletion of *GPR1* causes a defect in yeast morphogenesis, however this is overcome by exogenous cAMP (Maidan *et al.*, 2005). The gene encoding for adenylyl cyclase is *CDC35* and deletion leads to undetectable cAMP levels. The mutant strain grows very slowly and is defective for the morphological transition but the deletion is not lethal. Adenylyl cyclase deleted strains are avirulent in a mouse model (Rocha *et al.*, 2001).

The cAMP pathway in *C. albicans* displays some differences with that in *S. cerevisiae*, for example the deletion of *RAS* in *C. albicans* is not lethal but it is lethal in *S. cerevisiae*. The Ras pathway has been shown to be involved in programmed cell death in *C. albicans* (Braun and Johnson, 1997). In addition, Tpk2 of *S. cerevisiae* has a positive role in filamentous growth, whereas Tpk1 and 3 have the opposite effect; but in *C. albicans*, Tpk1 and Tpk2 have redundant positive roles in germ tube formation (Bockmuhl *et al.*, 2001; Souto *et al.*, 2006). Tpk2 complements the growth defect of *tpk1-3* temperature sensitive mutant *S. cerevisiae* SGY446 and it is involved in dimorphism (Sonneborn *et al.*, 2000).

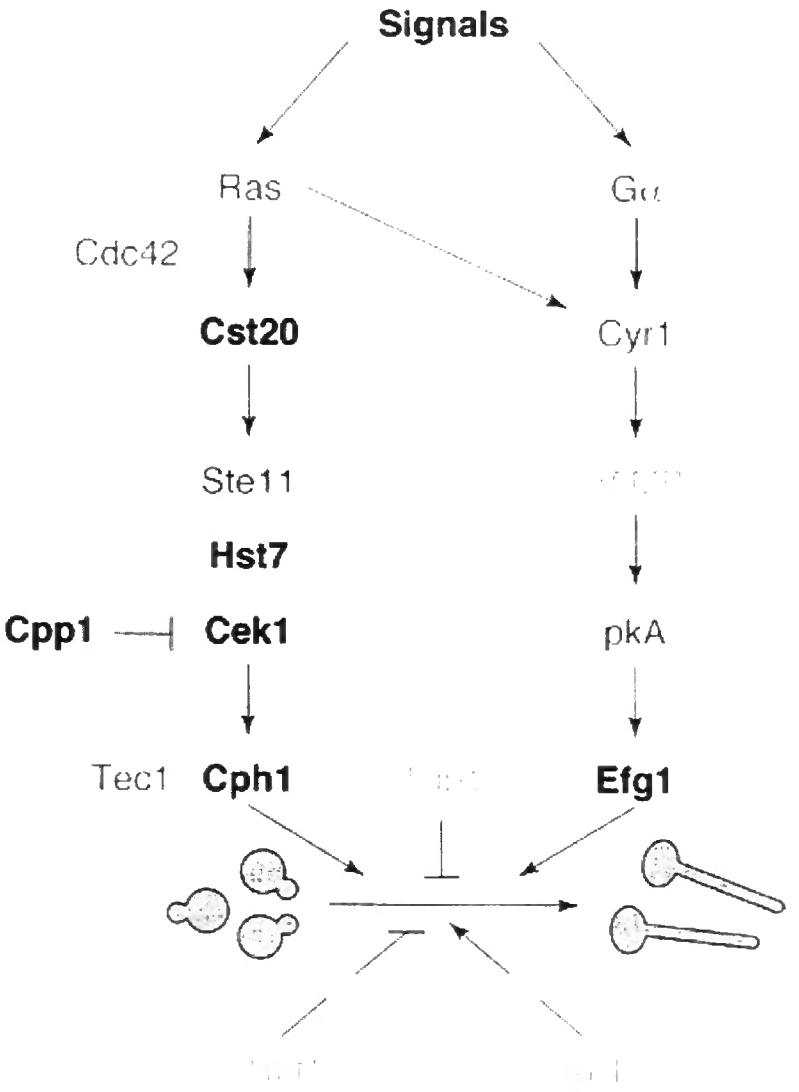

Figure 1.19.1.1 Efg1 and Cph1 pathways induce the yeast to hyphal transition in *C. albicans*. The MAPK components: Cph1 is similar to *S. cerevisiae* MAPK; Cst 20 is a *S. cerevisiae* Ste20 homologue, Hst7 is a *S. cerevisiae* Ste7 homologue, Cek1 is a *S. cerevisiae* Kss1 homologue. The cAMP/PKA pathway involves a traditional G protein, Ras, adenylyl cyclase (Cyr1), PKA and Efg1. The position of the transcriptional repressor Tup1 has not been characterised. Rbf1 and Int1 are DNA binding proteins, which have negative and positive roles in filamentation, respectively (Brown and Gow, 1999).

The transcriptional repressor Tup1 has a negative role in filamentous growth (Braun and Johnson, 1997). Rbf1 is a DNA binding protein that also has a negative role in filamentous growth (Brown and Gow, 1999). The *FLO8* gene encoding for a transcriptional factor has been identified in *C. albicans* by complementation in *S. cerevisiae*. Flo8 interacts with Efg1 to regulate dimorphism in *C. albicans*. A *flo8* deletion mutant is avirulent and defective for hyphal growth. (Cao *et al.*, 2006). Recent evidence also shows that cAMP is important for morphological transition; aminophylline, a phophodiesterase inhibitor, has a positive effect (increasing growth and inducing the transition) that corresponds to an increase in cAMP level and PKA activity; on the other hand atropine and trifluoperazine have the opposite effect (Singh *et al.*, 2007). A cAMP response element binding protein has been identified recently and it has been shown to have DNA binding activity and it is phosphorylated by PKA *in vitro* (Singh *et al.*, 2008).

1.19.2 The cAMP Pathway in *Ustilago maydis*

Ustilago maydis is a basidiomycete phytopathogenic fungus which is the causative agent of a smut disease of maize. *U. maydis* undergoes morphological changes from a non-pathogenic yeast form or teliospore to a pathogenic filamentous form; this transition is essential for pathogenesis. The cAMP pathway in *U. maydis* has been extensively studied (Borges-Walmsley and Walmsley, 2000; Chew *et al.*, 2008; Durrenberger *et al.*, 1998). The non pathogenic haploid cell exits in a yeast form that grows by budding. The mating process is essential for pathogenesis; during the mating process two haploid cells fuse and eventually form a dikaryon filamentous form (Durrenberger *et al.*, 1998; Gold *et al.*, 1994).

The dimorphic transition is induced by environmental factors, such as nutrient and oxygen availability. The gene encoding for adenylyl cyclase is *uac1*; deletion of *uac1* leads to constitutive filamentous growth that can be reversed by exogenous cAMP. However, the haploid filamentous *uac1* mutant is non-pathogenic and this suggests that filamentation is not necessary for pathogenesis. A mutation in the protein kinase regulatory subunit *ubc1* is defective for cytokinesis (mother

daughter cell separation) and shows changes in the bud site selection and is inhibited in filamentous growth (Gold *et al.*, 1994). The *ubc1* deleted mutant strain infection on maize plants revealed that they can colonize and grow on plant tissues but cannot produce tumours (Gold *et al.*, 1997). The cAMP/PKA catalytic subunits are encoded by two genes *ADR1* and *UKA1*: an *adr1* disrupted mutant displays a constitutive filamentous phenotype that is avirulent, whilst a *uka1* mutant shows no significant effect in mating, morphogenesis and virulence (Durrenberger *et al.*, 1998).

In contrast to other fungi, four Gα proteins Gpa1 to Gpa4 have been identified; Gpa1-3 are similar to Gα proteins in other fungi, but Gpa4 seems distinct. It has been shown that Gpa3 is involved in MAPK and cAMP/PKA pathways. Deletion mutants of *gpa1*, *gpa2* and *gpa4* exhibit no phenotypic change; whereas the *gpa3* mutant shows various phenotypes including elongation of the cells, which are usually aggregated in liquid medium. In addition, *gpa3* mutants produce grey coloured colonies with short aerial filaments on a charcoal containing medium. Interestingly the *gpa3* mutants are defective for mating, tumour formation and fail to respond to pheromones (Garcia-Pedrajas *et al.*, 2008; Regenfelder *et al.*, 1997).

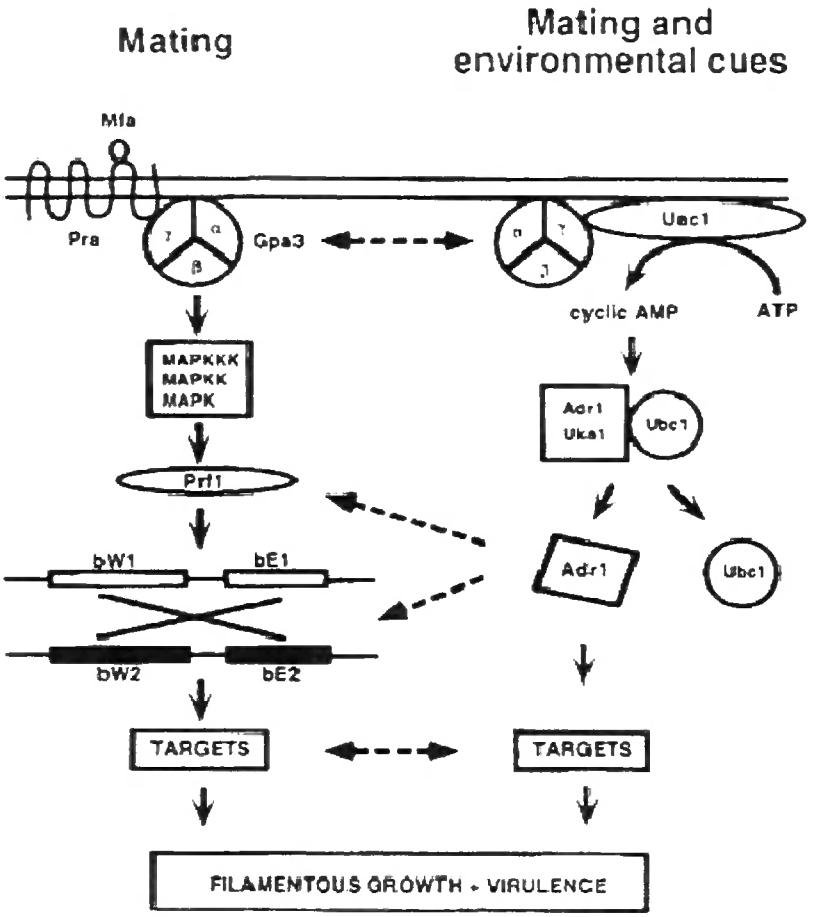

Figure 1.19.2.1 The pheromone response and cAMP signalling networks control mating, morphogenesis and virulence in *U. maydis*. In the pheromone signalling pathway the pheromone Mfa binds to the receptor Pra to activate the MAPK pathway via G protein Gpa3 and activation of the transcription factor Prf1. Prf1 increases the transcription of the other transcription factors bW1, bE1, bW2, bE2 (left side). In the cAMP pathway, Gpa3 activates adenylyl cyclase, then the major downstream molecule PKA catalytic subunit Adr1 is activated; in turn Adr1 phosphorylates downstream target transcription factors (Durrenberger *et al.*, 1998).

The gene encoding for Gβ *BPP1* has been cloned and encoded protein has the characteristic seven WD repeats. It has been suggested that Gpa3 and bpp1 are both components of the cAMP pathway. A *bpp1* deletion mutant shows filamentous growth in both liquid and solid medium. The mutants produced branched filaments and that are filled with cytoplasm. The Gβ mutant phenotype was suppressed by exogenous addition of cAMP (see fig. 1.19.2.2.). In addition, in the *bpp1* mutant, the expression of the pheromone induced gene *mfa* is completely suppressed. The *bpp*1 mutant can produce tumour in plant virulence studies, suggesting bpp1 is dispensable for virulence (Muller *et al.*, 2004).

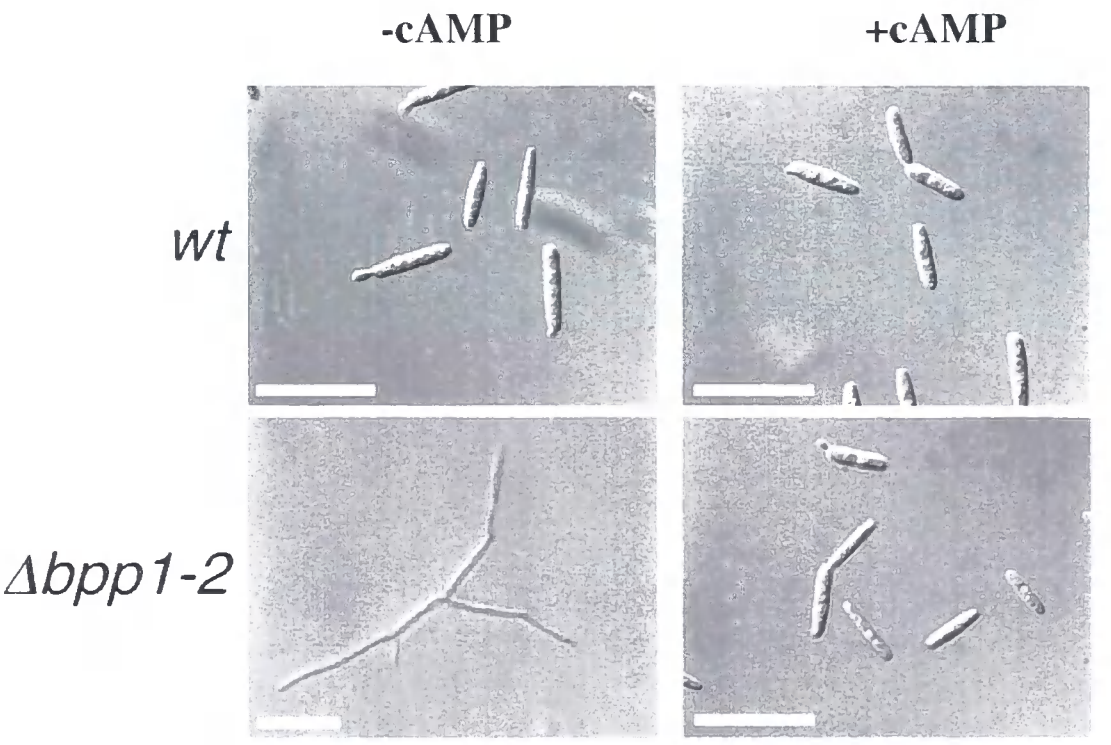

Figure 1.19.2.2 The Gβ *bpp1* mutant strain produces filamentous growth. *U. maydis* wild-type and Gβ *bpp*1 mutant were grown on Potato Dextrose liquid medium for 16 hours without cAMP (left side) and with 6 mM cAMP (right side). The Gβ mutant produced filamentous growth which was suppressed by exogenous cAMP (right side), scale bar: 20 μm (Muller *et al.*, 2004).

Recently *sep3* a gene encoding for septin was shown to be important for normal cell growth and budding. Early studies demonstrated that the PKA regulatory subunit *ubc1* mutant cannot separate the daughter cells from the mother cells (Gold *et al.*, 1994); similarly, a *sep3* mutant grows as a cluster of cells with multiple nuclei and the daughter cells cannot be separated from the mother cells. More recent studies of the *sep3* gene suggest that its expression may be promoted by PKA. Sep3 is also necessary for differentiation and germination of teliospores (Boyce *et al.*, 2005). Recently the gene has been identified is *fuz1* necessary for conjugation tube formation during the morphogenesis process (Chew *et al.*, 2008).

1.20 Glucose repression in yeast

In yeast, in the presence of glucose, the genes responsible for metabolizing other fermentable carbon sources, such as sucrose, maltose, galactose, and non fermentable carbon sources, such as ethanol, glycerol and acetate, are switched off at the transcriptional level in order to save energy; this is known as glucose repression (Ronne, 1995; Trumbly, 1992). The gene encoding for invertase which hydrolyses sucrose (*SUC2*) is the best studied glucose repressed system (Trumbly, 1992). The Snf1, Cat1 or Ccr1 have a vital role in the derepression of glucose repressed genes, because a *SNF1* deletion mutant cannot ferment carbon sources except glucose (Carlson, 1999; Papamichos-Chronakis *et al.*, 2004; Ronne, 1995).

1.20.1 Transcriptional repressors Tup1 (Thymidine Uptake) and Ssn6

In *S. cerevisiae*, the general transcriptional repressor *TUP1* has been cloned and characterised. The Tup1 protein seems to be rich in serine, threonine and, at the N-terminal glumatine (Williams and Trumbly, 1990). Tup1 is a phosphoprotein that contains WD40 repeats and each repeat has a different role in transcriptional repression. The N-terminus of Tup1 interacts with Ssn6; a mutation in N-terminal L62R abolishes the interaction (Carrico and Zitomer, 1998; Redd *et al.*, 1997). The N-terminal deleted *tup1* has a repressor function; moreover N-terminal deletion Tup1 cannot form a tetramer and remains as a monomer (Varanasi *et al.*, 1996). The N-

terminus has a α-helical coiled coil structure which helps Tup1 oligomerisation (Zhang *et al.*, 2002). It has been suggested that four Tup1 subunits forms a complex with one Ssn6 (4:1 ratio) (Varanasi *et al.*, 1996). Tup1 has six repeats of β-transducin domain in its C-terminal region (Williams and Trumbly, 1990).

SSN6 (*CYC8*) is a new family of genes encoding a protein containing 34 aa repeats called TPR motif (Tetratrico Peptide Repeat) (Goebl and Yanagida, 1991; Sikorski *et al.*, 1990). Cyc8 does not act as a functional repressor protein, despite the fact that it works as an adaptor between various DNA binding proteins (see fig.1.20.2.1) (Mig1 and Rox1) and Tup1 (Tzamarias and Struhl, 1994). The Ssn6 protein is rich in glutamine residues in both the N and C-terminus and does not contain conserved DNA binding domains (Trumbly, 1988).

Tup1 has been shown to repress several genes regulating various pathways, including the mating, oxygen use, glucose, DNA damage and stress response pathways (Wu *et al.*, 2001). The Tup1-Ssn6 co-repressor complex seems to regulate (repress) more than 150 genes in yeast. Cells deleted in this co-repressor complex can survive; however they show distinct phenotypes, such as flocculation, reduced sporulation, a mating deficiency in α strain and are deficient for glucose repression. In addition, the mutant take up thymidine from the medium, so it has been named as Tup1 (Thymidine Uptake), which is not seen in parental strains (Smith and Johnson, 2000).

1.20.2 Mig1, Ssn6-Tup1 complex in *S. cerevisiae*

MIG1 (Multicopy Inhibitor of *Gal1* gene expression) has been cloned and shown to be quite important in glucose repression. The major components of the glucose repression pathway are hexokinase PII (Hxk2, for glucose sensing), Snf1 kinase and the DNA binding repressor Mig1 (Klein *et al.*, 1998). Mig1 is a zinc finger protein and its localization is regulated by glucose. Mig1 is imported into the nucleus, in response to the addition of glucose (within a minute of addition of glucose in the medium), however, when glucose is removed from the medium it is exported back to the cytoplasm (De Vit *et al.*, 1997).

Mig1 has shown to be phosphorylated by Snf1 in response to a decrease in glucose; phosphorylation has a role in its subcellular localization and repression (De Vit *et al.*, 1997; Treitel and Carlson, 1995). Mig1 interacts with Ssn6 (Cyc8) in two hybrid assays (Treitel and Carlson, 1995). When glucose levels are high, Mig1 recruits the Ssn6-Tup1 co-repressor complex to bind to the promoter region of glucose-repressive genes in order to repress transcription (Klein *et al.*, 1998; Treitel and Carlson, 1995). In the absence of glucose Snf1 is activated and it phosphorylates Mig1; in turn phosphorylated Mig1 interacts with Msn5, which facilitates nuclear export of Mig1. This process results in the derepression of genes responsible for the utilization of alternative carbon sources (see fig. 1.20.2.1) (DeVit and Johnston, 1999). An *in vitro* experiment demonstrated that Ssn6-Tup1 complex represses transcription (Redd *et al.*, 1997).

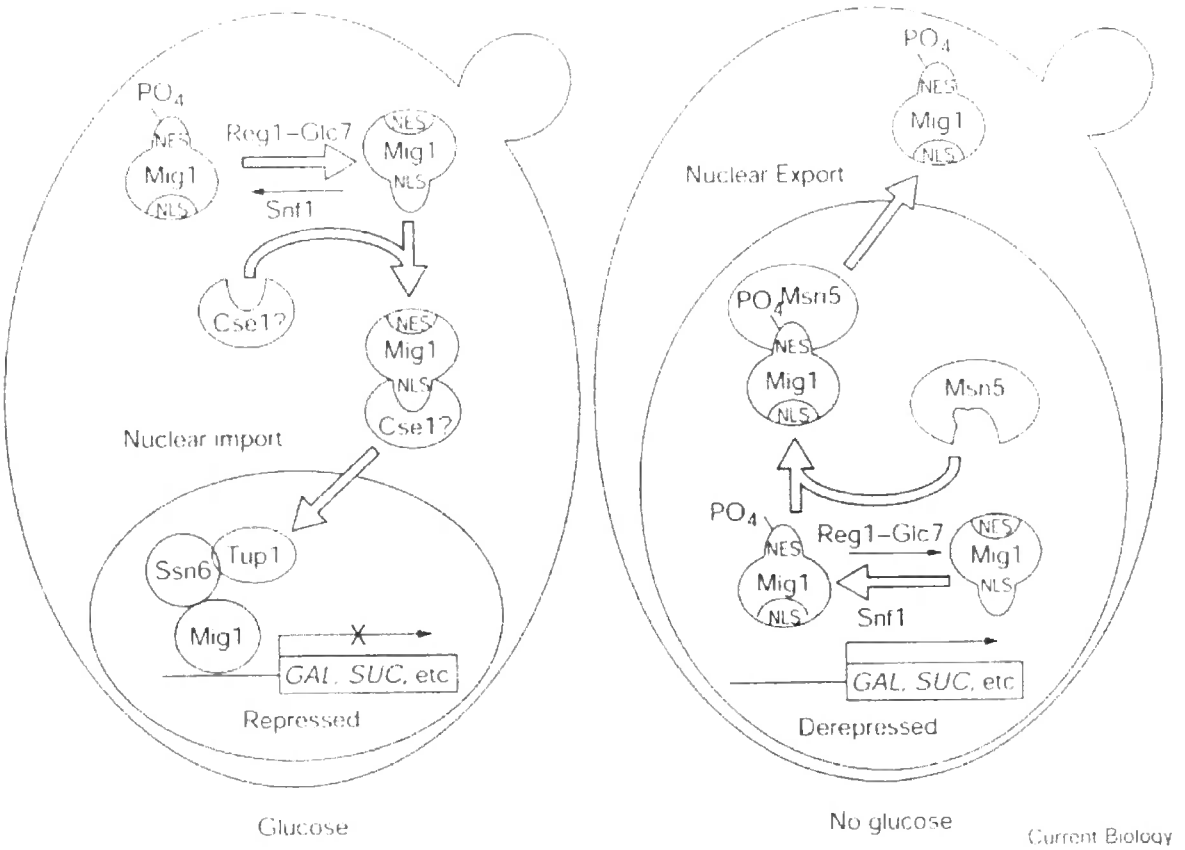

Figure 1.20.2.1 Mechanism of glucose repression in yeast. In the presence of glucose, Snf1 is inhibited and Reg1-Glc7 Phosphatase complex dephosphorylates the Mig1, which is then imported to the nucleus by Cse1 nuclear importin protein. Mig1 recruits Ssn6-Tup1 complex and binds to the promoter region of the genes to be repressed. In the absence of glucose, Snf1 is activated, in turn phosphorylates Mig1 which interacts with Msn5. Msn5 exports Mig1 from the nucleus to cytoplasm in order to relieve the repression (DeVit and Johnston, 1999).

In addition to glucose repression, the Mig1 Ssn6-Tup1 complex also represses mating (Ronne, 1995). An analysis of Tup1 showed that it has two non-overlapping transcriptional repression domains, with less similarity with one another, and has a separable binding site for Ssn6. It has been demonstrated that Tup1 can repress transcription without its partner Ssn6. Tup1 plays the main repressor function in the Ssn6-Tup1 complex and Ssn6 serves as a linker protein between Tup1 and specific DNA binding proteins (Ronne, 1995; Tzamarias and Struhl, 1994).

Gene sets repressed by Ssn6–Tup1	
Function	DNA binding protein
a-specific genes	α2/Mcm1
Haploid specific genes	a1/α2
Glucose-repressible genes	Mig1
DNA-damage-inducible genes	Crt1
Oxygen utilization genes	Rox1
Starch-degrading enzymes	Nrg1
Osmotic-stress-inducible genes	Sko1
Sporulation-specific genes	?
Meiosis specific genes	?
Flocculation genes	?

Table 1.20.2.2 Represents the list of DNA-binding proteins recruited by the Ssn6-Tup1 co-repressor complex for specific gene repression (Smith and Johnson, 2000).

1.20.3 Transcriptional activators

Snf/Swi (co-activators) is an extensively studied ATP-dependent chromatin remodelling nucleosome complex in *S. cerevisiae* (Kingston and Narlikar, 1999). This complex has been shown to control gene expression at the individual gene level rather than at the level of the whole chromosome. The Snf/Swi complex acts as an activator as well as repressor of transcription. In *S. cerevisiae*, only a certain number of genes have been shown to be controlled by this complex (Sudarsanam *et al.*, 2000).

1.21 Tup1 related to cAMP signalling pathway

It was previously demonstrated that Tpk2 can phosphorylate and interact with a heat shock factor-like repressor protein called Sfl1. Sfl1 binds to the promoter of *FLO11* and represses *FLO11* transcription, which is essential for pseudohyphal and invasive growth. This suggests that Tpk2 regulates Sfl1 (see fig. 1.16.1.1) (Pan and Heitman,

2002; Rupp *et al.*, 1999; Toda *et al.*, 1985). Further research has demonstrated that Sfl1 can also interact with Ssn6 within the TPR (Tetra trico peptide repeat) motif and suggests that Sfl1 recruits the Ssn6-Tup1 co-repressor complex to repress *SUC2*, *FLO11* and *HSP26*. These cumulative findings provide new insights into the relationship between Tup1 and the cAMP pathway (Conlan and Tzamarias, 2001).

1.22 Role of Tup1 in pathogenic fungi

In the human pathogenic fungus *Candida albicans* a Tup1 homologue has been identified, which seems to repress hyphal growth. Tup1 from *C. albicans* complements *S. cerevisiae tup1* mutant. A *TUP1* deletion mutant shows constitutively filamentous growth in *C. albicans*. In addition, the mutants grow faster with a higher accumulation of glycerol than wild type. It has been suggested that CaTup1 is different from ScTup1 in controlling gene expression because Ca*tup1* and Sc*tup1* mutants do not display the same phenotypes (Braun and Johnson, 1997; Brown and Gow, 1999). A negative regulator of growth, CaNrg1 has been suggested as a strong repressor that binds to the global co-repressor Tup1 and this complex inhibits filamentous growth. Serum is an inducer of germ tube and suggest that serum suppresses the repressor function of Nrg1 (see fig. 1.22.1) (Murad *et al.*, 2001).

It has recently shown that farnesol treated *C. albicans* display higher expression of Tup1 and also suggests that Tup1 is involved in farnesol mediated repression of growth (Kebaara *et al.*, 2008). The analysis of Ssn6 reveals that it has both activator and repressor functions because overexpression of Ssn6 causes enhanced filamentous growth and reduced virulence (Hwang *et al.*, 2003). Further studies have shown that Ssn6 may act independent of the Nrg1-Tup1 repressor complex. Hypha specific genes are repressed by Nrg1-Tup1 and this repression is not released in Ssn6 mutant cells. Nrg1 and Ssn6-Tup1 mediated repression takes place at some promoters, but in most other promoters, repression is by Nrg1-Tup1 (Garcia-Sanchez *et al.*, 2005). A recent report revealed that Swi1 acts as an activator and Tup1 acts as a repressor of growth (Mao *et al.*, 2008).

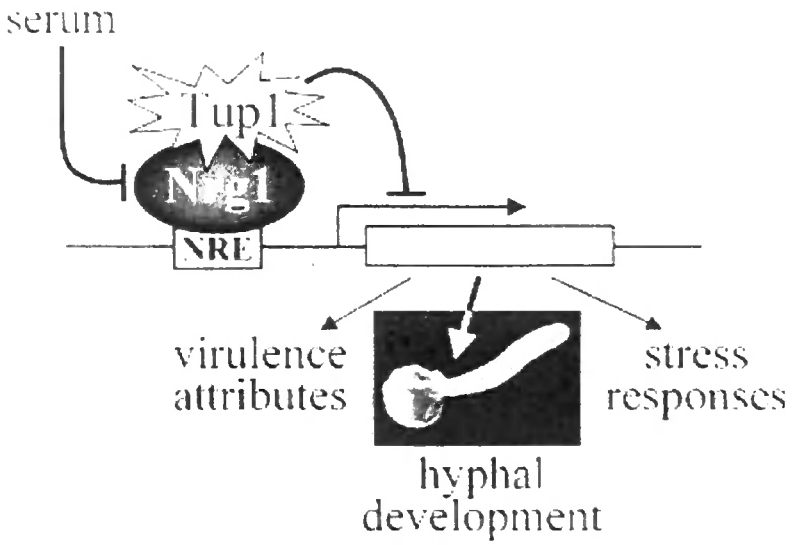

Figure 1.22.1 The mechanism of Nrg1-Tup1 mediated repression in *C. albicans*. Nrg1-Tup1 transcription of repression complex binds to the NRE site on the promoter and represses the genes regulating growth. Factors in serum down-regulate the Nrg1 level and release the repression (Murad *et al.*, 2001).

1.23 Aims and objectives

The aim of this study is to extend the level of understanding of the cAMP pathway in *Paracoccidioides brasiliensis* and elucidate its role in controlling the morphological transition from the saprobic mycelium to pathogenic yeast form of the fungus in order to identify potential drug targets.

The objectives of this study are as follows

1. To confirm the G protein interactions in the cAMP-signalling pathway, previously identified by yeast two-hybrid analyses, by conducting *in vitro* protein–protein interaction studies.

2. To measure intracellular cAMP levels during the mycelium to yeast transformation, so as to determine if these correlate with the changes in transcript numbers for adenylate cyclase and the G proteins with which it interacts.

3. To extend the yeast two-hybrid analyses to the Protein Kinase A (PKA) catalytic subunit Tpk1 and Tpk2; and, in particular, to determine if Tpk acts as a scaffold for assembly and control of the transcriptional complex.

4. To overexpress Tpk2 in *E. coli* for functional PKA assays, aimed at defining the phosphorylation targets of Tpk2. We are particularly interested in determining if the Gβ protein Gpb1 is a target for PKA phosphorylation, since this protein appears to play a key role in controlling the morphological switch.

5. To identify and characterize transcription factors and other components of the cAMP pathway that are downstream targets of PKA and are involved in the morphological switch of this fungus.

6. To undertake a functional characterisation of Pb Tpk1 and Tpk2 in *S. cerevisiae* *tpk2* mutants by PKA complememtation assays.

CHAPTER TWO

Materials and Methods

2.1. Computational methods

This thesis was written using Microsoft (MS) Office Word and graphical data were created by MS Excel program. Adobe Photoshop and MS office picture manager were used for the enhancement of the images and modification of diagrams. Vector NTI suite (Invitrogen) was used for mapping, analysis and alignments of DNA and protein sequences. http://www.promega.com/biomath/ was used for oligonucleotides design and Tm value calculations. http://db.yeastgenome.org/cgi-bin/locus was used to obtain the Sequence of *S. cerevisiae* Tpk1-3. Smart Analysis website; http://smart.embl-heidelberg.de/ was used to analyze the protein domains. Broad Institute website, http://www.broad.mit.edu/ was used for the Blast analysis with fungal database. http://www.candidagenome.org/ was used to acquire *C. albicans* Tpk2 sequence. The National Center for Biotechnology Information website (NCBI, http:// ncbi.nlm.nih.gov) was used frequently for downloading the reference journals and the ExPASy tools on this web site were used for translation. Blast searches and alignment of nucleotides and protein sequences. The complete p426 Vector sequence was obtained from seq.yeastgenome.org/vectordb/vector_descrip/COMPLETE/PRS426.SEQ.

2.2. Laboratory equipment

2.2.1. Sterilization

Laboratory glass ware and media were autoclaved in a Priorclave Tactrol 2 on a liquid cycle at 121°C for 15 minutes. Heat labile solutions such as antibiotics, DMSO (Dimethyl Sulfoxide), α-X-gal and PEG (poly ethylene glycol) and were filter-sterilized through 0.22 μm membranes (Millipore).

2.2.2 Centrifugation

Table 2.2.2.1 Centrifugation equipment used

Centrifuge	Rotor	Applications	Max Speed (rpm)	Temperature
Eppendorf bench top 5415D	F-45-24-11	1.5 ml & 0.5 ml microfuge tubes; various applications	13,000	RT
Jouan CR3i	T20	20 ml & 50 ml centrifuge tubes; various applications	4,100	4°C to RT
Sigma 3-16K	11180	20 ml & 50 ml centrifuge tubes; various applications	4,500	4°C to RT
Beckman Coulter Avanti J20-XP	JLA-8.1000	1 litre; cells harvesting	8,000	4°C to RT
Beckman Coulter Avanti JE	JA-10 JA-20	450 ml; cells harvesting; 40 ml tubes; pelleting cell debris	10,000 20,000	4°C to RT
Beckman L8-70M Ultracentrifuge	Type 50.2 Ti	22 ml ultracentrifuge tubes; pelleting cell membrane for Protein purification	50,000	4°C to RT

RT–Room Temperature

2.3. Bacterial Strains and Plasmids

Experimental procedures detailed have been followed according to Sambrook *et al.*, (1989) or as per manufacturers' instructions.

The bacterial strains and plasmids used in this study are listed below (2.3.1).

Table 2.3.1 Bacterial Strains and Plasmids

E. coli **Strains**	**Description/Genotypes**	**Source/Reference**
NovaBlue	K-12 strain with high transformation efficiency; blue/ white screening capability (with pGEM-T), *recA* and *endA* mutations resulting in high yields of quality plasmid DNA.	Novagen
BL21(DE3)	Deficient in *lon* & *ompT* proteases, general expression host.	Novagen
BL21(AI)	Deficient in *lon* & *ompT* proteases, general expression host; induced by the addition of arabinose.	Invitrogen
M15	Host strain for regulated high level expression for pBAD vectors.	QIAgen
LMG194	High level expression for toxic proteins (pBAD vectors).	Invitrogen
Top 10	*ara* mutant; host for general purpose cloning and plasmid propagation for pBAD vectors and pPICZ A vectors.	Invitrogen
Rosetta 2	Lactose permease mutant, deficient in *lon* and *ompT* proteases; Provides 7 rare tRNAs; eukaryotic protein expression host.	Novagen
Origami (DE3)	Strains carry *trxb* and *gor* mutations in the cytoplasmic disulfide reduction pathway; enhance disulfide bond formation in *E. coli* cytoplasm.	Novagen
BL21(DE3) STAR	RNaseE (*rne131*) mutant; general purpose expression host with reduced mRNA degradation.	Invitrogen

BL21(DE3) Codon plus	Deficient in *lon* and *ompT* proteases; allows expression of genes encoding tRNAs for rare argenine and proline codons.	Stratagene
BL21(DE3) PLysS	Deficient in *lon* and *ompT* proteases; high- stringency expression host.	Stratagene
DH5α	Non-expression host; general purpose cloning; plasmid propagation.	Life Technologies

Table 2.3.2 Commercial Plasmids and donated constructions

Plasmid	Description	Source/Reference
pGEM-T Easy	Cloning vector compatible with α-complementation; high copy number plasmid with Ampicillin resistance (Amp^R); TA cloning	Novagen
pET21a (+)	T7 *lac* expression vector for C-terminal His_6-tagged proteins. Amp^R	Novagen
pET21d (+)	T7 *lac* expression vector for C-terminal His_6- tagged proteins. Amp^R	Novagen
pQE-100	Derivative of MAP Kinase; tag-100; His_6-Tag; T5 promoter; Amp^R	QIAgen
pGEX6p-1-3	26 kDa N-terminal Glutathione S-transferase (GST) tag; *tac* promoter; cleaved by PreScission protease; Amp^R	GE Healthcare, Kindly supplied by Dr G Sharples
pBAD Myc His A	Arabinose inducible vector; Amp^R	Invitrogen
pET431a(+)	Protein expression; N-terminal Nus-A fusion; N-terminal & C-terminal His-tag; Amp^R	Novagen
pDNR-Lib	Pb01 cDNA library; Amp^R	Clontech, Dr Chen D. library construct (PhD thesis, 2006)

pGADT7-Lib	*Pb*01 cDNA library; Amp^R	Constructed by Chen G. (Chen D *et al.*, 2007)

2.4 Yeast Strains and Plasmids

Table 2.4.1 Yeast Strains

Strains	Description/Genotype	Source/Reference
Paracoccioides brasiliensis	Dimorphic, yeast form-37°C (requires Cys or Met as supplement and mycelial form-25°C (none required)	ATCC 90659
AH109	*MATa, trp1-901, leu2-3, 112, ura3-52, his3-200, gal4Δ, gal80Δ, LYS2 : : GAL1UAS-GAL1TATA-HIS3, GAL2UAS-GAL2TATA-ADE2, URA3 : : MEL1UAS-MEL1 TATA-lacZ*	Clontech
SGY446	*MATα tpk1Δ::ADE8 tpk2-63*(Ts) *tpk3::TRP1 BCY1 ura3-52 his3 leu2-3,112 trp1 ade8* PKA complementation assay.	Kindly supplied by Dr Claudio, Switzerland (Smith *et al.*,1998)
MLY61**a**/α	*ura3-52/ura3-52 MAT***a**/α; wild type; PKA complementation assay.	Pan X & Heitman (1999). (kindly supplied by Dr Joseph Heitman, USA)
XPY5**a**/α	Δ*tpk2::G418*/Δ*tpk2:: G418 ura3-52/ ura3-52 MAT***a**/α; PKA complementation assay.	Pan X & Heitman (1999). (Kindly supplied by Dr Joseph Heitman, USA)
GS115	*his4*	Kindly supplied by Dr P Yeo (Invitrogen)
KM71H	arg4 his 4 aox1::ARG4	Kindly supplied by Dr P Yeo (Invitrogen)

Table 2.4.2 Yeast Expression Plasmids

Plasmids	Descriptions/ Application	Source/reference
p426 MET25	Yeast expression vector; inducible by methionine starvation; *MET25* promoter; yeast complementation assay; Amp^R	(Mumberg *et al.*, 1994) Kindly supplied by Dr P Denny
pGADT7 (AD fusion)	Vector with Gal-4 activation domain; expressed at high level from the constitutive *ADH1* promoter; cloning vector for Two-hybrid assay; Amp^R	Clontech
pGBKT7 (BD)	Vector with Gal-4 binding domain; expressed at high level from the constitutive *ADH1* promoter; cloning vector for two-hybrid assay; Kan^R	Clontech
pGBKT7 Lamin	Vector with Gal-4 binding domain; expressed at high level from the constitutive *ADH1* promoter; negative control vector for two-hybrid assay; Kan^R	Clontech
pGADT7 Tag	Vector with Gal-4 activation domain; expressed at high level from the constitutive *ADH1* promoter; positive control vector for two-hybrid assay. Amp^R	Clontech
pGBKT7 P^{53}	Vector with Gal-4 binding domain; expressed at high level from the constitutive *ADH1* promoter; positive vector for two-hybrid assay; Kan^R	Clontech
pPICZ A	Cloning and expression vector for *Pichia pastoris; AOX* promoter. $Zeocin^R$	Kindly supplied by Dr P Yeo (Invitrogen)
pPIC9	Cloning and secretion expression vector for *Pichia pastoris;* α-factor signal sequence; *AOX* promoter; Amp^R	Kindly supplied by Dr P Yeo (Invitrogen)

2.5 Antibiotics and Reagents

Table 2.5.1 Antibiotics and Reagents

Antibiotics/ Reagents	Stock concentration	Storage condition	Working concentration
Ampicillin (Amp)	100 mg/ml	-20°C	100 μg/ml
Carbenicillin	100 mg/ml	-20°C	100 μg/ml
Chloramphenicol	30 mg/ml in 95% ethanol	-20°C	30 μg/ml
Kanamycin (Kan)	30 mg/ml	-20°C	30 μg/ml
Tetracycline	30 mg/ml	-20°C	30 μg/ml
Zeocin	25-100 mg/ml	-20°C	25 μg/ml for bacteria and 100 μg/ml for yeast
IPTG	100 mg/ml	-20°C	100 μg/ml
X-GAL	20 mg/ml in N,N-dimethyl formamide	-20°C	50 μl spread on to 90 mm plate
α-X-GAL	4 mg/ml in N,N-dimethyl formamide	-20°C	
ONPG	4 mg/ml in Z-buffer	Made fresh	
RNase A	10 mg/ml	-20°C	
DNase-I	1000 units/ml	-20°C	
Lyticase	100 mg/ml TE pH 7.5	-20°C	
L-Arabinose	20% in distilled H_2O	-20°C	0.02-0.2% (v/v)

2.6 Microbial Growth Media

All general media, chemicals, antibiotics and biological chemicals were purchased from Sigma, Melford, Fluka, BDH, Clontech and Merck. Microbiological growth medias were ordered from Oxoid, Difco and Clontech. Enzymes were obtained from Promega and New-England biolabes. Complete EDTA free protease inhibitor tablets were purchased from Roche Biochemicals.

Liquid and agar media used for culturing *E. coli* and *S. cerevisiae* were as follows:

Luria-Bertani (LB) Medium (Mu)

NaCl	10g/litre
Tryptone	10g/litre
Yeast extract	5g/litre

LB Agar

NaCl	10g/litre
Tryptone	10g/litre
Yeast extract	5g/litre
Agar	15g/litre

SOC Medium

NaCl	0.585g/litre
KCl	0.1865g/litre
Tryptone	20g/litre
Yeast extract	5g/litre

The above were autoclaved and the following filter-sterilized components were added:

1 M $MgCl_2 \cdot 6H_2O$	10 ml
1 M $MgSO_4$	10 ml

NZY$^+$ Medium

NZ amine (casein hydrolysate)	10g/litre
Yeast extract	5g/litre
NaCl	5g/litre

Medium adjusted to pH 7.5 using NaOH, autoclaved and the following filter-sterilized components added:

1 M $MgCl_2$	12.5 ml
1 M $MgSO_4$	12.5 ml
20% (w/v) glucose	20 ml

2x Yeast Tryptone (2x YT) Medium

NaCl	5g/litre
Tryptone	16g/litre
Yeast extract	10g/litre

RM Medium

Casamino acids	20g/litre
Glucose	2g/litre

The above were autoclaved and the following filter-sterilized components were added:

1 M $MgCl_2 \cdot 6H_2O$	1 ml
10x M9 Salts*	100 ml

<u>10xM9 Salts</u>

Na_2HPO4	60g/litre
KH_2PO_4	30g/litre
NaCl	5g/litre
NH_4Cl	10g/litre

Medium adjusted to pH 7.4 using 1 M NaOH, autoclaved and the following filter-sterilized component was added:

1 M Thiamine	1 ml/litre

ATCC medium for *P. brasiliensis*

Sabouraud Dextrose Broth	30g/litre
Agar	20g/litre
Distilled water	1000 ml

Adjusted pH 6.8-7.0.

YPD broth

Bacto-yeast extract	10g/litre
Peptone	20g/litre
Distilled water	900 ml pH -5.8

After autoclaving, 100 ml of 20% glucose was mixed.

YPD Agar

Bacto-yeast extract	10g/litre
Peptone	20g/litre
Distilled water	900 ml pH -5.8
Agar powder	20g/litre

After autoclaving, 100 ml of 20% glucose was mixed.

SLAD Agar (Synthetic Low Ammonium Dextrose)

Yeast nitrogen base	1.7g/litre (0.17%)

(without amino acids & ammonium sulfate)

Dextrose	20g/litre
Agar	20g/litre

500 μl of 100 mM ammonium sulfate was added to 1 litre to achieve 50 μM concentration. Ammonium sulfate stock 1.3214g/100 ml to make 100 mM solution and autoclaved separately.

SD Minimal Synthetic Dropout medium

SD base was purchased from Clontech, which comprised of nitrogen base, carbon source (glucose) and dropout supplement were added separately.

SD base	26.7g/litre
Agar	20g/litre

Dropouts (DO) (Clontech)

-Ura	0.77g/litre
-Trp-Leu-His-Ade	0.60g/litre
-Trp-Leu-His	0.62g/litre
-Trp-Leu	0.64g/litre

10x TE buffer/litre

	Stock	Required volume
10 mM Tris-Hcl	1 M	10 ml
1 mM EDTA	0.5 M	2 ml pH 7.5

2.7 Procedures

2.7.1 PCR Techniques (Polymerase Chain Reactions)

The PCR techniques were used to sub-clone the gene from the *Pb* cDNA library for the construction of plasmids.

Table 2.7.1.1 The PCR systems

PCR systems (DNA polymerases)	Applications	Comment	Source
Proofstart	Cloning for protein expression	High fidelity, 3'-5' exonuclease activity: blunt ended PCR product	QIAgen
Hotstart Taq	TA Cloning for smaller DNA	No 3'-5' exonuclease activity	QIAgen
AB gene Master Mix	Library screening	For amplifing large fragments; high fidelity	ABgene
Go Taq	Colony PCR screening	No proof reading activity	Promega

Proofstart reaction

Table 2.7.2 A general reaction with proofstart is described below

Reaction components	Final concentration
10x PCR buffer	1x
5x Q solution	1x
dNTPs (10 mM each)	200 μM
Forward primer (50 μMol)	0.3-0.5 μM
Reverse primer (50 μMol)	0.3-0.5 μM
Proofstart DNA polymerase	1 μl/1Kb DNA
Template cDNA library	0.5-1 μg/reaction
Total reaction volume	Made up to 50 μl

Cycling parameters

Initial denaturation	95°C	5 minutes
Denaturation	94 °C	10 seconds
Annealing temperature	55-68 °C	30 seconds
Extension temperature	72 °C	1 minute/reaction
35 cycles		
Final extension	72 °C	10 minutes
Indefinite	4 °C	

2.8 Oligonucleotides for PCR

Oligonucleotide primers were ordered online and synthesized by Invitrogen. Primers were reconstituted in sterile distilled water to a stock concentration of 50 μmole/μl and stored at -20°C.

Primers used in this thesis (The restriction sites are underlined)

Table 2.8.1 Primers for the constructions for two-hybrid assay

Constructions	primers
pADT7 *TPK2*$^{226-583}$	For *Eco*RI 5′ GAATTCATTCACAGCATCCACAGCAACAACAACAC 3′ Rev XhoI 5′ CTCGAGTCAAAAGTCCACGAAATAATCGCCATATGG 3′
pBKT7 *TPK2*$^{226-583}$	For *Nco*I 5′ CCATGGGCCATTCACAGCATCCACAGCAACAACAAC 3′ Rev *Bam*HI 5′ GGATCCAAAGTCCACGAAATAATCGCCATATGGATC 3′
pADT7 *TPK2*$^{1-270}$	For *Nco*I 5′ CCATGGAACGGGGTCTAGGCAATTTGCTGAAGAAG 3′ 1F Rev *Bam*HI 5′ GGATCCTTACGAGTATTTGCCCTTTGTCTG CCGC3′ 1R
pADT7 *TPK2*$^{1-583}$	For *Nco*I 5′ CCATGGAACGGGGTCTAGGCAATTTGCTGAAGAAG 3′1F Rev *Bam*HI 5′ GGATCCTTAAAAGTCCACGAAATAATCGCCATATGGATCATC 3′2R
pADT7 *TPK2*$^{265-583}$	For *Nco*I 5′ CCATGGAAACAAAGGGCAAATACTCGCTAGATGACTTTACG′ 3F Rev *Bam*HI 5′ GGATCCTTAAAAGTCCACGAAATAATCGCCATATGGATC 3′2R
pADT7 *GPG1*	For *Nco*1 5′ CCATGGAAGCCCCTGCCTACGAGCTTCGACCC 3′ Rev *Bam*H1 5′ GGATCCTTACATGATCATACAGCAGCCACCTGATTGTTGGGG 3′
pBKT7 *Pb* *TPK2*$^{1-270}$	For *Nco*I 5′ CCATGGAACGGGGTCTAGGCAATTTGCTGAAGAAG 3′ 1F Rev *Bam*HI 5′ GGATCCTTACGAGTATTTGCCCTTTGTCTGCCGC 3′ 1R
pBKT7 *TPK2*$^{1-583}$	For NcoI 5′ CCATGGAACGGGGTCTAGGCAATTTGCTGAAGAAG 3′1F Rev Rev *Bam*HI 5′ GGATCCTTAAAAGTCCACGAAATAATCGCCATATGGATC 3′ 2R
pBKT7 *TPK2*$^{265-583}$	For NcoI 5′ CCATGGAAACAAAGGGCAAATATCGCTAGATGACTTTACG 3′ 3F Rev *BamHI* 5′ GGATCCTTAAAAGTCCACGAAATAATCGCCATATGGATC 3′2R
ADT7 *TPK2* & BKT7 *TPK2*$^{1-174}$	For *Nco*I 5′ ATAATACCATGGAACGGGGTCTAGGCAATTTGCTG 3′ Rev *Bam*HI 3′ ATAATAGGATCCTTATTTGAAATGAGAGGGATCGCCCG 3′
pBKT7 *GPG1*	For *Nco*I 5′ CCATGGAAGCCCCTGCCTACGAGCTTCGACCC 3′ Rev *Bam*HI 5′ GGATCCTTACATGATCATACAGCAGCCACCTGATTGTTGGG 3′
pGADT7 & pGBKT7 *TUP 1*	For *Nco*I 5′ ATACTACCATGGGTATGTATAACCCACACCGTGGTATGGTTA 3′ Rev *Sma*I 5′ ATACTACCCGGGTGACCTTCTGGGATCCAATTG 3′

Table 2.8.2 Oligos for protein expression in yeast

p426 MET25 *GFP*	For *Eco*RI 5′ CATATGAATTCATGGTGAGCAAGGGCGAGGAGCTGTTC 3′ Rev *Sal*I 5′ ATATAGTCGACTTACTTGTACAGCTCGTCCATGCCGAGAGTG 3′
p426 MET25 *TPK2*$^{1\ 225}$_ GFP	For *Bam*HI 5′ AATATGGATCCATGCGGGGTCTAGGCAATTTGCTGAAG3′ Rev *Eco*RI 5′ ATAATGAATTCTCGTTGTTGTGCGGCATGTAGGCCATC 3′
p426 MET25 *TPK2*$^{226\text{-}583}$_ GFP	For *Bam*HI 5′ CATATGGATCCATGCATTCACAGCATCCCAGCAACAACAAC 3′ Rev *Eco*RI 5′ CTCCTGAATTCAAAGTCCACGAAATAATCGCCATATGGATC 3′
p426 MET25 *GPB-GFP*	For *Bam*HI 5′ ATACATGGATCCATGGCGGCCGATTTGAGCG 3′ Rev *Hin*dIII 5′ ATCTCTAAGCTTCCATGCCCAGACCTTGAGCAG 3′
p426 MET25 *TPK2*$^{1\ 583}$	For *Bam*HI 5′ ATTATAGGATCCATGCGGGGTCTAGGCAATTTG 3′ Rev *Eco*RI 5′ CTCCTGAATTCTTAAAAGTCCACGAAATAATCGCCATATG 3′
p426 MET25 *GFP*	For *Hin*dIII 5′ CATATAAGCTTATGGTGAGCAAGGGCGAGGAGC 3′ Rev *Sal*I 5′ ATATAATCGATTTACTTGTACAGCTCGTCCATGCCGAGAGTG 3′
p426 MET25 *TPK1*$^{135\text{-}560}$-*GFP*	For *Bam*H1 5′ ATAATAGGATCCATGGCCGCGGAAACGATAC 3′ Rev *Hin*dIII 5′ CTACTCAAGCTTAAAATCCGCAAACATAGCATCATGC 3′
ADT7 & BKT7 *TPK1*$^{135\ 560}$	For *Nco*I 5′ ATAATACCATGGAAATGGCCGCGGAAACGATAC 3′ Rev *Bam*HI 5′ ATAATCGGATCCTCAAAAATCCGCAAACATAGCATCATG 3′

Table 2.8.3 Adenylate cyclase (Cyr1) overexpression in *E. coli*

pGEX6p-3*CYR1*$^{453\ 505}$	For *Bam*HI 5′ AAGGATGGATCCGATAAAACCCATCAGGATAACTTTG 3′ Rev *Sal*I 5′ ATAATCGTCGACTTAATGTTCCGGCAGCGG 3′
pGEX6p-3*CYR1*$^{453\ 678}$	For *Bam*H1 5′ AAGGATGGATCCGATAAAACCCATCAGGAT 3′ Rev *Not*I 5′ CATATCGCGGCCGCTTAGTGGCTAAACTTTTGGTTCTCGTTG 3′
pGEX6p-3 *CYR1*$^{1\ 678}$	For *Bam*HI 5′ATAATCGGATCCATGGCAAGGAGACAGCGGGAGAAAG 3′ Rev *Not*I 5′ CATATCGCGGCCGCTTAGTGCTAAACTTTTGTTCTCGTTG 3′
pBAD cMyc His A *CYR1*$^{1\text{-}678}$	For *Nco*I 5′CCATGGAAGCAAGGAGACAGCGGGAGAAAGATAG 3′ Rev *Hin*dIII 5′ AAGCTTAGGAATTCGGTTTGACAGACTCCGCTCCG 3′

Table 2.8.4 Oligos for G protein overexpression in *E. coli*

pBAD cMycHis A *GPA1*	For *Kpn*I 5' ATAATAGGTACCATGGGGTGTGGAATGAGCACCGAG 3' Rev *Eco*RI 5' CTAATAGAATTCCATATCAGTCCACAGAGGGAAGGTTGTCC 3'
pET431a(+)*GPA1*	For *Eco*RI 5' GAATTCGGGTGTGGAATGAGCACCGAGGACAAGG 3' Rev *Hin*dIII 5' AAGCTTTATCAGTCCACAGAGGCGAAGGTTGTCCTG 3'
pET21a(+)*GPA1*	For *Eco*RI 5' GAATTCGGGTGTGGAATGAGCACCGAGGACAAGG 3' Rev *Hin*dIII 5' AAGCTTTATCAGTCCACAGAGGCGAAGGTTGTCCTG 3'
pGEX6p-1 *GPA1*	For *Eco*RI 5'GAATTCGGGTGTGGAATGAGCACCGAGGACAAGG 3' Rev *Not*I 5' ATACTAGCGGCCGCTCATATCAGTCCACGAGGC 3'
pET21a(+)*GPB1*	For *Nde*I 5' CATATGGCGGCCGATTTGAGCGGCGAGCAAATGCAG 3' Rev *Bam*HI 5' GGATCCCCATGCCCAGACCTTGAGCAGAGAATCCC 3'
pET21d(+)*GPB1*	For *Nco*I 5' CCATGGAAGCGGCCGATTTGAGCGGCGAGCAAATG 3' Rev *Hin*dIII 5' AAGCTTCCATGCCCAGACCTTGAGCAGAGAATCCC 3'
pET431a(+)*GPB1*	For *Bam*HI 5' GGATCCGCGGCCGATTTGAGCGGCGAG 3' Rev *Hin*dIII 5' AAGCTTCCATGCCCAGACCTTGAGCAGAGAATCCC 3'
pGEX6p-3 *GPB1*	For *Bam*HI 5' ATACATGGATCCATGGCGGCCGATTTGAGCGGCG 3' Rev *Not*I 5' ATATCTGCGGCCGCCTACCATGCCCAGACCTTG 3'
pET431a(+)*GPG1*	For *Bam*H1 5' GGATCCGCCCCTGCCTACGAGCTTCGACCC 3' Rev *Xho*I 5' CTCGAGCATGATCATACAGCAGCCACCTGATTGTTGGGG 3'
pGEX6p-3 *GPG1*	For *Bam*HI 5' ATCTATGGATCCATGGCCCCTGCCTACGAGCTTCG 3' Rev *Not*I 5' ATCTATGGATCCATGGCCCCTGCCTACGAGCTTCG 3'

Table 2.8.5 Oligos used for putative *Pb* Tpk2 protein overexpression in *E. coli*

pGEX6p-3 *TPK2*$^{1-583}$	For *Bam*HI 5′ GGATCCCGGGGTCTAGGCAATTTGCTGAAGAAG 3′ Rev *Sal*I 5′ GTCGACTTAAAAGTCCACGAAATAATCGCCATATGGATCATCC 3′
pGEX6p-3 *TPK2*$^{1-225}$	For *Bam*HI 5′ ATTATAGGATCCATGCGGGGTCTAGGCAATTTGCTGAAG 3′ Rev *Sal*I 5′ ATAATAGTCGACTTATCGTTGTTGGCGGCATGTAGGCC 3′
pPICZA *TPK2*$^{1-583}$	For *Kpn*I 5′ AATATAGGTACCATGCGGGGTCTAGGCAATTTGCTGAAG 3′ Rev ApaI 3′ CATATAGGGCCCAAAGTCCACGAAATAATCGCCATATGGATC 3′
pPIC9 *TPK2*$^{1-583}$	For *Eco*RI 5′ ATATCGAATTCATGCGGGGTCTAGGCAATTTGCTGAAGAAG 3′ Rev *Not*I 5′ ATATAGCGGCCGCAAAGTCCACGAAATAATCGCCATATG 3′
pET21d(+)*TPK2*$^{226-583}$	For *Nco*I 5′ CCATGGGACATTCACAGCATCCACAGCAACAAC 3′ Rev *Xho*I 5′ CTCGAGAAAGTCCACGAAATAATCGCCATATG 3′
pGEX6p-3 *TPK21*$^{528-583}$	For *Bam*HI 5′ ATATTAGGATCCGCGGAGGTGACGTGGGATC 3′ Rev *Sal*I 5′ ATCCTCGTCGACTTAAAAGTCCACGAAATAATCGCCATATGG 3′
pGEX6p-3 *TPK21*$^{272-511}$	For *Bam*HI 5′ ATAGGATCCTTTACGTTGCAACGGACGTTGGGGACG 3′ Rev *Sal*I 5′ AATGTCGACTTACAGGCGTACTGTGAGATCGGGAGTAATG 3′
pBAD Myc His A *TPK2*$^{1-583}$	For *Nco*I 5′ CCATGGACGGGGTCTAGGCAATTTGCTGAAGAAG 3′ Rev *Hind*III 5′ AAGCTTAAAGTCCACGAAATAATCGCCATATGGATCATC 3′
pGEX6P-3 *TPK2*$^{226-528}$	For *Bam*HI 5′ CATATGGATCCATGCATTCACAGCATCCACAGCAACAACAAC 3′ Rev *Sal*I 5′ CTAATAGTCGACTTAAAACCACGGATGATCCTTAACATCC 3′
pGEX6P-3 *TPK2*$^{152-271}$	For *Bam*HI 5′ ATAATAGGATCCATGAACCCCCTACATTCTCCCGGC 3′ Rev *Sal*I 5′ CTACTAGTCGACTTAGTCATCTAGCGAGTATTTGCCCTTTG 3′

pQE 100 *TPK2*$^{226-583}$	For *Bam*HI 5' AAGGATCCCATTCACAGCATCCACAGCAACAAC 3' Rev *Sac*I 5' TAGAGCTCAAAGTCCACGAAATAATCGCCATATG 3'
pET-43.1a(+)*TPK2*$^{226-583}$	For *Bam*HI 5' GGATCCCATTCACAGCATCCACAGCAAC 3' Rev *Xho*I 5' CTCGAGAAAGTCCACGAAATAATCGCCATATG 3'

Table 2.8.6 Oligos for Tup1 overexpression in *E. coli*

pET21d(+) *TUP1*	For *Nhe*I 5' ATACTAGCTAGCTATAACCCACACCGTGGTATGGTTAC 3' Rev *Xho*I 5' ATAATACTGGAGCCTTCTGGGATCCCAATTGGAATAGC 3'

Table 2.8.7 Universal primers

AOX primers	Forward 5' GACTGGTTCCAATTGACAAGC 3' Reverse 5' GCAAATGGCATTCTGACATCC 3'
M13 primers	Forward 5' GTAAAACGACGGCCAG 3' Reverse 5' CAGGAAACAGCTATGAC 3'
T7 sequencing	Promoter 5' TAATACGACTCACTATAGGGC 3'

2.9. Agarose gel electrophoresis

DNA agarose gel electrophoresis was routinely performed as described in Sambrook *et al.*, 1989. 1x TAE buffer was used (40 mM Tris-acetate, 1 mM EDTA).

10X TAE

Tris-base	48.4g/Litre
Glaceial acetic acid	11.4 ml/litre
EDTA	9.3g/litre

2.10. Cloning procedures

Plasmid mini preparations were performed with Plasmid miniprep kit (Wizard^{R} plus SV minipreps Cat No: A1460; Promega) as per manufacture's instructions. All the PCR products and restriction enzyme digested samples were gel extracted with QIAgen Gel Extraction kit (QIAgen. QIAquick Cat No: 28704) as per manufacture's protocol and eluted with sterile distilled water. Proofstart PCR blunt end DNA fragments and vectors were digested with respective endonucleases at suitable temperatures for 4-5 hours and gel extracted. Ligation reactions were performed with 1:3 molar ratio of vector to insert denatured at 45°C for 15 minutes and cooled on ice. Ligase buffer and T_4 DNA ligase were added to the reaction, incubated at 16°C for 1.5 hours and at 4°C for overnight.

Chemical competent cells were prepared as described in Sambrook *et al.*, 1989. Transformation was performed as follows. Competent cells were thawed on ice for 5 minutes; 2-5 μl of the ligation samples were mixed with the *E. coli* competent cells; incubated on ice for 30 minutes; heat shocked at 42°C for 30 seconds; cooled on ice for about 2 minutes; 300 μl of Soc or LB broth was added to the cells and incubated at 37°C for 1 hour. Finally the cells were plated on LB agar with appropriate antibiotics for selection. When doing TA cloning X-gal and IPTG (see table. 2.5.1) were spreaded on LB agar (ampicillin plates) before plating the cells. The transformants were randomly screened by colony PCR and restriction enzyme digestion of the plasmid. Then the positive plasmids were sent for DNA sequencing at DBS Genomics, University of Durham, UK. The sequence results were analyzed with the Vector NTI program.

2.11 Yeast transformation

Yeast transformation protocol was followed according to the Clontech's Matchmaker Gal-4 Two-Hybrid System 3 user manual. The bait gene was expressed as a fusion with Gal-4 DNA-binding domain (DNA-BD), while the prey gene or cDNA was expressed as a fusion to the Gal-4 activation domain (AD). When bait and prey proteins interact, the DNA-BD and AD brought into proximity and activates the transcription of three reporter genes. This technology is very sensitive to detect transient and weak interactions and moreover the proteins are supposed to be in native conditions *in vivo*. The primers and constructs used for the two-hybrid assays are represented in table 2.8.1.

The protocol for making yeast competent cells

The yeast strain AH109 was cultivated on YPD agar at 30°C for 2 to 3 days and stored at 4°C. Several 2-3 mm colonies were inoculated into 50 ml of YPD broth and incubated at 30°C at 230 rpm for 16-18 hours (OD_{600} >1.5). The overnight culture (5-7 ml) was transferred into 300 ml YPD broth in a 1 litre flask (enough to produce an OD_{600} 0.2-0.3) and incubated at 30°C at 230 rpm for 2-3 hours until the cells reached an OD_{600} 0.5. The cells were harvested in 50 ml centrifuge tubes at 1000x g for 5 minutes, resuspended in 35 ml of TE buffer pH 7.5 and centrifuged again. Finally the cell pellets were resuspended in 1.5 ml TE/LiAc (section. 2.6) solution and cells were stored on ice for transformation.

The following solutions were prepared freshly before the transformation

1. 1 M Lithium acetate (LiAc) stock; 1X TE buffer and DMSO

TE/LiAc prepared as; 1 ml of 1 M LiAc, 1 ml of 10x TE and 8 ml of sterile distilled water.

2. 50% PEG in TE/LiAc; 4g of PEG (3310) in 7 ml of TE/LiAc to make up to 10 ml & filter-sterilized.

For yeast transformation the following mixer was prepared as described below.

Table 2.11-1 Yeast transformation reaction

Small-scale co-transformation	Large- scale Pb library transformation
0.1 ml of fresh competent cells	1.5 ml of fresh competent cells
0.1 μg of AD fusion construction (ADT7)	0.1-0.5 mg of AD library
0.1 μg of BD fusion construction (BKT7)	0.2-0.1 mg of BD fusion construction
0.1 mg of Herring testes carrier DNA	2 mg of Herring testes carrier DNA
0.6 ml of PEG LiAc/TE	6 ml of PEG LiAc/TE

The above reaction was mixed by vortexing for 1 minute and incubated at 30°C for 30 minutes with shaking at 200 rpm. Sterile DMSO 70 μl was added to small-scale and 700 μl was added to library-scale transformation. The tubes were inverted a couple of times, heat shocked at 42°C for 15 minutes and tubes were inverted every 5 minutes during the heat shock. The tubes were chilled on ice for 2 minutes, centrifuged at 14k rpm for 5 seconds and cell pellets were resuspended in 0.5 ml of 1x TE for small-scale and 5-10 ml for library-scale.

The cells were plated on SD/-Trp/-Leu/-His plates for small-scale and SD/-Trp/-leu for library scale. The colonies from the above plates were replica plated on SD/-Trp/-leu/-His/-Ade. The plasmids were isolated from the positive clones by Clontech's yeast plasmid isolation kit (Cat No: PT3049-2) according to the user manual and sent for the DNA sequencing at DBS genomics. Positive clones were subjected to α-galactosidase assay and β-galactosidase colony lift and ONPG assays as described in section 2.12 & 2.13.

2.12. α-Galactosidase Assay

SD/-Leu/-His/-Trp/-Ade plate was prepared with 200 μl of α-X-Gal (4mg/ml). the positive colonies were streaked on the plates and incubated at 30°C for 2 to 4 days or until the blue colour developed.

2.13. β-Galactosidase Assay

2.13.1 Colony-lift assay

Colony-lift assay was used to screen a large number of co-transformants that survive on SD/-Leu/-His/-Trp/-Ade plates. The colonies from SD/-Leu/-His/-Trp/-Ade plates were streaked on fresh plates and incubated at 30°C for 2 to 4 days. Using sterile forceps the autoclaved Whatman 5 (VWR Grade 410 filter paper) was placed over the surface of the colonies, by gently pressing; the colonies were lifted on the paper and placed on a petri dish by colonies facing up. The filter paper was frozen on dry ice for 10 minutes, thawed at room temperature for 10 minutes and this was repeated for 3 cycles. The filter paper was placed over the presoaked two layers of filter paper (pre-soaked on Z-buffer + β-mercaptoethanol + X-Gal solution). The filter paper setup was incubated at 30°C and checked periodically for the appearance of blue color on the colonies lifted area of the filter paper.

Z-buffer for 1 litre

$NaHP0_4.7H_20$	16.1g pH 7.0	Autoclaved
$NaH_2P0_4.H_20$	5.50g	
KCl	0.75g	
$MgS0_4.7H_20$	0.246g	
Distilled water	1000 ml	
β-mercaptoethanol	0.27 ml	
X-Gal solution (20mg/ml)	1.67 ml	

2.13.2. β-Galactosidase assay using ONPG (Ortho-nitrophenyl-β-D-galactopyranoside) as a substrate

The β-galactosidase assay is a quantitative assay to confirm the two-hybrid interactions. Two-hybrid positive clones were inoculated in 5 ml of SD/-Leu/-His/-Trp/-Ade broth and incubated overnight at 30°C. Overnight culture clumps were dispersed by vortex for 0.5-1 minute; then 2 ml was inoculated in to 8 ml of fresh YPD broth and further incubated at 30°C at 250 rpm for 3-5 hours or until reached an OD_{600} 0.5 to 0.8. ONPG was prepared 4 mg/ml in Z-buffer and left on the end-over-end-rotator for about 1 to 2 hours to dissolve completely. After mid log phase (OD_{600} 0.8) cells were harvested in 3, 1.5 ml micro centrifuge tubes and centrifuged at 14K rpm for 30 seconds. The supernatants were removed and the cell pellets were resuspended in 1.5 ml Z-buffer, centrifuged, the supernatants removed and resuspended in 0.3 ml of Z-buffer (The concentration factor was 1.5/0.3 = 5 fold). 0.1 ml was transferred to a fresh tube and frozen on dry ice. The freeze thaw cycles were repeated 5 to 6 times and 100 µl of Z buffer was added into 2 blank tubes. Z-buffer + β-mercaptoethanol was prepared (8.3 µl of β-mercaptoethanol for 5 ml Z-buffer) freshly, 0.7 ml of Z-buffer + β-mercaptoethanol was added to the reaction and blank tubes, 160 µl of ONPG was added to all the reaction and blank tubes and the timer was started. All the tubes were incubated in 30°C until the yellow colour developed, then 0.4 ml of 1 M Na_2Co_3 was added to the reaction and blank tubes. The tubes were centrifuged at 14K rpm for 10 minutes to pellet cell debris. The supernatant was transferred to the clean cuvette and the OD_{420} measured against the blank tubes in the spectrophotometer (Spectra manager V530/C0295908).

2.14 Overexpression of GST-fusion proteins in *E. coli*

P. brasiliensis adenylate cyclase $CYR1^{453\text{-}678}$ and $CYR1^{453\text{-}505}$, which incorporate the Ras and Gα binding domains, *GPB1*, *GPG1*, $TPK2^{1\text{-}225}$, $TPK2^{1\text{-}272}$, $TPK2^{151\text{-}272}$, $TPK2^{226\text{-}528}$, $TPK2^{272\text{-}527}$, $TPK2^{1\text{-}583}$ $TPK2^{528\text{-}583}$ and *GPA1* were sub-cloned into pGEX6p1-3 (for primers see table: 2.8.3, 2.8.4 & 2.8.5). The PCR products were gel extracted, restriction enzymes digested and ligated into pGEX6p-3 as described in the cloning procedure in section 2.10. The constructs were sent for DNA sequencing at DBS genomics.

The plasmids were transformed into *E. coli* Codon Plus and the cells were induced with 0.1 mM IPTG overnight at 25°C. 500ml LB and 2YT mediums were used in 2 litre flasks with vigorous shaking (200 rpm). Cells were harvested by centrifuging (Beckman Coulter) at 6000 rpm for 5 minutes. The cells were resuspended in lysis buffer (PBS) with complete EDTA free protease inhibitor tablet (Roche), lysozyme, DNase-I and incubated on ice for 15 minutes. Then the cells were passed through a constant cell disruption system for cell lysis at 15 psi twice, 0.1% Triton X-100 was added and centrifuged at 43K rpm (Beckman Ultracentrifuge) for 1 hour. The supernatant was mixed with GST beads and incubated at 4°C on an end-over-end-rotator for 30 minutes. Then the supernatants were passed through the column, washed 3 times with 1x PBS and finally eluted with GST elution buffer (50 mM Tris HCl pH 8.0 & 10 mM Glutathione). The elution fractions were run on 4 to 12% SDS (NuPAGE precast, Invitrogen) polyacrylamide gel. The protein concentrations were measured by BCA™ protein assay as described in section 2.27. The purified proteins were confirmed by Western blot.

2.15 Western blotting

The Western blot technique was routinely used for the detection of recombinant proteins expressed from *E. coli* and yeast. Expressed proteins were resolved by SDS PAGE using NuPAGE precast gels with appropriate controls and marker (See Blue, Pre-stained

Protein Standard Marker, Invitrogen). The gel was removed, placed on a square petri dish and soaked for 10 minutes in 25 ml transfer buffer. In the mean time a 8.5 cm x 8.5 cm square size PVDF membrane (Immobilon) was cut and soaked in 100% ethanol for 30 seconds and immersed in transfer buffer for 15 minutes (Gloves were worn to prevent skin contamination on the membrane).

The blotting apparatus (BIORAD) setup was prepared as follows; 3 nylon sponge pads (previously well immersed in transfer buffer) were placed on the negative charge side (cathode), followed by filter paper (8.5 cm x 8.5 cm), gel, PVDF membrane, (anode) filter paper and 3 nylon sponge pads. The proteins migrate from negative charge to positive charged PVDF membrane by applying 175mAmperes voltage for 1.5 hours. The membrane was removed, placed in a square petri dish with 25 ml wash buffer (2.15.1-C) with shaking at room temperature for 10 minutes, decanted and blocked with wash buffer with 3% BSA at room temperature for an hour. Then the membrane was incubated at 4°C without shaking for overnight with the same blocking buffer.

The blocking buffer was decanted; 25 ml of fresh buffer with 0.5% BSA was added with primary antibody and incubated with shaking at room temperature for an hour. The membrane was washed 3 times, each for 5 minutes with wash buffer. The membrane was incubated with secondary antibody for an hour at room temperature and the membrane was washed as previously. Finally the membrane was incubated with the substrate for 5 minutes and autoradiographed.

The primary antibody used for the His_6-tag was anti-polyhistidine monoclonal antibodies (1:5000 dilution, Sigma). The secondary antibody was goat anti-mouse IgG alkaline phosphatase conjugate (1:5000 dilution, BIORAD Cat No: S3660). Primary antibodies for the GST-tag were monoclonal anti-GST antibodies (1:12,500 dilution, Novagen Cat No: 71097). Immune-Star™ AP (BIORAD Cat No: 170-5018) was used as a substrate.

Polyclonal antibodies were produced from rabbit by Invitrogen for specific proteins, such as Gpa1, Gpb1, Gpg1 and Tpk2 and were used as primary antibodies at a dilution of 1:1000, and anti-rabbit IgG HRP conjugate (1:5000 dilution Sigma Cat No: A6154) was used as secondary antibodies. ECL reagent (mixture of equal proportion of solution I & II) was used as a substrate. (solution I- 1 ml luminol, 0.44 ml of coumaric acid, 10 ml of 1 M Tris, pH 8.5, made up to 100 ml with distilled water and solution II– 64 μl of 30% H_2O_2, 10 ml of 1 M Tris, pH 8.5 and made up to 100 ml with distilled water).

2.15.1 Buffers

a) Transfer buffer

Glycine	2.9g/litre
Tris-base	5.8g/litre
SDS	0.37g/litre
Methanol	20% (v/v)

b) **Phosphate stock**

KH_2PO_4	6.465g/litre
K_2HPO_4	35.3g/litre

c) Wash buffer

Phosphate stock	60 ml/litre
NaCl	8.76g/litre
Tween 20	0.05% (v/v)

2.15.2 SDS running buffers

a) MES buffer/1 litre

		Stock	**Required**
Tris base	50 mM	1 M	50 ml
EDTA	0.1%	200 mM	5 ml
MES	50 mM	-	9.76g
SDS	0.1%	10	10 ml

b) MOPS buffer for 2.5 litres

MOPS	26.25g
Trisbase	15.15g
SDS	2.5g
EDTA	0.75g

c) Phosphate Buffered Saline (PBS)/litre

		Stock	**Required**
NaCl	140 mM	3 M	46.6 ml
KH_2P0_4	1.8 mM	1 M	1.8 ml
KCl	2.7 mM	3 M	0.9 ml
Na_2HP0_4	10 mM	1 M	10 ml

2.16 *In vitro* coupled Transcription and Translation (^{35}S labelling)

The TNT^{R} Coupled reticulocyte Lysate Systems was used for *in vitro* translation. This system can be used for transcription and translation of genes cloned downstream from the SP6, T3 and T7 RNA polymerase promoter. The two-hybrid assay BKT7 construction circular plasmids were used as a template for *in vitro* translation. *Pb* Cyr1$^{1-678}$, full length Gpa1 & full length Gpg1 proteins were synthesized by *in vitro* coupled transcription and translation system (Promega cat No: L4600) labelled with Redivue^{TM}L^{35}S methionine (Amersham cat No: AG1094) using rabbit reticulocyte lysate, since these proteins were formed inclusion bodies in several attempts in *E. coli*. An *in vitro* translation was performed as below

TNT Rabbit reticulocyte lysate	25 µl
TNT Reaction buffer	2 µl
TNT RNA polymerase (SP6, T3 or T7)	1 µl
Amino acid mixture minus Met	1 µl
^{35}S Met Redivue™L^{35}S methionine (500ci/mmol)	2 µl (GE Healthcare)
RNasin Ribonuclease inhibitor	1 µl (Promega)
Plasmid DNA template (ethanol precipitated)	2 µl (0.5 µg/µl)
Nuclease free water (Promega)	16 µl
Total volume	50 µl

The reaction was incubated at 30°C for 2 hours and 2.5 µl of the translated samples were loaded on SDS-polyacrylamide gel to verify the translation. The translated proteins were stored at 4°C and used for GST Pull-down assays.

2.17 GST Pull-down Assay

In order to confirm the results of the yeast two-hybrid assay the GST pull-down assay was performed with fusion proteins consisting of GST-tag (Glutathione S-transferase). The prey proteins were labelled with ^{35}S by TNT coupled transcription and translation system as described in section 2.16. The GST pull-down assay was performed according to the protocol-A (section. 2.17.1) adapted in this study.

2.17.1 GST pull-down assay protocol-A

The GST-fusion proteins were dialysed in PBS and immobilized on 40 µl of GST beads (Glutathione sepharose 4B beads, GE healthcare) at 4°C for 30 minutes (CYR1$^{453-678}$-GST & Gpb1-GST). Then the beads were washed 4 times with PBS to remove unbound proteins. The protein immobilized beads were preblocked with 200 µl of binding buffer (20 mM HEPES pH 7.9, 600 mM NaCl, 0.1 % Tween 20, 5% Glycerol, 1 mM DTT, 5%

skimmed milk and 1% BSA) for 10-15 minutes at room temperature with 10 µl of EDTA free protease inhibitor (1/4 tablet in 0.2 ml PBS; made fresh stock). 10 µl of *In vitro* translated prey protein was mixed with immobilized proteins. 10 mM GDP (Sigma G7127) of final concentration was mixed in the pull-down of GPb1-GST with 35^S Gpa1 & 10 mM GTP final concentration (30 µl of 100 mM stock was used, Sigma G-8877) was mixed in case of $Cyr1^{453-678}$-GST with ^{35}S Gpa1 pull-down reaction. The same reactions were performed without GTP and GDP. The proteins were incubated in an end-over-end-rotator at room temperature for 2 hours. Then 1 ml of binding buffer (without 5% skimmed milk & 1% BSA) was added to this reaction tube, inverted for 5 times, incubated at room temperature for 10 minutes, centrifuged at 7K rpm for 10 seconds at table top centrifuge and the supernatant was discarded. 1 ml of buffer was added to the beads, inverted 2-4 times, again incubated at room temperature for 5 minutes and centrifuged as above. 1 ml of wash buffer was added, mixed well and centrifuged (no incubation). In total 7 washes were performed each with 1 ml of wash buffer. At the final wash all the supernatants were discarded, the beads were resuspended in 100 µl of the wash buffer, transferred to a fresh eppendorf tube, centrifuged and the supernatants were completely removed. The proteins were eluted by the addition of 30 µl of NuPAGE 4x LDS sample buffer followed by boiling at 90°C for 5 minutes and separated on 4-12% SDS-polyacrylamide gel (NuPAGE-precast Bis-Tris) under denaturing conditions. The gels were fixed (20% ethanol and 10% acetic acid) for 30 minutes and soaked on 5-10 ml of fluorographic reagent NAMP 100 (GE Healthcare) to amplify the signal. The gels were dried at 80°C for 35 minutes under vacuum and autoradiographed (2-3 days exposed at -80°C).

2.18. Tpk2 $^{226-583}$-His_6 & Tup1-His_6 expression in *E. coli*

The pET21d(+) *TPK2*$^{226-583}$ construct was transformed into *E. coli* BL21(DE3), BL21(DE3) Codon plus, BL21(DE3) STAR, BL21-AI, C-41(DE3), C-43(DE3), Rosetta 2 and Origami (DE3) and these strains were used for protein overexpression. 5 ml of overnight culture was used as a starter culture for 1 litre 2YT medium. Cells were

induced with 30-100 μM IPTG at an OD_{600} 0.5 and the overexpression was allowed to proceed for 5 hours at temperatures between 16 and 28°C with various shaking conditions. The cells were harvested, resuspended in lysis buffer A (20 mM Tris HCl, pH 7.5, 300 mM NaCl, 10 mM imidazole and 10% glycerol) with DNase-I and incubated on ice for 15 minutes. The cells were twice passed through a constant cell disruption system in order to lyse the cells at 15k psi and then centrifuged at 43K rpm (Beckman-Coulter Ultracentrifuge) for an hour. The supernatant was then mixed with 1 ml nickel sepharose beads (50% slurry) and incubated at 4°C on an end-over-end-rotator for 30 minutes. This mixture was then poured into a 50 ml glass column (Bio-Rad), washed twice with 50 ml of buffer A with 25 and 50 mM imidazole and finally eluted with elution buffer A with 100-500 mM imidazole gradient. The elution fractions, cell debris, flow through, washes and cell pellets were, after 43k rpm centrifugation, examined on a 4 to 12% SDS (NuPAGE precast) polyacrylamide gradient gel. Tpk2 formed inclusion bodies therefore the following protocol has been adapted.

Tpk2 and Tup1 pET21d(+) constructs were transformed into *E. coli* pLysS and used for protein expression. 10 ml of a 3-4 hour culture was used as a starter culture for 1 litre of medium. Cells were induced with 0.1 mM IPTG at an OD_{600} 1.1 (Tpk2) and 0.5 (Tup1) for 5 hours at 20°C in LB. The cells were harvested, resuspended in lysis buffer A (2.18.1) with DNase-I (500 units) and incubated on ice for 15 minutes. Then the cells were passed through a constant cell disruption system for cell lysis at 15k psi for twice and centrifuged at 43K rpm (Beckman Ultracentrifuge) for an hour. The supernatant was mixed with nickel sepharose beads and incubated at 4°C on end-over-end-rotator for 30 minutes. Then the supernatants were passed through a column and washed 3 times with buffer A with 25, 50 and 75 mM imidazole and finally eluted with elution buffer A with a 100-500 mM imidazole gradient. The elution fractions were run on 4 to 12% SDS (NuPAGE precast) polyacrylamide gels. The purified proteins were confirmed by Western blotting as described in section 2.15. The protein concentrations were measured using the BCA™ protein assay as mentioned in section 2.27.

2.18.1 Lysis Buffer A

20 mM Tris HCl, pH- 8, 500 mM NaCl, 1% Triton X-100, 1 mM β-mercaptoethanol, 10 mM imidazole, 5 mM DTT and 10% glycerol.

2.19 Tpk2-His_6 Pull-down $Cyr1^{453-678}$-GST, Gpb1-GST, Gpg1-GST and GST tag

$Cyr1^{453-678}$-GST, Gpb1-GST, Gpg1-GST and GST-tag alone were dialyzed in PBS and immobilized on 40 μl GST beads by incubation at 4°C for 40 minutes. GST beads were washed with PBS 5 times. 1 ml of $Tpk2^{226-583}$, about 2.3 mg/ml (dialyzed with pull-down buffer), was mixed with GST beads. The beads were incubated on end-over-end- rotator at 4°C for overnight (12 hrs). GST beads were washed 7 times (1 ml) with pull-down assay buffer (section. 2.19.1) and the tubes were inverted ten times in each wash. 30 μl of 4x LDS sample buffer was mixed with the beads and boiled at 92°C for 5 minutes. 20 μl was loaded on 12% SDS-polyacrylamide gel. The gel was then transferred to a PVDF membrane and Tpk2 was detected by anti-polyhistidine monoclonal antibodies.

2.19.1 Pull-down assay buffer

HEPES	20 mM pH 7.9
NaCl	600 mM
DTT	1 mM
Tween 20	0.05%
Glycerol	5%

2.20 $Tpk2^{1-225}$-GST and Tup1-His_6 Pull-down assay protocol

$Tpk2^{1-225}$-GST and GST-tag were dialyzed in PBS and immobilized on 30 μl of GST beads by incubation at 4°C for 40 minutes. The GST beads were washed with PBS 5 times. 400 μl of purified Tup1 protein, about 2.0 mg/ml (dialyzed with pull-down

buffer as described previously), was mixed with previously immobilized Tpk2 and GST tag. The beads were incubated on an end-over-end-rotator at room temperature for 2 hours. The GST beads were washed 9 times each with 1 ml of pull-down assay buffer and the tubes were inverted ten times in each wash. The buffer was completely removed in the final wash. 30 µl of 4x LDS sample buffer was mixed with the beads and boiled at 92°C for 5 minutes; 20 µl was loaded on a 4-12% SDS-polyacrylamide gel. The gel was then transferred to a PVDF membrane and Tup1 was detected by anti-polyhistidine monoclonal antibodies.

2.21 Overexpression of Gpa1

The G protein G-α subunit encoding gene *GPA1* was cloned into pGEX 6p-1, for GST-fusion, and pET21a(+). pGEX 6p-1 Gpa1 was expressed as described in section 2.14 and the pET21a(+) construct was expressed as explained in section 2.18. These constructs were tested in various *E. coli* strains with various induction conditions; since Gpa1 formed inclusion bodies. Finally Gpa1 was expressed from the *in vitro* translation system (section. 2.16).

2.22 Intracellular protein overexpression in *Pichia pastoris*

P. brasiliensis putative *TPK2* was sub-cloned into the *Pichia* expression vector pPICZA with *Kpn*I and *Apa*I in the forward and reverse primers, respectively (for primers see table. 2.8.5). *E. coli* Top 10 F' was used for basic construction and plasmid propagation. 10 ng of pPICZA *TPK2* construction and pPICZA vector were linearized by digesting with *Pme*I and transformed to GS115 and KM71H *Pichia* strains by the lithium chloride method according to the manufacture's protocol in the *Pichia* expression manual. The transformants were selected by plating on YPD agar with 100 µg/ml zeocin. The genomic DNA was extracted from the positive clones and verified by PCR analysis using 5' and 3' *AOX* primers.

Protein expression was achieved by inoculating a single colony into 5 ml of MGH (Minimal Glycerol Histidine Medium) for 24 hours at 30°C, centrifuged, resuspended into 5 ml of MMH (Minimal methanol histidine medium) and induced with 0.5% methanol for every 24 hours. After 144 hours, the cells were harvested, mixed with an equal amount of acid washed glass beads and resuspended in 100 µl of breaking buffer. The cells were vortexed 10 times for 30 seconds interval, kept on ice, between vortexing and centrifuged at 14k rpm for 10 minutes at 4°C. 50 µl of supernatant was mixed with 25 µl of 4x LDS buffer, boiled at 90°C for 2 minutes and 20 µl was loaded on an SDS-polyacrylamide gel. Protein expression was analyzed by Western blot.

2.22.1 Media and buffers

a) Minimal Glycerol medium		**b) Minimal Methanol Medium**	
Yeast Nitrogen Base	1.34%	Yeast Nitrogen Base	1.34%
Glycerol	1%	Methanol	0.5%
Biotin	4×10^{-5}%	Biotin	4×10^{-5}%

c) Breaking buffer

Sodium phosphate	50 mM pH 7.4
PMSF	1 mM (Phenylmethylsulfonyl fluoride)
EDTA	1 mM
Glycerol	5%

2.23. Extracellular Protein overexpression in *Pichia pastoris*

P. brasiliensis putative *TPK2* was cloned into the *Pichia* expression vector pPIC9 with an α-factor secretion signal for extracellular expression, with *Eco*RI and *Not*I in the forward and reverse primers, respectively (for primers see table. 2.8.5). *E. coli* Top 10 F' was used for basic construction and plasmid propagation. The construction and empty

vector were linearised with *Sal*I, transformed into GS115 and KM71H by the lithium chloride method, selected by plating on MD (section. 2.23.1.a) plates without histidine and incubated at 30°C for 3 days. Genomic DNA was isolated from positive clones and subjected to PCR using gene specific and *AOX* 5' and 3' primers.

Positive clones were replica plated from MD to MM (section. 2.23.1.b) plates to select the Mut^+ and Mut^S (methanol slow utilizing) phenotypes. The positive clones were inoculated into 5 ml of BMGY (buffered glycerol-complex medium), incubated at 28°C for 24 hours, harvested and resuspended in 2 ml of BMMY (buffered methanol-complex medium). The cells were induced with 10 μl of 100% methanol, after 72 and 144 hours. 0.5 ml cultures were harvested and the supernatant was analyzed for secreted proteins. The colonies from MM plates were patched on to PVDF membranes and subjected to Western blot.

2.23.1 Media recipes

a) MD Agar (Minimal Dextrose medium without Histidine)

Yeast Nitrogen Base	1.34%
Dextrose	2%
Biotin	4×10^{-5}%
Agar powder	2%

b) BMGY (Buffered Glycerol-complex Medium) c) BMGY (Buffered Methanol-complex Medium)

Yeast extract	1%
Peptone	2%
Yeast Nitrogen Base	1.34%
Biotin	4×10^{-5}%
Sodium phosphate	100 mM
Glycerol	1% (for methanol medium 0.5% of 100% methanol)

2.24. Antibody production

Polyclonal antibodies for components of the cAMP pathway, such as adenylyl cyclase Cyr1, G protein α-subunit Gpa1, β-subunit Gpb1 and γ-subunit Gpg1 and cAMP dependent protein kinase A Tpk2 were produced in rabbits. The protein sequence for each component was sent to Invitrogen peptides design team to design synthetic peptide for antibody production (Standard protocol Cat No: M0300). They designed suitable peptides, synthesized 20 mg of the peptide, injected into two rabbits and collected serum after 4, 8 and 10 weeks. The ELISA test was performed with serum against the peptide. The serum was directly used at 1:1000 dilution as antibodies for the protein detection. Synthetic peptides used for the antibody production were as follows:

Gpa1, P. brasiliensis # 139 - 153 : *C* **FRRSREYQLNDSAR** - *amide* ---------- 15 residues

Gpb1, P. brasiliensis # 266 - 279 : *C* **DIRADRELNTYQSD** - *amide* ---------- 15 residues

Gpg1, P. brasiliensis # 71 - 84 : *C* **QIDKREDPYAPQQS** - *amide* ----------15 residues

Cyr1, P. brasiliensis # 1623 - 1636 : *C* **SDLKRRGERPKLRS** - *amide* ----------15 residues

Tpk2, P. brasiliensis # 556 - 569 : *C* **SQFDRYPEETEPYG** - *amide* ----------15 residues

2.25. Protein concentration

Purified proteins were concentrated using Vivaspin (Sartorius group) 2 ml ultra filtration spin columns. A column of 30-50 kDa cut-off less than the protein of interest was used. Proteins purified by nickel sepharose and GST resins were further concentrated by columns. 1.5 ml to 2 ml of protein samples were transferred to the column and centrifuged at 5,000 x g in a Beckman JA-10 fixed angle rotor for 5 minutes. The flow through was discarded, more sample was added on to the top of the column and the process was repeated until concentrated to the required volume. 30 kDa cut-off columns were used for concentrating all the proteins in this study. The centrifugation speed and time were varied for each protein according to the final concentration needed. Finally

the protein concentration was measured by the BCA™ Protein assay (Pierce) described in section 2.27.

2.26 Desalting and buffer change

PD-10 desalting columns (GE Healthcare) were routinely used for desalting and buffer change. The columns, prepacked with Sephadex™ G-25 Medium, are disposable and used for the group separation of high molecular weight (greater than 5 kDa) and low molecular weight (smaller than 1 kDa). This is very quick and efficient means of desalting a solution. The column was first equilibrated with 25 ml of buffer of interest for the protein and the flow through was discarded. A protein sample solution of 2.5 ml was passed through the column (if the protein sample was less then it was 2.5 ml, made up to 2.5 ml with buffer) and the flow through was discarded. Finally the protein was eluted with 3.5 ml of buffer. The proteins concentrated in this manner were used for pull-down and enzymatic assays.

2.27 BCA™ Protein Assay

The BCA™ protein assay is based on bicinchoninic acid (BCA) for the colorimetric detection and quantitation of total protein. The principle behind the reaction is reduction of Cu^{2+} to Cu^{1+} by the protein in an alkaline medium and detected by a reagent containing bicinchoninic acid. The purple color developed by chelating two molecules of BCA with one cuprous ion. This complex is water soluble and exhibits a strong absorbance at 562 nm. The protein concentration between 20-2,000 μg/ml can be detected.

The working reagent was prepared by mixing 50 parts of BCA™ reagent A with 1 part of BCA™ reagent B. A standard graph was prepared by using BSA (Bovine serum albumin) provided by in kit by taking an average of replicate values and plotting

the protein concentration (μg/ml) on X-axis and absorbance on the Y-axis so that the value could be deducted from the blank standard.

The following mixture was prepared to find out the concentration of the unknown sample:

Protein	water	Working reagent (A+B)
10 μl	90 μl	2 ml
20 μl	80 μl	2 ml
-	100 μl	2 ml (control blank)

The above reaction was immediately incubated at 37°C in a water bath for 30 minutes. The tubes were cooled at room temperature for a minute and the absorbance was measured at 562 nm against the water blank within 10 minutes.

2.28 Assay for cAMP production (Intracellular cAMP measurement using the non-acetylated EIA procedure with novel lysis reagent)

P. brasiliensis mycelium form was grown in a 50 ml of modified liquid YPD media at 26°C for 6 days and 5 ml was inoculated into a fresh 50 ml medium and subjected to an increase in temperature to 37°C to induce the morphological transition to the yeast form. Cells were harvested; 1 ml and 5 ml aliquots at different time interval (0 and 340 hours) during the transition and immediately stored at -80°C. To thawed cells, collected by centrifugation, 4% formic acid solution mix (9.2 ml 100% formic acid, 190.8 ml distilled water and 50 ml butanol) was added and agitated for 5 hours to disrupt the cells. The cell debris was removed by centrifugation at 14k rpm for 10 minutes and the supernatants containing cAMP were lyophilized in a Jouan LR3 lyophilyser. Subsequently, the lyophilized pellet was made up in assay buffer 1B, containing 0.25% dodecyl-trimethylammonium-bromide, and 100 μl was assayed using a Biotrak Enzyme Immuno Assay (EIA kit RPN 225 from Amersham) according to the manufacturer's protocol #3. Measurements were normalized by using an equivalent wet weight of cells during the

disruption procedure. A set of standards for cAMP were prepared from 12.5 fmol to 3200 fmol and used to generate a standard curve. The values of the unknown samples were calculated from the standard curve.

2.29 Green fluorescent Protein (GFP) expression in Yeast

The *GFP* gene (pEGFP-Actin vector as a template (Clontech)) was PCR amplified and (for primers see table. 2.8.2) cloned into the *Eco*RI and *Sal*I sites of p426 MET25 vector with stop codon. Vector p426 MET25 (Fig. 2.29.1) has a constitutive promoter (from *MET25*) and a *CYC1* transcription terminator (Mumberg *et al.*, 1994). p426 MET25-*GFP* was transformed into wild-type *S. cerevisiae* MLY61**a**/α and the expression of GFP was verified by observing under (100x) oil immersion fluorescent microscopy (Olympus 1X71 attached with camera). A yeast colony was smeared on a microscope slide with saline, air dried and fixed with 4% formaldehyde for 20 minutes. The slide was washed thrice with PBS, dried, covered with a cover slip and observed under a microscope. GFP expression was also observed in liquid cultures grown in YPD at 30°C for 4-5 hours.

Figure 2.29.1 Map of p426 MET25 Vector with multi cloning site

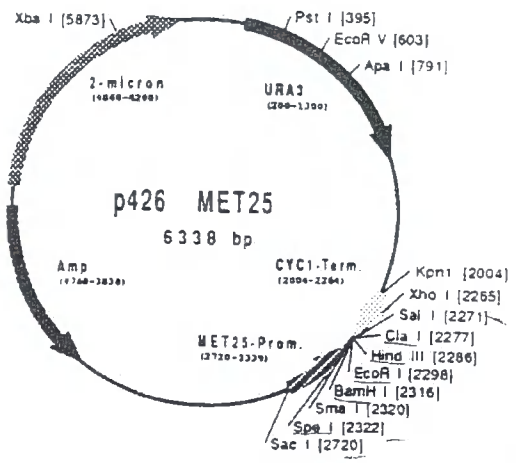

2.30 Complementation in yeast Δ*tpk2* (temperature sensitive) SGY446 PKA mutant.

2.30.1 Tpk2-GFP fusion

P. brasiliensis putative *TPK2* gene encoding protein was truncated into the N-terminus 1-225 and C-terminus 226-583. The *TPK2* truncates were fused to the N-terminus of *GFP* via *Bam*HI and *Eco*RI sites in the p426 MET25 GFP vector. The 6 base pairs of the *Eco*RI restriction site was used to link the genes (for primers see table. 2.8.2). These constructs were transformed into yeast strain SGY446 by the lithium acetate method as described in section 2.11. Transformants were selected by the uracil marker on SD minus uracil plates and incubated at 25°C for 5 to 6 days then the transformants were further streaked on SD minus uracil plates and incubated at 37°C and 25°C. GFP expression was verified by microscopy as described in 2.29. Tpk2 complementation was analyzed by observing growth at 37°C.

2.31 Pseudohyphae analysis

The empty vector and *TPK2-GFP* constructs (see table. 2.8.2) were transformed into yeast by the lithium acetate method as described in section 2.11.

Table 2.31.1 Yeast transformation for pseudohyphae analysis

Vector/ constructs	**Transformed into yeast strain (diploid strains)**
p426 MET25	WT *S. cerevisiae* MLY61**a**/α & Δ*tpk2*
p426 MET25 GFP	*S. cerevisiae tpk2* mutant XPY5**a**/α
p426 MET25 *P. brasiliensis* putative *TPK2* N-terminus 1-225-GFP fusion	*S. cerevisiae tpk2* mutant XPY5**a**/α
p426 MET25 *P. brasiliensis* putative *TPK2* C-terminus 226-583-GFP fusion	*S. cerevisiae tpk2* mutant XPY5**a**/α

The transformants were selected on SD minus uracil plates. For the pseudohyphal analysis, the diploid transformants were streaked on SLAD medium (0.17% yeast nitrogen base, 2% dextrose, 50-200 μM ammonium sulfate, 2% agar) and incubated at 30°C for 6 days. Individual single colonies on the SLAD agar plates were observed under a microscope at 20x magnification (e.g. using a Nickon Eclipse E400 digital camera attached microscope). The colonies on plates were periodically observed after 3 days of incubation until 6 days.

2.32 Expression of *P. brasiliensis* Tpk2 full length

P. brasiliensis TPK2 full length was cloned into p426 MET25 vector via the *Bam*HI and *Eco*RI sites, with a stop codon and transformed into the *S. cerevisiae tpk2* mutant XPY5**a**/α and *tpk2* temperature sensitive mutant strain SGY446. Induction of pseudohyphae was analyzed on SLAD medium and growth at 37°C was observed.

2.33 Construction of *P. brasiliensis* G protein β-subunit Gpb1-GFP fusion

The *GFP* gene was sub-cloned with a stop codon into the p426 MET25 vector via the *Hin*dIII and *Sal*I sites which were introduced into the forward and reverse primers, respectively (table 2.8.2). The *GFP* construct was transformed into *S. cerevisiae* wild-type MLY61**a**/α and GFP expression was verified as described previously (section. 2.29). *P. brasiliensis* G protein β-subunit *GPB1* was sub-cloned into the N-terminus of *GFP* via the *Bam*HI and *Hin*dIII sites; using the 6 base pairs of *Hin*dIII restriction site to join the two genes (for primers see table. 2.8.2).

2.34 Co-expression of *P. brasiliensis* Tpk2 with G-protein β-subunit Gpb1

In order to investigate the role of Tpk2 interaction on Gpb1, competent cells were prepared from *S. cerevisiae*, Δ*tpk2* XPY5**a**/α and transformed with *P. brasiliensis TPK2* full length (described in 2.32). The Gpb1-GFP fusion was transformed into above competent cells and plated on SD-uracil to a lower cell density in order to get well isolated colonies. The Gpb1-GFP transformants were screened by observing GFP as described in section 2.29.

The *S. cerevisiae* XPY5**a**/α transformed with *P. brasiliensis TPK2* and *GPB1-GFP* were streaked on SLAD agar and analyzed for the induction of pseudohyphae as described in section 2.31.

2.35. DAPI staining and confocal microscopy

The GFP fusion transformed yeast cells nuclei were analyzed by DAPI staining by smearing a colony on a microscopy slide with saline, air dried and fixed with 4% formaldehyde for 20 minutes. The slide was washed 3 times with PBS (Phosphate buffered saline) and a drop of mounting medium with DAPI solution (Vectashield mounting medium H-1200) was placed over the slide, covered with a cover slip, left at room temperature for 30 minutes to dry and then observed under a Zeiss LSM 510 META confocal microscopy with 40x oil immersion objective. All the pictures were processed using the LSM 5 image browser and Image J software.

2.36 Protein extraction from the yeast

Fresh colonies of *S. cerevisiae* haploid SGY446 and diploid strains (MLY61**a**/α & XPY5**a**/α) were inoculated into 10 ml of SD-uracil broth and incubated at 30°C overnight with shaking. Cell clumps in over night cultures were dispersed by vortexing vigorously for 1 minute, transferred into fresh 50 ml YPD medium and incubated at 30°C for 3 hours. Then the cells were harvested at 3000 rpm for 5 minutes and frozen at -80°C. The cells were thawed on ice, 200 μl of yeast breaking buffer (as described in section 2.22) and 100 μl of acid washed glass beads were added. The samples were incubated at 70°C for 10 minutes, vortexed vigorously for 1 minute and centrifuged at 14k rpm for 5 minutes. The supernatant was transferred to a fresh tube and stored at -20°C. 20 μl of the sample was briefly boiled, immediately loaded on a SDS-PAGE (12% precast) gel and then the gel was transferred to a PVDF membrane for Western blotting.

2.37 Western blotting with anti-GFP antibodies for GFP and Tpk2 N-terminus

The polyclonal anti-GFP antibodies (Clontech, kindly supplied by Dr Paul Denny in our lab) were used for the detection of GFP and Tpk2 N-terminus 1-225-GFP fusion proteins expressed from the yeast strains. A Western blot was performed as described in section 2.15. An anti-GFP antibodies 1:100 dilution as a primary antibodies and an anti-rabbit IgG HRP conjugate 1:2500 dilution as a secondary antibodies were used. ECL substrate was used for the detection.

2.38 Western blot with polyclonal specific antibodies for Tpk2 C-terminus 226-583, Tp2 full length and Gpb1

P. brasiliensis Tpk2 polyclonal antibodies, produced for the peptide sequence 556-569 in the Tpk2 C-terminus (as described in section 2.23) were used for the detection of Tpk2 C-terminus and full length protein expression in yeast. The peptide sequence 266-279 was used to produce the antibodies for Gpb1. The above polyclonal specific antibodies 1:1650 dilution as a primary and anti-rabbit IgG HRP conjugate 1:3000 dilution as secondary antibodies were used in the Western blotting (described in section 2.15).

2.39 PKA Assay ProFluor™ PKA Assay (Promega Cat No V1240)

P. brasiliensis putative cAMP-dependent PKA catalytic subunit Tpk2 C-terminus 226-583 was partially purified from *E. coli* (section 2.18) and used for PKA assays.

2.39.1 Reaction solutions

a) Protein sample preparation

5x Reaction buffer	20 µl
Substrate PKAR110	0.1 µl
Protein sample dialyzed in the assay buffer (1.5 mg/ml, 40 mM Tris HCl pH 7.5 & 20 mM $MgCl_2$, 50 µM DTT)	80 µl
Total volume	100 µl

25 µl was used for each well.

b) ATP solution

5x Reaction buffer	20 µl
rATP	1 µl
Water	79 µl
Total	100 µl

c) Protease solution

5x termination buffer	20 µl
Protease reagent	2 µl
Water	78 µl
Total	100 µl

d) Stabilizer Solution

5x Termination buffer	60 µl
Stabilizer reagent	0.1 µl
Water	79.9 µl
Total	100 µl

e) Assay Buffer

40 mM Tris HCl-pH 7.5

20 mM Magnesium chloride

Protocol

1. 25 µl of the above proteins (described in 2.39.1) were added in to each well of a micro titer plate (black plate with flat bottom).
2. 25 µl of ATP solution was added to the wells, some of the wells (used as controls), only buffer was added (reaction buffer without ATP).
3. The reagents were mixed well and incubated for 30 minutes at 30°C.
4. 25 µl of protease solution was added to each of the wells, mixed well and incubated at room temperature for 30 minutes.
5. 25 µl of stabilizer solution was added to each of the wells.
6. The plate was mixed well and readings were taken at an excitation wavelength of 485 nm and an emission wavelength of 530 nm.

The reactions were carried out with and without cAMP and ATP. The catalytic subunit of bovine heart cAMP-dependent protein kinase, (Promega Cat No: V5161) was used as a positive control in these assays.

2.40 *P. brasiliensis TPK1* cloning

The complete gene sequence of *P. brasiliensis TPK1* was obtained from the Broad institute web site http://www.broad.mit.edu/ and cloned into p426 MET25-GFP using the restriction enzymes *Bam*HI and *Hind*III in the forward and reverse primers, respectively (see table 2.8.2 for construct and primers). The PCR was performed with Proofstart DNA polymerase (QIAgen) using Pb cDNA library as a template as described in 2.7.2. The PCR products were digested with the above restriction enzymes and ligated into p426 MET25-GFP vector in the *Hind*III site, which was used to link the *TPK1* with *GFP*. $TPK1^{135\text{-}560}$ was also cloned into two-hybrid assay vectors pGADT7 and pGBKT7

with *Nco*I and *Bam*HI restriction sites (for constructs and primers see table. 2.8.2) as mentioned above. The cloning was performed as described in section 2.10. The recombinant plasmid was subjected to restriction enzyme digestion and DNA sequencing.

2.40.1 Tpk1 complementation and pseudohyphal analysis

The *P. brasiliensis TPK1*$^{135\text{-}560}$ p426 MET25-*GFP* construct was transformed into *S. cerevisiae* haploid and diploid strains by the lithium acetate method as described in section 2.11. The transformants were plated on SD-ura and incubated at 30°C for 3-4 days. Then GFP expression was analyzed under fluorescence microscopy as described in section 2.29. For pseudohyphae induction studies, the transformants were streaked on SLAD agar and analyzed as described in section 2.3. The proteins were extracted from the yeast cells as described in section 2.36 and a Western blot (section. 2.15) was performed with anti-GFP antibodies as described in section 2.37. The yeast cells nuclei was stained with DAPI as described in section 2.35 and the GFP localization observed under confocal microscopy.

2.40.2 Tpk1 two-hybrid analysis

TPK1 was cloned into the AD-fusion and DNA-BD vectors as described in section 2.40 and used for two-hybrid assays with *Pb* Gpb1, Cyr1 and Tup1. The constructs were co-transformed into *S. cerevisiae* AH109 strain as described in section 2.11. The transformants were plated on SD-Leu/-Trp/-His and incubated at 30°C for 5-7 days. The positive colonies from the above plates were further streaked on SD-Leu/-Trp/-His/-Ade with α-X-gal in order to do α-galactosidase assays.

CHAPTER THREE: PART ONE

G proteins association and their interaction with Adenylyl cyclase

---

G proteins are heterotrimeric guanine-nucleotide binding proteins that comprise Gα, Gβ and Gγ subunits which transmit signals from the external environment to intracellular effectors (Sprang, 1997). In *P. brasiliensis*, G proteins have been cloned in our lab by Dr. Daliang Chen and Dr. Gongyou Chen and two-hybrid analyses have been under taken. The two-hybrid analyses confirm the interaction of G protein (Gα) Gpa1 with (Gβ) Gpb1 and (Gγ) Gpg1 which form a heterotrimeric complex. Gpa1 and Gpb1 also interact with adenylyl cyclase N-terminus (Chen *et al.*, 2007). In order to confirm the two-hybrid analyses these three proteins were overexpressed in *E. coli* and GST pull-down assays were performed as described in this chapter.

3.1 Constructs for Cyr1 and G protein overexpression

For *in vitro* protein-protein interaction studies the gene fragments encoding the N-terminus of $CYR1^{1\text{-}678}$, $CYR1^{453\text{-}505}$, $CYR1^{453\text{-}678}$, and the G protein encoding genes *GPA1*, *GPB1* and *GPG1* were sub-cloned into pGEX6p1-3 vector for overexpression in *E. coli* for the GST-fusion proteins. Throughout the research performed in this thesis, the *P. brasiliensis* pDNR cDNA library was used as a template for the PCR reactions to amplify the genes and gene fragments.

Figure 3.1.1 Agarose gel electrophoresis of PCR amplifications. Lane M: 1Kb ladder, lanes 1-4: PCR products of *GPA1* and lanes 5-8: PCR products of $CYR1^{1\text{-}678}$.

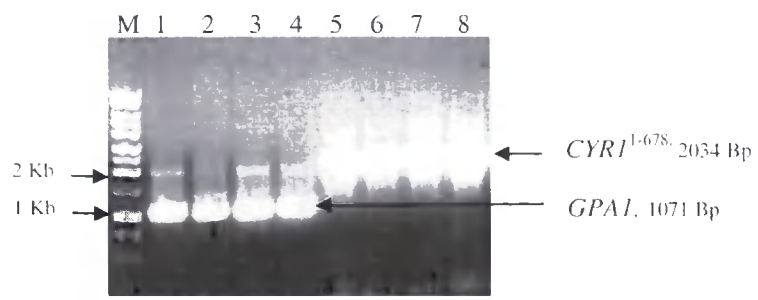

CYR1$^{1-678}$, *CYR1*$^{435-678}$, *GPB1* and *GPG1* were sub-cloned into pGEX6p-3 GST-fusion vector with *Bam*HI and *Not*I in the forward and reverse primers, respectively. *GPA1* was sub-cloned into pGEX6p-1 with *Eco*RI and *Not*I in the forward and reverse primers, respectively. The constructs and primers are described in table 2.8.3 and 2.8.4. The constructs mentioned here and throughout this thesis were DNA sequenced at Durham Biological Sciences (DBS) Genomics at the University of Durham, UK.

Figure-3.1.2 a) Agarose gel electrophoresis of PCR amplifications. Lanes 1 & 2: *CYR1*$^{453-505}$, lane 3 & 4: *GPB1* and lane 5 & 6: *GPG1* PCR products to clone into pGEX 6p-3 for GST-fusion protein overexpression. Lane M: 1Kb ladder.

Figure-3.1.2 b) Agarose gel electrophoresis of *CYR1*$^{453-678}$ PCR products. Lanes 1 & 2: CYR1$^{453-678}$ to clone into pGEX 6p-3 for GST-fusion protein expression. Lane M: 1Kb ladder.

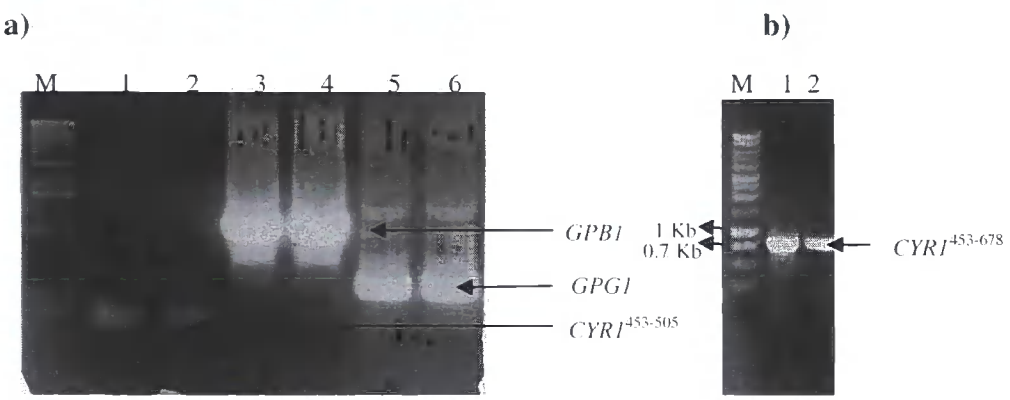

The PCR products were gel extracted, restriction enzyme digested, ligated into pGEX6p-3 vector and transformed into *E. coli* NovaBlue. The recombinant plasmids were verified by DNA sequencing.

3.2 Overexpression of adenylyl cyclase (Cyr1) and other GST-fusion proteins

When the Cyr1 N-terminus protein was overexpressed it formed inclusion bodies, although several attempts at various induction conditions with different *E. coli* strains with both GST and His_6-fusions expression from pBAD vectors were tried. The same happened with Cyr1 catalytic domain with a His-tag from a pET21a(+) construct (this was constructed by D.Chen in our lab).

The catalytic domain was cloned on its own, after showing that the N-terminus, which is quite a large fragment, cannot be overexpressed. The fragment of $CYR1^{453\text{-}505}$, which comprises the Gα and Ras binding domains, was fused to a GST-tag in an attempt to overexpress it in a soluble form. This fragment was overexpressed in a soluble form in *E. coli* (Fig. 3.2.2.a) and then a larger fragment $Cyr1^{453\text{-}678}$, was successfully overexpressed in *E. coli* (Fig. 3.2.2.c & d). Full length Cyr1 N-terminus 1-678 was produced from an *in vitro* translation method and labelled with ^{35}S and used for pull-down assays (section. 3.6.1).

The GST-fusion constructs of Cyr1, G proteins and vector with only GST-tag were transformed into *E. coli* Codon Plus. 5 ml of overnight *E. coli* culture was used as a starter culture for 500 ml 2YT broth in a 2 litre flask and incubated at 37°C with 200 rpm shaking. The cells were induced at an OD_{600} 0.5 with 0.1 mM IPTG overnight at 25°C. The cells were harvested, resuspended in lysis buffer (Phosphate Buffered Saline (PBS)) with complete protease inhibitor cocktail and DNaseI. 0.1% Triton x-100 (Sigma) was added to the disrupted cells and then the suspension was centrifuged at 43K rpm. The supernatant was pooled and 1 ml of GST beads were added and suspension incubated at 4°C with end-over-end rotation for 30 minutes. The beads were poured into a 50 ml glass column (Bio-Rad), washed three times with 50 ml of PBS and finally eluted with 6 aliquots of 1 ml of GST elution buffer (50 mM Tris HCl pH 8.0 & 10 mM Glutathione). The elution fractions were run on 4

to 12% SDS (Invitrogen NuPAGE, precast) polyacrylamide gradient gel. The protein concentrations were measured by BCA™ protein assay (Pierce). The concentrations were Cyr1$^{453-678}$-GST = 7.2 mg/ml, Gpb1-GST = 4.8 mg/ml, Gpg1-GST = 12 mg/ml and GST alone = 3 mg/ml. The purified proteins were confirmed by Western blot as described in section 2.15.

Figure 3.2.1 SDS-PAGE of Cyr1$^{1-678}$-GST fusion small-scale expression in *E. coli*.

Mini overexpression of *CYR1*$^{1-678}$ pGEX6p-3 construct was performed in 10 ml of LB and 2YT broths. 1.5 ml of culture was harvested at uninduced condition and at various times after induction, resuspended in 100 µl of MOPS buffer, 50 µl of 4x NuPAGE LDS sample loading buffer and boiled at 100°C for 10 minutes, briefly centrifuged and 10 µl was loaded on gel.

Lane M: protein marker, lane 1: total proteins from uninduced culture grown in LB medium, lane 2: total proteins from induced culture (4 hrs) in LB, lane 3 & 5: total proteins from uniduced culture from 2YT medium, lane 4 & 6: total proteins from induced culture (4 hrs) from 2YT medium.

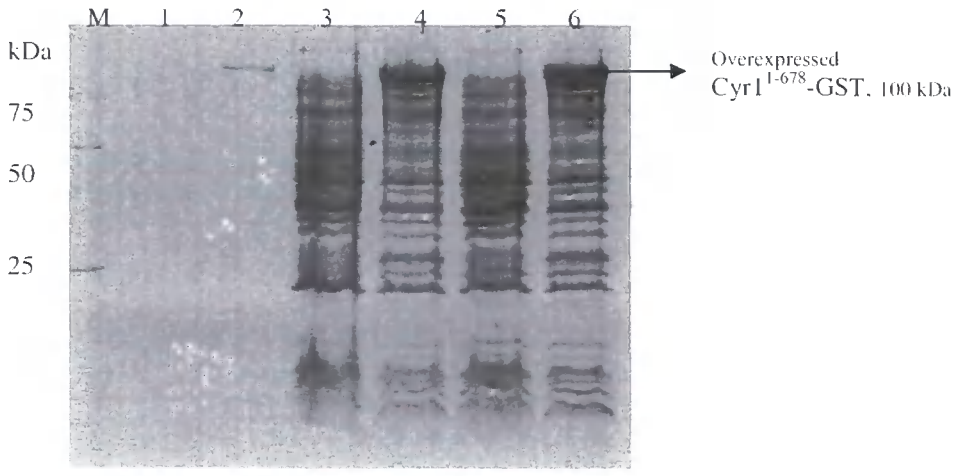

Figure shows that the total proteins from the *E. coli* Codon Plus overexpressing the Cyr1$^{1-678}$ (AC N-terminus including Gα binding domain) GST-fusion protein (GST 26 kDa + Cyr1$^{1-678}$ 74 kDa), in a small-scale overexpression, but large-scale preparation resulted in inclusion bodies.

Figure 3.2.2 a) SDS-PAGE of Cyr1$^{453-505}$-GST. Lanes 1-4: soluble fractions from the GST column: lane M: marker SeeBlue (Invitrogen).

Figure 3.2.2 b) Western blot for Cyr1$^{453-505}$ with monoclonal anti-GST antibodies (1:12500 dilution) as primary antibodies, goat anti-mouse IgG-AP (alkaline phosphatase) conjugate (1:5000 dilution) as secondary antibodies and Immune Star^{TM} (BIORAD) AP was used as a substrate.

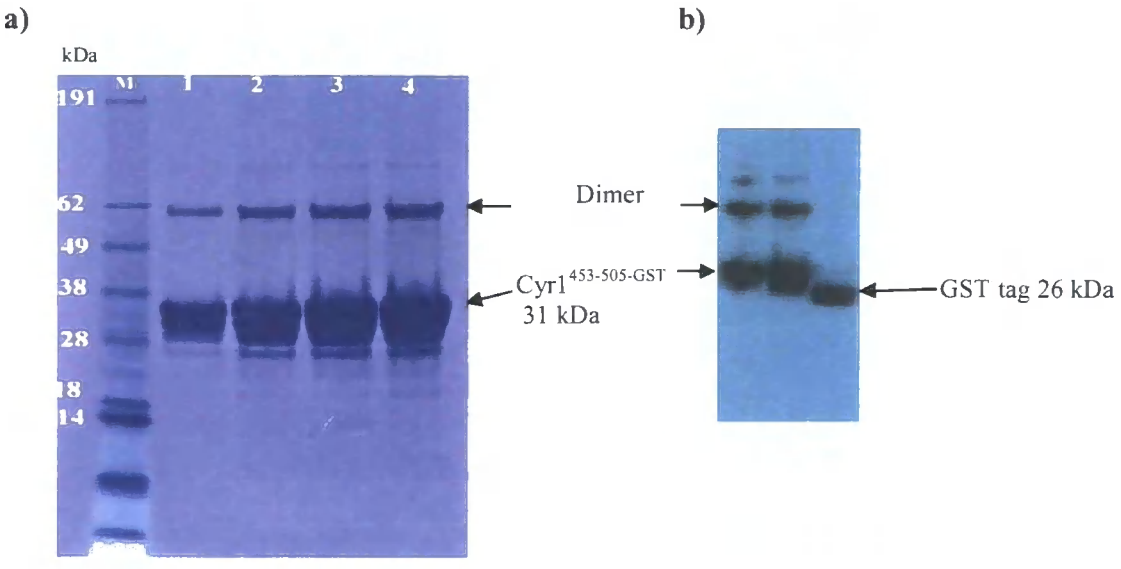

These figures demonstrate that Cyr1$^{453-505}$ can be overexpressed and purified, via a GST column, as a soluble protein. The Western blot confirms the identity of the protein.

Figure 3.2.2 c) SDS-PAGE of Cyr1$^{453-678}$-GST. Lane cell: cell debris after cell lysis, FT: flow through, lanes 1-6: soluble fractions from the GST column, lane 7: cell pellets showing the inclusion bodies and lane M: marker.

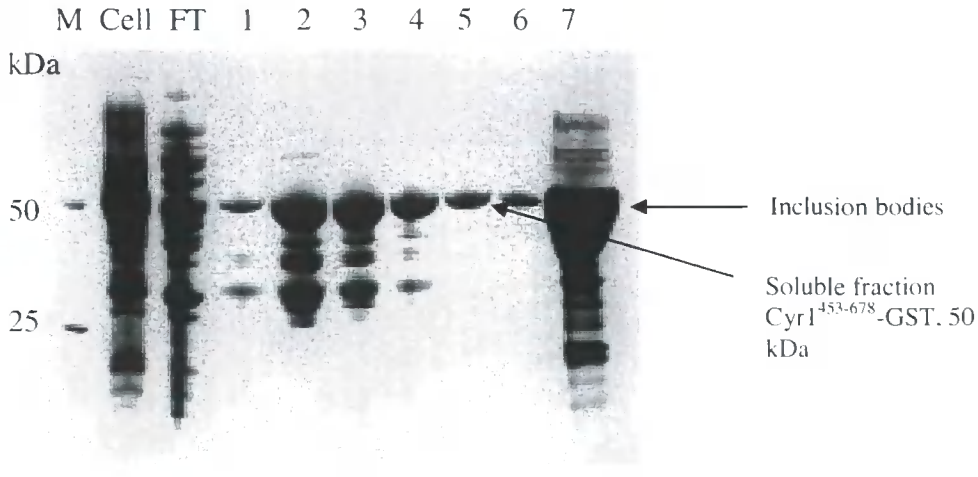

This figure demonstrates the overexpression of soluble Cyr1$^{453-678}$ (adenylyl cyclase N-terminus, with an extended Gα and Ras association domain 453-505), in *E. coli* Codon Plus, which was purified on a GST column. The soluble proteins were used for the pull-down assays. Lane 7 indicates that the part of the overexpressed protein formed inclusion bodies.

Figure 3.2.2 d) SDS-PAGE of Cyr1$^{453-678}$-GST. Lanes 1-3: soluble fractions from the GST column, lane 4 GST only: GST-tag overexpressed in *E. coli* and lane M: marker SeeBlue (Invitrogen).

Figure 3.2.2 e) Western blot with monoclonal anti-GST antibodies (1:12,500 dilution) as primary antibodies, goat anti-mouse IgG-AP (alkaline phosphatase) conjugate (1:5000 dilution) as secondary antibodies and Immune star^{TM} (BIORAD) AP was used as a substrate.

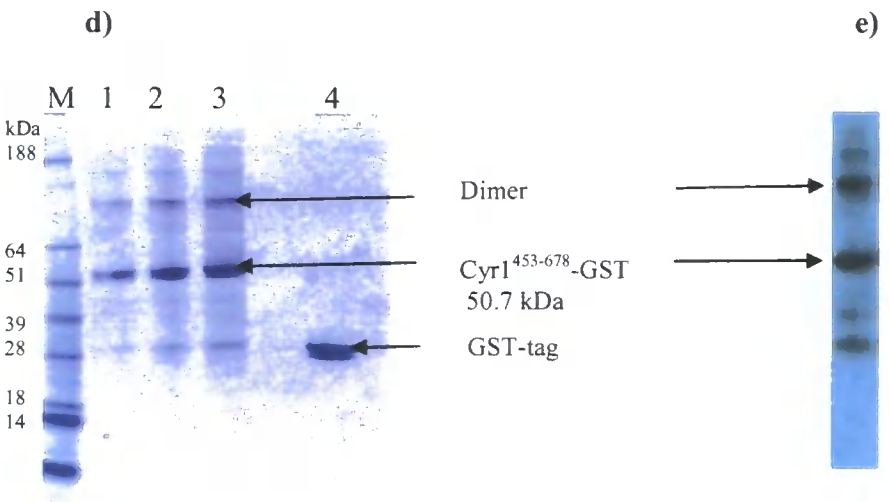

This figure demonstrates that Cyr1 can be purified as a soluble protein. The identity of the protein was confirmed by Western blotting with anti-GST antibodies.

3.3 Overexpression of Gpa1

The G protein Gα subunit *GPA1* was sub-cloned for protein overexpression in *E. coli* with His_6-tag and GST-fusions, because Gpa1 is necessary for the protein-protein interaction study for investigating the formation of the heterotrimeric G protein complex and GTP hydrolysis.

Figure 3.3.1 SDS-PAGE of Gpa1-GST fusion small-scale overexpression in *E. coli* Codon Plus. Lane M: protein marker, lane 1: total proteins from uninduced culture, lane 2: induced culture (3 hrs) and lane 3: induced culture (4 hrs) at 25°C (as described in 3.2.1).

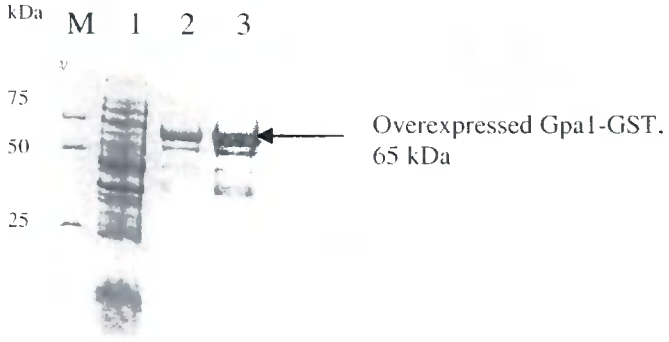

Figure 3.3.2 SDS-PAGE of Gpa1-His_6 (pET21a (+)) inclusion bodies in *E. coli* Codon plus and its corresponding Western blot with anti-polyhistidine antibodies

Lane M: marker, lane 1: imidazole elution fraction, lane 2: total proteins from untransformed *E. coli* & lane 3: pellets from the *GPA1* transformed cells

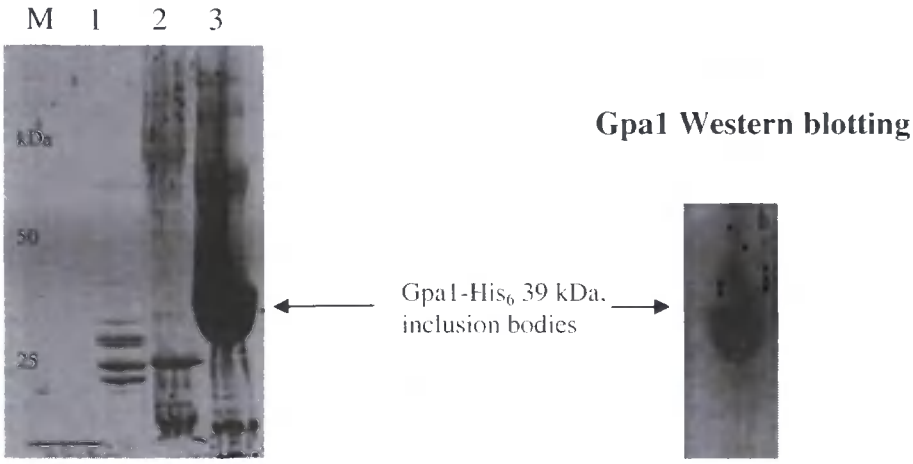

Gpa1 formed inclusion bodies during several overexpression attempts under various induction conditions and with different *E. coli* strains, both with GST-fusion (pGEX6p-1) and His_6-tag (pBAD, pET21a(+) and pET43.1a(+)) constructs. Finally Gpa1 was produced from *in vitro* translation system labelled with ^{35}S and used for pull-down assays (section 3.6).

3.4 Over expression of Gpb1

The G-protein ß-subunit *GPB1* was initially cloned into pET21a(+), pET21d(+) and pET431a(+) for the purpose of *in vitro* protein-protein interactions with Gpa1, adenylyl cyclase and Gpg1. The Gpb1 protein could not be overexpressed using any of the above constructs; nor did it form inclusion bodies. Then Gpb1 was fused to GST using the pGEX6p-3 vector and successfully overexpressed as described in the section 3.2. The overexpressed Gpb1 (Fig. 3.4.1 a) was confirmed by Western blot (Fig. 3.4.1 b) with polyclonal specific antibodies.

Figure 3.4.1 a) SDS-PAGE of G protein ß-subunit Gpb1-GST. Lanes 1-7: soluble fractions from the GST column, lane C: cell debris after cell lysis, FT: flow through from GST column and lane M: marker.

Figure 3.4.1 b) Western blot for Gpb1 with polyclonal specific antibodies (1:1000 dilution) as primary antibodies, goat anti-rabbit IgG HRP (Horseradish Peroxidase) conjugate (1:3000 dilution) as secondary antibodies and ECL was used as a substrate.

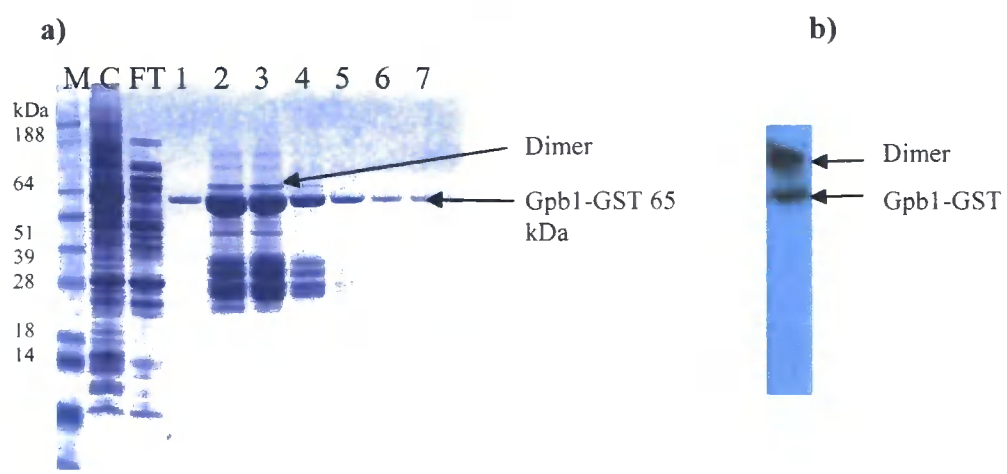

3.5 Overexpression of Gpg1

The G protein γ-subunit is a small protein (10 kDa), which is essential for the *in vitro* protein-protein interaction with other G proteins. Gpg1 was overexpressed with a GST-fusion tag as described in section 3.2. The overexpressed Gpg1 (Fig. 3.5.1 a) was further confirmed by Western-blot (Fig. 3.5.1 b) using specific polyclonal antibodies.

Figure 3.5.1 a) SDS-PAGE of G protein γ-subunit Gpg1-GST. Lanes 1-3: soluble fractions from the GST column, lane cell: cell debris after cell lysis and lane M: marker (Bench Mark, Invitrogen)

Figure 3.5.1 b) Western blot with polyclonal specific antibodies (1:1000 dilution) as primary antibodies, goat anti-rabbit IgG HRP (Horseradish Peroxidase) conjugate (1:3000 dilution) as secondary antibodies and ECL was used as a substrate.

a) **b)**

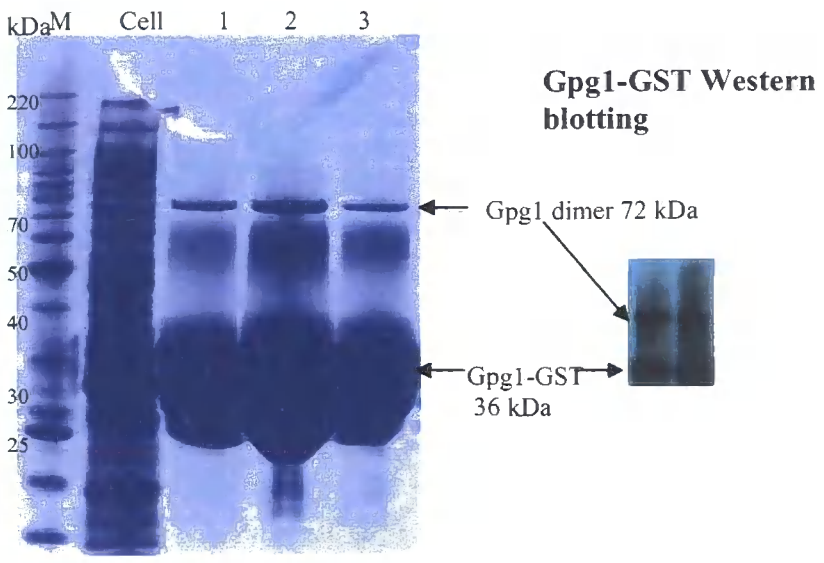

3.6 *In vitro* translation of proteins

A TNT® coupled Reticulocyte Lysate System (Promega) was used for the coupled transcription/translation of proteins labelled with Redivue™ L ^{35}S Methionine (Amersham). Cyr1$^{1-678}$, Gpa1 and Gpg1 were produced from this system, because several attempts at overexpressing Cyr1$^{1-678}$ and Gpa1 in *E. coli* only produced inclusion bodies. The genes and fragments of the above genes were sub-cloned into the two-hybrid assay, BKT7 vector and used as a template. The proteins were overexpressed using the rabbit reticulocyte RNA polymerase provided by the kit, RNasin Ribonuclease inhibitor and RNase-free tubes and pipette tips. The proteins were expressed as described in section 2.16 and 2.5 μl of the translated proteins were run on a 4-12% SDS-polyacrylamide gradient gel and fixed with 20% ethanol and 10% acetic acid. The gel was then soaked in a fluorographic reagent NAMP 100 (GE Healthcare) to amplify the signal, dried in a vacuum and autoradiographed at -80°C for 2-3 days. The translated proteins are shown, with corresponding molecular weight band (marker), in figure 3.6.1. These proteins were used for the GST pull-down assays.

Figure 3.6.1 ***In vitro* translated proteins.** The three translated proteins were shown in the figure as lane 1: Gpa1^{35}S translated, lane 2: Cyr1$^{1-678}$ ^{35}S translated and lane 3: Gpg1 ^{35}S translated proteins.

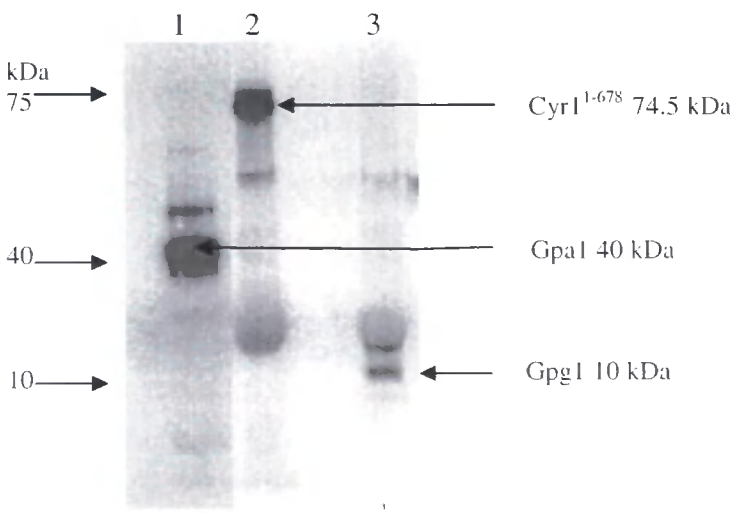

3.7 Interaction of G protein α-subunit Gpa1 with G protein β-subunit Gpb1

The GST and Gpb1-GST proteins were purified from bacteria as described in section 3.2 & 3.4, loaded on to glutathione sepharose beads and incubated with *in vitro* translated ^{35}S-Gpa1 and nucleotide. After washing the beads, the proteins were eluted by the addition of 4x NuPAGE LDS sample buffer, followed by heating at 90°C for 5 minutes and separated on a 4–12% NuPAGE gel under denaturing conditions. Gpa1 interacts with Gpb1 (Fig. 3.7.1). Bound Gpa1 was detected as a gel band by autoradiography.

Fig 3.7.1 Pull-down assays to demonstrate that ^{35}S Gpa1 interacts with Gpb1-GST. Lane 1: input *in vitro* translated ^{35}S Gpa1, lanes 2, 4 and 6: establish that Gpa1 binds to immobilized Gpb1-GST, but the apparent affinity decreases in the order of incubation with GDP (lane 2), no nucleotide (lane 4) and GTP (lane 6). Negative controls, using immobilized GST are shown in lanes 3, 5 and 7.

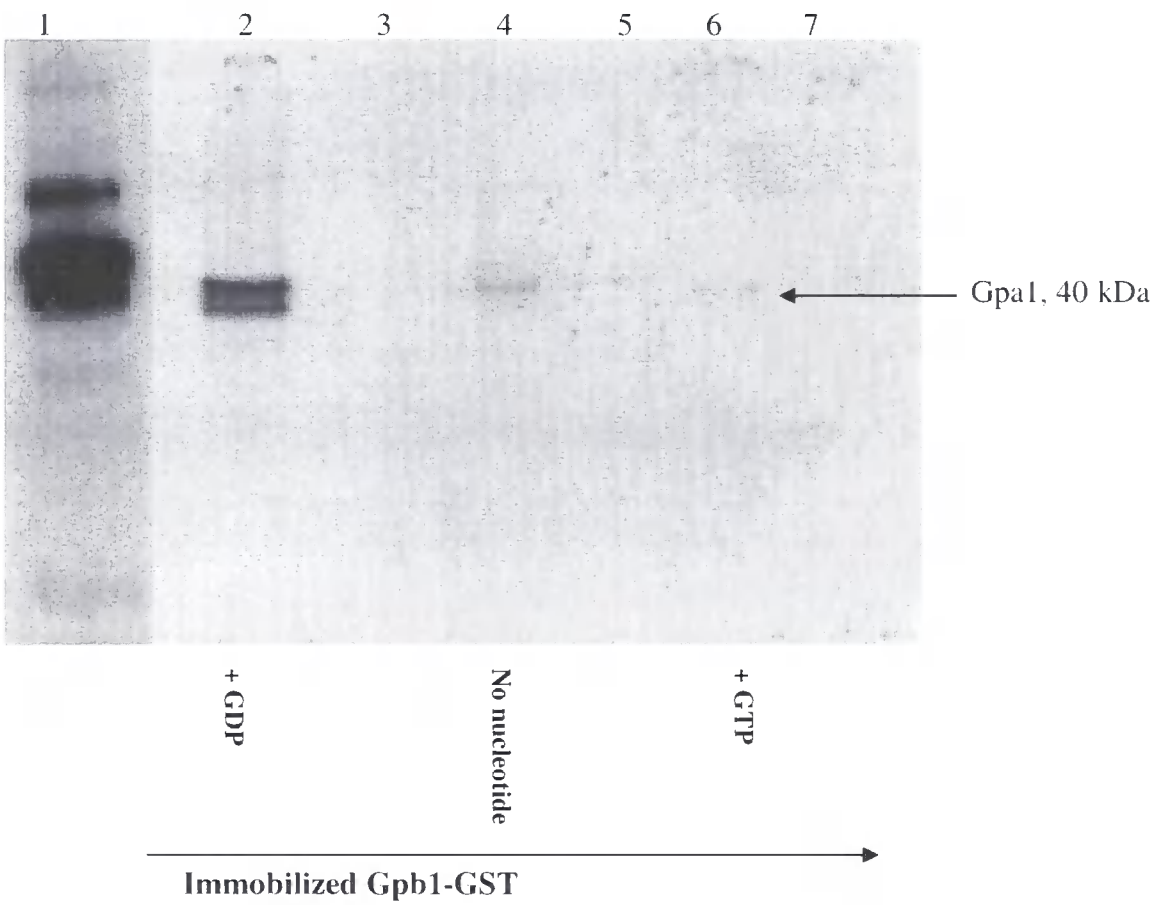

3.8 Interaction of G protein β-subunit Gpb1 with Gpg1

The Gpb1-GST and GST tag proteins were immobilized on GST beads and ^{35}S Gpg1 was mixed with 10 mM GDP and incubated at room temperature for 2 hours. The pull-down assay was performed as described in section 3.7. Gpb1 did not pull down Gpg1 (Fig. 3.8.1; lane 2).

Figure 3.8.1 Pull-down assay to demonstrate that Gpb1-GST interacts with ^{35}S Gpg1. Lane 1: *In vitro* translated ^{35}S Gpg1 input, lane 2: immobilized Gpb1 GST incubated with ^{35}S Gpg1 (no pull-down) lane 3: immobilized GST incubated with ^{35}S Gpg1 as a negative control.

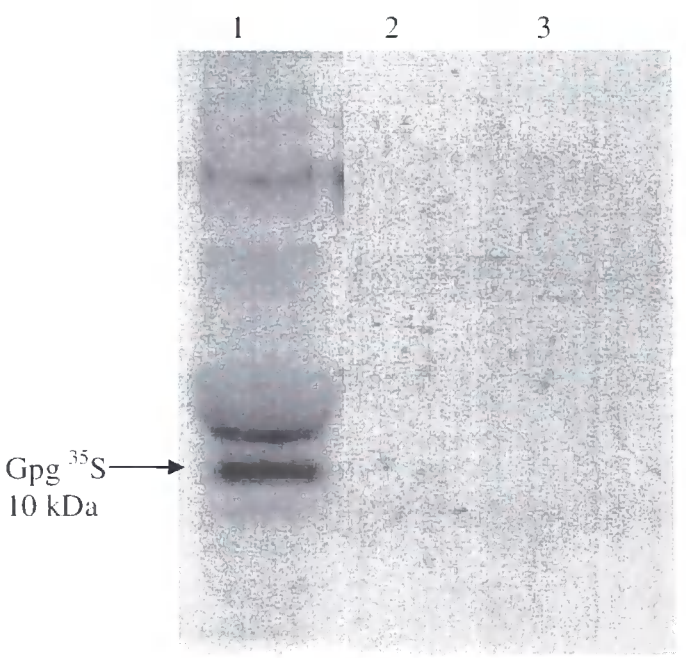

3.9 Interaction of G protein α-subunit Gpa1 with Cyr1

The GST and Cyr1$^{453-678}$- GST proteins were purified from bacteria as described in section 3.2, then loaded on to glutathione sepharose beads and incubated with *in vitro* translated ^{35}S Gpa1 and 10 mM nucleotide. The GST beads were washed, the proteins were eluted by the addition of 4x NuPAGE LDS sample buffer, followed by heating at 90°C for 5 minutes and separated on a 4–12% gradient gel under denaturing conditions. Bound Gpa1 was detected as a gel band by autoradiography. Gpa1 interacts with adenylyl cyclase (e.g. the Cyr1$^{453-678}$ Gα and Ras binding domain) which is shown in figure 3.9.1.

Figure 3.9.1 Pull-down assays to demonstrate that Gpa1 interacts with Cyr1$^{453-678}$. Lanes 2, 4 and 6: establish that Gpa1 binds to immobilized Cyr1, but there was little difference in apparent affinity after incubation with GTP (lane 2), no nucleotide (lane 4) or GDP (lane 6). Negative controls, using immobilized GST are shown in lanes 3, 5 and 7.

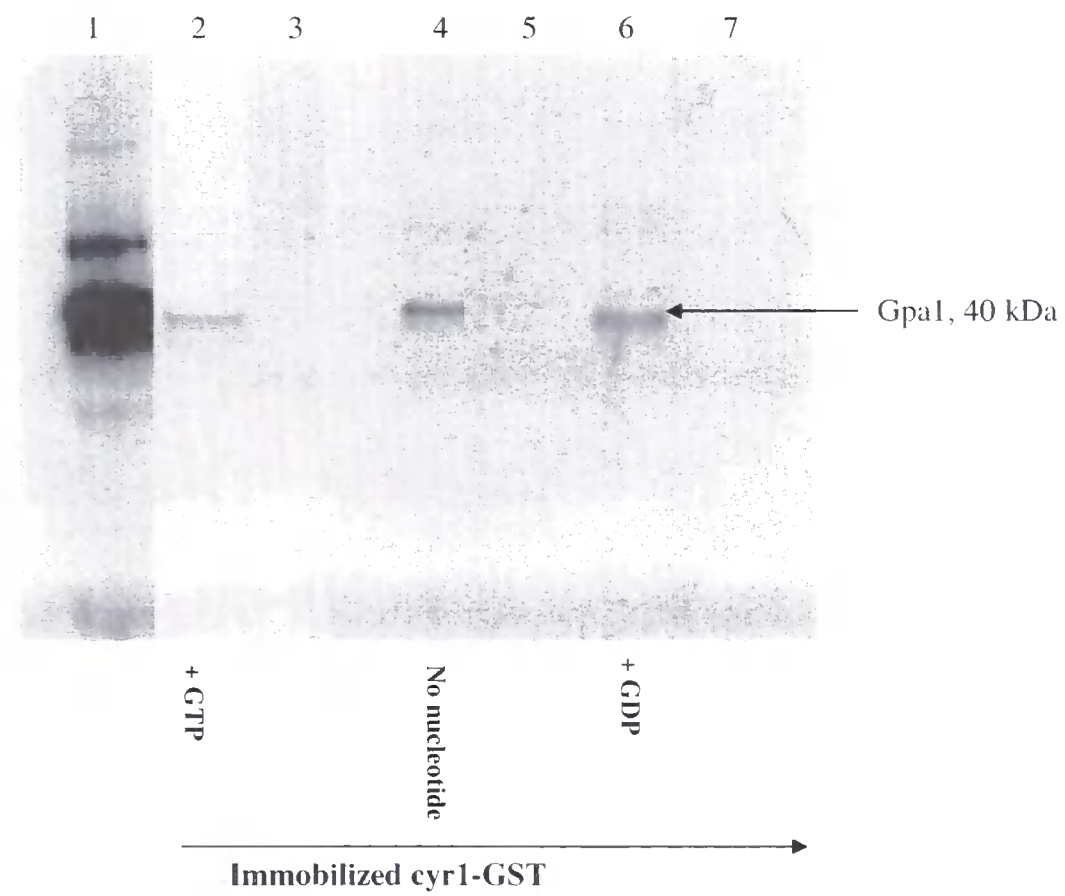

3.10 Interaction of G protein β-subunit Gpb1 with Cyr1$^{1-678}$

The GST and Gpb1-GST proteins were purified from *E. coli* as described in section 3.2 and 3.4, immobilized on GST beads, ^{35}S Cyr1$^{1-678}$ was mixed, incubated at room temperature for 2 hours and a pull-down assay was performed as described in section 3.7. The Gpb1 pulled-down the Cyr1 N-terminus 1-678, which incorporates the Gα binding domain, is shown in figure 3.10.1 lane 2.

Figure 3.10.1 Pull-down assays to demonstrate that Gpb1-GST interacts with Cyr1$^{1-678}$. Lane 1: *In vitro* translated ^{35}S Cyr1$^{1-678}$ input, lane 2: immobilized Gpb1-GST incubated with ^{35}S Cyr1$^{1-678}$ and lane 3: immobilized GST incubated with ^{35}S Cyr1$^{1-678}$.

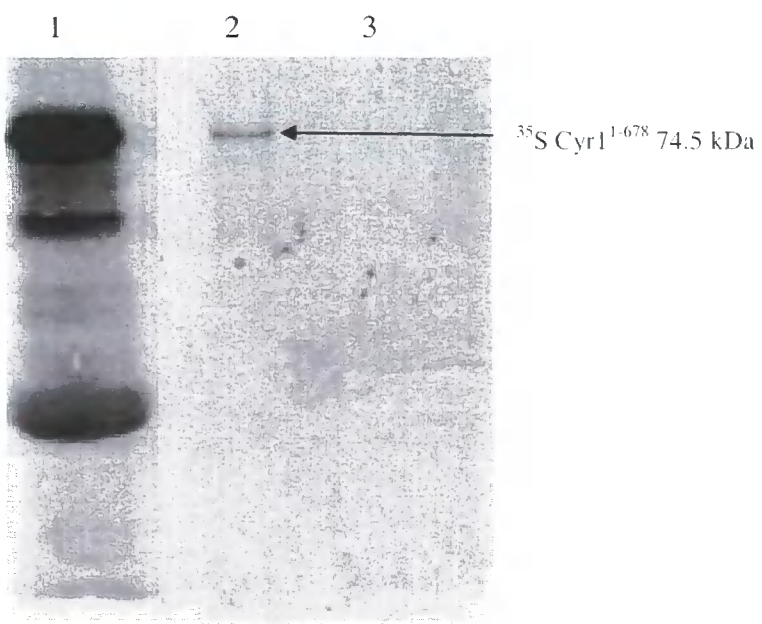

3.11 cAMP Assay

cAMP controls many physiological function in fungi such as utilization of carbon sources, conidiation, dimorphism and sexual processes in several fungi (Alspaugh *et al.*, 2002; Borges-Walmsley and Walmsley, 2000; Pall, 1981). Therefore we sought to measure the level of cAMP during the period of transition from mycelial to yeast form in *P. brasiliensis*. *P. brasiliensis* mycelial cells were grown at 26°C and shifted to 37°C to induce the transition to the yeast form. Cells were harvested between 0 and 340 hours of the transition and the intracellular cAMP levels were measured as described in section 2.28, using the non acetylated EIA procedure (protocol 3) of the cAMP Biotrak Enzyme Immuno Assay (EIA, RPN 225, Amersham) System.

3.11.1 cAMP assay Principle

The cAMP assay is based upon a competitive enzyme immunoassay system, in which there is competition between unlabelled cAMP (cAMP from test samples) and a fixed amount of peroxidase-labelled cAMP. This method utilizes a micro titre plate that had been coated with donkey anti-rabbit immunoglobulin. The test samples were incubated with antiserum (rabbit anti-cAMP), then a fixed volume of cAMP-peroxidase conjugate was added and finally after the addition of enzyme substrate, the absorbance at 450 nm was measured (see figure 3.11.1.1).

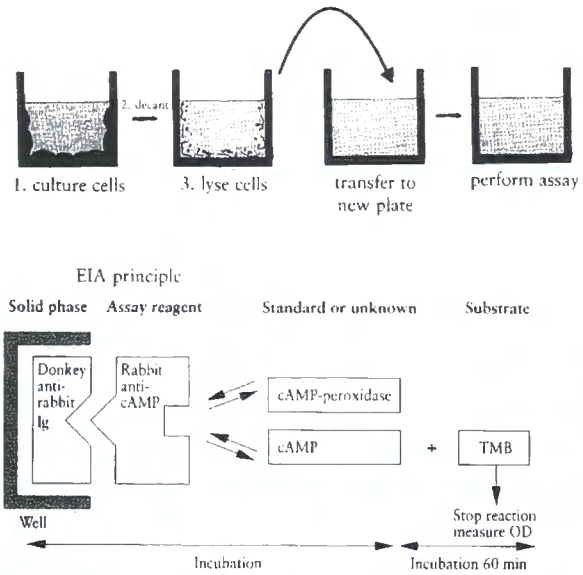

Figure 3.11.1.1 Cell lysis and principle of cAMP assay.

3.11.2 cAMP Standard curve

A cAMP standard curve was prepared for a concentration range between 12.5 fmol and 3200 fmol according to the manufactures protocol. Mean value from the duplicate test (OD-1 and OD-2) were plotted on the standard curve (Fig.3.11.2.2). The values are shown in table 3.11.2.1.

3.11.2.1 Table- Data for cAMP standard curve

Concentration fmol	OD-1 at 450 nm	OD-2 at 450 nm	Mean OD	%B/Bo
12.5 fmol	2.198	2.313	2.2555	114
25	1.834	1.833	1.833	91
50	1.534	2.683	1.534	75
100	1.462	1.722	1.462	71
200	1.519	1.286	1.286	61
400	1.178	0.859	1.178	56
800	0.679	0.882	0.7805	34
1600	0.654	0.624	0.639	27
3200	0.456	0.479	0.4675	17

Figure 3.11.2.2 Standard curve for cAMP

The cAMP concentration was plotted on X-axis and the value of the percent bound (%B/Bo) was plotted on the Y-axis to generate a standard curve on semi log paper. The values of cAMP standard are in table 3.11.2.1.

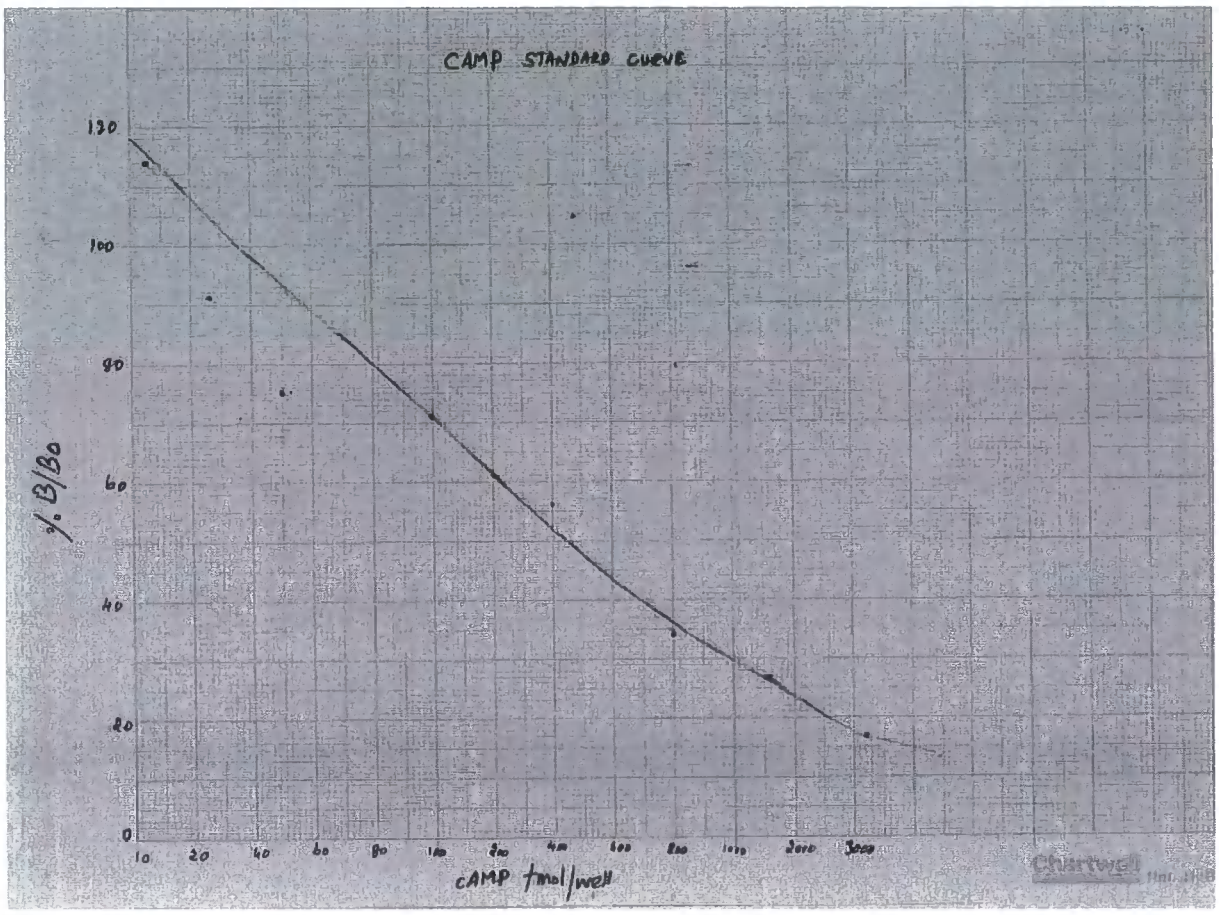

3.11.3 Calculation of unknown value using the standard curve

P. brasiliensis cells were subjected to the mycelial to yeast transformation and the samples were collected at the various time intervals shown in column 1 (table. 3.11.3.1). The samples were lyophilized and resuspended in assay buffer and 100 μl was used for the assay, which is described in the section 2.28. The absorbance for two independent test samples were taken at 450 nm which is shown in column 2. The mean absorbance is shown in column 3.

Using the following formula and data the percent bound (% B/Bo) for each sample was calculated

Zero standard OD = 2.001

NSB OD (Non Specific Binding) = 0.145

Zero standard - NSB OD (2.001-0.145) = 1.856

$$\text{Calculation of \%B/Bo} = \frac{(\text{Sample OD or Standard OD- NSB OD})}{\text{Zero standard-NSB OD (2.001- 0.145)}} \times 100$$

$$\text{0- hour- \%B/Bo} = \frac{(1.588\text{-}0.145)\times 100}{1.856} = 78$$

In a similar way the percent bound was calculated for all the samples which are shown in column 4 (table. 3.11.3.1). The level of cAMP was calculated from the cAMP standard curve using the percent bound values, which are shown in column 5 (table. 3.11.3.1). Finally the cAMP (fmol) values were plotted as shown in graph 3.11.4.

Table 3.11.3.1 cAMP levels

The cAMP values were calculated as described in section 3.11.3 which is shown below table. These data are used in the figure 3.11.4.

Hours	OD_{450} nm for culture harvest 1 ml	5 ml	Mean OD_{450}	Mean OD-NSB OD	cAMP Concentration fmol
0	1.922	1.254	1.588	(1.588-0.145)/ *100/1.856 = %B/Bo = 78	84
3	1.960	0.768	1.379	66	150
6	1.382	1.193	1.2875	62	200
12	1.013	0.927	0.97	44	600
24	1.039	1.474	1.2565	60	240
48	1.637	1.267	1.452	70	110
72	1.490	1.541	1.5155	74	92
96	1.355	1.400	1.3775	66	170
120	1.571	1.320	1.4455	70	110
240	0.903	0.603	0.753	33	820
340	0.517	0.457	0.342	18	1800

Figure 3.11.4 cAMP Assay: cAMP levels of mycelial to yeast transformation

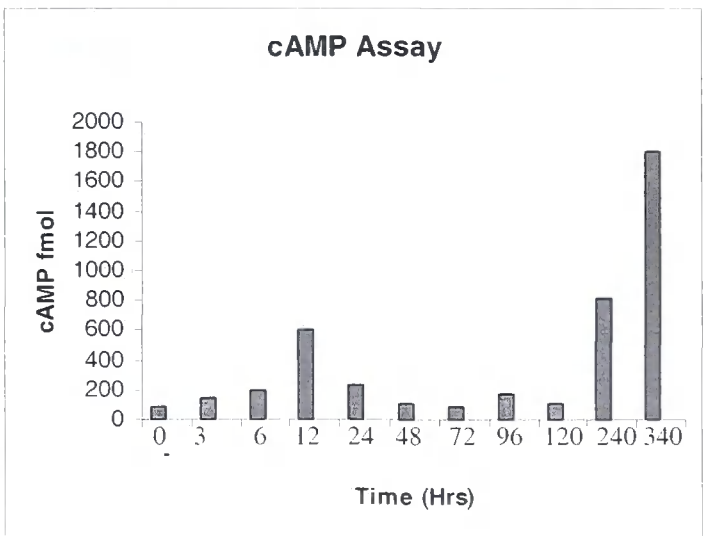

This figure represents the intracellular cAMP levels during the transition from mycelial to yeast form of *P. brasiliensis*. The level of cellular cAMP increases

progressively from the onset of transition and reached a peak at 12 hours and then progressively increased from a minimum at 72 hours. The average values from the test were plotted in this graph.

3.12 Discussion

G proteins are activated by seven-transmembrane helix cell surface receptors and these receptor catalyses the exchange of GDP for GTP on the Gα subunit. Activated GTP-bound Gα dissociates from the trimer (Gαβγ) and either Gα or Gβγ are free to regulate downstream effector molecules, such as adenylyl cyclase, phospholipase C and ion channels (Dohlman, 2002; Sprang, 1997).

The components of the cAMP pathway have been cloned from *P. brasiliensis*. Three Gα subunits (namely *GPA1-3*) Gβ *GPB1*, Gγ *GPG1*, adenylyl cyclase (AC) (*CYR1*) and cAMP-dependent PKA catalytic subunit *TPK2*. GST pull-down assays have confirmed that Gpa1 directly interacts with Gpb1 and the interaction is strengthened by GDP and blocked by GTP (Fig. 3.7.1 lane 2 & 6, respectively). The two-hybrid assays have confirmed that the N-terminus of Gpb1 (WD1+3) interacts with Gpg1 and Gpa1 but not with Gpa2 and 3 (Chen *et al.*, 2007). Consistent with these two-hybrid assays, GST pull-down assays have shown that the Gγ Gpg1 did not interact with full length Gpb1 (Fig. 3.8.1, lane 2). A recent report reveals that Gβγ assembly needs a molecular chaperone PhLP (Phosducin Like Protein) as a stabilizer (Lukov *et al.*, 2005). This indicates that Gpa1 can form a trimer complex as Gαβγ. The plant pathogen *Ustilago maydis* has four Gα subunits (namely *GPA1-4*) but only Gpa3 is involved in the cAMP pathway and in forming a dimer with the Gβ subunit Bpp1 (Muller *et al.*, 2004). In *S. cerevisiae*, the Gα subunit Gpa2 responds to nitrogen starvation and induces pseudohyphal growth via the cAMP signalling pathway (Lorenz and Heitman, 1997).

In *Schizosaccharomyces pombe*, adenylyl cyclase the Gα binding domain has been identified and aligned with other fungal Gα binding domains recently (Ivey and Hoffman, 2005). In *P. brasiliensis*, the conserved Gα binding domain lies in the

region between residues 448-503. *P. brasiliensis* adenylyl cyclase has 4 major domains when analysed with SMART (EMBL): 1-678 (Gα-binding domain), 752-1244 leucine-rich repeats, 1341-1627 a serine/threonine phosphatase family 2C catalytic domain and 1574-1856 adenylyl/guanylyl cyclase catalytic domain. The AC N-terminus 1-678 was sub-cloned and tested for protein overexpression in various strains of *E. coli* with different constructs, but the protein could not be overexpressed in a soluble form. Then part of the AC N-terminus 453-678 (comprises Gα-binding domain 448-503) was successfully overexpressed with a GST-fusion in *E. coli* (Fig. 3.2.2) and used as the bait protein in a GST pull-down assay; however, adenylyl cyclase full length N-terminus was expressed from the *in vitro* translation system (Fig. 3.6.1).

G protein Gα-subunit Gpa1 of *Cryptococcus neoformans* is involved in the cAMP pathway, which activates adenylyl cyclase and is responsible for an increase in intracellular cAMP levels (Alspaugh *et al.*, 2002). The G protein Gpa2 of *S. pombe* activates adenylyl cyclase and causes an increase in intracellular cAMP levels (Ivey and Hoffman, 2005; Ogihara *et al.*, 2004; Peeters *et al.*, 2006). In a similar manner, *P. brasiliensis* Gpa1 interacts with adenylyl cyclase N-terminus 453-678 (Gα binding domain) and it is able to bind in the presence of GTP/GDP or in the absence of nucleotides, indicating that the binding is independent of nucleotides (Fig. 3.9.1). This suggests that the Gpa1 activates adenylyl cyclase. GDP-Gpa1 had higher affinity for Gpb1 than adenylyl cyclase (Fig. 3.7.1, lane 2).

In *S. pombe*, the G protein Gβ Git5 interacts and activates adenylyl cyclase (Landry *et al.*, 2000). *P. brasiliensis* Gpb1 interacts with adenylyl cyclase N-terminus 1-678 produced from *in vitro* translation (Fig. 3.10.1). It has been shown that fungal adenylyl cyclase interacts with Gpb1 (Chen *et al.*, 2007). AC 453-678 Gα binding domain interacted with both Gpa1 and Gpb1, suggesting that this domain plays a major role in the protein-protein interaction (Chen *et al.*, 2007).

cAMP is a second messenger molecule which regulates intracellular processes in many organisms (Pall, 1981). It has been shown that cAMP controls the

morphological transition in *S. cerevisiae* (Borges-Walmsley and Walmsley, 2000), in *C. albicans* (Niimi *et al.*, 1980), in *Mucor rouxii* (Cassola *et al.*, 2004), and in *N.crassa* (Scott and Solomon, 1975). It has been demonstrated that cAMP is responsible for the morphological transition of the non-pathogenic yeast form to the pathogenic filamentous form of the plant pathogen *Ustilago maydis*. The yeast form exhibits increased cAMP levels and the hyphal form shows decreased cAMP levels (Durrenberger *et al.*, 1998). In *C. albicans* an increase in the cellular cAMP level has been observed during the morphological transition that is associated with its virulence (Sabie and Gadd, 1992). RT PCR analysis revealed that *P. brasiliensis CYR1* transcript levels peaked at 24 hours after the onset of the morphological transition, which correlates with mycelial differentiation; and a further progressive increase in *CYR1* transcripts from about 72 hours, as the fungus attained the yeast form. The addition of exogenous cAMP after 12 hours of transition has less effect than addition at 120 hours, which induced a partial reversal of the transition from mycelial to yeast form (Chen *et al.*, 2007). In *S. cerevisiae* exogenous cAMP modulates pseudohyphal growth; the addition of 10 mM exogenous cAMP to the wild-type and Δ*pde*2/Δ*pde*2 cells showed enhanced pseuohyphae (Lorenz and Heitman, 1997).

Considering the above findings, intracellular cAMP levels were measured to check if the increase in Cyr1 transcript levels correlated with the cellular cAMP levels. The results demonstrated that the level of cellular cAMP peaked at about 12 hours and then progressively increased from a minimum at 72 hours so that the cAMP levels were higher in the yeast form (Fig. 3.11.4) (Chen *et al.*, 2007). This suggests that the increase in cAMP levels regulates the morphological transition in *P. brasiliensis*.

In this study, we have established that the Gβ and Gγ proteins interact with only Gα subunit (Gpa1) to form the heterotrimeric complex Gpa1/Gpb1/Gpg1 and that the Gpa1/Gpb1 binding site lies in the residue between 453-678 of adenylyl cyclase (Chen *et al.*, 2007).

CHAPTER FOUR

Interaction of cAMP-dependent PKA catalytic subunit Tpk2 with G proteins, Adenylyl cyclase (Cyr1) and the transcriptional repressor Tup1

---

4 Yeast Two-Hybrid Analyses

P. brasiliensis genes and gene fragments encoding two known proteins were sub-cloned into the two-hybrid assay vectors as described in table 2.8.1. The 'bait' protein was fused to the Gal-4 DNA-binding domain (DNA-BD) and the 'prey' protein was fused to the Gal-4 activation domain (AD). When the proteins interact with each other; the DNA-BD and AD are brought into proximity and this facilitates the transcription of the reporter gene (Chien *et al.*, 1991; Fields and Song, 1989). This two-hybrid assay technique has been used to discover the interaction between cAMP-dependent Protein Kinase A (PKA) catalytic subunit Tpk2 with adenylyl cyclase, G proteins and the transcriptional repressor Tup1. This research is described in this chapter.

An *in vitro* GST pull-down assays have been performed with GST-fusion proteins as bait protein and His_6 proteins as prey proteins in order to confirm the two-hybrid assay interactions. These assays are described in the second part of this chapter.

4.1 Constructions for Yeast Two-Hybrid Analyses

The components of the cAMP pathway of *P. brasiliensis* were sub-cloned into DNA-BD and AD fusion plasmids. *TPK2* was truncated at its N-terminus (e.g 1-174, 1-270) and its C-terminus (e.g. 265-583) and these truncations and Tpk2 full length (1-583) were sub-cloned into two-hybrid assay cloning vectors pGADT7 (AD fusion) and pGBkT7 (DNA-BD). The transcriptional repressor *TUP1* and the G protein *GPG1* were also sub-cloned in-frame with the above vectors (for constructs, see table.

2.8.1). The high fidelity ProofStart DNA polymerase (QIAgen) was used to sub-clone the genes from the Pb cDNA library. The adenylyl cyclase *CYR1*$^{1-678}$, *CYR1*$^{600-1314}$, *CYR1*$^{1302-1876}$, *CYR1*$^{1648-2100}$ and *GPA1-3* genes were constructed by Dr. Daliang and the *GPB1 gene* was constructed by Dr G. Chen in our lab: these constructs were used for two-hybrid assays. Constructions of truncated *TPK2* and *GPG1* are shown below (Fig. 4.1.1 to 4.1.5). These constructs had their DNA sequenced at the DBS Genomics at the University of Durham.

Figure 4.1.1 Agarose gel electrophoresis of *P. brasiliensis* truncated *TPK2* PCR products. Lane M: 1 DNA ladder, lanes 1 & 2: *TPK2*$^{1-270}$ PCR products, lanes 3 & 4: *TPK2* full length PCR products and lanes 5-6: *TPK2*$^{265-583}$ PCR products.

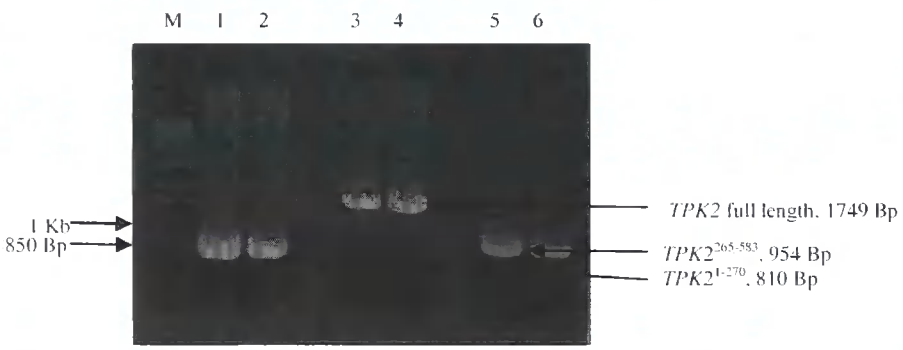

These PCR products were gel extracted and ligated into pGEMT-Easy vector. The insert was subsequently digested from the pGEMT-Easy vector (Fig. 4.1.2) and further cloned into the two-hybrid assay vectors pGADT7 and pGBKT7 (Fig. 4.1.3 and 4.1.4).

Fig 4.1.2 Agarose gel electrophoresis of digestion screens of pGEMT-truncated *TPK2* with *Nco*I and *Bam*HI. Lanes 1-4: pGEMT *TPK2*$^{1-270}$ digested, lane 5: undigested pGEMT sample 1, lanes 6-9: pGEMT *TPK2* full length digested, lane 10: undigested sample 6, lane M: 1 KB DNA ladder, lanes 11-14: pGEMT *TPK2*$^{265-583}$ digested and lane 15: undigested sample 11.

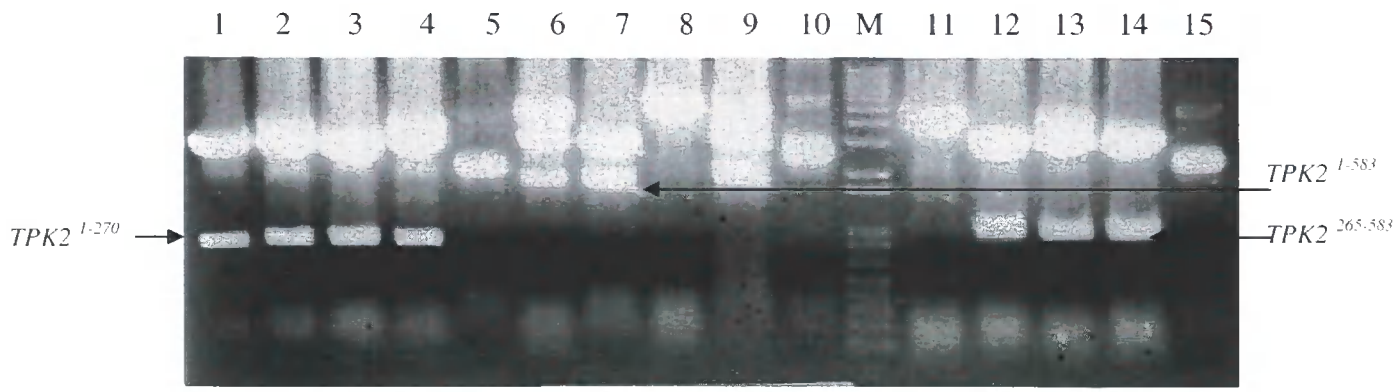

Fig 4.1.3 Agarose gel electrophoresis of digestion screens of pGBKT7 truncated *TPK2*$^{1-270}$ with *Nco*I and *Bam*HI. Lane M: 1KB Ladder, lanes 1-3: pGBKT7 *TPK2*$^{1-270}$ digested. Lane 1 has the correct insert.

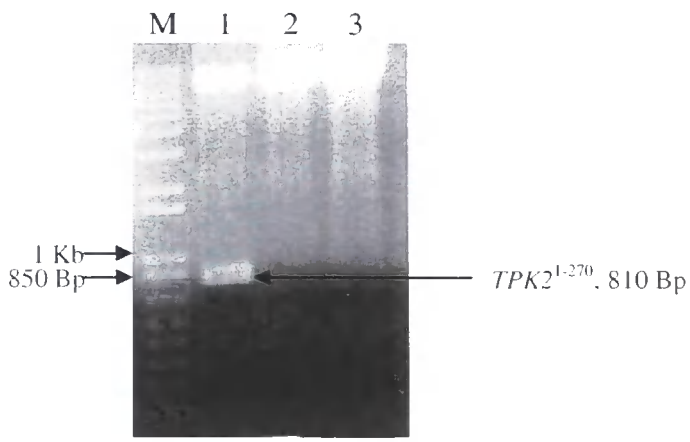

Fig 4.1.4 Agarose gel electrophoresis of digestion screens of pGBKT7 full length *TPK2* with *Nco*I and *Bam*HI. Lane M: 1 Kb ladder, lanes 1-3: pGADT7 *TPK2* full length digested and lane 4: undigested sample 1.

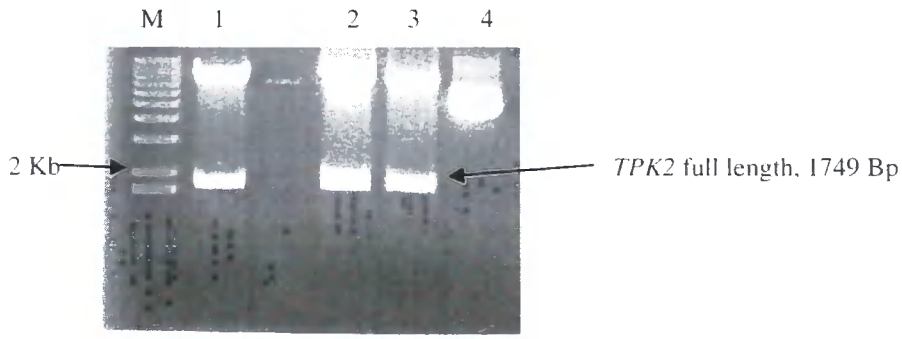

Fig 4.1.5 Agarose gel electrophoresis of digestion screens of *GPG1* with *Nco*I and *Bam*HI.

a) Digestion screening of pGEMT *GPG1* **b) Digestion screening of pGBKT7 *GPG1***

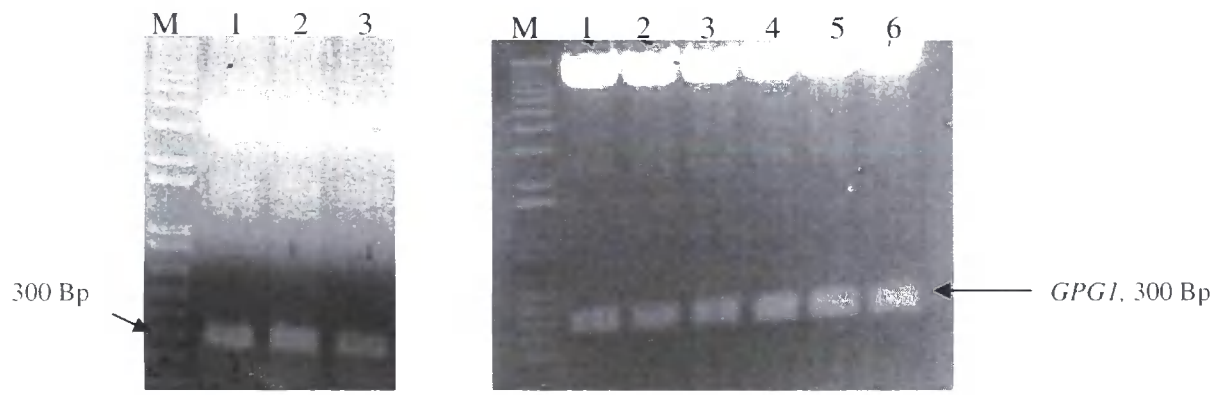

a) Lane M: 1 Kb ladder and lanes 1-3: pGEMT *GPG1* digested.

b) Lane M: 1 Kb ladder and lanes 1-6: pGBKT7 *GPG1* digested.

4.2 Yeast transformation

The components of the cAMP pathway of *P. brasiliensis* AD and DNA-BD constructs were independently transformed into *S. cerevisiae* AH109 strain and these were plated on SD/-Leu and SD/-Trp plates, respectively, with α-X-Gal in the agar medium in order to verify the self activation of *MEL1*. The *MEL1* reporter gene codes for α-Galactosidase, which can be detected by blue coloured colonies on α-X-Gal medium. None of the constructs activated the *MEL1* reporter independently. In order to investigate the protein-protein interactions, 750ng of AD-fusion and 750ng of DNA-BD vector constructs were co-transformed into the yeast AH109 strain as described in section 2.11. The transformation was initially carried out on SD/-Leu/-Trp/-His plates and incubated at 30°C. Colonies from the above plates were streaked on to SD/-Leu/-Trp/-His/-Ade. The colonies from the above plates were further subjected to α-galactosidase and β-galactosidase assays for confirmation.

Table 4.2.1 Two-Hybrid Assay results

Interacting partners	**$Tpk2^{1-174}$**	**$Tpk2^{1-270}$**	**$Tpk2^{226-583}$**	**$Tpk2^{265-583}$**	**$Tpk2^{1-583}$**
$Cyr1^{1-678}$	-	+	+	+	+
$Cyr1^{600-1316}$	-	+	NT	-	+
$Cyr1^{1302-1876}$	-	-	NT	+	+
$Cyr1^{1648-2100}$	-	+	NT	-	+
Gpa1	-	-	NT	+	+
Gpa2	NT	-	NT	-	-
Gpa3	NT	-	NT	-	-
Gpg1	-	+	NT	+	+
Gpb1	-	-	+	+	+
Ras	NT	-	NT	-	-
Tup1	-	+	-	-	+

+ Positive, -Negative and NT-Not Tested

P. brasiliensis truncated Tpk2 was analysed for protein-protein interactions, by yeast two-hybrid analyses, with adenylyl cyclase, G proteins and Tup1. The Tpk2 N and C-terminus interact with adenylyl cyclase N-terminus 1-678. $Cyr1^{1-678}$, which

incorporates the Gα binding and Ras association domain, is the major domain involved in protein-protein interactions (Chen *et al.*, 2007). $Cyr1^{600-1316}$ interacts with the N-terminus of Tpk2 and the $Cyr1^{1302-1876}$ catalytic domain interacts with the C-terminal of Tpk2; almost all the Cyr1 domains interact with Tpk2. The G protein α-subunit Gpa1 and G protein β-subunit Gpb1 both can interact with the Tpk2 C-terminus. The G-protein γ-subunit can interact with both N-and C-terminus of Tpk2. Tup1 interacts with the N-terminus 1-225 of Tpk2. None of these interacted with $Tpk2^{1-174}$ which has no 'Q' residues (see results table. 4.2.1). In order to exclude the false positives, the negative control vector BKT7 lamin (Clontech) was co-transformed with the ADT7 construct made for the two-hybrid assay (table. 4.2.2). Empty vectors were also used to co-transform with the bait and prey constructs as negative controls. ADT7-T (SV40 T antigen) and $BKT7P^{53}$ were used as a positive control throughout the assays.

Table 4.2.2 Negative controls

ADT7	BKT7 Lamin
$Tpk2^{1-174}$	-
$Tpk2^{1-270}$	-
$Tpk2^{1-583}$	-
$Tpk2^{265-583}$	-
Gpg1	-
Tup1	-

-Negative (no interaction)

4.3 α-Galactosidase assay

The colonies from SD/-Leu/-Trp/-His/-Ade plates were further subjected to α-galactosidase assays using α-X-Gal on SD/-Leu/-Trp/-His/-Ade agar plates to study the activation of the *MEL1* reporter gene. 200 μl of 4mg/ml α-X-Gal solution was mixed while making the SD/-Leu/-Trp/-His/-Ade plates and the colonies were streaked on to this medium and blue colour colonies were seen after 3-4 days of incubation at 30°C (Fig. 4.3.1).

Figure 4.3.1 a-Galactosidase assay for Tpk2. a-Galactosidase assay positive colonies on SD-Trp/-Leu/-His/-Ade with a-X-Gal.

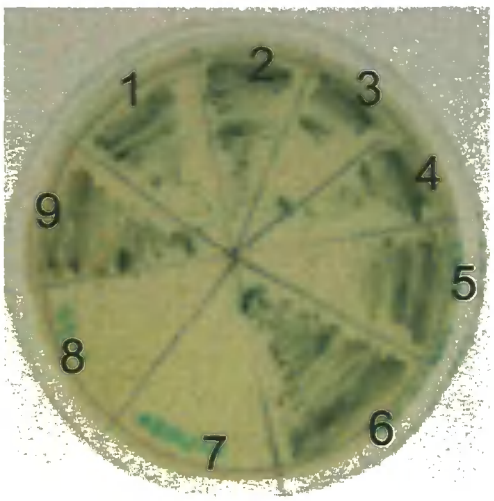

1 Tpk2 + Cyr1$^{(1-678)}$
2 Tpk2 + Gpa1
3 Tpk2 + Gpb1
4 Tpk2 + Gpg1
5 Tpk2 + Tup1
6 Tpk2$^{(1-270)}$ + Tup1
7/8 -ve control (BK Lamin & ADT7 Tpk2)
9 +ve control

4.4 ß-Galactosidase Assay

The positive colonies from the a-galactosidase assay were subjected to ß-galactosidase assays; colony lift assays and ONPG assays. The *LACZ* reporter gene encodes for ß-galactosidase.

4.4.1 Colony lift assay (X-gal filter assay)

The positives colonies from the a-galactosidase assay were streaked on SD/-Leu/-Trp/-His/-Ade agar plates and incubated for 2 days at 30°C. Then the colonies were transferred to filter paper, lysed by repeated freezing and thawing as described in methods section 2.13.1. The filter paper was then incubated at 30°C in Z-buffer with X-gal solution and the blue colour was observed after 5-6 hours of incubation. All the colonies from Tpk2 with Cyr1 and Tup1 interaction produced the blue colour, but in the case of Tpk2 with Gpa1, Gpb1 and Gpg1 only a few colonies produced the blue colour, while the other colonies produced the blue colour after 8 hours of incubation (Fig. 4.4.1.1). This assay is more sensitive than a-galactosidase and ß-

galactosidase ONPG assays but it is not a quantitative assay; therefore the ß-galactosidase ONPG assay was performed to quantify the interaction.

Figure 4.4.1.1 Colony lift assay: Y2H positive colonies on filter paper

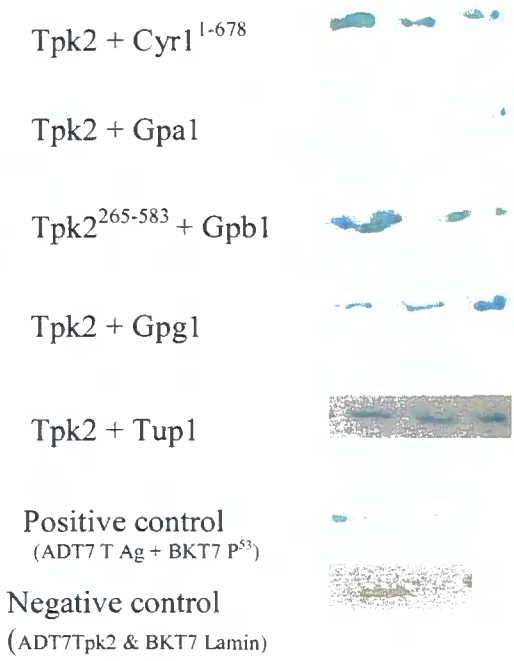

The blue colour on the filter paper represents a positive ß-galactosidase assay.

4.4.2 ß-Galactosidase ONPG assay

Positive colonies from the colony lift assay were subjected to ß-galactosidase ONPG assay. Colonies were grown in 5 ml of SD/-Leu/-Trp/-His/-Ade broth overnight and 2 ml was inoculated into 8 ml of fresh YPD. A negative control was grown on SD/-Leu/-Trp and AD-fusion Tpk2 and ADT7 vectors were grown on SD/-Leu/ broth. Cells were grown until log phase and then the cells were harvested, washed and resuspended in Z-buffer as described in section 2.13.2. Then the cells were lysed by repeated freezing and thawing cycles (5 cycles), ONPG was added to the tubes and incubated at 30°C (incubation times varied for each protein), when a strong yellow colour developed in the reaction tube, 400 µl of 1 M Na_2Co_3 was mixed, centrifuged

at 14k rpm for 10 minutes; the supernatant was transferred to a cuvette and the absorbance at OD_{420} was measured using a spectrophotometer (table. 4.4.2.1).

Table 4.4.2.1 β-Galactosidase ONPG assay data

Protein-protein interaction	OD_{600} of 1 ml culture	Incubation time-t Minutes	Test OD_{420} in triplicates	$\frac{1000 \times OD_{420}}{t \times V \times OD_{600}}$ Miller units	Mean value Miller units	Mean-highest value = + Value & Mean - lowest value= - Value
$Cyr1^{1-678}$ + Tpk2	0.8566	300	1. 0.2055 2. 0.1693 3. 0.207	1. 0.16 2. 0.1318 3. 0.2360	0.1759	+ 0.0601 - 0.0441
Gpa1+ Tpk2	1.1785	900	1. 0.6477 2. 0.7223 3. 0.7710	1. 0.1212 2. 0.1362 3. 0.1454	0.1345	+ 0.0109 - 0.0133
Gpb1+ Tpk2	1.3471	300	1. 0.4907 2. 0.8002 3. 0.6811	1. 0.1289 2. 0.1369 3. 0.1344	0.2495	+ 0.0524 - 0.061
Gpg1+ Tpk2	1.0359	300	1. 0.3817 2. 0.3334 3. 0.3681	1. 0.2457 2. 0.2146 3. 0.2369	0.2324	+ 0.0133 - 0.0178
Tup1+ Tpk2	0.6398	300	1. 0.3429 2. 0.3672 3. 0.2700	1. 0.3574 2. 0.3827 3. 0.2814	0.3405	+ 0.0422 - 0.0591
Positive control	1.31	1200	1. 2.9982 2. 3.0571 3. 2.9336	1. 0.381 2. 0.3889 3. 0.3732	0.381	+ 0.0079 - 0.0078
Negative control	1.5909	1140	1. 0.2320 2. 0.1754 3. 0.2056	1. 0.0271 2. 0.0251 3. 0.0240	0.0238	+ 0.0032 - 0.0.0033
ADT7 vector	1.56	1140	1. 0.1977 2. 0.22473 3. 0.2508	1. 0.0222 2. 0.0252 3. 0.0282	0.0252	+ 0.003 - 0.003
ADT7 Tpk2	1.04	1140	1. 0.1315 2. 0.1324 3. 0.1396	1. 0.02218 2. 0.02233 3. 0.02354	0.0226	+ 0.00094 - 0.00042

β-galactosidase units were calculated as follows

t = elapsed time (in minutes) incubation

V = 0.1 ml x concentration factor = 5

OD_{600} = A_{600} of 1 ml of culture

OD_{420} = A_{420} of test sample

$$\frac{1{,}000 \times OD_{420}}{t \times V \times OD_{600}}$$

1 miller unit of β-galactosidase is the amount which hydrolyzes 1 μmol of ONPG to-nitro phenol and D-galactose per min per cell.

Figure 4.4.2.2 β-Galactosidase Assay

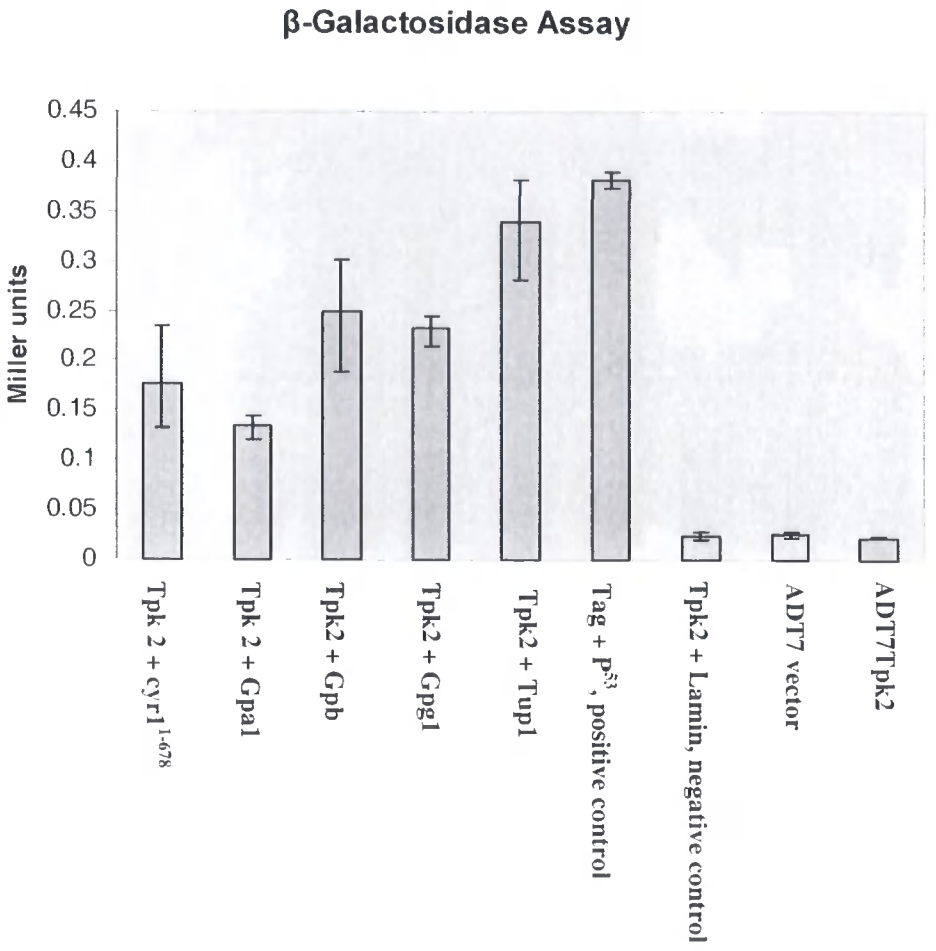

This assay quantifies the interaction of Tpk2 with other proteins. The result shows that Tup1 has highest affinity with Tpk2 and then decreasing order of affinity to Gpb1, Gpg1, Cyr1 N-terminus and Gpa1.

4.5 Negative results of Two-hybrid assays

The two-hybrid assay was extended to investigate interaction between Tpk2 N-terminus with the C-terminus, but there was no interaction detected between them. Tpk2 neither interact with Ras nor the G proteins Gpa2 and Gpa3. In another experiment no interaction was observed between Tup1 and Gpb1.

4.6 Protein kinase A catalytic subunit Tpk2 overexpression in *E. coli*

The cAMP-dependent Protein kinase A (PKA) is the main downstream component of the cAMP/PKA pathway, which acts downstream of adenylyl cyclase. *TPK2* has been sub-cloned for protein overexpression for functional analysis and for *in vitro* protein-protein interaction studies with G proteins and adenylyl cyclase.

Full length *TPK2* was cloned into pBAD Myc HisA, pGEX6p-3 (GST-fusion), pPICZA (*Pichia pastoris* intracellular expression vector) and pPIC9 (*Pichia pastoris* extracellular expression vector). Tpk2 cannot be overexpressed from any of the above constructs as a full length protein. Then Tpk2 C-terminus, comprising the catalytic domain 226-583, was cloned into pQE100, pET431a(+), pET21d(+) and pGEX6p-3 (GST-fusion) for protein over expression (for constructs see table 2.8.5). $Tpk2^{226\text{-}583}$ has been overexpressed via a pET21d(+) construct and partially purified from *E. coli* (Fig. 4.7.3.1).

4.7 Tpk2 C-terminus overexpression in *E. coli*

4.7.1 Tpk2 C-terminus 226-583 construction

The TPK2 fragment, encoding the C-terminus 226-583 was PCR amplified with *Nco*I and *Xho*I in the forward and reverse primers, respectively. *P. brasiliensis* pDNR cDNA was used as a PCR template for the proofstart DNA polymerase (QIAgen). The PCR products are shown in figure 4.7.1.1.

Figure 4.7.1.1 Agarose gel electrophoresis of PCR amplifications. Lanes 1, 2 and 3: PCR products of *TPK2*$^{226\text{-}583}$ to clone into pET21d(+) for protein overexpression.

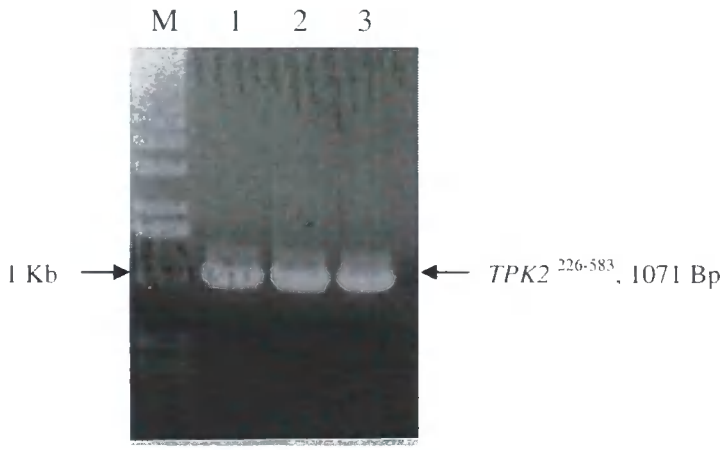

TPK2 PCR products were ligated into pGEMT easy vector and digested with *Nco*I and *Xho*I and further ligated into the pET21d(+) vector. The pET21d(+) *TPK2* was screened with restriction digestion with *Nco*I and *Xho*I enzymes as shown below (Fig. 4.7.1.2).

Figure 4.7.1.2 Agarose gel electrophoresis of pET21d(+)*TPK2*$^{226\text{-}583}$ digestion screens with *Nco*I and *Xho*I; lanes 1, 3, 5, & 7: undigested plasmids, lanes 2, 4, 6, & 8: digested plasmids which have the correct size inserts *TPK2*$^{226\text{-}583}$ and lane M: 1 Kb ladder.

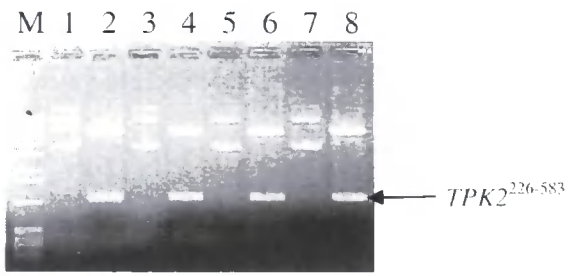

4.7.2 Tpk2 protein overexpression

P. brasiliensis TPK2 has been sub-cloned into various expression vectors to overexpress in *E. coli* and *Pichia* system (for contructs see table 2.8.2 and 2.8.5). In an attempt to overexpress Tpk2 full length and C-terminal protein in *E. coli* BL21(DE3), BL21(DE3) Codon plus, BL21(DE3) STAR, BL21-AI, C-41(DE3), C-43(DE3), Rosetta 2 and Origami (DE3) always formed inclusion bodies, which is described in methods section 2.18 and fig. 4.7.2.1. The protein overexpressed from the pQE100 *TPK2* construct also formed inclusion bodies in M15 *E. coli*. There was no overexpression observed from pBAD vector constructs in LMG and M15 *E. coli*. There was no protein expression detected in *Pichia pastoris* KS71H and GS115 strains. The Rosetta 2 cells died during overexpression due to the protein being toxic to *E. coli*. Finally Tpk2 was overexpressed in *E. coli* pLysS and partially purified as described in section 4.7.3.

Figure 4.7.2.1 SDS-PAGE of Tpk$^{226-583}$ cell pellet showing the inclusion bodies from BL21(DE3).

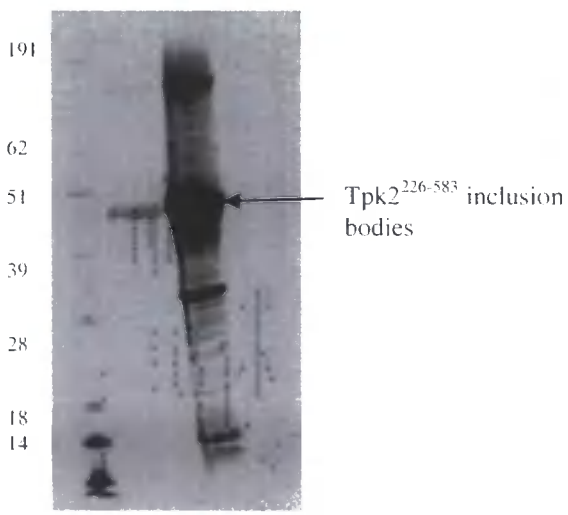

4.7.3 Partially purified Tpk2$^{226\text{-}583}$-His$_6$

The *TPK2* C-terminus 226-583 pET21d(+) construct was transformed into *E. coli* pLysS and fresh transformants were used for protein overexpression and the purification was carried out as described in methods section 2.18. After several attempts the protein was partially purified (Fig. 4.7.3.1) and confirmed by Western blot with monoclonal anti-polyhistidine and anti-mouse IgG AP conjugate antibodies (Fig. 4.7.3.2). Tpk2 was further concentrated using a Vivaspin column 30 kDa cut-off (see methods section. 2.25) and used for pull-down (see section. 4.8) and protein kinase assays (Fig. 4.9.2). The Tpk2 protein band was cut off from the SDS-polyacrylamide gel and verified by MALDI-TOF analysis at the School of Biological and Biomedical sciences, University of Durham, UK.

Figure 4.7.3.1 SDS-PAGE of Tpk$^{226-583}$-His$_6$ partially purified from *E. coli* pLysS.

Lane M: marker, lane cell: total proteins after cell disruption, lane FT: flow through, lanes 1-11: imidazole gradient elutions and lane 12: inclusion bodies from the cell pellets.

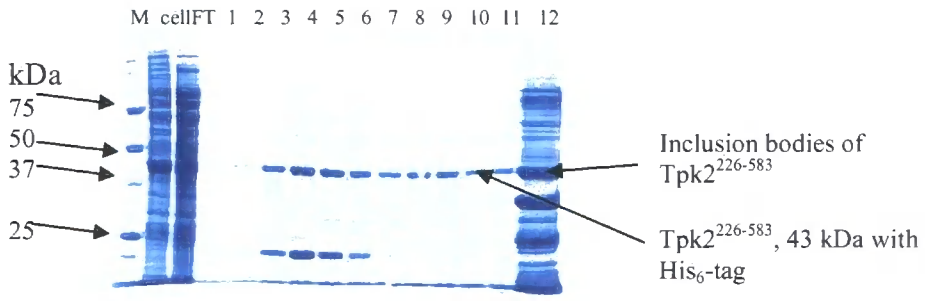

Figure 4.7.3.2 Tpk2$^{226-583}$-His$_6$ Western blot with monoclonal anti-polyhistidine antibodies 1; 5000 dilution (Sigma H-1029) and anti-mouse IgG AP conjugate (Sigma A-3562) as a secondary antibody as 1:5000 dilution)

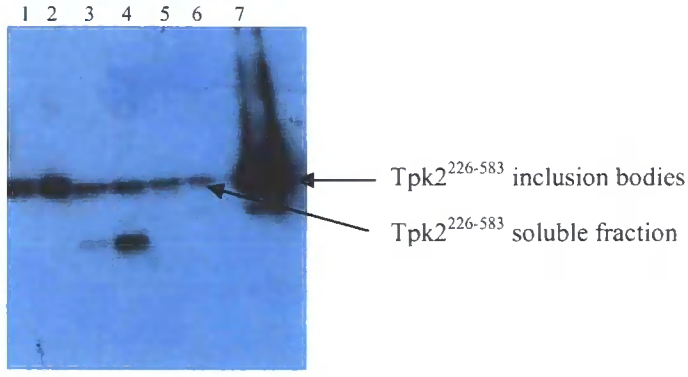

Lanes 1-6: Tpk2 imidazole gradient elutions from *E. coli* pLysS and lane 7: Tpk2 inclusion bodies.

4.8 Pull-down assay for Tpk2$^{226-583}$ with adenylyl cyclase and the G proteins, Gpb1 and Gpg1

P. brasiliensis cAMP-dependent PKA catalytic subunit Tpk2 C-terminus 226-583 was overexpressed from *E. coli* pLysS with His-tag (section. 4.7.3). The purified protein was used pull-down assay with adenylyl cyclase (Cyr1) Gα and Ras association domain 453-678-GST, Gpb1-GST and Gpg-GST. The GST-fusion proteins and GST-tag were also overexpressed from the vector pGEX6p-3 in *E. coli* Codon Plus (section. 3.2-3.5).

The GST fusion proteins Cyr1$^{453-678}$, Gpb1, Gpg and GST were immobilized on GST beads, Tpk2 C-terminal 226-583 with His-tag was mixed with the above beads and incubated at 4°C for 12 hours with end-over-end-rotation as described in section 2.19. The beads were centrifuged, washed in wash buffer seven times (20 mM HEPES pH 7.9, 600 mM NaCl, 1 mM DTT, 0.05% Tween 20 and 5% glycerol) and the proteins were then eluted from the beads with 4x LDS buffer by heating at 92°C for 5 minutes. 20 µl of the eluted protein was loaded on a 12% SDS polyacrylamide gel. The gel was then transferred to a PVDF membrane and a Western blot was performed as described in section 2.15. Tpk2 was detected by anti-polyhistidine monoclonal antibodies. The results confirmed the interaction of Tpk2 with Cyr1$^{453-678}$ and Gpb1 but not with Gpg1. Purified GST-tag was used as a negative control in all these assays (Fig. 4.8.1).

Figure 4.8.1 Pull-down assay: Tpk2$^{226-583}$-His$_6$ Western blot with monoclonal anti-polyhistidine antibodies 1; 5000 dilution (Sigma H-1029) and anti-mouse IgG AP conjugate (Sigma A-3562) as a secondary antibody as 1:5000 dilution) for the detection of Tpk2$^{226-583}$ His$_6$.

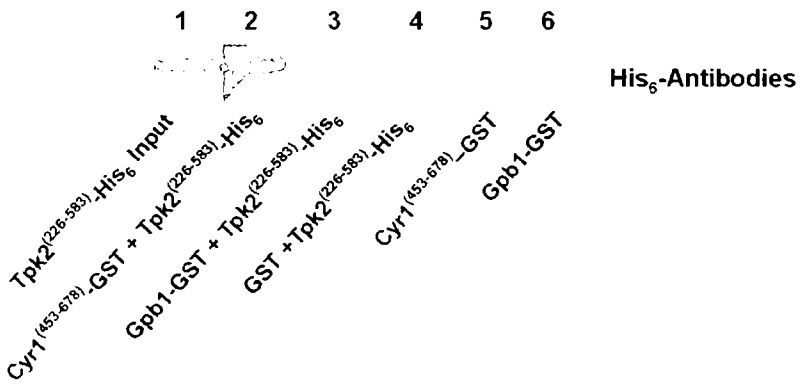

4.9 Protein Kinase A (PKA) Assay

Protein kinases, which carryout phosphorylation reactions, play a vital role in the integration of signalling networks in eukaryotic cells. The chemical activity of the kinase involves the removal of phosphate group from ATP and covalently attaching it to the free hydroxyl group of the target substrate. Partially purified *P. brasiliensis* cAMP-dependent PKA catalytic subunit $Tpk2^{226-583}$ from *E. coli* (section. 4.7.3) has been used for PKA assays. The PKA assay was performed using a ProFlour™ PKA assay (Promega) in a black 96-well flat bottom plate as described in section 2.39. The reaction uses PKA R110 (bisamide rhodamine 110) as a substrate, which is nonfluorescent. After the kinase reaction, the termination buffer (contains protease reagent) was added to the wells to stop the reaction. The protease reagent in the termination buffer specifically cleaves the amino acids from the nonphosphorylated PKA R110 substrate and the released R110 substrate is highly fluorescent where as the phosphorylated PKA R110 is resistant to protease digestion and remains nonfluorescent. Therefore the fluorescent intensity is inversely proportional to the kinase activity (table.4.9.1 & fig. 4.9.2). Using this assay we established that Pb $Tpk2^{226-583}$, C-terminus has PKA activity (Fig. 4.9.1). The 40 kDa cAMP-dependent protein kinase A purified from bovine heart (Promega) was used as a positive control.

Table 4.9.1 PKA assay-Fluorescent units

Proteins	Fluorescent units /FLU
No enzyme (buffer control)	1. 57603 2. 59598 3. 57907
No ATP	1. 59732 2. 59235 3. 60568
Bovine heart PKA (positive control)	1. 276 2. 293 3. 334
***P. brasiliensis* $Tpk2^{226-583}$**	1. 269 2. 311 3. 884

Figure 4.9.2 PKA Assay

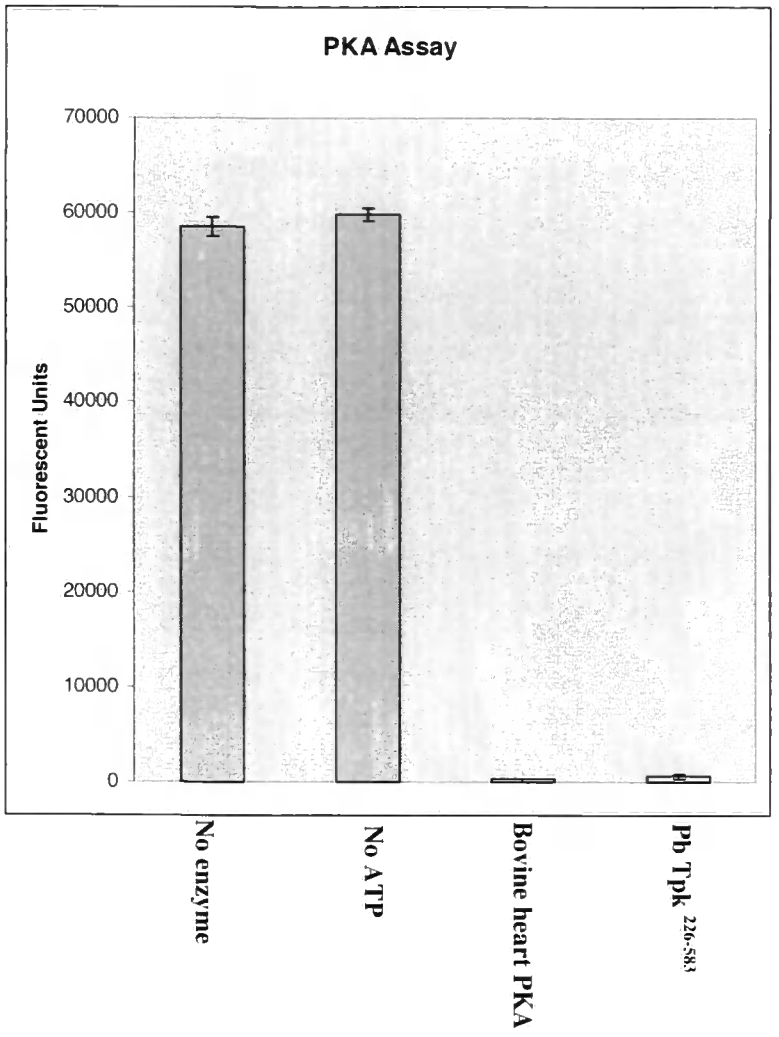

Figure representing bovine heart PKA (Promega) and *P. brasiliensis* Tpk2$^{226\text{-}583}$ have reduced fluorescence indicative of PKA activity; and the negative controls (no enzyme and no ATP) have high fluorescence indicative of no PKA activity.

4.10 Tpk2 N-terminus 1-225-GST overexpression in *E. coli*

A *TPK2* gene fragment encoding N-terminus 1-225 was sub-cloned into pGEX6p-3 with *Bam*H1 and *Sal*1 in the forward and reverse primers, respectively, for the overexpression of the GST-fusion protein for pull-down assays with Tup1. The *TPK2*$^{1-225}$*-GST* construct was transformed into *E. coli* Codon Plus and the culture was induced at an OD_{600} 0.5 with 0.1 mM IPTG for 5 hours at 25°C with 160 rpm in LB broth. The protein purification was performed as described in section 2.14 with increased washing conditions. The overexpressed Tpk2 N-terminus was cleaved by *E. coli*; in order to minimize the amount of cleavage, the protein was induced for a shorter duration (e.g. 5 hours) at 25°C. Those Fractions with less cleavage were further concentrated using a Vivaspin column as described in section 2.24. The proteins were confirmed by Western blot with anti-GST antibodies (Fig. 4.10.1.b).

Figure 4.10.1 a) SDS-PAGE of Tpk2$^{1-225}$ purified from *E. coli* codon plus.
Lane M: marker, lanes 1-8: elution from GST column.

b) Western blotting for Tpk2$^{1-225}$ with anti-GST antibodies (Novagen, 1:12,500 dilution as a primary antibody) and anti-mouse IgG AP conjugate (Sigma A 3562, 1:5000 dilution as a secondary antibody as 1:5000 dilution).

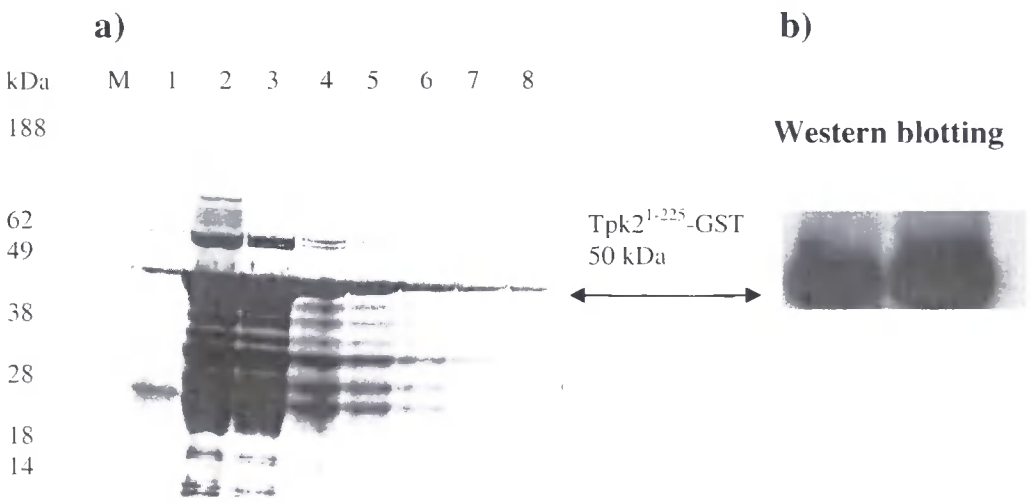

4.11 Overexpression and purification of Tup1-His_6

P. brasiliensis transcriptional repressor *TUP1* was sub-cloned into pET21d(+) vector with *Nhe*1 and *Xho*1 in the forward and reverse primers, respectively, for the overexpression of the protein with a His-tag in *E. coli*; in order to provide protein for the pull-down assays with the Tpk2 N-terminus. The *TUP1* construct was transformed into *E. coli* pLysS and 10 ml of 3 hours starter culture was used for 1 litre of medium. The cells were induced with 0.1 mM IPTG at an OD_{600} 0.5 for 5 hours at 25°C with 160 rpm in LB broth: 6 litres of culture were used for the overexpression and purification of Tup1. Purification was performed as described in section 2.18 with some modifications in the column washing. Initially the column was washed with 50 ml of buffer A with 25 mM and 50 mM imidazole concentration and then the protein was eluted with a 100-500 mM imidazole gradient. The eluted fractions were run on a 4-12% SDS-polyacrylamide gradient gel, which revealed that the Tup1 had several contaminating proteins (Fig. 4.11.1). Therefore in an attempt to further purify the protein by anion exchange using 'Q' sepharose column, the protein was dialysed into different buffers: 20 mM Tris with 30 mM NaCl and 20 mM Tris with 100 mM NaCl. In both buffer conditions the proteins precipitated and it seems that Tup1 is not stable at low salt concentration. Finally the proteins were purified from 9 litres of culture with a different column washing protocol. The column was washed with 100 ml of buffer A with 10 mM imidazole followed by 100 ml of 25, 50 and 75 mM imidazole (Fig. 4.11.2). The eluted fractions were further concentrated using a Vivaspin column as described in section 2.24. The protein concentration was 2.5 mg/ml (BCA™ protein assay kit, Pierce). The purified protein was confirmed by Western blot with anti-polyhistidine monoclonal antibodies (Fig. 4.11.3).

Figure 4.11.1 SDS-PAGE of Tup1-His_6 purification from the *E. coli* pLysS. Lane M: Seeblue marker, FT: flow through and lanes 1-10: 100-500 mM imidazole gradient elutions from nickel sepharose column.

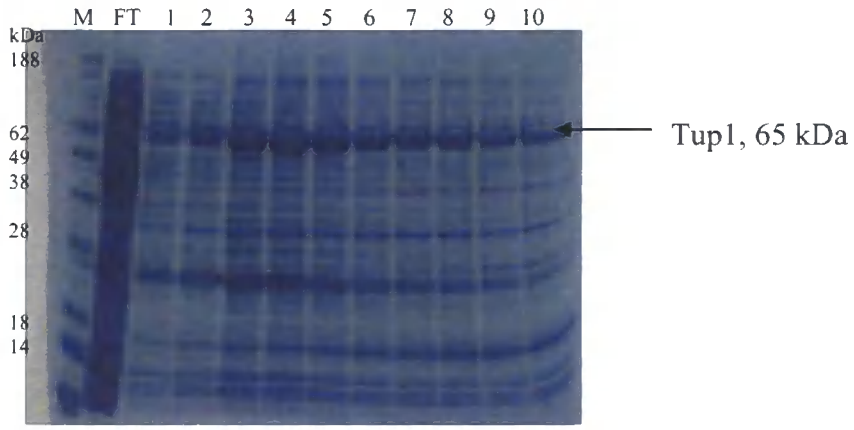

Figure 4.11.2 SDS-PAGE of Tup1-His_6 purification from *E. coli* pLysS.

Lane M: marker, lanes 1-7: imidazole gradient elutions.

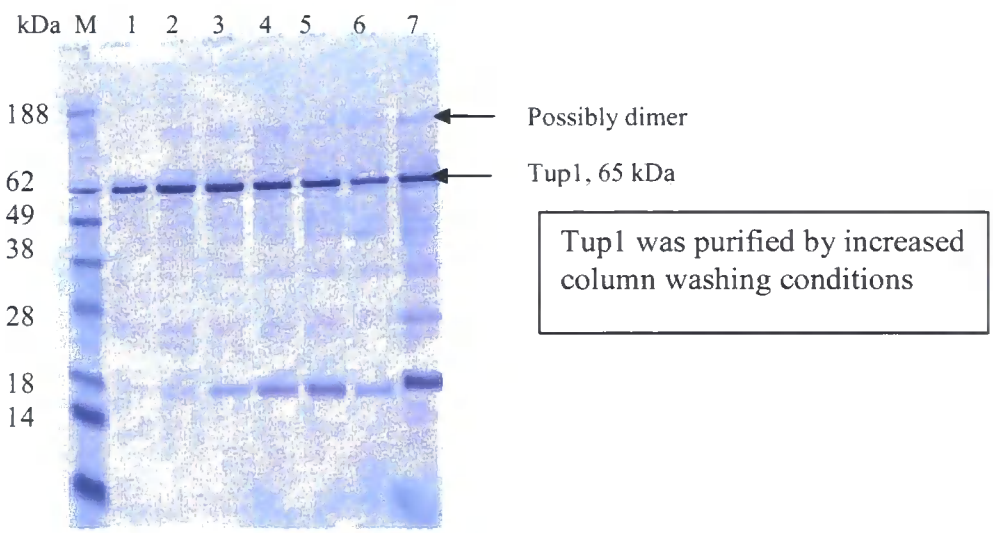

Figure 4.11.3 Tup1-His$_6$ Western blot with monoclonal anti-polyhistidine antibodies 1: 5000 dilution (Sigma H-1029) and anti-mouse IgG AP conjugate (Sigma A-3562) as a secondary antibody (1:5000 dilution)

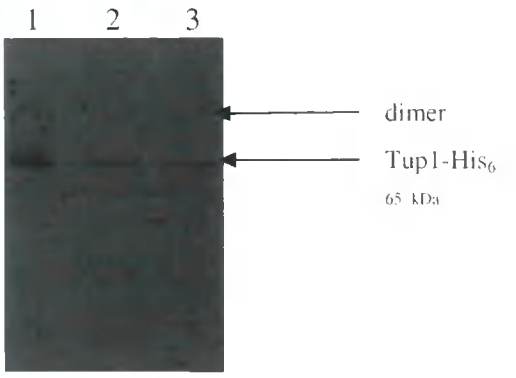

4.12 Pull-down assay for Tpk2 N-terminus-GST with Tup1-His$_6$

Tpk2 N-terminus 1-225-GST and GST-tag were immobilized on GST beads and washed 5 times with PBS. Tup1-His$_6$ was dialysed into pull-down buffer (for recipe see section. 2.19.1), mixed with the GST beads and the pull-down assay was performed as described in section 4.8 with some modifications. The reaction tubes were incubated at room temperature for 2 hours instead of 12 hours at 4°C. The Tup1 interaction with Tpk1$^{1-225}$ was detected by Western blot with anti-polyhistidine monoclonal antibodies as shown below (Fig. 4.12.1).

Figure 4.12.1 Pull-down assay: Tup1-His$_6$ Western blot with monoclonal anti-polyhistidine antibodies 1; 5000 dilution and anti-mouse IgG AP conjugate as a secondary antibody as 1:5000 dilution).

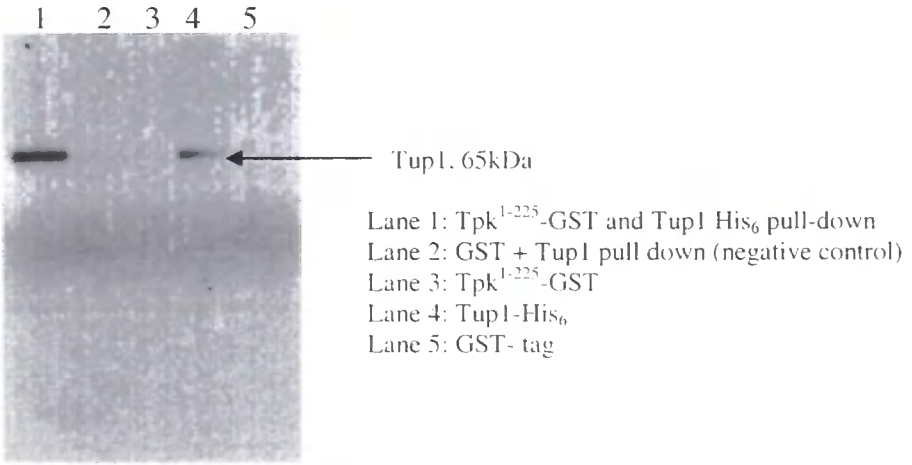

4.13 Library screening with Tup1

In order to find any co-transcription factor (e.g. Nrg1) which binds to Tup1 and any other potential candidates that interact with Tup1, a two-hybrid library transformation was performed. The *P. brasiliensis* pGAD library (table 2.3.2) was used for screening with Tup1. The BKT7 Tup1 construct was co-transformed with pGAD library as described in section 2.11. The transformants grown on SD-Leu/-Trp were further streaked on SD-Leu/-Trp/-His and then the colonies from SD-Leu/-Trp/-His were streaked on SD-Leu/-Trp/-His/-Ade with a-X-Gal for a-galactosidase assay. The positive colonies were selected by their blue colour (Fig. 4.13.1) and further subjected to ß-galactosidase assay colony lift assay in which the colonies were lifted to filter paper as described in section 2.13.1. The positive clones were selected by blue colour on the filter paper (Fig. 4.13.2). Plasmids were isolated from the positive clones using Clontech's yeast plasmid isolation kit described in section 2.11. The isolated plasmids were transformed into *E. coli* NovaBlue and ampicillin resistant clones selected. The ADT7 library plasmids were prepared using a QIAgen miniprep kit and the inserts were DNA sequenced with ADT7 sequencing primers at DBS genomics. The DNA sequence results were analysed with Broad Institute data base (www.broad.mit.edu). The proteins interacting with Tup1 are described in table. 4.13.3.

Figure 4.13.1 a-Galactosidase assay for Tup1 library screening, SD-Leu/-Trp/-His/-Ade agar plate with a-X gal

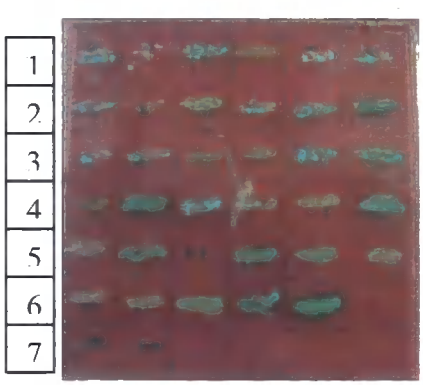

SD-Leu/-Trp/-His/-Ade with X-a- gal plate showing the blue colour colonies representing the positive for a-Galactosidase assay
Lanes 1-5: library transformants showing a-gal assay
Lane 6: Positive control
Lane 7: Negative control

Figure 4.13.2 ß-Galactosidase Assay; colony lift Assay

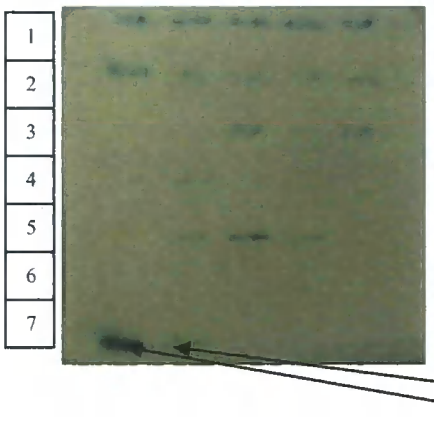

Blue colour colonies on whatman 5 filter paper representing positive for ß-galactosidase assay

Lanes 1-6: library transformants showing the ß-gal assay

Lane 7: positive/negative control

Table 4.13.3 Tup1 interacting proteins

1	Adenylsulfate kinase
2	Ubiquinone oxidoreductase
3	Actin family proteins
4	30 kDa Heat shock protein

The data base analysis of the DNA sequence of the library screening clones showed that Tup1 interacted with the above proteins (table. 4.13.3) in two hybrid library screening. These interactions need to be further confirmed by using full length gene sequences cloned from cDNA library.

4.14 Discussion

The upstream components of the cAMP pathway in *P. brasiliensis* such as the G proteins that interact with adenylyl cyclase have been described previously in chapter 3. The same analytic strategy was extended to find the potential upstream components interacting with downstream component of cAMP-dependent PKA. *Pb* cAMP-dependent PKA C-subunit *TPK2* was cloned previously in our lab using cDNA and gDNA library screening. The cloned *P. brasiliensis* Tpk2 has highest homology with Tpk2 of *S. cerevisiae* and *C. albicans* (chapter 5, see table. 5.9.1), therefore it has been named Tpk2.

The two-hybrid analyses for Tpk2 with G proteins and adenylyl cyclase were performed to investigate the role of PKA in the cAMP pathway. Fungal cAMP-dependent PKA has several conserved 'Q' residues at the N-terminus and these are responsible for protein-protein interactions (Liebman *et al.*, 2004; Sonneborn *et al.*, 2000). *P. brasiliensis* Tpk2 has 583 amino acids and includes 2 glutamine 'Q' stretches that total 36 'Q' residues in the N-terminus located between 175 to 186 and 229 to 254 and these are interrupted by proline and histidine residues (see fig. 5.1.3) In contrast, other fungi have only one stretch of 'Q' residues interrupted by proline. *P. brasiliensis* Tpk2 has a long N-terminus which is absent in mammalian Tpk and a few fungal Tpks (Liebmann *et al.*, 2004; Sonneborn *et al.*, 2000). In order to find the interaction domains; *P. brasiliensis* Tpk2 was truncated into its N-terminal (e.g $Tpk2^{(1-174)}$ and $Tpk2^{(1-270)}$ with and without 'Q' residues, respectively) and at its C-terminal (e.g $Tpk2^{(226-583)}$ and $Tpk2^{(265-583)}$ with and without 'Q' residues, respectively) domains. The full length $Tpk2^{(1-583)}$ was also assayed (see table. 2.8.1). *P. brasiliensis* adenylyl cyclase has 4 major domains when analysed with SMART (EMBL) (see section 3.12, Chen *et al.*, 2007). Tpk2 truncates and full length *TPK2* was tested by two-hybrid assay for interactions with the 4 domains of adenylyl cyclase and G proteins.

Two-hybrid assays confirmed the interaction of Tpk2 N-terminus 1-270 with adenylyl cyclase N-terminus 1-678 (Gα and Ras association domain) and the serine/threonine phosphatase family 2C catalytic domain (PP2Cc) domain. All the truncations of Tpk2 and full length interacted with the adenylyl cyclase N-terminus 1-678 (Gα and Ras association domain), which appears to be used as a scaffold for protein binding. The Tpk2 catalytic domain (C-terminus 265-583) interacts the with adenylyl cyclase catalytic domain (CYCc) (table. 4.2.1); possibly this interaction could enable Tpk2 to modulate the catalytic activity of AC. The interaction of Tpk2 with adenylyl cyclase N-terminus 1-678 was further confirmed by both α-galactosidase assay (Fig. 4.3.1) and β-galactosidase assay colony lift and ONPG (quantitative assay) (Fig. 4.4.1.1 & 4.4.2.2). The adenylyl cyclase catalytic domain and N-terminus 1-678 formed inclusion bodies (chapter. 3, section. 3.2), therefore the Gα binding domain was used for the pull-down assays. The GST pull-down assay confirmed the interaction of Tpk2 C-terminus 226-583 (catalytic domain) with

AC Gα binding domain 453-678 (Fig. 4.8.1). Previously it was shown that the AC N-terminus (Gα binding domain) can interact with Gpa1 and Gpb1 (chapter 3, fig. 3.9.1 & 3.10.1, Chen *et al.*, 2007). *S. cerevisiae tpk* mutant shows hyper-accumulation of cAMP, suggesting that PKA activity is required as part of a feedback mechanism to reduce cAMP levels (Mbonyi *et al.*, 1990; Nikawa *et al.*, 1987). PKA acts as a strong feed back inhibitor of cAMP, by activating the phosphodiesterase Pde1 by phosphorylation has been shown in several fungi (Hicks *et al.*, 2005; Ma *et al.*, 1999). For the first time we have shown that *P. brasiliensis* Tpk2 directly interact with adenylyl cyclase.

Two-hybrid assays and GST pull-down assays confirmed the interaction of Tpk2 C-terminus 226-583 (catalytic domain) with G protein Gpb1 (Fig. 3.8.1). In *S. cerevisiae*, the G protein mimics Krh1 interacts with the protein kinase A catalytic subunits Tpk1-3, causing them to interact with the regulatory subunit Bcy1 to reduce PKA activity. The *krh1/2* mutants show high PKA activity indicating that G proteins bypass adenylyl cyclase and directly act on protein kinase A (Peeters *et al.*, 2006; Peeters *et al.*, 2007). In haploid *S. cerevisiae*, the Gβ mimics *krh1/2* mutants have a hyperinvasive and showing high levels of expression of *FLO11* (Batlle *et al.*, 2003). This indicates that the G proteins down-regulate PKA activity.

The Tpk2 C-terminus also interacts with the G proteins Gpa1 and Gpg1 in two-hybrid assays (figures. 4.3.1, 4.4.1.1. & 4.4.2.2), but no interaction was detected between Tpk2 and Gpg1 in the GST pull-down assay and, previously, we found that there is no interaction between Gpb1 and Gpg1 in a pull-down assay (chapter 3, fig. 3.8), since molecular chaperones are required for Gpb1 and Gpg1 interaction (Lukov *et al.*, 2005). It could be that in a similar way, the Gpg1 requires some molecular chaperones that enable it to interact with Tpk2 *in vivo*, why Gpg1 and Gpa1 interact with Tpk2 is unclear.

A two-hybrid assay confirmed the interaction of Tpk2 N-terminus 1-270 with the WD-repeat transcription factor (transcriptional repressor) Tup1 (α-galactosidase assay fig. 4.3.1 & β-gal assay figures 4.4.1.1 & 4.4.2.2) and establishes that it binds to a region between residues 175-265, which has two stretches of 'Q' residues (see

table. 4.2.1). In order to confirm these interactions, Tpk2 N-terminus 1-225 and Tup1 were overexpressed in *E. coli* with a GST-tag and His-tag, respectively. The GST pull-down assay confirmed the interaction between Tup1 and Tpk2 N-terminus (Fig. 4.12.1); establishing for the first time in fungi that Tup1 can interact with PKA. Tup1 is involved in many pathways: for example, in *P. marneffei* Tup1 homologue supports the filamentous form of the fungus and represses yeast morphogenesis (Todd *et al.*, 2003). Tup1 has WD-repeats that are similar to these in the G protein Gβ subunit, which we previously found to interact with Tpk2, suggesting that Tpk2 can bind to proteins with similar WD repeats.

In *S. cerevisiae,* Tup1 represses the transcription of many functionally related genes by interacting with their cognate transcription factors and specific DNA binding proteins (Keleher *et al.*, 1992; Park *et al.*, 1999; Ronne, 1995; Treitel and Carlson, 1995). A two-hybrid library screening was performed to find any cognate transcription factor such as an homologue of Nrg1; but Tup1 was found to interact with proteins such as adenylate sulphate kinase, actin family protein and Heat shock protein 30 (table. 4.13.3). The biological significance of these interactions has to be investigated.

P. brasiliensis Tpk2 is involved in various interactions, but the biological significant interactions are as follows:

1) Interaction with AC probably acts as a feed back inhibitor of cAMP.

2) Interaction with G protein Gpb1 down-regulates its own activity (PKA activity).

$Tpk2^{1-174}$ (without 'Q' residues) had no interaction with any of the proteins specified in this chapter, which confirms that the 'Q' residues are necessary for protein-protein interactions (table 4.2.1).

CHAPTER FIVE

P. brasiliensis Tpk2 Complements *S. cerevisiae Δtpk2*

The *P. brasiliensis* cAMP-dependent protein kinase A catalytic subunit *TPK2* has been cloned previously in our lab. A recent genome sequence search revealed the presence of a second cAMP-dependent protein kinase A subunit, which we term *TPK1*. The current study has focused on the functional characterisation of *Pb* Tpk1 and Tpk2. *Pb* Tpk2 has the highest homology with Tpk2 of *S. cerevisiae* and *C. albicans* (see table. 5.1.1); whilst *P. brasiliensis* Tpk1 is homologous to Tpk3 of *S. cerevisiae*. Therefore *S. cerevisiae* has been used as a model system to analyse the function of *P. brasiliensis* in complementation assays. Two *S. cerevisiae tpk2* mutants were used in this study; an haploid temperature sensitive (Ts) strain, which cannot grow at 37°C (Smith *et al.*, 1998), and a diploid strain XPY5**a**/α, which cannot produce pseudohyphae under low nitrogen conditions (Pan and Heitman, 1999) were used to study *Pb* Tpk in complementation assays. The use of these strains for complementation is described in this chapter.

5.1 *P. brasiliensis* Tpk2 characterisation

The *P. brasiliensis* PKA catalytic subunit Tpk2 has a long N-terminal region that is absent in other PKAs. Therefore *P. brasiliensis* Tpk2 has been truncated into its N- and C-terminus and these were analyzed by the vector NTI program; the results of this analysis are shown in figure 5.1.3. The C-terminus of *P. brasiliensis* Tpk2 is similar to Tpk of other organisms (see table 5.1.1)

Table 5.1.1 ***P. brasiliensis*** **Tpk2 homology with other fungi as listed below.**

S.No	Organism/protein	Identity with *Pb* Tpk2 (226-583) (C-terminus)	Identity with *Pb* Tpk2 Full length(1-583)
1	*S. cerevisiae* Tpk1	54%	37.7%
2	*S. cerevisiae* Tpk2	65%	43.4%
3	*S. cerevisiae* Tpk3	56.4%	39.5%
4	*C. albicans* Tpk2	65%	43.4%
5	*A. fumigatus* pkaC1	60.6%	57.7%
6	*A. nidulans* AnpkaA	58.1%	53.5%
7	*U. maydis* Uka1	42%	28.6%
8	*U. maydis* Adr-1	53.9%	39.4%
9	*A. fumigatus* Afpka-EAL9142	40.6%	27.8%
10	*P. brasiliensis* Tpk1	28.1%	27.8%

Figure 5.1.2 Phylogenetic relationship of cAMP-dependent PKA

The phylogenetic tree was constructed by Vector NTI alignX (Informax), which explains the relationship between *Pb* cAMP-dependent PKA catalytic subunit Tpk with other related organisms PKAs.

The abbreviations are: Pb, *P. brasiliensis*; Sc, *S. cerevisiae*; Af, *Aspergillus fumigatus;* An, *Aspergillus nidulans;* Ca, *Candida albicans;* Um, *Ustilago maydis.*

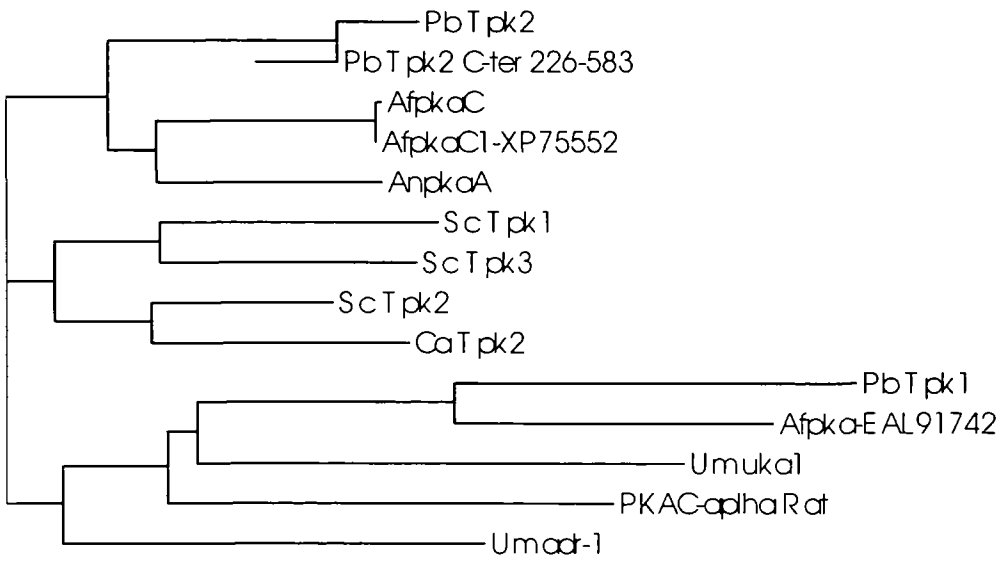

Figure 5.1.3 Comparative alignment of cAMP-dependent PKA catalytic subunits. The proteins were aligned by Vector NTI alignment (Informax). The abbreviations are: Pb, *P. brasiliensis*; Sc, *S. cerevisiae*; Af, *Aspergillus fumigatus;* An, *Aspergillus nidulans;* Ca, *Candida albicans;* Um, *Ustilago maydis*. The following symbols indicate conserved sequences.

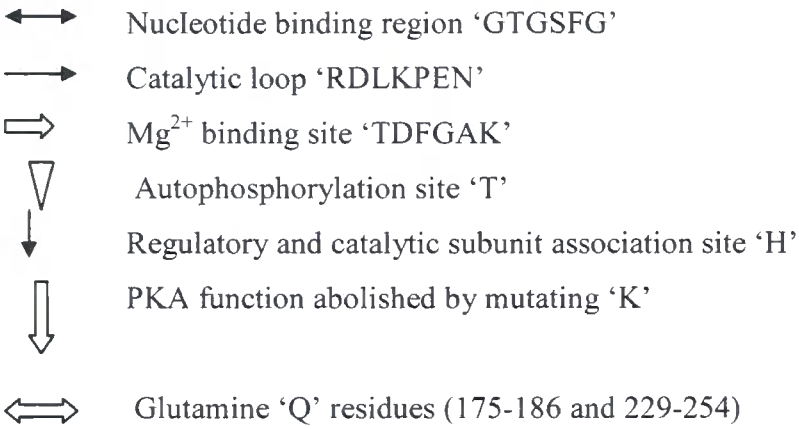

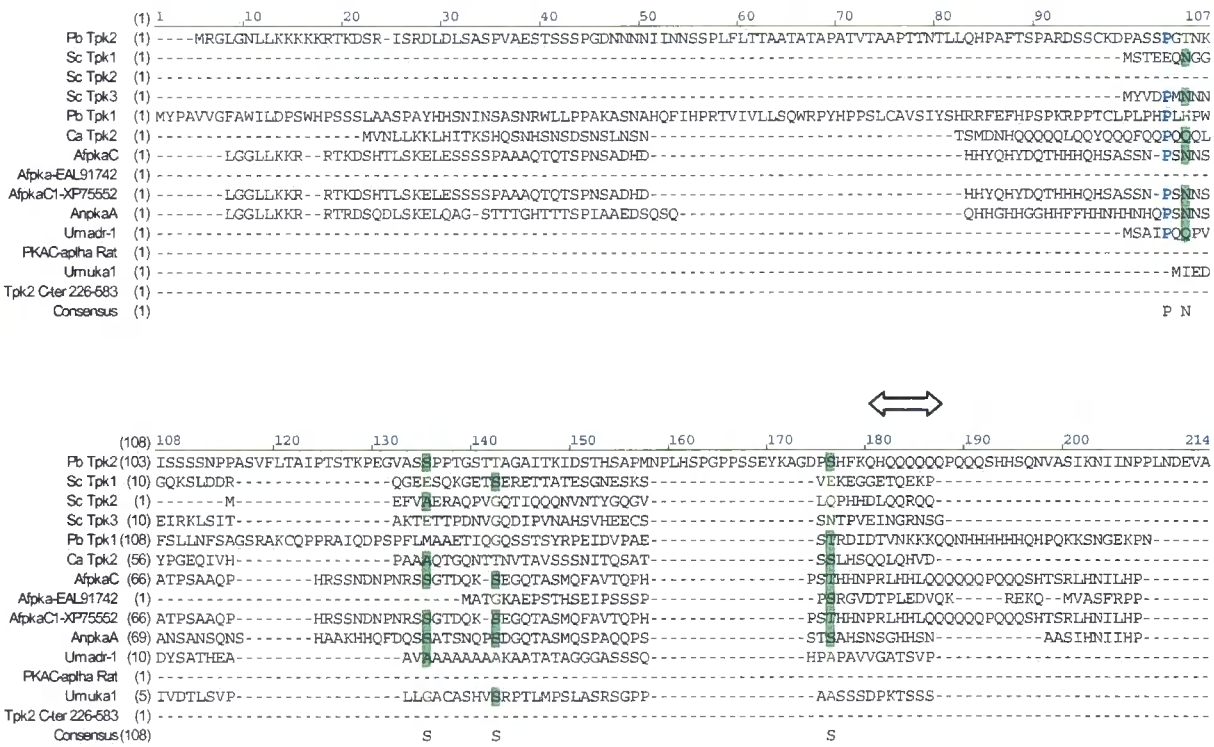

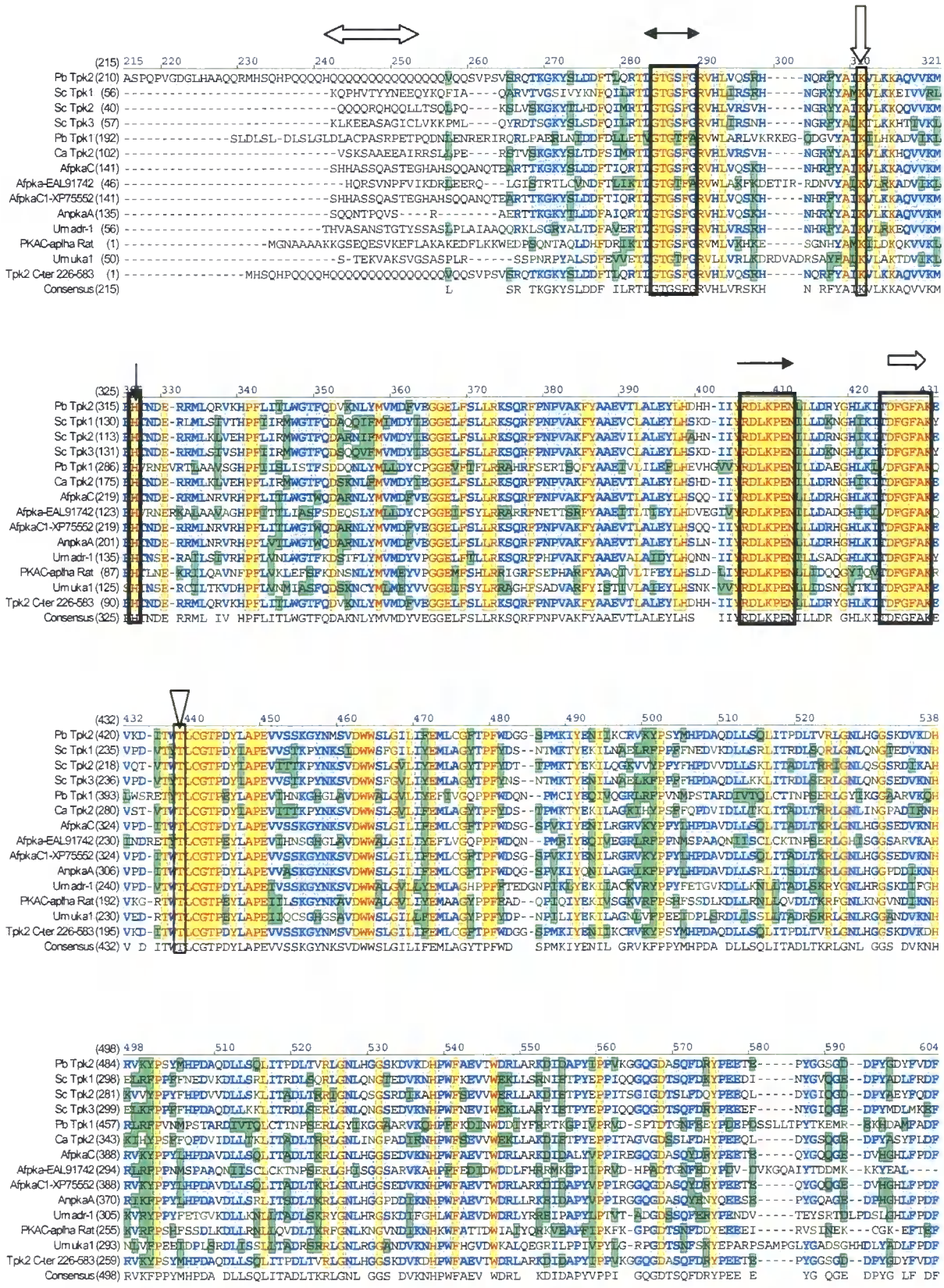
Pb Tpk2 (210)
Sc Tpk1 (56)
Sc Tpk2 (40)
Sc Tpk3 (57)
Pb Tpk1 (192)
Ca Tpk2 (102)
AfpkaC (141)
Afpka-EAL91742 (46)
AfpkaC1-XP75552 (141)
AnpkaA (135)
Um adr-1 (56)
PKACaptha Rat (1)
Um uka1 (50)
Tpk2 C-ter 226-583 (1)
Consensus (215)
Pb Tpk2 (315)
Sc Tpk1 (130)
Sc Tpk2 (113)
Sc Tpk3 (131)
Pb Tpk1 (286)
Ca Tpk2 (175)
AfpkaC (219)
Afpka-EAL91742 (123)
AfpkaC1-XP75552 (219)
AnpkaA (201)
Um adr-1 (135)
PKACaptha Rat (87)
Um uka1 (125)
Tpk2 C-ter 226-583 (90)
Consensus (325)
Pb Tpk2 (420)
Sc Tpk1 (235)
Sc Tpk2 (218)
Sc Tpk3 (236)
Pb Tpk1 (393)
Ca Tpk2 (280)
AfpkaC (324)
Afpka-EAL91742 (230)
AfpkaC1-XP75552 (324)
AnpkaA (306)
Um adr-1 (240)
PKACaptha Rat (192)
Um uka1 (230)
Tpk2 C-ter 226-583 (195)
Consensus (432)
Pb Tpk2 (484)
Sc Tpk1 (298)
Sc Tpk2 (281)
Sc Tpk3 (299)
Pb Tpk1 (457)
Ca Tpk2 (343)
AfpkaC (388)
Afpka-EAL91742 (294)
AfpkaC1-XP75552 (388)
AnpkaA (370)
Um adr-1 (305)
PKACaptha Rat (255)
Um uka1 (293)
Tpk2 C-ter 226-583 (259)
Consensus (498)

5.1.4 SMART Analysis of *P. brasiliensis* Tpk2

P. brasiliensis Tpk2 was analysed with SMART (EMBL) and this analysis revealed two major domains; a serine/threonine protein kinase catalytic domain 272-527 (S_TKc) and an extension to the serine/threonine protein kinase domian 528-583 (S_TKc_X). The other domains are marked as low complexity regions, which are shown in the figure 5.1.4.1 and table 5.1.4.2. This predicts that the *Pb* cAMP-dependent PKA catalytic domain is present at its C-terminus.

Figure 5.1.4.1 Domains of *Pb* Tpk2

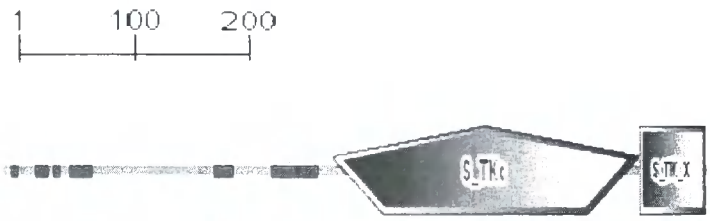

Table 5.1.4.2 Tpk1 Domain positions

Name	Begin	End	E-value
low complexity	7	13	-
low complexity	27	39	-
low complexity	42	49	-
low complexity	56	75	-
low complexity	175	191	-
low complexity	223	262	-
S_TKc	272	527	5.27e-105
S_TK_X	528	583	1.61e-08

The figure and table are retrieved from the SMART (EMBL) software analysis.

5.2 *TPK2* constructions

The *P. brasiliensis* cAMP-dependent PKA catalytic subunit *TPK2* full length (FL), N-terminus 1-225-*GFP* and C-terminus 226-583-*GFP* were sub-cloned into p426MET25 vector (for constructs; see table. 2.8.2). First the gene encoding *GFP* (EGFP,Clontech) was amplified by high fidelity proofstart DNA polymerase (QIAgen) and sub-cloned into p426 (Fig. 2.29.1; vector map), with *Eco*RI and *Sal*I sites as shown in figure 5.2.1, and then the Tpk2 N-terminus and C-terminus were fused to the *GFP* gene via the *Eco*RI site. *TPK2* (FL) and its fragments were amplified from a *P. brasiliensis* cDNA library (Fig. 5.2.2). These were subsequently digested with the restriction enzymes (Fig. 5.2.1; restriction sites) and the PCR products ligated into p426MET25 vector, which had been digested with same restriction enzymes. The recombinant plasmids were then transformed into *E. coli* NovaBlue and these were grown, the plasmid was extracted and screened by restriction digestion (Fig. 5.2.3-5.2.5). The positive plasmids were DNA sequenced at Durham Biological Science (DBS) Genomics facility.

Figure 5.2.1 Construction Map of *TPK2* for p426 MET25 Vector

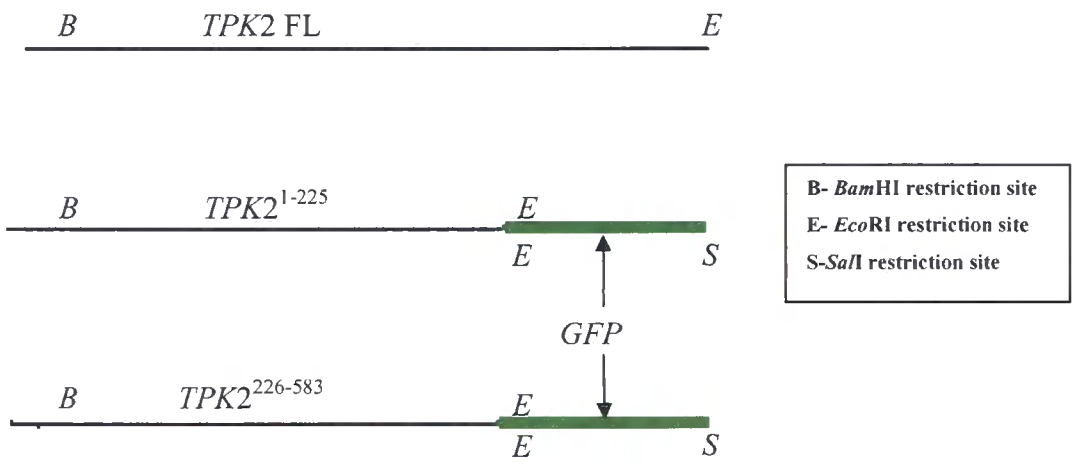

Figure 5.2.1 represents *TPK2* full length (FL) was constructed with stop codon and without *GFP* fusion. The N-terminus $TPK2^{1\text{-}225}$ and C-terminus $TPK2^{226\text{-}583}$ were constructed with *GFP* fusion.

Figure 5.2.2 Agarose gel electrophoresis of *TPK2* and *GFP* PCR products to clone into p426MET25 vector.

(a) Lane M: 1 Kb ladder and lane 1 & 2 *TPK2* full length (FL) PCR products

(b) Lane M: 1 Kb ladder; lane 2: $TPK2^{1-225}$ PCR products and

(c) Lane 1 & 2: $TPK2^{226-583}$ PCR products, lane M: 1 Kb ladder and lane 3 & 4: *GFP* PCR products.

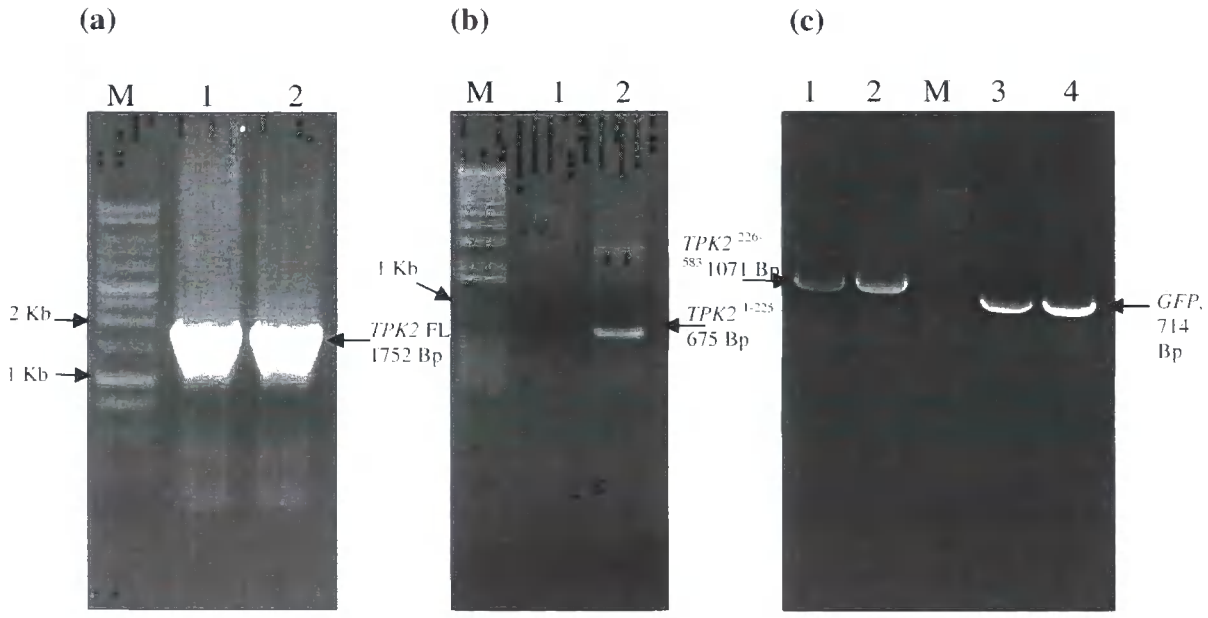

The PCR products were gel extracted. *TPK2* full length PCR product was restriction enzyme digested with *Bam*HI and *Eco*RI and ligated into the p426MET25 vector. The *GFP* PCR product was restriction enzyme digested with *Eco*RI and *Sal*I and ligated into the p426MET25 vector. The *TPK2* N-terminus 1-225 and C-terminus 226-583 were restriction enzyme digested with *Bam*HI and *Eco*RI and ligated into the p426MET25-GFP vector. After ligation and transformation, restriction digestion screens were performed (Fig. 5.2.3-5.2.5) to identify successful clones.

Figure 5.2.3 **Agarose gel electrophoresis of *TPK2*$^{1-583}$ (FL)** p426MET25 digestion screens with *Bam*HI and *Eco*RI. Lanes 1-6: digested *TPK2* and lane 7: undigested plasmids

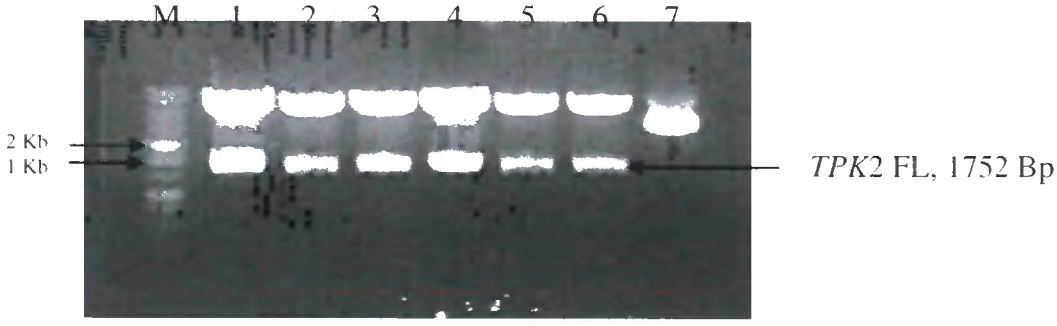

All the digested plasmids had the *TPK2* full length insert.

Figure 5.2.4 **Agarose gel electrophoresis of p426MET25 -*GFP*** digestion screens with *Eco*RI and *Sal*I,

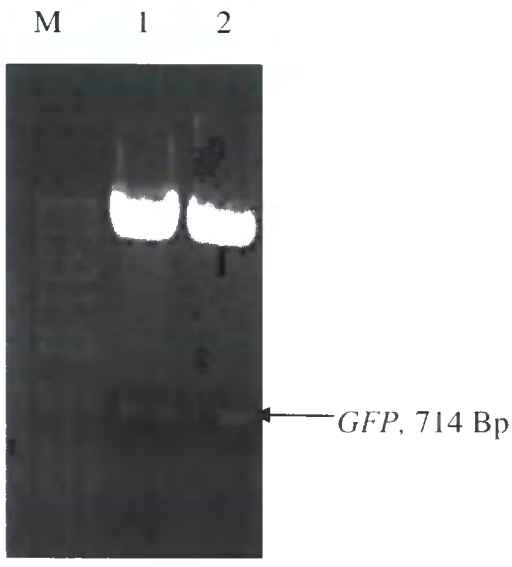

Lane 1 and 2 both have the insert (*GFP*). This p426MET25-GFP construct was restriction enzyme digested with *Bam*HI and *Eco*RI and *TPK2* 1-225 and 226-583 PCR products were ligated to make the *GFP* fusion proteins. The screening of the *TPK2* truncated *GFP* fusion was performed by restriction digestion (Fig. 5.2.5).

Figure 5.2.5 **Agarose gel electrophoresis of *TPK2* N & C-terminus** p426MET25-*GFP* digestion screens with *Bam*HI and *Eco*RI. Lane 1 and 3: digested $TPK2^{1-225}$ (lane 1 has the insert) lane 2 and 4: undigested $TPK2^{1-225}$, lane 5 and 7: digested *TPK2* C-terminus 226-583 (both lanes have inserts) and lane 4 & 6: undigested *TPK2* p426MET25-*GFP*

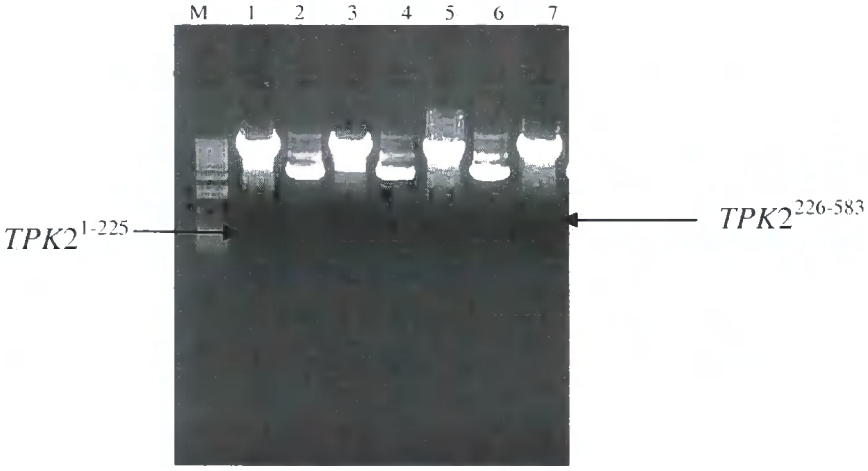

5.3 Tpk2 complementation in *S. cerevisiae tpk2* temperature sensitive mutant SGY446

The *S. cerevisiae* haploid strain SGY446, a *tpk2* temperature sensitive mutant (Smith *et al.*, 1998), has been used to study the function of *P. brasiliensis* Tpk2 by complementation assay. *P. brasiliensis TPK2* truncated at its N-terminus 1-225-*GFP*, its C-terminus, comprising of the catalytic domain 226-583-*GFP*, and full length constructs (section 5.1) were transformed into *S. cerevisiae* SGY446. Transformants were streaked on SD-uracil plates and incubated at 25°C and 37°C as described in section 2.30. It was shown that the SGY446 haploid strain does not grow at 37°C; whilst strains transformed with *P. brasiliensis* Tpk2 C-terminus and full length were able to grow at 37°C and complemented the functional PKA (Fig. 5.3.1). The GFP-fusion constructs expressed the green fluorescence protein, which is shown in section 5.7. These proteins were extracted from these transformants and confirmed by Western blot which is described in section. 5.6.

Figure 5.3.1 ***P. brasiliensis*** **Tpk2 complements** ***S. cerevisiae tpk2*** **Ts mutant SGY446**

(a) SD-URA 25°C

(b) SD-URA 37°C

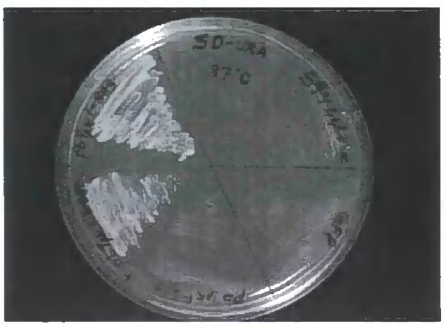

(c) Streak pattern

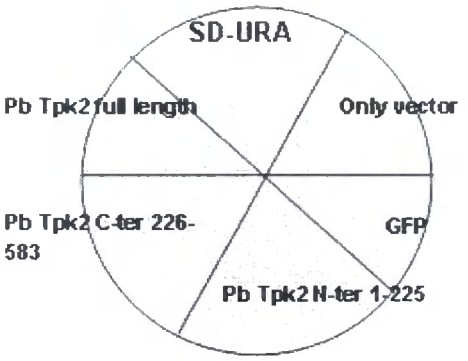

Figure 5.3.1

(a): *S. cerevisiae* SGY446 haploid strain transformed with empty plasmid (p426MET25), plasmid with only *GFP*, *P. brasiliensis TPK2* N-terminus 1-225 and C-terminus 226-583 and *TPK2* full length 1-583 were streaked on SD-uracil plate and incubated at 25°C; all the transformants were able to grow.

(b): the same colonies mentioned as above were streaked on another plate and incubated at 37°C; the transformants carrying the functional PKA (C-terminus & full length) have grown.

(c): the streaking pattern.

5.4 *P. brasiliensis* Tpk2 induce pseudohyphae in *S. cerevisiae tpk2* mutant

The diploid *S. cerevisiae* wild-type MLY61**a**/α and *tpk2* mutant XPY5**a**/α (Pan and Heitman, 1999) strains were used to study the function of *P. brasiliensis* Tpk2. The wild type can produce pseudohyphae at low nitrogen conditions, but the mutant XPY5**a**/α cannot. *P. brasiliensis* Tpk2 truncated N-terminus 1-225-*GFP*, C-terminus 226-583-*GFP* and full length without *GFP*-fusion constructs were transformed into the diploid *S. cerevisiae* wild-type and *tpk2* mutant strains. For pseudohyphae analysis, the transformants were streaked on SLAD agar with 50-200 μM ammonium sulphate and pseudohyphae were observed under 20x magnification, using an Eclipse E-400 microscope as described in the section 2.30. *P. brasiliensis TPK2* FL and C-terminus 226-583 transformants were able to produce pseudohyphae (Fig. 5.4.1) but the N-terminus could not.

Figure 5.4.1 Pb Tpk2, pseudohyphae analysis in *S. cerevisiae tpk2*Δ

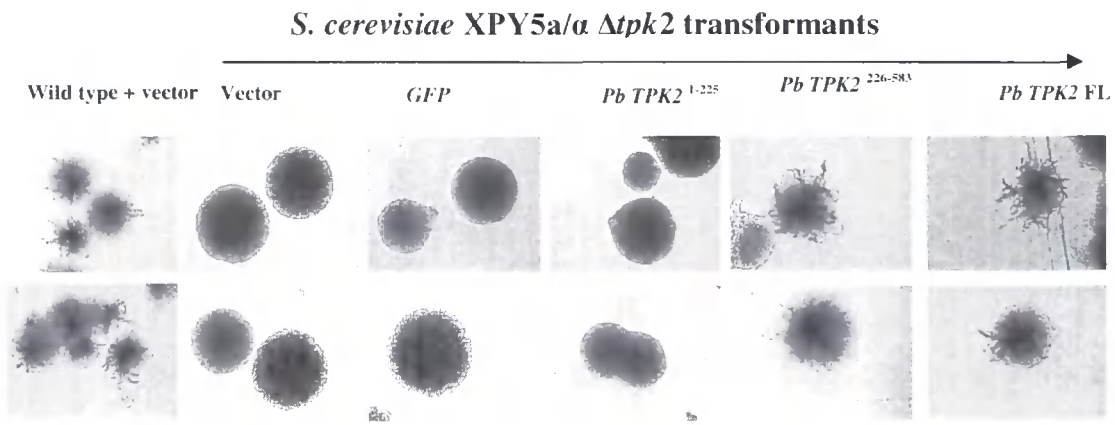

Upper panels-SLAD agar with 50 μM ammonium sulphate

Lower panels-SLAD agar with 200 μM ammonium sulphate

Arrow indicates the pseudohyphae and scale bar for the whole picture: 0.72 mm

5.5 Gpb1-GFP inhibits the function of Tpk2

5.5.1 Construction of *GPB1-GFP*

The G protein Gpb1 was fused to GFP for co-expression with Tpk2 FL (no GFP fusion). For *GPB1* fusion another *GFP* construct was made with *Hin*dIII and *Sal*I and then *GPB1* was fused to the *Hin*dIII site as described in 2.33 (for constructs see table. 2.8.2).

Figure 5.5.1.1 Construction map of *GPB1-GFP*

GPB1 was fused to N-terminus of *GFP* in *Hin*dIII restriction site.

5.5.2 Coexpression of Tpk2 and Gpb1-GFP

The interaction of Gpb1 with the Tpk2 C-terminal (226-583) functional catalytic domain was confirmed by two-hybrid and GST pull-down analyses (Fig. 4.3.1 & 4.8.1). In order to discern the effect of the interaction *in vivo,* Gpb1-GFP was co-expressed with Tpk2 full length. *S. cerevisiae* SGY446 haploid *tpk2* temperature sensitive mutant and diploid *Δtpk2* XPY5**a**/a strains had been transformed with *P. brasiliensis TPK2*$^{1\text{-}583}$ (FL), were further transformed with the *GPB1-GFP* and the transformants selected on the basis of their green fluorescence due to the expression of GFP. As a control, *GPB1-GFP* was also transformed into the *S. cerevisiae* wild-type MLY61**a**/a and *tpk2* mutant strains. The diploid transformants were streaked on SLAD agar with 50-200 μM ammonium sulphate and the effect on pseudohyphae was analysed as described in section 5.3. The haploid SGY446 transformants were streaked on SD-uracil plates and incubated at 25°C and 37°C as described in section 5.3.

We found that *Pb* Gpb1-GFP inhibits the formation pseudohyphae by interacting with Tpk2 (Fig. 5.5.2.2; right end) but has no effect on wild-type and *S. cerevisiae* Δ*tpk2* cells. *P. brasiliensis* Gpb1-GFP inhibited the growth of the *S. cerevisiae* SGY446 strain at 37°C (Fig. 5.5.2.1). The expression of both Tpk2 and Gpb1-GFP in both the transformants was confirmed by Western blot with specific antibodies (section. 5.6).

Figure 5.5.2.1 Pb Gpb1-GFP inhibits the growth (SGY446) of Pb *TPK2* transformants at 37°C

(a) SD-Ura 25°C **(b) SD-Ura 37°C**

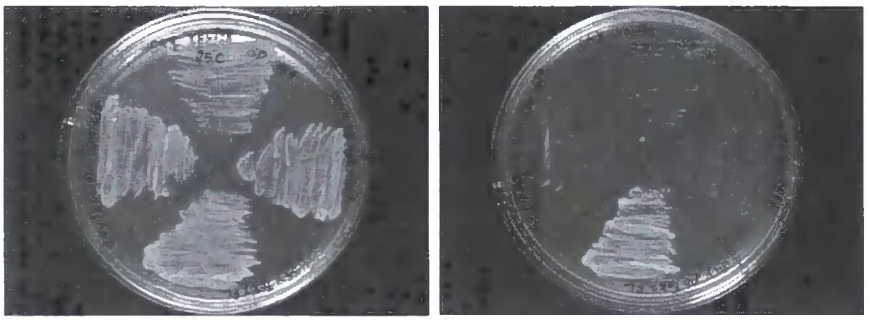

(c) Streak pattern

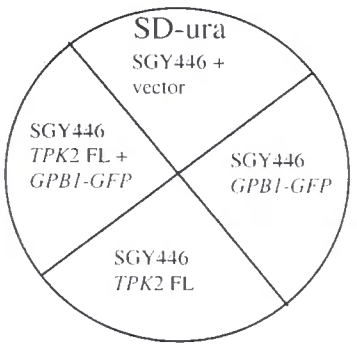

Figure 5.5.2.1

(a): The host *S. cerevisiae* SGY446 transformed with vector p426MET25, *Pb GPB1-GFP*, *Pb TPK2* FL and *Pb TPK2* FL + *GPB1-GFP* co-transformed, all can grow at 25°C.

(b): *P. brasiliensis TPK2* FL transformant only able to grow at 37°C; whilst co-transformant (*TPK2* FL + *GPB1-GFP*) did not growth at 37°C.

(c): the streak pattern.

Figure 5.5.2.2 Co-expression of Gpb1-GFP with Tpk2 full length inhibits pseudohyphae

Consistent with the previous results, where *Pb* Gpb1 interacts with *Pb* Tpk2 C-terminus (functional domain) and this interaction blocked the function of Tpk2 by inhibiting pseudohyphal growth.

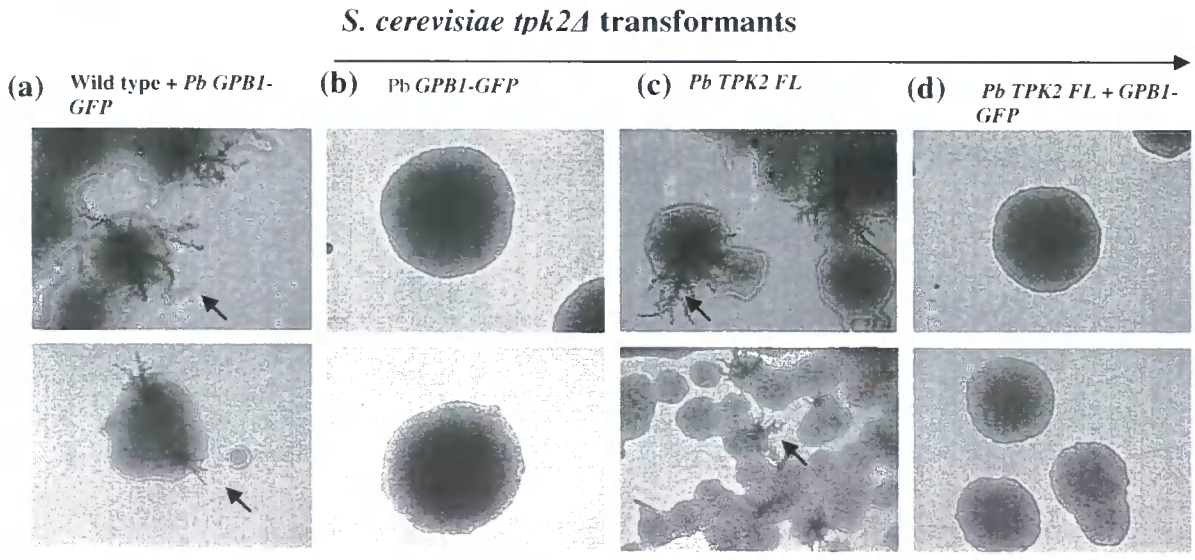

Upper panels-SLAD agar with 50 μM ammonium sulphate

Lower panels-SLAD agar with 200 μM ammonium sulphate

Arrow indicates the pseudohyphae and scale bar for the whole picture: 0.72 mm

Figure 5.5.2.2

P. brasiliensis GPB1-GFP transformed diploid *S. cerevisiae*

(a) Wild type can still produce the pseudohyphae

(b) *tpk2* mutant shows no phenotype change

(c) *tpk2* mutant transformed with only *Pb TPK2* FL can produce pseudohyphae.

(d) *tpk2* mutant co-transformant (carrying *Pb TPK2FL & GPB1-GFP)* did not produce pseudohyphae.

5.6 Western blot for Tpk2 and Gpb1-GFP

5.6.1 Western blot for GFP and Tpk2 N-terminus 1-225-GFP

The yeast transformants were grown on SD-uracil broth and the total proteins were extracted from the yeast cells as described in section 2.36. The extracted proteins were examined by Western blot with anti-GFP polyclonal antibodies (Clontech) in order to detect Tpk2 N-terminus 1-225-GFP and GFP as described in section 2.37 (Fig. 5.6.1.1).

Figure 5.6.1.1 Western blot for Tpk2 N-terminus 1-225-GFP and GFP with anti-GFP antibodies

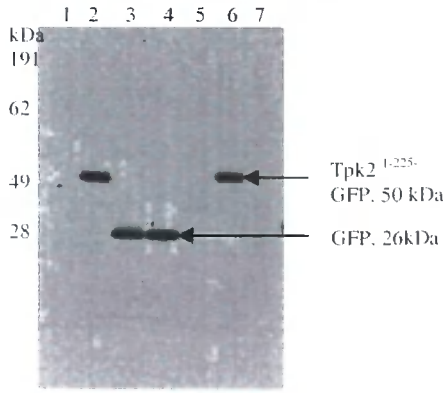

Lane 1: XPY5a/α (Δ*tpk2*) transformed with vector only
Lane 2: XPY5a/α transformed with *Pb TPK2* N-terminus 1-225-GFP
Lane 3: XPY5a/α transformed with GFP only
Lane 4: SGY446 (Δ*tpk2* Ts) transformed with GFP only
Lane 5: Empty
Lane 6: SGY446 transformed with *Pb TPK2* N-terminus 1-225 -GFP
Lane 7: SGY446 transformed with vector only

5.6.2 Western blot for Tpk2 C-terminus 226-583-GFP with Tpk2 polyclonal antibodies (Invitrogen)

The antibody for Tpk2 was raised against the peptide sequence Tpk2 556-569 (i.e., the C-terminus of Tpk2). Therefore the Tpk2 specific antibodies were used only for the detection of Tpk2 C-terminus 226-583 and full length. The N-terminus fusion was detected with anti-GFP polyclonal antibodies as shown in figure 5.6.1.1.

Figure 5.6.2.1 Western blot for Tpk2 C-terminus with specific antibodies

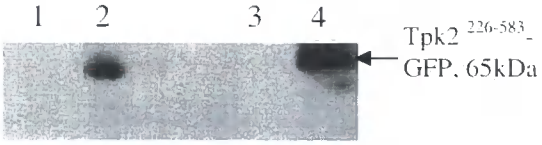

Lane 1: Xpy5a/α (Δ*tpk2*) transformed with vector only
Lane 2: XPY5a/α transformed with *Pb TPK2* $^{226\text{-}583}$-GFP
Lane 3: SGY446 (Δ*tpk2* Ts) transformed with vector only
Lane 4: SGY446 transformed with *Pb TPK2* $^{226\text{-}583}$-GFP

5.6.3 Western blot for Tpk2 FL

The Tpk2 FL expression from both haploid and diploid *S. cerevisiae* strains was verified by Western blot (section. 2.38). A specific polyclonal antibody was used to detect Tpk2 (Fig. 5.5.3.1).

Figure 5.6.3.1 Western blot for Tpk2 with specific antibodies

Lane 1: SGY446 (Δ*tpk2* Ts) transformed with vector only
Lane 2: Xpy5a/α (Δ*tpk2*) transformed with vector only
Lane 3: SGY446 transformed with *Pb TPK2* full length
Lane 4: XPY5a/α transformed with *Pb TPK2* full length

5.6.4 Western blot for Gpb1-GFP

The G protein Gpb1-GFP was detected from co-expressed yeast cells using specific antibodies raised against the peptide *Pb* Gpb1 266-279 and the Western blot was performed as described in section 2.38.

Figure 5.6.4.1 Western blot for Gpb1-GFP with specific antibodies

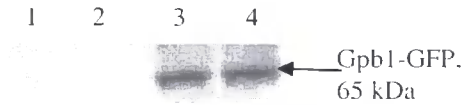

Lane 1: SGY446 (Δ*tpk2* Ts) transformed with vector only
Lane 2: Xpy5a/α (Δ*tpk2*) transformed with vector only
Lane 3: SGY446 transformed with *Pb GPB1-GFP*
Lane 4: XPY5a/α transformed with *Pb GPB1-GFP*

5.7 Subcellular localization of Tpk2-GFP

In order to investigate the subcellular localization of the GFP-fusion proteins, Tpk2 N-terminus-GFP, C-terminus-GFP and GFP expressing yeast cells nuclei were stained with DAPI as described in section 2.34. DAPI strongly binds to DNA and helps to visualize the nucleus in the cell. DAPI stained cells were observed under a confocal microscope.

Figure 5.7.1 Subcellular localization of Pb Tpk2 in *S. cerevisiae*

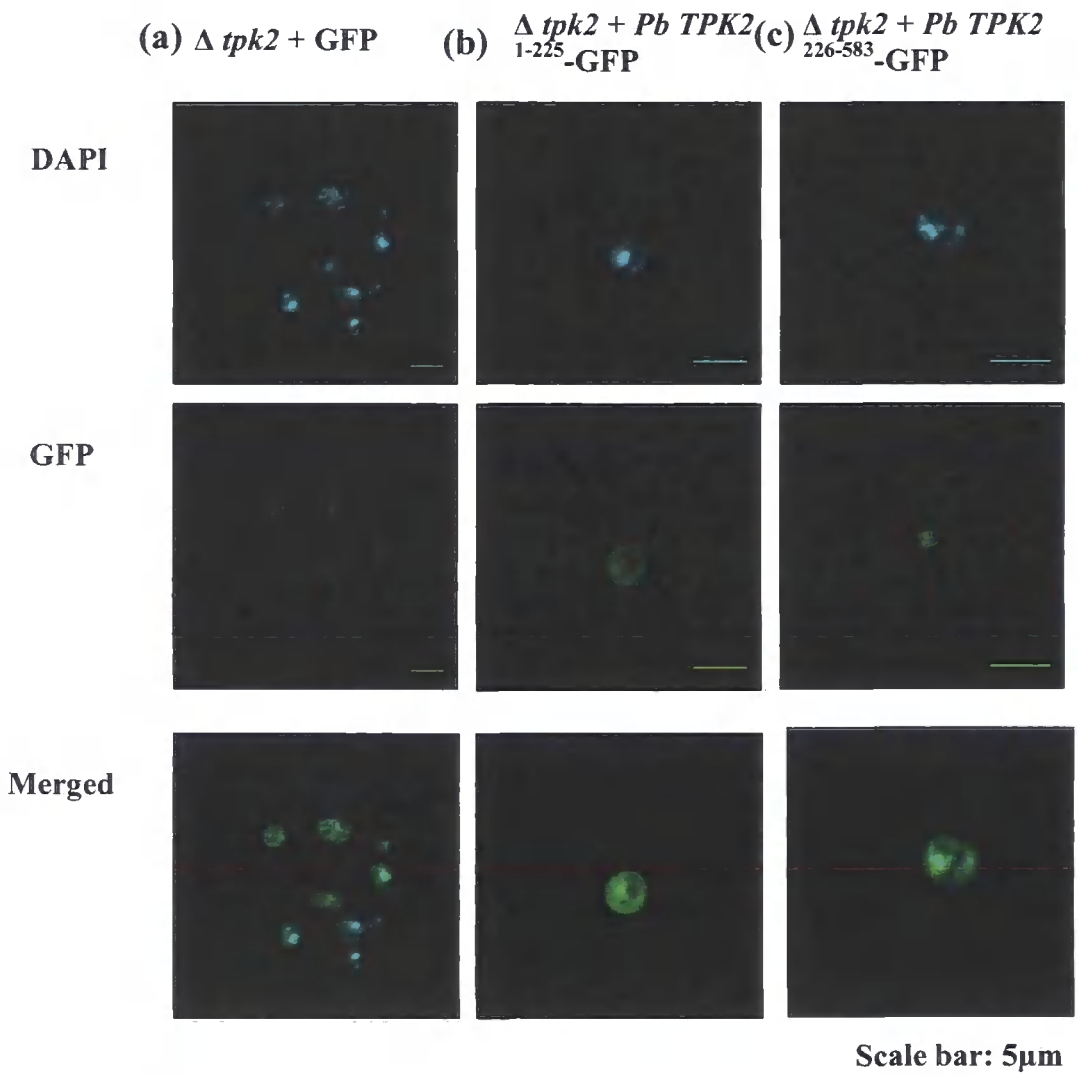

Figure 5.7.1- Δ *tpk*2 transformants carrying *Pb TPK2-GFP* fusions analyzed by confocal microscope

(a) GFP, expressed from p426MET25 was distributed throughout the cell.
(b) *Pb* Tpk2 N-terminus 1-225-GFP was distributed throughout the cell.
(c) *Pb* Tpk2 C-terminus 226-583-GFP was concentrated in the nucleus.

5.8 Subcellular localization of Tpk2 & Gpb-GFP in cells co-expressing these proteins

We have previously shown that *Pb* Gpb1-GFP inhibits Tpk2 function, inhibiting pseudohyphae and cell growth at 37°C (Fig. 5.5.2.1 and 5.5.2.2). Since Tpk2 localizes in the nucleus (Fig. 5.7.1), the interaction of Tpk2 with Gpb1 possibly re-target the Tpk2 from the nucleus to the cytoplasm. In order to investigate this, Gpb1-GFP was co-expressed with Tpk2 full length, as described in section 5.4.2, and the cells stained with DAPI to see the subcellular localization of Gpb1-GFP (e.g. identified by their GFP fluorescence).

Figure 5.8.1 Subcellular localization of Pb Gpb1-GFP in *TPK2* transformed *S. cerevisiae tpk2Δ*

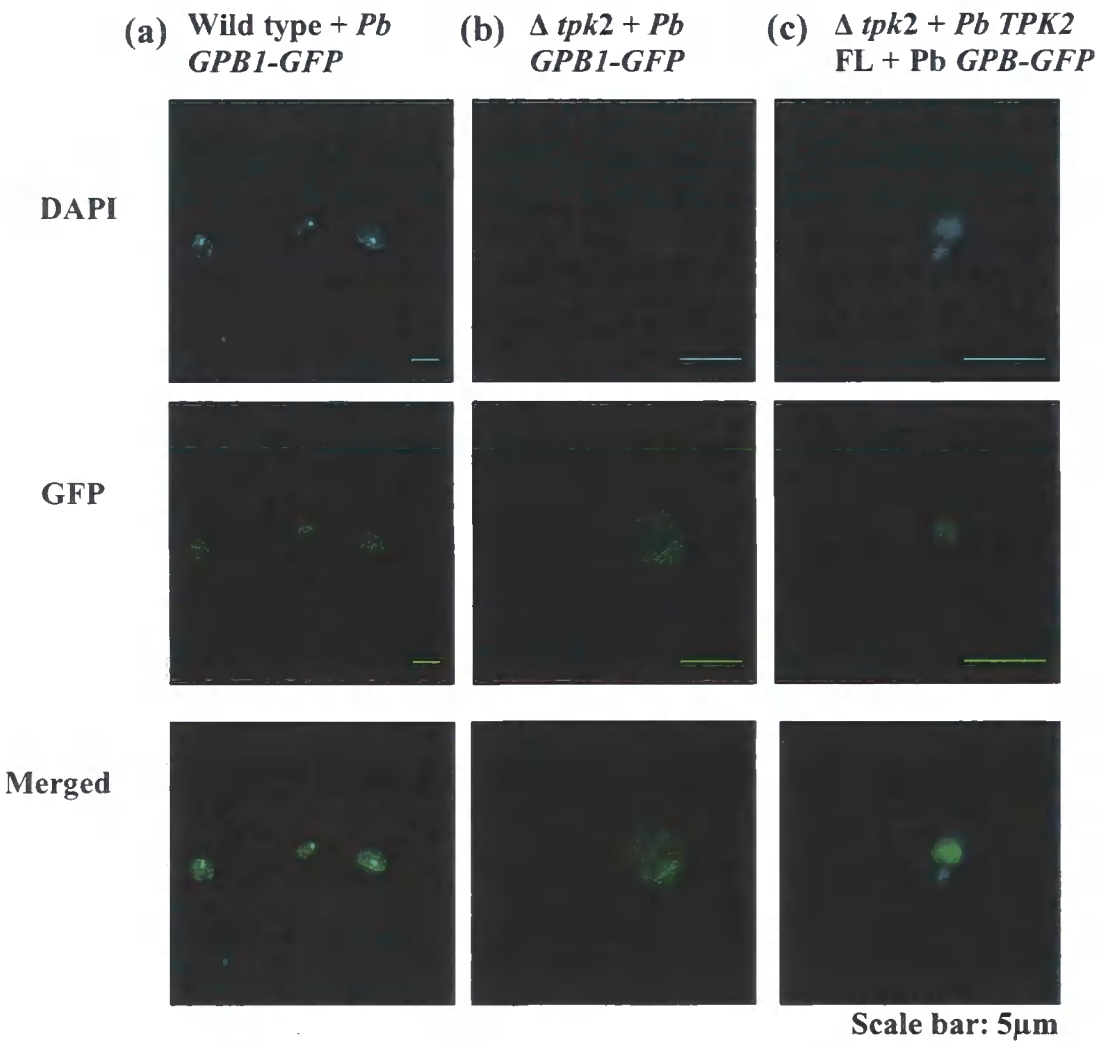

Figure 5.8.1 Δ*tpk2* transformants carrying *Pb* Gpb1-GFP fusions analyzed by confocal microscopy.

(a) Gpb1-GFP was distributed throughout the cell in the wild-type (MLY61**a**/α) strain.

(b) Gpb1-GFP was distributed throughout the cell in the *tpk2* mutant (XPY5**a**/α) strain.

(c) Gpb1-GFP was concentrated in the nucleus when co-expressed with *Pb TPK2* FL in the Δ*tpk2* cells.

5.9 *Pb TPK1* Cloning and characterization

We under took a *P. brasiliensis* genome sequence search that revealed another cAMP-dependent PKA catalytic subunit (Tpk1), which has 560 amino acids and has highest homology with *Aspergillus fumigatus* Afpka EAL91742 but only 31.5 % homology with *P. brasiliensis* Tpk2 (see table. 5.9.1). *P. brasiliensis* Tpk1 has been aligned with other Tpks by Vector NTI alignment programme as shown in figure 5.1.3. The conserved nucleotide binding site in all Tpk's is GTGSFG, but Tpk1 of *P. brasiliensis* and *Aspergillus fumigatus* Afpka EAL91742 are slightly different by having GTGTFA; however, the catalytic loop RDLKPEN is similar in both. The conserved Mg^{2+} binding region is TDFGFAK but Tpk1 of *P. brasiliensis* and *Aspergillus fumigatus* Afpka EAL91742 have a change in the first amino acid position as VDFGFAK (see figure. 5.1.3).

Table 5.9.1 Tpk1 homology with other PKAs

S.No	Organisms	Identity with *Pb* Tpk1
1	*S. cerevisiae* Tpk1	27.2%
2	*S. cerevisiae* Tpk2	27.3%
3	*S. cerevisiae* Tpk3	27.9%
4	*C. albicans* Tpk2	29.2%
5	*A. fumigatus* AfpkaC1	31.5%
6	*A. fumigatus* AfpkaC	31.3%
7	*A. nidulans* AnpkaC1	30.4%
8	A. fumigatus Afpka-EAL91742	43.6%
9	*P. brasiliensis* Tpk2	31.5%
10	*U. maydis* Adr-1	27.6%
11	*U. maydis* Uka1	29%

5.9.2 SMART Analysis of *P. brasiliensis* Tpk1

An analysis of *P. brasiliensis* Tpk1 with SMART (EMBL) revealed two major domains; (239-500) a serine/threonine phosphorylation domain (S_TKc) and (501-560) an extension of the serine/threonine phosphorylation domain (S_TKc_X). The N-terminus is similar to Tpk2 and is a low complexity region (89-205).

Figure 5.9.2.1 Major domains of Tpk1

Table 5.9.2.2 Tpk1 domains and its positions

Name	Begin	End	E-value
low complexity	89	111	-
low complexity	166	184	-
low complexity	192	205	-
S_TKc	239	500	8.45e-95
S_TK_X	501	560	5.22e-08

The figure and table are the output of the SMART analysis.

5.9.3 Tpk1: Two-hybrid analyses

We have previously demonstrated that *Pb* Gpb1 interacts with *Pb* Tpk2 and inhibits its function. Our analysis was extended in order to see whether Tpk1 interacts with Gpb1, Tup1 and adenylyl cyclase. *Pb* Tpk1$^{135\text{-}560}$ was sub-cloned into the pGADT7 and pGBKT7 vectors with *Nco*I and *Bam*HI sites in the forward and reverse primers,

respectively (for constructs and primers see table. 2.8.2). Two-hybrid analyses were performed to analyse the interactions, which revealed that Tpk1 interacts with adenylyl cyclase N-terminus 1-678 (see table. 5.8.3.1).

Table 5.9.3.1 Tpk1 two-hybrid results

Interacting proteins with *Pb* Tpk1	Interactions
Pb Cyr1 $^{1-678}$	+
Pb Gpb	-
Pb Tup1	-
Tpk2 1-174 (control)	-
ADT7 vector (control)	-
BKT7 vector (control)	-
pGADT7 Lamin & pGBKT7 lamin (negative control)	-
Pb Actin (negative control)	-

+ Positive and – negative interactions

5.9.4 Tpk1 complementation Assay

P. brasiliensis Tpk2 complemented the *S. cerevisiae tpk2* mutant haploid (SGY446) and diploid strains (XPY5**a**/α). To test whether *Pb* Tpk1 has a similar function to Tpk2 or a distinct role, the gene fragment encoding *Pb TPK1* $^{135-560}$ was cloned into p426MET25-GFP vector and transformed into the *S. cerevisiae tpk2* mutant strains (XPY5**a**/α) and a complementation assay was performed as described in sections 5.2 and 5.3. Tpk1 did not induce pseudohyphal growth (Fig. 5.9.4.1). Confocal microscope analyses revealed that Tpk1 localised in the cytoplasm but was not distributed throughout the cytoplasm (Fig. 5.9.4.3). The proteins were extracted from the yeast cells and verified by Western blot with anti-GFP antibodies (Fig. 5.9.4.3).

Figure 5.9.4.1 Pseudohyphal analysis of Tpk1-GFP

P. brasiliensis TPK1-GFP was transformed into the *S. cerevisiae tpk2* mutant XPY5**a**/α and then the transformants were streaked on SLAD agar and an individual colony was observed under 20x magnifications as described in section 5.3.

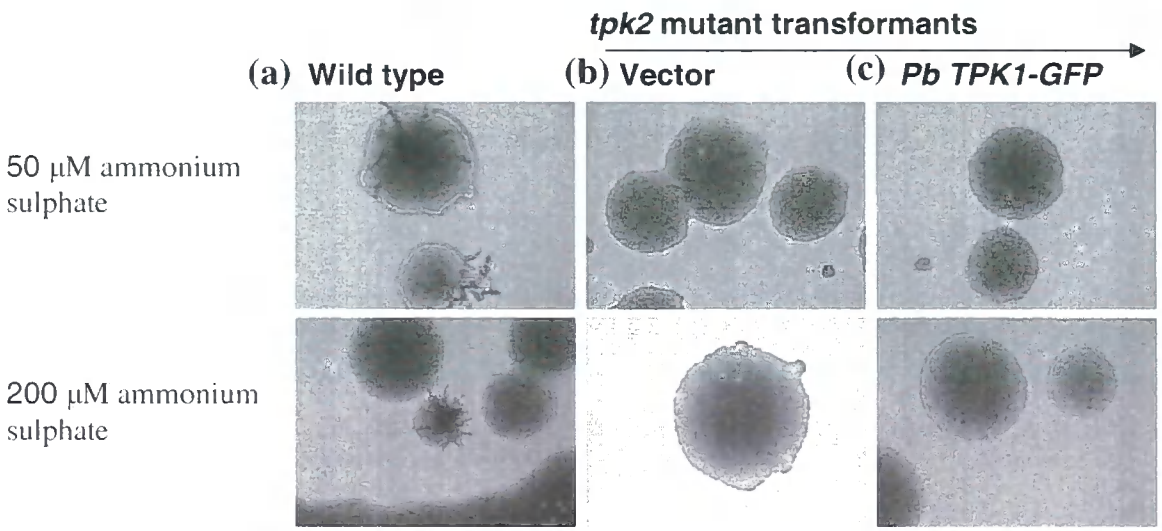

Scale bar for the whole picture: 0.72 mm

Figure 5.9.4.1: Represents diploid *S. cerevisiae tpk2* mutant transformed with *P. brasiliensis TPK1*

(a) Wild type MLY61**a**/α can produce pseudohyphae

(b) *tpk2* mutant XPY5**a**/α cannot produce pseudohyphae

(c) *Pb* Tpk1-GFP did not induce pseudohyphae in a *tpk2* mutant.

Figure 5.9.4.2 Subcellular localization of Tpk1-GFP in *S. cerevisiae* Δ*tpk2* XPY5a/a

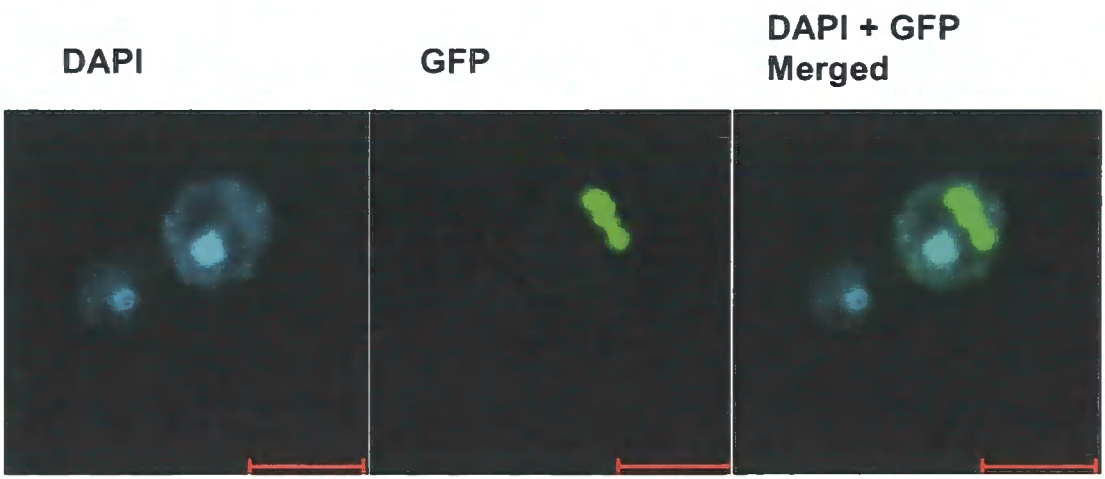

Scale bar: 5μm

P. brasiliensis TPK1-GFP fusion construct in p426MET25 vector was transformed into the *S. cerevisiae tpk2* mutant XPY5**a**/a strain to test for complementation, because previously we had shown that *Pb* Tpk2 can complement the *S. cerevisiae tpk2* mutant haploid SGY446 Ts mutant and diploid XPY5**a**/a strains. Pb Tpk1 did not complement the *S. cerevisiae tpk2* mutant XPY5**a**/a. The Tpk1-GFP fusion protein was located in the cytoplasm (Fig. 5.9.4.2) but Tpk2 was concentrated in the nucleus.

Figure 5.9.4.3 Western blot for Tpk1-GFP fusion

Total proteins were extracted from yeast cells as described in section 2.36 and a Western blot was performed as described in sections 2.37 and 5.5.1 with anti-GFP antibodies.

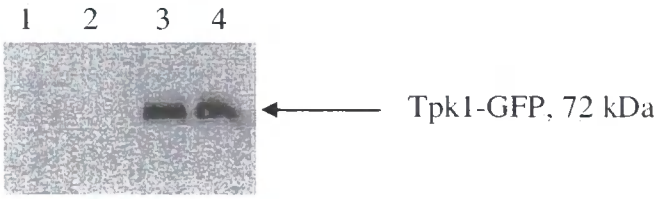

Lane 1 & 2: *tpk2* mutant XPY5**a**/α transformed with vector only

Lane 3 and 4: *tpk2* mutant XPY5**a**/α transformed with *Pb TPK1-GFP*

5.10 Discussion

The *P. brasiliensis* PKA catalytic subunit Tpk2 has 583 amino acids and contains the conserved nucleotide binding region 279-284 (GTGSFG), catalytic loop 394-400 (RDLKPEN) and Mg^{2+} binding region 412-418 (TDFGFAK) (Bockmuhl *et al.*, 2001; Liebmann *et al.*, 2004). The autophosphorylation site lies at threonine-426 and histidine-316 is responsible for the catalytic and regulatory subunit association (Durrenberger *et al.*, 1998; Liebmann *et al.*, 2004) The function of Tpk2 in *S. cerevisiae* was knocked out by mutation of K99R (Pan and Heitman, 2002).

P. brasiliensis Tpk2 has conserved PKA sequences and is similar to Tpk2 of *S. cerevisiae* and *C. albicans* (see table. 5.1.1 and figure. 5.1.3). *Pb* Tpk2 shows two major domains on SMART analysis (Fig. 5.1.4.1) that are conserved among fungal PKAs. A previous study has revealed that Tpk2 of *C. albicans* complements the *S. cerevisiae tpk2* temperature-sensitive (Ts) mutant SGY446 (Bockmuhl *et al.*, 2001). In a similar way the Tpk2 complementation assay was performed to see if *P. brasiliensis* Tpk2 could complement haploid *S. cerevisiae tpk2* Ts SGY446 (Smith *et al.*, 1998), which is unable to grow at 37°C and the diploid *S. cerevisiae* Δ*tpk2* XPY5**a**/α, (Pan Heitman, 1999), which is unable to produce pseudohyphae under low nitrogen condition. *P. brasiliensis TPK2* full length was transformed into the *tpk2* mutant haploid (SGY446) and diploid (XPY5**a**/α) strains and found to complement their phenotypes, enabling growth at 37°C and formation of pseudohyphae, respectively (Fig. 5.3.1 & 5.4.1).

To investigate the functional domain, the complementation assay was performed with truncated Tpk2 at its N-terminus 1-225-GFP and its C-terminus 226-583-GFP and the results clearly demonstrated that the C-terminal region was able to complement both strains, but the N-terminal region could not (Fig. 5.3.1 & 5.4.1). We previously demonstrated that the C-terminus 226-583 expressed from the *E.coli* has PKA activity (Fig. 4.9.2; chapter 4), indicating that the C-terminus is the catalytic domain and is sufficient for its function in inducing filamentous growth. The protein expressions were verified by Western blot with anti-GFP and specific

polyclonal antibodies (Fig. 5.6.1.1, 5.6.2.1 & 5.6.3.1). *TPK2* transformed yeast cells nuclei were stained with DAPI and the GFP localization was analysed using a confocal microscope; then Tpk2 C-terminus 226-583-GFP was shown to localise in the nucleus, whereas the N-terminal was distributed throughout the cells (Fig. 5.7.1). Previously it has been shown that *C. albicans* Tpk1-GFP and Bcy1-GFP localise in the nucleus (Cassola *et al.*, 2004). Similarly *S. cerevisiae* Tpk2 localises in the nucleus (Pan and Heitman, 2002). This suggests that PKA is targeted to the nucleus, presumably to phosphorylate target transcription factors.

Since two-hybrid and pull-down assays confirmed the interaction of Gpb1 with Tpk2 C-terminus; we sought to test whether the G protein Gpb1 has an inhibitory effect on PKA function (see table. 4.2.1 and fig. 4.8.1; chapter 4). The *S. cerevisiae* haploid (SGY446) and diploid (XPY5**a**/α) *tpk2* mutant strains were used as recipients of *Pb TPK2* FL and into these *Pb GPB1-GFP* was transformed and selected on the basis of GFP expression. These studies indicated that Gpb1-GFP inhibited the ability of Tpk2 to complement growth at 37°C (*tpk2* Ts mutant SGY446) and to produce pseudohyphae (*tpk2* mutant XPY5**a**/α) (Fig. 5.5.2.1 & 5.5.2.2), suggesting that Gpb1 interacts directly with the Tpk2 C-terminus catalytic domain and inhibits its activity.

There is a possibility that Gpb1 relocates Tpk2 from the nucleus to the cytoplasm. In order to investigate this possibility Tpk2 and Gpb1-GFP co-transformed yeast cells nuclei were stained with DAPI and the subcellular localization of GFP was analysed. The Tpk2 and Gpb1-GFP complex concentrated in the nucleus, however part of the Gpb1-GFP was present in the cytoplasm but Gpb1-GFP alone was distributed throughout the cells in both wild type and mutants (Fig. 5.8.1). This indicates that Gpb1 interacts with Tpk2 and this complex localizes in the nucleus. This strongly suggests that Gpb1 inhibits Tpk2 from phosphorylating transcription factors necessary for the production of pseudohyphae. In *S. cerevisiae*, the kelch repeat proteins (Gβ mimics) Gpb1 and Gpb2 acts downstream of Gpa2 and these regulate the invasive and pseudohyphal growth by inhibiting PKA activity in a cAMP-independent manner (Lu and Hirsch, 2005). The kelch repeat proteins Krh1/2

(Gpb2/1) act as a strong down-regulator of PKA activity by interacting with the catalytic subunit of cAMP dependent PKA (Peeters *et al.*, 2006). A *S. cerevisiae* kelch repeat proteins *krh1/2* deletion mutant exhibited a hyperinvasive phenotype with a high level of *FLO11* expression (cell surface flocculin), which is responsible for pseudohyphal and invasive growth (Batlle *et al.*, 2003). This strongly indicates that G proteins down-regulate the activity of PKA.

Three isoforms of cAMP-dependent PKA catalytic subunits have been identified in *S. cerevisiae* (namely *TPK1*, *TPK2* and *TPK3*) and all have homology in their C-terminus but the N-terminals are not homologous and are of different lengths. It was shown that at least one subunit is required for cell viability (Toda *et al.*, 1987). The three subunits do not have a functionally redundant role in pseudohyphal growth; Tpk2 induces, whereas Tpk1 and Tpk3 inhibit the pseudohyphal growth (Robertson and Fink, 1998). In contrast, PKA isoforms (Tpk1 and Tpk2) in *C. albicans* have similar roles in hyphal morphogenesis (Bockmuhl *et al.*, 2001).

The PKA from the plant pathogen *Ustilago maydis* has two catalytic subunits, namely *adr1* and *uka1*. Adr1, which has the highest homology with Tpk2 of *S. cerevisiae*, is required for the virulence and for the yeasts to pathogenic mycelial morphogenesis. It has been shown that in addition to the above function, Adr1 confers resistance to dicarboximide fungicide vinclozolin. The gene encoding for *uka1* is not essential for virulence, mating or morphogenesis (Durrenberger *et al.*, 1998; Orth *et al.*, 1995). A previous report showed that *S. cerevisiae* PKA confers resistance to polymixcin B (Boguslawski and Polazzi, 1987). The protein kinase conferring fungicide resistance is not well understood. In *P. brasiliensis*, *TPK2* has been previously cloned in our lab, we sought to search the data base; a search of the recent genome sequence (Broad Institute) revealed the presence of another catalytic subunit in *Pb*, which has 31.5% homology with *Pb* Tpk2 and decreasing order of homology with *Aspergillus fumigatus* Afpka-EAL91742 (43.6%), *Ustilago maydis* Uka1 (29%) and *S. cerevisiae* Tpk3 (27.9%) (see table. 5.8.1). Further investigation will be needed to determine if *Pb* Tpk1 and Tpk2 confer any antifungal activity.

P. brasiliensis TPK1 has been cloned by specific primers designed on the basis of the sequence downloaded from the Broad Institute data base. *P. brasiliensis* $TPK1^{135\text{-}560}$ was transformed into the *S. cerevisiae* haploid (SGY446 *tpk2* Ts mutant) and diploid (XPY5**a**/α, *tpk2* mutant) strains, which were analysed for complementation as observed for *P. brasiliensis* Tpk2. *Pb* Tpk1 neither complements the haploid strain nor the diploid strains for growth at 37°C and pseudohyphal growth under low nitrogen conditions, respectively (Fig. 5.9.4.1). Confocal microscope analyses revealed that Tpk1 localises in the cytoplasm (Fig 5.9.4.2). Previous studies indicated that *S. cerevisiae* Tpk1 localization is controlled by nutrients. During active growth and cAMP depleted conditions Tpk1-GFP localizes in the nucleus, whereas exogenous addition of 3 mm cAMP causes rapid dissociation of Tpk1 from regulatory subunit Bcy1 and enters in to the cytoplasm, but Bcy1 remains in the nucleus (Griffioen *et al.*, 2000). Therefore it is not surprising that *P. brasiliensis* Tpk1-GFP localizes in the cytoplasm.

For two-hybrid analyses, *Pb* $TPK1^{135\text{-}560}$ was sub-cloned into both of the two-hybrid assay vectors and ADT7 Tpk was co-transformed with BKT7 Cyr1, Gpb1 and Tup1 and vice versa. It has been shown that Tpk1 can interact with only adenylyl cyclase but not with Tup1 and Gpb1 with both vector constructs (see table 5.9.3.1). It seems that the adenylyl cyclase acts as a central component of the cAMP/PKA pathway, which can interact with many proteins.

Pb Tpk2 induced pseudohyphal growth in a diploid *S. cerevisiae tpk2* mutant strain but Tpk1 did not. This suggests that Tpk2 of *Pb* has a role in the filamentous growth of the mycelial form and Tpk1 has no role in morphological transition. This behaviour correlates with the transcript levels, in that Tpk2 levels are higher in mycelial. During the morphological transition the Tpk2 transcript levels decreased and Gpb transcript levels rose after 24 hours of the onset of the transition (Chen *et al.*, 2007). This suggests that Gpb1 down-regulates Tpk2 and inhibits filamentous growth.

CHAPTER SIX

Final discussion

In order to identify potential drug targets, a molecular level study of *P. brasiliensis* was under taken. Due to a lack of genetic tools in *P. brasiliensis*, we have used various approaches to study the components of the cAMP signalling pathway. We measured the intracellular cAMP levels; a transient increase in cAMP was observed with the onset of the morphological transition from mycelium to yeast (figure. 3.11.4) that correlates with an increase in the transcripts of adenylyl cyclase (Chen *et al.*, 2007). In general adenylyl cyclase is activated by G proteins, consistent with this, in this study we have shown that adenylyl cyclase interacts with the G protein Gpa1 (figure. 3.9.1), this suggests adenylyl cyclase could be activated by this interaction. Similarly, in *S.pombe*, adenylyl cyclase is activated by the G protein Gpa2 when it interacts with the N-terminus of adenylyl cyclase (Ivey and Hoffman, 2005). Recently, it was demonstrated that Gpa2 interacts with adenylyl cyclase in *S. cerevisiae* (Peeters *et al.*, 2006).

In addition, we have established for the first time that a Gβ subunit Gpb1 interacts with adenylyl cyclase in a filamentous fungus, which is required for the regulation of adenylyl cyclase activity (figure. 3.10.1). Interestingly both Gα Gpa1 and Gβ Gpb1 interact with the N-terminus of adenylyl cyclase (453-678). Most filamentous fungi, including *P. brasiliensis* have more than one Gα subunit, but there is no evidence that the Gβ and Gγ subunit, and which there is generally single copied, forms a complex with different Gα. In this study, we have shown for the first time that the G protein Gα Gpa1 forms a complex with Gβ Gpb1 and Gγ Gpg1 (Chen *et al.*, 2007). Work in our lab indicated that Gpa2 and Gpa3 do not interact with Gpb1 and Gpg1 (Chen *et al.*, 2007).

The cAMP-dependent PKA is the main downstream component of the cAMP/PKA pathway in *S. cerevisiae* (Thevelein and de Winde 1999; Ivey and Hoffman, 2005). Initially the *Pb* PKA catalytic subunit *TPK2* was cloned in our lab,

which is highly homologous to *S. cerevisiae* Tpk2, but a recent genome sequencing project revealed the presence of another *TPK*, we named as *TPK1*, which is similar to *A.fumigatus* catalytic subunit, Afpka-EAL91742. It has been shown that PKA shows a strong feed back inhibition on cAMP synthesis by activating phosphodiesterase via phosphorylation activity (Nikawa *et al.*, 1987; Mbonyi *et al.*, 1990; Ma *et al.*, 1999). However, a strong feed back inhibition was also seen in phosphodiesterase mutant strains, this suggests that adenylyl cyclase itself is a target for the feed back inhibition (Thevelein and de Winde 1999; Colombo *et al.*, 1998). In this study, we have shown for the first time that Tpk2 directly interacts with the N and C-terminus of adenylyl cyclase (see table 4.2.1). The N-terminal interaction is used as a scaffold for protein binding and probably the C-terminal (catalytic domain of adenylyl cyclase) interaction inhibits cAMP synthesis.

The Tpk2 of *C. albicans* complements *S. cerevisiae tpk2* mutant (Sonneborn *et al.*, 2000), similarly we sought to test if Tpk2 of *P. brasiliensis* complements *S. cerevisiae* Δ*tpk2*. We found *P. brasiliensis* Tpk2 complemented the *S. cerevisiae tpk2* mutant haploid strain (SGY446, Ts mutant) and induced the formation of pseudohyphae in a *tpk2* mutant diploid strain (XPY5**a**/α) (figure 5.3.1 and 5.4.1), but Tpk1 did not (figure. 5.9.4.1). Moreover, Tpk2 localised to the nucleus and Tpk1 to the cytoplasm of *S. cerevisiae* (figure 5.7.1 and 5.9.4). Consistent with this, Tpk2 of *S. cerevisiae* localised to the nucleus (Pan and Heitman, 2002)

The *P. brasiliensis* Gβ protein Gpb1 interacts with Tpk2 C-terminus (catalytic domain). We sought to test whether this interaction could affect Tpk's function. Consistent with this, Gpb1 interacts with Tpk2 *in vivo* and inhibits the pseudohyphae induced by Tpk2 (figure. 5.5.2.2). This indicates that Gpb1 inhibits the catalytic activity of Tpk2. In addition, Gpb1 was targeted to the nucleus in the presence of Tpk2 (figure. 5.8.1), there is a possibility that Gpb1 could be phosphorylated by Tpk2, but this needs to be determined. However, the mechanism in *S. cerevisiae* is different: Gβ mimics Krh1/2 interact with Tpk2 causing it to interact with its regulatory subunit Bcy1 (Peeters *et al.*, 2006 and 2007).

P. brasiliensis Tpk2 N-terminus also interacts with the global transcriptional repressor Tup1 (figure. 4.12.1 and table. 4.2.1). We have established for the first time

that the glutamine-rich domain of Tpk2 is necessary for this interaction (table. 4.2.1), but the position of Tup1 in the cAMP pathway and the role of the interaction have to be characterised. Previously it was shown that the 'Q' residues are necessary for protein-protein interactions (Liebman *et al.*, 2004; Sonneborn *et al.*, 2000).

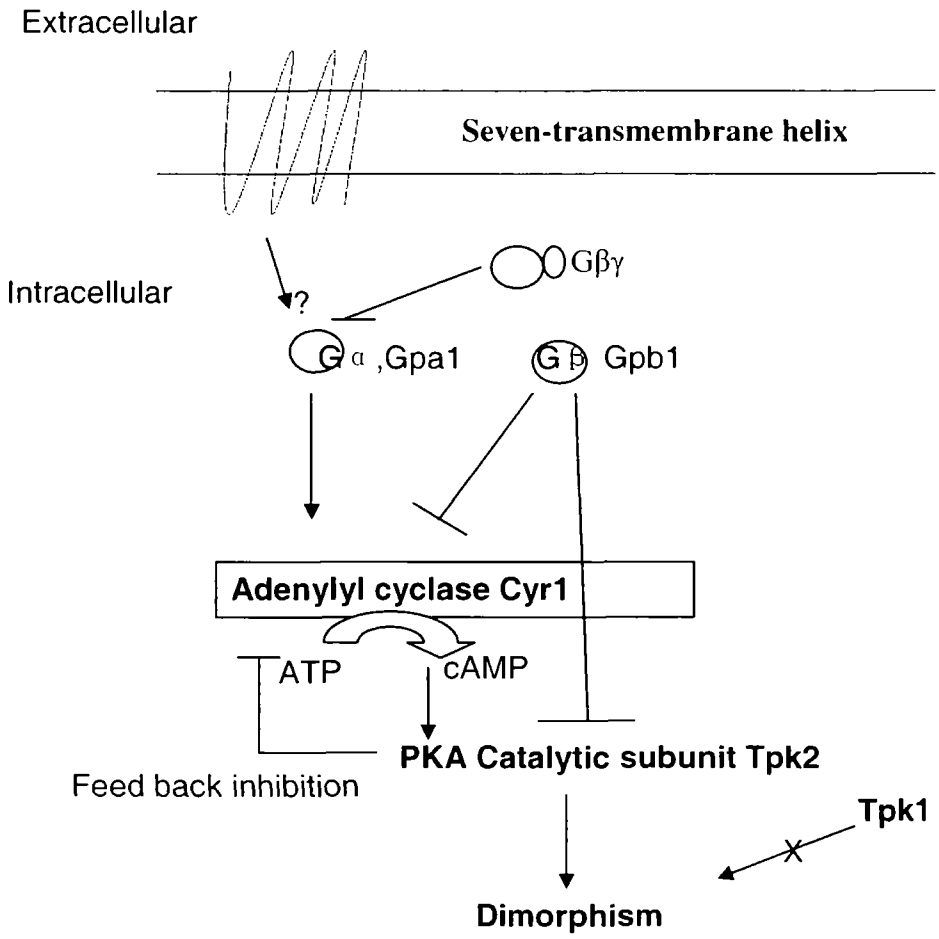

Figure 6.1 The cAMP pathway in *P. brasiliensis*. Gpa1 dissociates from the Gβγ dimer, and in turn adenylyl cyclase is activated by Gpa1. Gpb1 also interacts and regulates the adenylyl cyclase activity probably in an inhibitory manner. Tpk2 interacts with adenylyl cyclase and acts as a feed back inhibitor of cAMP. Tpk2 involves in the dimorphism. Blunt arrow indicates negative effect.

In conclusion, we have shown that the change in cAMP levels during the morphological transition suggesting that cAMP modulates this transition. Despite phosphodiesterase feed back inhibition of cAMP; we showed here, Tpk2 directly interacts with adenylyl cyclase; therefore adenylyl cyclase itself acts as a target for

feed back inhibition of cAMP. The G protein Gβ Gpb1 interacts with both adenylyl cyclase and Tpk2 in order to switch off the signalling pathway. In addition, we presume that, the interaction of Gpb1 with Tpk2 blocks the interaction with adenylyl cyclase. We suggest that G protein Gβ Gpb1 regulates both upstream and downstream components of the cAMP signalling pathway.

REFERENCES

Ajello, L., and Polonelli, L. (1985) Imported paracoccidioidomycosis: a public health problem in non-endemic areas. *Eur J Epidemiol* **1**: 160-165.

Alspaugh, J.A., Pukkila-Worley, R., Harashima, T., Cavallo, L.M., Funnell, D., Cox, G.M., Perfect, J.R., Kronstad, J.W., and Heitman, J. (2002) Adenylyl cyclase functions downstream of the Galpha protein Gpa1 and controls mating and pathogenicity of Cryptococcus neoformans. *Eukaryot Cell* **1**: 75-84.

Ansari, K., Martin, S., Farkasovsky, M., Ehbrecht, I.M., and Kuntzel, H. (1999) Phospholipase C binds to the receptor-like GPR1 protein and controls pseudohyphal differentiation in Saccharomyces cerevisiae. *J Biol Chem* **274**: 30052-30058.

Aristizabal, B.H., Clemons, K.V., Stevens, D.A., and Restrepo, A. (1998) Morphological transition of Paracoccidioides brasiliensis conidia to yeast cells: in vivo inhibition in females. *Infect Immun* **66**: 5587-5591.

Azambuja, R., Matsunaga, T., and Segura, J.C. (1981) [Paracoccidioidomycosis (South American blastomycosis)]. *Hautarzt* **32**: 249-252.

Batlle, M., Lu, A., Green, D.A., Xue, Y., and Hirsch, J.P. (2003) Krh1p and Krh2p act downstream of the Gpa2p G(alpha) subunit to negatively regulate haploid invasive growth. *J Cell Sci* **116**: 701-710.

Belozerskaia, T.A., Sokolovskii, V., and Kritskii, M.S. (1994) [Cyclic nucleotides and membrane electrogenesis in cell differentiation in Neurospora crassa]. *Vopr Med Khim* **40**: 2-5.

Biswas, K., and Morschhauser, J. (2005) The Mep2p ammonium permease controls nitrogen starvation-induced filamentous growth in Candida albicans. *Mol Microbiol* **56**: 649-669.

Bockmuhl, D.P., Krishnamurthy, S., Gerads, M., Sonneborn, A., and Ernst, J.F. (2001) Distinct and redundant roles of the two protein kinase A isoforms Tpk1p and Tpk2p in morphogenesis and growth of Candida albicans. *Mol Microbiol* **42**: 1243-1257.

Boguslawski, G., and Polazzi, J.O. (1987) Complete nucleotide sequence of a gene conferring polymyxin B resistance on yeast: similarity of the predicted polypeptide to protein kinases. *Proc Natl Acad Sci U S A* **84**: 5848-5852.

Borges-Walmsley, M.I., and Walmsley, A.R. (2000) cAMP signalling in pathogenic fungi: control of dimorphic switching and pathogenicity. *Trends Microbiol* **8**: 133-141.

Borges-Walmsley, M.I., Chen, D., Shu, X., and Walmsley, A.R. (2002) The pathobiology of Paracoccidioides brasiliensis. *Trends Microbiol* **10**: 80-87.

Boyce, K.J., Chang, H., D'Souza, C.A., and Kronstad, J.W. (2005) An Ustilago maydis septin is required for filamentous growth in culture and for full symptom development on maize. *Eukaryot Cell* **4**: 2044-2056.

Braun, B.R., and Johnson, A.D. (1997) Control of filament formation in Candida albicans by the transcriptional repressor TUP1. *Science* **277**: 105-109.

Broek, D., Samiy, N., Fasano, O., Fujiyama, A., Tamanoi, F., Northup, J., and Wigler, M. (1985) Differential activation of yeast adenylate cyclase by wild-type and mutant RAS proteins. *Cell* **41**: 763-769.

Brown, A.J., and Gow, N.A. (1999) Regulatory networks controlling Candida albicans morphogenesis. *Trends Microbiol* **7**: 333-338.

Brummer, E., Hanson, L.H., Restrepo, A., and Stevens, D.A. (1988) In vivo and in vitro activation of pulmonary macrophages by IFN-gamma for enhanced killing of Paracoccidioides brasiliensis or Blastomyces dermatitidis. *J Immunol* **140**: 2786-2789.

Brummer, E., Hanson, L.H., and Stevens, D.A. (1988) Gamma-interferon activation of macrophages for killing of Paracoccidioides brasiliensis and evidence for nonoxidative mechanisms. *Int J Immunopharmacol* **10**: 945-952.

Brummer, E., Hanson, L.H., Restrepo, A., and Stevens, D.A. (1989) Intracellular multiplication of Paracoccidioides brasiliensis in macrophages: killing and restriction of multiplication by activated macrophages. *Infect Immun* **57**: 2289-2294.

Brummer, E., Castaneda, E., and Restrepo, A. (1993) Paracoccidioidomycosis: an update. *Clin Microbiol Rev* **6**: 89-117.

Camargo, Z.P., Gesztesi, J.L., Saraiva, E.C., Taborda, C.P., Vicentini, A.P., and Lopes, J.D. (1994) Monoclonal antibody capture enzyme immunoassay for detection of Paracoccidioides brasiliensis antibodies in paracoccidioidomycosis. *J Clin Microbiol* **32**: 2377-2381.

Cantore, M.L., Galvagno, M.A., and Passeron, S. (1983) cAMP levels and in situ measurement of adenylate cyclase and cAMP phosphodiesterase activities during yeast-to-hyphae transition in the dimorphic fungus Mucor rouxii. *Cell Biol Int Rep* **7**: 947-954.

Cao, F., Lane, S., Raniga, P.P., Lu, Y., Zhou, Z., Ramon, K., Chen, J., and Liu, H. (2006) The Flo8 transcription factor is essential for hyphal development and virulence in Candida albicans. *Mol Biol Cell* **17**: 295-307.

Carbonell, L.M. (1969) Ultrastructure of dimorphic transformation in paracoccidioides brasiliensis. *J Bacteriol* **100**: 1076-1082.

Carlson, M. (1999) Glucose repression in yeast. *Curr Opin Microbiol* **2**: 202-207.

Carrico, P.M., and Zitomer, R.S. (1998) Mutational analysis of the Tup1 general repressor of yeast. *Genetics* **148**: 637-644.

Cassola, A., Parrot, M., Silberstein, S., Magee, B.B., Passeron, S., Giasson, L., and Cantore, M.L. (2004) Candida albicans lacking the gene encoding the regulatory subunit of protein kinase A displays a defect in hyphal formation and an altered localization of the catalytic subunit. *Eukaryot Cell* **3**: 190-199.

Celenza, J.L., Eng, F.J., and Carlson, M. (1989) Molecular analysis of the SNF4 gene of Saccharomyces cerevisiae: evidence for physical association of the SNF4 protein with the SNF1 protein kinase. *Mol Cell Biol* **9**: 5045-5054.

Chen, D., Janganan, T.K., Chen, G., Marques, E.R., Kress, M.R., Goldman, G.H., Walmsley, A.R., and Borges-Walmsley, M.I. (2007) The cAMP pathway is important for controlling the morphological switch to the pathogenic yeast form of Paracoccidioides brasiliensis. *Mol Microbiol* **65**: 761-779.

Chew, E., Aweiss, Y., Lu, C.Y., and Banuett, F. (2008) Fuz1, a MYND domain protein, is required for cell morphogenesis in Ustilago maydis. *Mycologia* **100**: 31-46.

Cloutier, M., Castilla, R., Bolduc, N., Zelada, A., Martineau, P., Bouillon, M., Magee, B.B., Passeron, S., Giasson, L., and Cantore, M.L. (2003) The two isoforms of the cAMP-dependent protein kinase catalytic subunit are involved in the control of dimorphism in the human fungal pathogen Candida albicans. *Fungal Genet Biol* **38**: 133-141.

Colombo, S., Ma, P., Cauwenberg, L., Winderickx, J., Crauwels, M., Teunissen, A., Nauwelaers, D., de Winde, J.H., Gorwa, M.F., Colavizza, D., and Thevelein, J.M. (1998) Involvement of distinct G-proteins, Gpa2 and Ras, in glucose- and intracellular acidification-induced cAMP signalling in the yeast Saccharomyces cerevisiae. *Embo J* **17**: 3326-3341.

Conlan, R.S., and Tzamarias, D. (2001) Sfl1 functions via the co-repressor Ssn6-Tup1 and the cAMP-dependent protein kinase Tpk2. *J Mol Biol* **309**: 1007-1015.

Cook, J.G., Bardwell, L., and Thorner, J. (1997) Inhibitory and activating functions for MAPK Kss1 in the S. cerevisiae filamentous-growth signalling pathway. *Nature* **390**: 85-88.

da Silva, S.P., Borges-Walmsley, M.I., Pereira, I.S., Soares, C.M., Walmsley, A.R., and Felipe, M.S. (1999) Differential expression of an hsp70 gene during transition from the mycelial to the infective yeast form of the human pathogenic fungus Paracoccidioides brasiliensis. *Mol Microbiol* **31**: 1039-1050.

da Silva, M.B., Marques, A.F., Nosanchuk, J.D., Casadevall, A., Travassos, L.R., and Taborda, C.P. (2006) Melanin in the dimorphic fungal pathogen Paracoccidioides brasiliensis: effects on phagocytosis, intracellular resistance and drug susceptibility. *Microbes Infect* **8**: 197-205.

de Assis, C.M., Gandra, R.F., Gambale, W., Shimizu, M.T., and Paula, C.R. (2003) Biosynthesis of chondroitinase and hyaluronidase by different strains of Paracoccidioides brasiliensis. *J Med Microbiol* **52**: 479-481.

De Vit, M.J., Waddle, J.A., and Johnston, M. (1997) Regulated nuclear translocation of the Mig1 glucose repressor. *Mol Biol Cell* **8**: 1603-1618.

De Vries, L., and Gist Farquhar, M. (1999) RGS proteins: more than just GAPs for heterotrimeric G proteins. *Trends Cell Biol* **9**: 138-144.

De Vries, L., Zheng, B., Fischer, T., Elenko, E., and Farquhar, M.G. (2000) The regulator of G protein signaling family. *Annu Rev Pharmacol Toxicol* **40**: 235-271.

DeVit, M.J., and Johnston, M. (1999) The nuclear exportin Msn5 is required for nuclear export of the Mig1 glucose repressor of Saccharomyces cerevisiae. *Curr Biol* **9**: 1231-1241.

Dohlman, H.G. (2002) G proteins and pheromone signaling. *Annu Rev Physiol* **64**: 129-152.

Durrenberger, F., Wong, K., and Kronstad, J.W. (1998) Identification of a cAMP-dependent protein kinase catalytic subunit required for virulence and morphogenesis in Ustilago maydis. *Proc Natl Acad Sci U S A* **95**: 5684-5689.

Elias, J., Jr., dos Santos, A.C., Carlotti, C.G., Jr., Colli, B.O., Canheu, A., Matias, C., Furlanetti, L., Martinez, R., Takayanagui, O.M., Sakamoto, A.C., Serafini, L.N., and Chimelli, L. (2005) Central nervous system paracoccidioidomycosis: diagnosis and treatment. *Surg Neurol* **63 Suppl 1**: S13-21; discussion S21.

Engelberg, D., Simchen, G., and Levitzki, A. (1990) In vitro reconstitution of cdc25 regulated S. cerevisiae adenylyl cyclase and its kinetic properties. *Embo J* **9**: 641-651.

Field, J., Vojtek, A., Ballester, R., Bolger, G., Colicelli, J., Ferguson, K., Gerst, J., Kataoka, T., Michaeli, T., Powers, S., and et al. (1990) Cloning and characterization of CAP, the S. cerevisiae gene encoding the 70 kd adenylyl cyclase-associated protein. *Cell* **61**: 319-327.

Franzen, A.J., Cunha, M.M., Miranda, K., Hentschel, J., Plattner, H., da Silva, M.B., Salgado, C.G., de Souza, W., and Rozental, S. (2008) Ultrastructural characterization of melanosomes of the human pathogenic fungus Fonsecaea pedrosoi. *J Struct Biol* **162**: 75-84.

Gancedo, J.M. (1998) Yeast carbon catabolite repression. *Microbiol Mol Biol Rev* **62**: 334-361.

Garcia-Pedrajas, M.D., Nadal, M., Bolker, M., Gold, S.E., and Perlin, M.H. (2008) Sending mixed signals: Redundancy vs. uniqueness of signaling components in the plant pathogen, Ustilago maydis. *Fungal Genet Biol.*

Garcia-Sanchez, S., Mavor, A.L., Russell, C.L., Argimon, S., Dennison, P., Enjalbert, B., and Brown, A.J. (2005) Global roles of Ssn6 in Tup1- and Nrg1-dependent gene regulation in the fungal pathogen, Candida albicans. *Mol Biol Cell* **16**: 2913-2925.

Gilman, A.G. (1984) G proteins and dual control of adenylate cyclase. *Cell* **36**: 577-579.

Goebl, M., and Yanagida, M. (1991) The TPR snap helix: a novel protein repeat motif from mitosis to transcription. *Trends Biochem Sci* **16**: 173-177.

Gold, S., Duncan, G., Barrett, K., and Kronstad, J. (1994) cAMP regulates morphogenesis in the fungal pathogen Ustilago maydis. *Genes Dev* **8**: 2805-2816.

Gold, S.E., Brogdon, S.M., Mayorga, M.E., and Kronstad, J.W. (1997) The Ustilago maydis regulatory subunit of a cAMP-dependent protein kinase is required for gall formation in maize. *Plant Cell* **9**: 1585-1594.

Goldani, L.Z., and Sugar, A.M. (1995) Paracoccidioidomycosis and AIDS: an overview. *Clin Infect Dis* **21**: 1275-1281.

Gomes, G.M., Cisalpino, P.S., Taborda, C.P., and de Camargo, Z.P. (2000) PCR for diagnosis of paracoccidioidomycosis. *J Clin Microbiol* **38**: 3478-3480.

Gomez, B.L., Nosanchuk, J.D., Diez, S., Youngchim, S., Aisen, P., Cano, L.E., Restrepo, A., Casadevall, A., and Hamilton, A.J. (2001) Detection of melanin-like pigments in the dimorphic fungal pathogen Paracoccidioides brasiliensis in vitro and during infection. *Infect Immun* **69**: 5760-5767.

Granot, D., and Snyder, M. (1991) Glucose induces cAMP-independent growth-related changes in stationary-phase cells of Saccharomyces cerevisiae. *Proc Natl Acad Sci U S A* **88**: 5724-5728.

Griffioen, G., Anghileri, P., Imre, E., Baroni, M.D., and Ruis, H. (2000) Nutritional control of nucleocytoplasmic localization of cAMP-dependent protein kinase catalytic and regulatory subunits in Saccharomyces cerevisiae. *J Biol Chem* **275**: 1449-1456.

Hanna, S.A., Monteiro da Silva, J.L., and Giannini, M.J. (2000) Adherence and intracellular parasitism of Paracoccidioides brasiliensis in Vero cells. *Microbes Infect* **2**: 877-884.

Harashima, T., and Heitman, J. (2002) The Galpha protein Gpa2 controls yeast differentiation by interacting with kelch repeat proteins that mimic Gbeta subunits. *Mol Cell* **10**: 163-173.

Hedbacker, K., and Carlson, M. (2008) SNF1/AMPK pathways in yeast. *Front Biosci* **13**: 2408-2420.

Hoffman, C.S. (2005) Glucose sensing via the protein kinase A pathway in Schizosaccharomyces pombe. *Biochem Soc Trans* **33**: 257-260.

Hoffman, C.S. (2005) Except in every detail: comparing and contrasting G-protein signaling in Saccharomyces cerevisiae and Schizosaccharomyces pombe. *Eukaryot Cell* **4**: 495-503.

Hogan, L.H., Klein, B.S., and Levitz, S.M. (1996) Virulence factors of medically important fungi. *Clin Microbiol Rev* **9**: 469-488.

Hsueh, Y.P., Xue, C., and Heitman, J. (2007) G protein signaling governing cell fate decisions involves opposing Galpha subunits in Cryptococcus neoformans. *Mol Biol Cell* **18**: 3237-3249.

Hwang, C.S., Oh, J.H., Huh, W.K., Yim, H.S., and Kang, S.O. (2003) Ssn6, an important factor of morphological conversion and virulence in Candida albicans. *Mol Microbiol* **47**: 1029-1043.

Ivey, F.D., and Hoffman, C.S. (2002) Pseudostructural inhibitors of G protein signaling during development. *Dev Cell* **3**: 154-155.

Ivey, F.D., and Hoffman, C.S. (2005) Direct activation of fission yeast adenylate cyclase by the Gpa2 Galpha of the glucose signaling pathway. *Proc Natl Acad Sci U S A* **102**: 6108-6113.

Jiang, R., and Carlson, M. (1997) The Snf1 protein kinase and its activating subunit, Snf4, interact with distinct domains of the Sip1/Sip2/Gal83 component in the kinase complex. *Mol Cell Biol* **17**: 2099-2106.

Jones, S., Vignais, M.L., and Broach, J.R. (1991) The CDC25 protein of Saccharomyces cerevisiae promotes exchange of guanine nucleotides bound to ras. *Mol Cell Biol* **11**: 2641-2646.

Kanetsuna, F., Carbonell, L.M., Moreno, R.E., and Rodriguez, J. (1969) Cell wall composition of the yeast and mycelial forms of Paracoccidioides brasiliensis. *J Bacteriol* **97**: 1036-1041.

Kao, R.S., Morreale, E., Wang, L., Ivey, F.D., and Hoffman, C.S. (2006) Schizosaccharomyces pombe Git1 is a C2-domain protein required for glucose activation of adenylate cyclase. *Genetics* **173**: 49-61.

Kataoka, T., Broek, D., and Wigler, M. (1985) DNA sequence and characterization of the S. cerevisiae gene encoding adenylate cyclase. *Cell* **43**: 493-505.

Kawamukai, M., Gerst, J., Field, J., Riggs, M., Rodgers, L., Wigler, M., and Young, D. (1992) Genetic and biochemical analysis of the adenylyl cyclase-associated protein, cap, in Schizosaccharomyces pombe. *Mol Biol Cell* **3**: 167-180.

Kebaara, B.W., Langford, M.L., Navarathna, D.H., Dumitru, R., Nickerson, K.W., and Atkin, A.L. (2008) Candida albicans Tup1 is involved in farnesol-mediated inhibition of filamentous-growth induction. *Eukaryot Cell* **7**: 980-987.

Keleher, C.A., Redd, M.J., Schultz, J., Carlson, M., and Johnson, A.D. (1992) Ssn6-Tup1 is a general repressor of transcription in yeast. *Cell* **68**: 709-719.

Kingston, R.E., and Narlikar, G.J. (1999) ATP-dependent remodeling and acetylation as regulators of chromatin fluidity. *Genes Dev* **13**: 2339-2352.

Klein, C.J., Olsson, L., and Nielsen, J. (1998) Glucose control in Saccharomyces cerevisiae: the role of Mig1 in metabolic functions. *Microbiology* **144 (Pt 1)**: 13-24.

Kontoyiannis, D.P., and Lewis, R.E. (2002) Antifungal drug resistance of pathogenic fungi. *Lancet* **359**: 1135-1144.

Kronstad, J., De Maria, A.D., Funnell, D., Laidlaw, R.D., Lee, N., de Sa, M.M., and Ramesh, M. (1998) Signaling via cAMP in fungi: interconnections with mitogen-activated protein kinase pathways. *Arch Microbiol* **170**: 395-404.

Kubler, E., Mosch, H.U., Rupp, S., and Lisanti, M.P. (1997) Gpa2p, a G-protein alpha-subunit, regulates growth and pseudohyphal development in Saccharomyces cerevisiae via a cAMP-dependent mechanism. *J Biol Chem* **272**: 20321-20323.

Kubler, E., Mosch, H.U., Rupp, S., and Lisanti, M.P. (1997) Gpa2p, a G-protein alpha-subunit, regulates growth and pseudohyphal development in Saccharomyces cerevisiae via a cAMP-dependent mechanism. *J Biol Chem* **272**: 20321-20323.

Kurita, N., Oarada, M., Ito, E., and Miyaji, M. (1999) Antifungal activity of human polymorphonuclear leucocytes against yeast cells of Paracoccidioides brasiliensis. *Med Mycol* **37**: 261-267.

Kuroda, Y., Suzuki, N., and Kataoka, T. (1993) The effect of posttranslational modifications on the interaction of Ras2 with adenylyl cyclase. *Science* **259**: 683-686.

Landry, S., Pettit, M.T., Apolinario, E., and Hoffman, C.S. (2000) The fission yeast git5 gene encodes a Gbeta subunit required for glucose-triggered adenylate cyclase activation. *Genetics* **154**: 1463-1471.

Landry, S., and Hoffman, C.S. (2001) The git5 Gbeta and git11 Ggamma form an atypical Gbetagamma dimer acting in the fission yeast glucose/cAMP pathway. *Genetics* **157**: 1159-1168.

Lee, N., and Kronstad, J.W. (2002) ras2 Controls morphogenesis, pheromone response, and pathogenicity in the fungal pathogen Ustilago maydis. *Eukaryot Cell* **1**: 954-966.

Lengeler, K.B., Davidson, R.C., D'Souza, C., Harashima, T., Shen, W.C., Wang, P., Pan, X., Waugh, M., and Heitman, J. (2000) Signal transduction cascades regulating fungal development and virulence. *Microbiol Mol Biol Rev* **64**: 746-785.

Liebmann, B., Muhleisen, T.W., Muller, M., Hecht, M., Weidner, G., Braun, A., Brock, M., and Brakhage, A.A. (2004) Deletion of the Aspergillus fumigatus lysine biosynthesis gene lysF encoding homoaconitase leads to attenuated virulence in a low-dose mouse infection model of invasive aspergillosis. *Arch Microbiol* **181**: 378-383.

Lo, W.S., and Dranginis, A.M. (1996) FLO11, a yeast gene related to the STA genes, encodes a novel cell surface flocculin. *J Bacteriol* **178**: 7144-7151.

Lo, H.J., Kohler, J.R., DiDomenico, B., Loebenberg, D., Cacciapuoti, A., and Fink, G.R. (1997) Nonfilamentous C. albicans mutants are avirulent. *Cell* **90**: 939-949.

Lo, W.S., and Dranginis, A.M. (1998) The cell surface flocculin Flo11 is required for pseudohyphae formation and invasion by Saccharomyces cerevisiae. *Mol Biol Cell* **9**: 161-171.

Loose, D.S., Stover, E.P., Restrepo, A., Stevens, D.A., and Feldman, D. (1983) Estradiol binds to a receptor-like cytosol binding protein and initiates a biological response in Paracoccidioides brasiliensis. *Proc Natl Acad Sci U S A* **80**: 7659-7663.

Lorenz, M.C., and Heitman, J. (1997) Yeast pseudohyphal growth is regulated by GPA2, a G protein alpha homolog. *Embo J* **16**: 7008-7018.

Lorenz, M.C., and Heitman, J. (1998) The MEP2 ammonium permease regulates pseudohyphal differentiation in Saccharomyces cerevisiae. *Embo J* **17**: 1236-1247.

Lortholary, O., Denning, D.W., and Dupont, B. (1999) Endemic mycoses: a treatment update. *J Antimicrob Chemother* **43**: 321-331.

Lu, A., and Hirsch, J.P. (2005) Cyclic AMP-independent regulation of protein kinase A substrate phosphorylation by Kelch repeat proteins. *Eukaryot Cell* **4**: 1794-1800.

Lukov, G.L., Hu, T., McLaughlin, J.N., Hamm, H.E., and Willardson, B.M. (2005) Phosducin-like protein acts as a molecular chaperone for G protein betagamma dimer assembly. *Embo J* **24**: 1965-1975.

Ma, P., Wera, S., Van Dijck, P., and Thevelein, J.M. (1999) The PDE1-encoded low-affinity phosphodiesterase in the yeast Saccharomyces cerevisiae has a specific function in controlling agonist-induced cAMP signaling. *Mol Biol Cell* **10**: 91-104.

Madhani, H.D., Styles, C.A., and Fink, G.R. (1997) MAP kinases with distinct inhibitory functions impart signaling specificity during yeast differentiation. *Cell* **91**: 673-684.

Madhani, H.D., and Fink, G.R. (1998) The control of filamentous differentiation and virulence in fungi. *Trends Cell Biol* **8**: 348-353.

Maidan, M.M., De Rop, L., Serneels, J., Exler, S., Rupp, S., Tournu, H., Thevelein, J.M., and Van Dijck, P. (2005) The G protein-coupled receptor Gpr1 and the Galpha protein Gpa2 act through the cAMP-protein kinase A pathway to induce morphogenesis in Candida albicans. *Mol Biol Cell* **16**: 1971-1986.

Mao, X., Li, Y., Wang, H., Cao, F., and Chen, J. (2008) Antagonistic interplay of Swi1 and Tup1 on filamentous growth of Candida albicans. *FEMS Microbiol Lett.*

Mbonyi, K., van Aelst, L., Arguelles, J.C., Jans, A.W., and Thevelein, J.M. (1990) Glucose-induced hyperaccumulation of cyclic AMP and defective glucose repression in yeast strains with reduced activity of cyclic AMP-dependent protein kinase. *Mol Cell Biol* **10**: 4518-4523.

McGowan, K.L., and Buckley, H.R. (1985) Preparation and use of cytoplasmic antigens for the serodiagnosis of paracoccidioidomycosis. *J Clin Microbiol* **22**: 39-43.

Mendes-Giannini, M.J., Bueno, J.P., Shikanai-Yasuda, M.A., Ferreira, A.W., and Masuda, A. (1989) Detection of the 43,000-molecular-weight glycoprotein in sera of patients with paracoccidioidomycosis. *J Clin Microbiol* **27**: 2842-2845.

Merson-Davies, L.A., and Odds, F.C. (1989) A morphology index for characterization of cell shape in Candida albicans. *J Gen Microbiol* **135**: 3143-3152.

Michelin, M.A., Figueiredo, F., and Cunha, F.Q. (2002) Involvement of prostaglandins in the immunosuppression occurring during experimental infection by Paracoccidioides brasiliensis. *Exp Parasitol* **102**: 170-177.

Mintzer, K.A., and Field, J. (1999) The SH3 domain of the S. cerevisiae Cdc25p binds adenylyl cyclase and facilitates Ras regulation of cAMP signalling. *Cell Signal* **11**: 127-135.

Mitts, M.R., Grant, D.B., and Heideman, W. (1990) Adenylate cyclase in Saccharomyces cerevisiae is a peripheral membrane protein. *Mol Cell Biol* **10**: 3873-3883.

Mitts, M.R., Bradshaw-Rouse, J., and Heideman, W. (1991) Interactions between adenylate cyclase and the yeast GTPase-activating protein IRA1. *Mol Cell Biol* **11**: 4591-4598.

Muller, P., Leibbrandt, A., Teunissen, H., Cubasch, S., Aichinger, C., and Kahmann, R. (2004) The Gbeta-subunit-encoding gene bpp1 controls cyclic-AMP signaling in Ustilago maydis. *Eukaryot Cell* **3**: 806-814.

Mumberg, D., Muller, R., and Funk, M. (1994) Regulatable promoters of Saccharomyces cerevisiae: comparison of transcriptional activity and their use for heterologous expression. *Nucleic Acids Res* **22**: 5767-5768.

Munder, T., and Kuntzel, H. (1989) Glucose-induced cAMP signaling in Saccharomyces cerevisiae is mediated by the CDC25 protein. *FEBS Lett* **242**: 341-345.

Murad, A.M., Leng, P., Straffon, M., Wishart, J., Macaskill, S., MacCallum, D., Schnell, N., Talibi, D., Marechal, D., Tekaia, F., d'Enfert, C., Gaillardin, C., Odds, F.C., and Brown, A.J. (2001) NRG1 represses yeast-hypha morphogenesis and hypha-specific gene expression in Candida albicans. *Embo J* **20**: 4742-4752.

Nemecek, J.C., Wuthrich, M., and Klein, B.S. (2006) Global control of dimorphism and virulence in fungi. *Science* **312**: 583-588.

Niimi, M., Niimi, K., Tokunaga, J., and Nakayama, H. (1980) Changes in cyclic nucleotide levels and dimorphic transition in Candida albicans. *J Bacteriol* **142**: 1010-1014.

Nikawa, J., Cameron, S., Toda, T., Ferguson, K.M., and Wigler, M. (1987) Rigorous feedback control of cAMP levels in Saccharomyces cerevisiae. *Genes Dev* **1**: 931-937.

Obara, T., Nakafuku, M., Yamamoto, M., and Kaziro, Y. (1991) Isolation and characterization of a gene encoding a G-protein alpha subunit from Schizosaccharomyces pombe: involvement in mating and sporulation pathways. *Proc Natl Acad Sci U S A* **88**: 5877-5881.

Odds, F.C. (1987) Candida infections: an overview. *Crit Rev Microbiol* **15**: 1-5.

Ogihara, H., Shima, F., Naito, K., Asato, T., Kariya, K., and Kataoka, T. (2004) Direct activation of fission yeast adenylyl cyclase by heterotrimeric G protein gpa2. *Kobe J Med Sci* **50**: 111-121.

Orth, A.B., Rzhetskaya, M., Pell, E.J., and Tien, M. (1995) A serine (threonine) protein kinase confers fungicide resistance in the phytopathogenic fungus Ustilago maydis. *Appl Environ Microbiol* **61**: 2341-2345.

O'Toole, G., Kaplan, H.B., and Kolter, R. (2000) Biofilm formation as microbial development. *Annu Rev Microbiol* **54**: 49-79.

Pall, M.L. (1981) Adenosine 3',5'-phosphate in fungi. *Microbiol Rev* **45**: 462-480.

Pan, X., and Heitman, J. (1999) Cyclic AMP-dependent protein kinase regulates pseudohyphal differentiation in Saccharomyces cerevisiae. *Mol Cell Biol* **19**: 4874-4887.

Pan, X., and Heitman, J. (2002) Protein kinase A operates a molecular switch that governs yeast pseudohyphal differentiation. *Mol Cell Biol* **22**: 3981-3993.

Papamichos-Chronakis, M., Gligoris, T., and Tzamarias, D. (2004) The Snf1 kinase controls glucose repression in yeast by modulating interactions between the Mig1 repressor and the Cyc8-Tup1 co-repressor. *EMBO Rep* **5**: 368-372.

Paris, S., and Duran, S. (1985) Cyclic adenosine 3',5' monophosphate (cAMP) and dimorphism in the pathogenic fungus Paracoccidioides brasiliensis. *Mycopathologia* **92**: 115-120.

Park, S.H., Koh, S.S., Chun, J.H., Hwang, H.J., and Kang, H.S. (1999) Nrg1 is a transcriptional repressor for glucose repression of STA1 gene expression in Saccharomyces cerevisiae. *Mol Cell Biol* **19**: 2044-2050.

Peeters, T., Louwet, W., Gelade, R., Nauwelaers, D., Thevelein, J.M., and Versele, M. (2006) Kelch-repeat proteins interacting with the Galpha protein Gpa2 bypass adenylate cyclase for direct regulation of protein kinase A in yeast. *Proc Natl Acad Sci U S A* **103**: 13034-13039.

Peeters, T., Versele, M., and Thevelein, J.M. (2007) Directly from Galpha to protein kinase A: the kelch repeat protein bypass of adenylate cyclase. *Trends Biochem Sci* **32**: 547-554.

Pryciak, P.M., and Huntress, F.A. (1998) Membrane recruitment of the kinase cascade scaffold protein Ste5 by the Gbetagamma complex underlies activation of the yeast pheromone response pathway. *Genes Dev* **12**: 2684-2697.

Puccia, R., Carmona, A.K., Gesztesi, J.L., Juliano, L., and Travassos, L.R. (1998) Exocellular proteolytic activity of Paracoccidioides brasiliensis: cleavage of components associated with the basement membrane. *Med Mycol* **36**: 345-348.

Redd, M.J., Arnaud, M.B., and Johnson, A.D. (1997) A complex composed of tup1 and ssn6 represses transcription in vitro. *J Biol Chem* **272**: 11193-11197.

Regenfelder, E., Spellig, T., Hartmann, A., Lauenstein, S., Bolker, M., and Kahmann, R. (1997) G proteins in Ustilago maydis: transmission of multiple signals? *Embo J* **16**: 1934-1942.

Restrepo, A., Salazar, M.E., Cano, L.E., Stover, E.P., Feldman, D., and Stevens, D.A. (1984) Estrogens inhibit mycelium-to-yeast transformation in the fungus Paracoccidioides brasiliensis: implications for resistance of females to paracoccidioidomycosis. *Infect Immun* **46**: 346-353.

Restrepo-Moreno, A. 1993. Paracoccioidomycosis. p 33-45. In J.W.Murphy, H. Friedman, and M. Bendinelli (ed.), Fungal infections and immune responses. Penum Press, New York.

Reynolds, T.B., and Fink, G.R. (2001) Bakers' yeast, a model for fungal biofilm formation. *Science* **291**: 878-881.

Robertson, L.S., and Fink, G.R. (1998) The three yeast A kinases have specific signaling functions in pseudohyphal growth. *Proc Natl Acad Sci U S A* **95**: 13783-13787.

Rocha, C.R., Schroppel, K., Harcus, D., Marcil, A., Dignard, D., Taylor, B.N., Thomas, D.Y., Whiteway, M., and Leberer, E. (2001) Signaling through adenylyl cyclase is essential for hyphal growth and virulence in the pathogenic fungus Candida albicans. *Mol Biol Cell* **12**: 3631-3643.

Ronne, H. (1995) Glucose repression in fungi. *Trends Genet* **11**: 12-17.

Rupp, S., Summers, E., Lo, H.J., Madhani, H., and Fink, G. (1999) MAP kinase and cAMP filamentation signaling pathways converge on the unusually large promoter of the yeast FLO11 gene. *Embo J* **18**: 1257-1269.

Sabie, F.T., and Gadd, G.M. (1992) Effect of nucleosides and nucleotides and the relationship between cellular adenosine 3':5'-cyclic monophosphate (cyclic AMP) and germ tube formation in Candida albicans. *Mycopathologia* **119**: 147-156.

Salazar, M.E., Restrepo, A., and Stevens, D.A. (1988) Inhibition by estrogens of conidium-to-yeast conversion in the fungus Paracoccidioides brasiliensis. *Infect Immun* **56**: 711-713.

Sambrook J. Fritish EF and Maniatis T. 1989. Molecular Cloning- A Laboratory Manual, 2nd edition. Cold spring Harbour Laboratory Press. New york.

San-Blas, G., and San-Blas, F. (1977) Paracoccidioides brasiliensis: cell wall structure and virulence. A review. *Mycopathologia* **62**: 77-86.

San-Blas, G., Nino-Vega, G., and Iturriaga, T. (2002) Paracoccidioides brasiliensis and paracoccidioidomycosis: molecular approaches to morphogenesis, diagnosis, epidemiology, taxonomy and genetics. *Med Mycol* **40**: 225-242.

Sato, M., Blumer, J.B., Simon, V., and Lanier, S.M. (2006) Accessory proteins for G proteins: partners in signaling. *Annu Rev Pharmacol Toxicol* **46**: 151-187.

Scott, W.A., and Solomon, B. (1975) Adenosine 3',5'-cyclic monophosphate and morphology in Neurospora crassa: drug-induced alterations. *J Bacteriol* **122**: 454-463.

Shima, F., Okada, T., Kido, M., Sen, H., Tanaka, Y., Tamada, M., Hu, C.D., Yamawaki-Kataoka, Y., Kariya, K., and Kataoka, T. (2000) Association of yeast adenylyl cyclase with cyclase-associated protein CAP forms a second Ras-binding site which mediates its Ras-dependent activation. *Mol Cell Biol* **20**: 26-33.

Sikorski, R.S., Boguski, M.S., Goebl, M., and Hieter, P. (1990) A repeating amino acid motif in CDC23 defines a family of proteins and a new relationship among genes required for mitosis and RNA synthesis. *Cell* **60**: 307-317.

Singh, A., Sharma, S., and Khuller, G.K. (2007) cAMP regulates vegetative growth and cell cycle in Candida albicans. *Mol Cell Biochem* **304**: 331-341.

Singh, A., Dhillon, N.K., Sharma, S., and Khuller, G.K. (2008) Identification and purification of CREB like protein in Candida albicans. *Mol Cell Biochem* **308**: 237-245.

Slessareva, J.E., and Dohlman, H.G. (2006) G protein signaling in yeast: new components, new connections, new compartments. *Science* **314**: 1412-1413.

Smith, A., Ward, M.P., and Garrett, S. (1998) Yeast PKA represses Msn2p/Msn4p-dependent gene expression to regulate growth, stress response and glycogen accumulation. *Embo J* **17**: 3556-3564.

Smith, R.L., and Johnson, A.D. (2000) Turning genes off by Ssn6-Tup1: a conserved system of transcriptional repression in eukaryotes. *Trends Biochem Sci* **25**: 325-330.

Soares, A.M., Calvi, S.A., Peracoli, M.T., Fernandez, A.C., Dias, L.A., and Dos Anjos, A.R. (2001) Modulatory effect of prostaglandins on human monocyte activation for killing of high- and low-virulence strains of Paracoccidioides brasiliensis. *Immunology* **102**: 480-485.

Sonneborn, A., Bockmuhl, D.P., Gerads, M., Kurpanek, K., Sanglard, D., and Ernst, J.F. (2000) Protein kinase A encoded by TPK2 regulates dimorphism of Candida albicans. *Mol Microbiol* **35**: 386-396.

Souto, J.T., Figueiredo, F., Furlanetto, A., Pfeffer, K., Rossi, M.A., and Silva, J.S. (2000) Interferon-gamma and tumor necrosis factor-alpha determine resistance to Paracoccidioides brasiliensis infection in mice. *Am J Pathol* **156**: 1811-1820.

Souto, G., Giacometti, R., Silberstein, S., Giasson, L., Cantore, M.L., and Passeron, S. (2006) Expression of TPK1 and TPK2 genes encoding PKA catalytic subunits during growth and morphogenesis in Candida albicans. *Yeast* **23**: 591-603.

Sprang, S.R. (1997) G protein mechanisms: insights from structural analysis. *Annu Rev Biochem* **66**: 639-678.

Stevens, D.A. (1989) The interface of mycology and endocrinology. *J Med Vet Mycol* **27**: 133-140.

Sudarsanam, P., Iyer, V.R., Brown, P.O., and Winston, F. (2000) Whole-genome expression analysis of snf/swi mutants of Saccharomyces cerevisiae. *Proc Natl Acad Sci U S A* **97**: 3364-3369.

Tamaki, H. (2007) Glucose-stimulated cAMP-protein kinase A pathway in yeast Saccharomyces cerevisiae. *J Biosci Bioeng* **104**: 245-250.

Tanaka, K., Nakafuku, M., Satoh, T., Marshall, M.S., Gibbs, J.B., Matsumoto, K., Kaziro, Y., and Toh-e, A. (1990) S. cerevisiae genes IRA1 and IRA2 encode proteins that may be functionally equivalent to mammalian ras GTPase activating protein. *Cell* **60**: 803-807.

Tanaka, K., Nakafuku, M., Tamanoi, F., Kaziro, Y., Matsumoto, K., and Toh-e, A. (1990) IRA2, a second gene of Saccharomyces cerevisiae that encodes a protein with a domain homologous to mammalian ras GTPase-activating protein. *Mol Cell Biol* **10**: 4303-4313.

Taylor, S.S., Kim, C., Cheng, C.Y., Brown, S.H., Wu, J., and Kannan, N. (2008) Signaling through cAMP and cAMP-dependent protein kinase: diverse strategies for drug design. *Biochim Biophys Acta* **1784**: 16-26.

Thevelein, J.M., and de Winde, J.H. (1999) Novel sensing mechanisms and targets for the cAMP-protein kinase A pathway in the yeast Saccharomyces cerevisiae. *Mol Microbiol* **33**: 904-918.

Tisi, R., Baldassa, S., Belotti, F., and Martegani, E. (2002) Phospholipase C is required for glucose-induced calcium influx in budding yeast. *FEBS Lett* **520**: 133-138.

Toda, T., Uno, I., Ishikawa, T., Powers, S., Kataoka, T., Broek, D., Cameron, S., Broach, J., Matsumoto, K., and Wigler, M. (1985) In yeast, RAS proteins are controlling elements of adenylate cyclase. *Cell* **40**: 27-36.

Toda, T., Cameron, S., Sass, P., Zoller, M., and Wigler, M. (1987) Three different genes in S. cerevisiae encode the catalytic subunits of the cAMP-dependent protein kinase. *Cell* **50**: 277-287.

Todd, R.B., Greenhalgh, J.R., Hynes, M.J., and Andrianopoulos, A. (2003) TupA, the Penicillium marneffei Tup1p homologue, represses both yeast and spore development. *Mol Microbiol* **48**: 85-94.

Treitel, M.A., and Carlson, M. (1995) Repression by SSN6-TUP1 is directed by MIG1, a repressor/activator protein. *Proc Natl Acad Sci U S A* **92**: 3132-3136.

Tristano, A.G., and Diaz, L. (2007) A case of laryngeal paracoccidioidomycosis masquerading as chronic obstructive lung disease. *South Med J* **100**: 709-711.

Trumbly, R.J. (1988) Cloning and characterization of the CYC8 gene mediating glucose repression in yeast. *Gene* **73**: 97-111.

Trumbly, R.J. (1992) Glucose repression in the yeast Saccharomyces cerevisiae. *Mol Microbiol* **6**: 15-21.

Tzamarias, D., and Struhl, K. (1994) Functional dissection of the yeast Cyc8-Tup1 transcriptional co-repressor complex. *Nature* **369**: 758-761.

Van de Velde, S., and Thevelein, J.M. (2008) Cyclic AMP-protein kinase A and Snf1 signaling mechanisms underlie the superior potency of sucrose for induction of filamentation in Saccharomyces cerevisiae. *Eukaryot Cell* **7**: 286-293.

van Duin, D., Casadevall, A., and Nosanchuk, J.D. (2002) Melanization of Cryptococcus neoformans and Histoplasma capsulatum reduces their susceptibilities to amphotericin B and caspofungin. *Antimicrob Agents Chemother* **46**: 3394-3400.

Vanhalewyn, M., Dumortier, F., Debast, G., Colombo, S., Ma, P., Winderickx, J., Van Dijck, P., and Thevelein, J.M. (1999) A mutation in Saccharomyces cerevisiae adenylate cyclase, Cyr1K1876M, specifically affects glucose- and acidification-induced cAMP signalling and not the basal cAMP level. *Mol Microbiol* **33**: 363-376.

Varanasi, U.S., Klis, M., Mikesell, P.B., and Trumbly, R.J. (1996) The Cyc8 (Ssn6)-Tup1 corepressor complex is composed of one Cyc8 and four Tup1 subunits. *Mol Cell Biol* **16**: 6707-6714.

Vicentini, A.P., Gesztesi, J.L., Franco, M.F., de Souza, W., de Moraes, J.Z., Travassos, L.R., and Lopes, J.D. (1994) Binding of Paracoccidioides brasiliensis to laminin through surface glycoprotein gp43 leads to enhancement of fungal pathogenesis. *Infect Immun* **62**: 1465-1469.

Whiteway, M., Clark, K.L., Leberer, E., Dignard, D., and Thomas, D.Y. (1994) Genetic identification of residues involved in association of alpha and beta G-protein subunits. *Mol Cell Biol* **14**: 3223-3229.

Whiteway, M.S., and Thomas, D.Y. (1994) Site-directed mutations altering the CAAX box of Ste18, the yeast pheromone-response pathway G gamma subunit. *Genetics* **137**: 967-976.

Williams, F.E., and Trumbly, R.J. (1990) Characterization of TUP1, a mediator of glucose repression in Saccharomyces cerevisiae. *Mol Cell Biol* **10**: 6500-6511.

Wu, J., Suka, N., Carlson, M., and Grunstein, M. (2001) TUP1 utilizes histone H3/H2B-specific HDA1 deacetylase to repress gene activity in yeast. *Mol Cell* **7**: 117-126.

Yamagishi, D., Otani, H., and Kodama, M. (2006) G protein signaling mediates developmental processes and pathogenesis of Alternaria alternata. *Mol Plant Microbe Interact* **19**: 1280-1288.

Yamawaki-Kataoka, Y., Tamaoki, T., Choe, H.R., Tanaka, H., and Kataoka, T. (1989) Adenylate cyclases in yeast: a comparison of the genes from Schizosaccharomyces pombe and Saccharomyces cerevisiae. *Proc Natl Acad Sci U S A* **86**: 5693-5697.

Yu, G., Li, J., and Young, D. (1994) The Schizosaccharomyces pombe pka1 gene, encoding a homolog of cAMP-dependent protein kinase. *Gene* **151**: 215-220.

Zelicof, A., Gatica, J., and Gerst, J.E. (1993) Molecular cloning and characterization of a rat homolog of CAP, the adenylyl cyclase-associated protein from Saccharomyces cerevisiae. *J Biol Chem* **268**: 13448-13453.

Zhang, Z., Varanasi, U., and Trumbly, R.J. (2002) Functional dissection of the global repressor Tup1 in yeast: dominant role of the C-terminal repression domain. *Genetics* **161**: 957-969.

Ziv, C., Gorovits, R., and Yarden, O. (2008) Carbon source affects PKA-dependent polarity of Neurospora crassa in a CRE-1-dependent and independent manner. *Fungal Genet Biol* **45**: 103-116.

Molecular Microbiology (2007) 65(3), 761–779 doi:10.1111/j.1365-2958.2007.05824.x

The cAMP pathway is important for controlling the morphological switch to the pathogenic yeast form of *Paracoccidioides brasiliensis*

Daliang Chen,[1‡] Thamarai K. Janganan,[1‡] Gongyou Chen,[1†‡] Everaldo R. Marques,[2] Marcia R. Kress,[2] Gustavo H. Goldman,[2] Adrian R. Walmsley[1*] and M. Inês Borges-Walmsley[1*]

[1]*Centre for Infectious Diseases, Wolfson Research Institute, School of Biological and Biomedical Sciences, University of Durham – Queen's Campus, Stockton-on-Tees TS17 6BH, UK.*

[2]*Departamento de Ciencias Farmaceuticas, Faculdade de Ciencias Farmaceuticas de Ribeirao Preto, Universidade de Sao Paulo, Av. do Cafe S/N, CEP 14040-903, Ribeirao Preto, Sao Paulo, Brazil.*

Summary

***Paracoccidioides brasiliensis* is a human pathogenic fungus that switches from a saprobic mycelium to a pathogenic yeast. Consistent with the morphological transition being regulated by the cAMP-signalling pathway, there is an increase in cellular cAMP levels both transiently at the onset (< 24 h) and progressively in the later stages (> 120 h) of the transition to the yeast form, and this transition can be modulated by exogenous cAMP. We have cloned the *cyr1* gene encoding adenylate cyclase (AC) and established that its transcript levels correlate with cAMP levels. In addition, we have cloned the genes encoding three Gα (Gpa1–3), Gβ (Gpb1) and Gγ (Gpg1) G proteins. Gpa1 and Gpb1 interact with one another and the N-terminus of AC, but neither Gpa2 nor Gpa3 interacted with Gpb1 or AC. The interaction of Gpa1 with Gpb1 was blocked by GTP, but its interaction with AC was independent of bound nucleotide. The transcript levels for *gpa1*, *gpb1* and *gpg1* were similar in mycelium, but there was a transient excess of *gpb1* during the transition, and an excess of *gpa1* in yeast. We have interpreted our findings in terms of a novel signalling mechanism in which the activity of AC is differentially modulated by Gpa1 and Gpb1 to maintain the signal over the 10 days needed for the morphological switch.**

Accepted 7 June, 2007. *For correspondence. E-mail a.r.walmsley@durham.ac.uk, m.i.borges-walmsley@durham.ac.uk; Tel. (+44) (0)191 334 0465 or 0467; Fax (+44) (0)191 334 0468. †Present address: Department of Plant Pathology, Nanjing Agricultural University, 1 Weigang, 210095, Nanjing, China. ‡These authors contributed equally to the work.

Introduction

The phylogenetically related ascomycete fungi *Paracoccidioides brasiliensis*, *Histoplasma capsulatum*, *Blastomyces dermatitidis*, *Coccidioides immitis*, *Penicillium marneffei* and *Sporothrix schenkii* from more than hundred thousand different species of environmental fungi are able to adapt for survival in mammalian hosts (Borges-Walmsley *et al.*, 2002; Morris-Jones, 2002; San-Blas *et al.*, 2002; Bradsher *et al.*, 2003; DiCaudo, 2006; Vanittanakom *et al.*, 2006; Kauffman, 2007). These are known as dimorphic fungi because they undergo extensive changes that allow them to switch from mycelium, a non-pathogenic filamentous form, to pathogenic single-cellular yeast that causes infections in millions of people across the globe every year. Infection is the result of the release from mycelium, frequently found in soil, of fragments or spores, which are inhaled by the host, exposing them to an elevated temperature that triggers the morphological switch. The pathogenicity of these fungi is intimately linked to the morphological change because strains that are unable to transform from mycelium to yeast are often avirulent (Nemecek *et al.*, 2006). However, our knowledge of how these fungi sense and respond to the temperature change is still rudimentary.

In eukaryotes, many cell-signalling processes are mediated by guanine-nucleotide binding proteins known as G proteins (for a review, see Sprang, 1997). Generally these are activated when they interact with a G protein-coupled receptor (GPCR) and transmit signals to downstream effectors such as adenylate cyclase (AC) and protein kinases. Typically these G proteins function as heterotrimeric complexes, composed of Gα, Gβ and Gγ subunits, which are activated when GTP binds to, and replaces bound GDP on, the Gα subunit to cause its dissociation from the Gβγ dimer. The signal can be mediated by Gα-GTP, Gβγ or both, depending on the pathway, and is attenuated as the GTP is hydrolysed to allow the

re-association of the trimeric complex (Sprang, 1997). Although this is a generally held view of the function of heterotrimeric G proteins, there is recent evidence that complex dissociation is not needed for signalling by all G proteins (Frank *et al.*, 2005).

Fungi possess between two and four, but most have three, Gα proteins. However, they only appear to have a single Gβ and Gγ protein, suggesting that either some Gα proteins can act independently or multiple Gα proteins can interact with the Gβγ dimer (Lafon *et al.*, 2006; Yu, 2006). *Saccharomyces cerevisiae* has two Gα proteins, Gpa1 and Gpa2, which have been shown to regulate mating, in response to pheromones, and filamentous growth, in response to glucose, via mitogen-activated protein kinase (MAPK) and cAMP-signalling pathways respectively (for a recent review, see Hoffman, 2005). Gpa1 interacts with the Gβγ dimer, composed of Ste4 and Ste18, preventing activation of the MAPK-signalling pathway by the Ste4–Ste18 dimer, which binds to the scaffold protein Ste5 (Whiteway *et al.*, 1995; Pryciak and Huntress, 1998) and the p21-activated kinase Ste20 (Leeuw *et al.*, 1998). In contrast, the cAMP-signalling pathway is activated by Gpa2 and Ras (Lorenz and Heitman, 1997; Colombo *et al.*, 1998; 2004; Xue *et al.*, 1998; Kraakman *et al.*, 1999; Lorenz *et al.*, 2000), both of which are presumed to bind directly to AC. Although Gpa2 does not appear to have a Gβ partner, it can bind the kelch-repeat proteins Gpb1 and Gpb2 that may mimic Gβ subunits to control the level of the free protein (Harashim and Heitman, 2002). *Schizosaccharomyces pombe* also possesses two Gα proteins that regulate pheromone-activated MAPK and glucose-activated cAMP-signalling pathways. However, the pheromone pathway is activated by the Gα protein Gpa1, rather than by a Gβγ dimer, but its target is unknown (Obara *et al.*, 1991; Ladds *et al.*, 2005); while Gpa2, which binds to the Gβγ dimer, composed of Git5 and Git11 (Landry and Hoffman, 2001), binds to and activates AC (Ogihara *et al.*, 2004; Ivey and Hoffman, 2005). *Ustilago maydis* has four Gα proteins, but it is not known whether they work independently of a Gβ or whether they all interact with the same Gβ, or even if they have kelch-repeat protein partners (Regenfelder *et al.*, 1997; Muller *et al.*, 2004). *Aspergillus nidulans* possesses three Gα proteins, FadA (Yu *et al.*, 1996), GanA and GanB (Chang *et al.*, 2004), and apparently a single Gβ, sfaD (Rosen *et al.*, 1999), and Gγ, GpgA (Seo *et al.*, 2005), protein, but does not appear to possess kelch-repeat proteins that are related to Gpb1 or Gpb2. There is evidence from the phenotypes of disruption mutants that a sfaD–GpgA dimer can interact with both FadA and GanB (Lafon *et al.*, 2005), but a direct interaction has not been demonstrated.

Gβ proteins have been found to be involved in developmental pathways of several filamentous fungi: for example, in controlling the development and/or virulence of the plant pathogens *Cryphonectria parasitica* (Kasahara and Nuss, 1997), *Magnaporthe grisea* (Nishimura *et al.*, 2003), *Fusarium oxysporum* (Jain *et al.*, 2003; Delgado-Jarana *et al.*, 2005), *U. maydis* (Muller *et al.*, 2004) and *Cochliobolus heterostrophus* (Ganem *et al.*, 2004), and in the development of *Neurospora crassa* (Krystofova and Borkovich, 2005), *A. nidulans* (Rosen *et al.*, 1999) and *Cryptococcus neoformans* (Wang *et al.*, 2000). Although the Gβ proteins MBP1 and GPB1, from *M. grisea* and *C. neoformans*, appear to function through MAPK-signalling pathways in analogy with Ste4, the other Gβ proteins function, at least partially, through cAMP-signalling pathways. In several cases, exogenous cAMP can suppress some, if not all, of the defects caused by deleting these genes. For example, the filamentous growth of a *bpp1* deletion in *U. maydis* can be suppressed by exogenous cAMP (Muller *et al.*, 2004). A constitutively active allele of *gpa3* also suppresses this phenotype, suggesting that Bpp1 and Gpa3 are components of the same heterotrimeric G protein that acts on AC. However, in contrast to Δ*bbp1* strains, Δ*gpa3* strains are impaired in pathogenicity, suggesting that Gpa3 operates independently of Bpp1. In *N. crassa*, deletion of the Gβ protein Gnb-1 causes a reduction in cAMP levels, but this was attributed to a reduction in Gα proteins that activate AC (Krystofova and Borkovich, 2005). In *S. pombe*, deletion of the Gβ protein Git5 does not affect basal cAMP levels but inhibits the glucose-induced elevation of cAMP levels (Landry *et al.*, 2000), and one proposal is that Git5 interacts directly with AC. Thus, there is evidence that Gα and Gβ proteins can independently activate different signalling processes.

If Gα and Gβ, and the Gβγ and Gαβγ complexes can all elicit signalling, then there is no reason why these subunits should be expressed equivalently. Signalling could be brought about by the increased expression of either the Gα or Gβ subunit, above that of its cognate subunit, so that there would be a pool of uncomplexed G protein that would be free to interact with other proteins in the signalling pathway. In the case of *S. cerevisiae*, it has been reported that there is an excess of Gpa1 over Ste4 (Ghaemmaghami *et al.*, 2003) that might be needed to prevent pheromone-independent signalling by the Ste4–Ste18 dimer (Hoffman, 2005). This balance in the subunits is important because a twofold increase in Ste4 is sufficient to activate the pathway (Hao *et al.*, 2003). A similar imbalance has been noted in *S. pombe*, where the Gβ Git5 is transcribed at much lower levels than the Gα Gpa2 and Gγ Git11 (Hoffman, 2005). It has been hypothesized that the uncomplexed Gpa2 is associated with AC to form an inactive complex: glucose activation of the signalling pathway would lead to Gpa2-GTP, released from the Git5–Git11 dimer, being swapped for Gpa2-GDP bound to AC that would then become activated (Hoffman, 2005).

The cAMP-signalling pathway has been shown to be important in controlling morphological changes and the pathogenicity of several fungi (Borges-Walmsley and Walmsley, 2000). For example, signalling through AC controls the virulence of *Candida albicans* (Rocha *et al.*, 2001), *C. neoformans* (Alspaugh *et al.*, 2002) and *A. fumigatus* (Liebmann *et al.*, 2003). In contrast to the ACs of *C. neoformans* (Vallim *et al.*, 2005) and *A. fumigatus* (Liebmann *et al.*, 2003) that only appear to be regulated via Gα proteins, *C. albicans* is regulated by both Ras (Rocha *et al.*, 2001) and Gpa2 (Miwa *et al.*, 2004; Maidan *et al.*, 2005), which can also interact with the MAPK pathway (Sanchez-Martinez and Perez-Martin, 2002; Bennett and Johnson, 2006). In the plant pathogen *M. grisea*, the morphological changes that are involved in pathogenicity are dependent upon G protein-mediated cAMP signalling, and exogenous cAMP induces formation of the infective appressorium (Nishimura *et al.*, 2003).

Paracoccidioides brasiliensis, the aetiological agent of paracoccidioidomycosis (for a review, see San-Blas *et al.*, 2002; Borges-Walmsley *et al.*, 2002), the most prevalent systemic mycosis in Latin America, where it is estimated that throughout the endemic region as many as 10 million individuals, out of a population of about 90 million, may be infected (Restrepo *et al.*, 2001). The fungus is dimorphic undergoing a complex transformation *in vivo*, in which mycelia and conidia transform to the pathogenic yeast form (Medoff *et al.*, 1987; Borges-Walmsley *et al.*, 2002; San-Blas *et al.*, 2002), while strains that are unable to undergo the mycelium-to-yeast transformation are avirulent (San-Blas and Niño-Veja, 2001). Herein we establish that this process is regulated by the cAMP-signalling pathway, and we have cloned the gene encoding AC and genes that encode a set of G proteins, which potentially function upstream of AC. In the absence of molecular tools for forward and reverse genetic approaches for studying gene function in *P. brasiliensis*, we have investigated the interaction of these proteins using yeast two-hybrid and pull-down assays. Our data indicate that the Gβ and Gγ proteins Gpb1 and Gpg1 interact specifically with the Gα Gpa1, but not with Gpa2 or Gpa3, to form a trimeric complex. This trimer can dissociate to release Gpa1 and Gpb1 that can independently interact with the N-terminus of AC. We propose that the ability of AC to bind both Gpa1 and Gpb1 enables maintenance of a long-term signal that is required to direct the morphological transition from the saprobic mycelium to pathogenic yeast, which occurs over a period of about 10 days.

Results

The P. brasiliensis *morphological transition is controlled by cAMP*

The cAMP-signalling pathway has been implicated in controlling morphological changes and the virulence of a number of fungi. We sought to determine whether cAMP would affect the morphological transition, which underlies the virulence, of *P. brasiliensis*. As a prerequisite for such an analysis, we monitored the morphology of *P. brasiliensis* cells, growing in liquid culture, which had been induced to undergo the mycelium-to-yeast transition by increasing the temperature from 26°C to 37°C, and established parameters to quantify the different morphotypes that are produced during this process. We classified the transition into four different morphological states (Fig. 1A): (i) hyphae; (ii) differentiating hyphae, characterized by the development of chlamydospore-like cells, produced by intercalary or lateral swellings in the fertile hyphae; (iii) transforming yeast, characterized by the production of multiple buds by the chlamydospore; and (iv) mature, multibudding yeast. This classification helped us establish quantitative parameters to assess the morphological transition at successive time point: after 336 h, 92% of the cells were yeast, indicating that the transition had gone to near completion (Fig. 1B, left graphic). In contrast, when the mycelial cells were treated with 10 mM dibutyryl-cAMP and the morphological switch induced, only 32% of the cells were yeast after 336 h, indicating that cAMP retarded the morphological transition (Fig. 1B, right graphic). We did not find any appreciable effect of dibutyryl-cAMP, at concentrations up to 20 mM, upon the yeast-to-mycelium transition induced by decreasing the incubation temperature from 37°C to 26°C (data not shown). This latter finding contrasts with an earlier study that indicated that cAMP retarded the yeast-to-mycelium transition (Paris and Duran, 1985), but we cannot identify any clear reason for this difference.

Identification of the components of a cAMP-signalling pathway in P. brasiliensis

In an attempt to identify genes from the cAMP-signalling pathway, which our studies clearly implicated in the control of the morphological switch from the mycelium to pathogenic yeast form of *P. brasiliensis*, we used homology-based strategies to clone the genes that encode AC (e.g. *CYR1*) and several G proteins, including three Gα (e.g. *GPA1*, *GPA2* and *GPA3*), Gβ (e.g. *GPB1*) and Gγ (e.g. *GPG1*) subunits, which might be expected to be involved in its regulation (see *Supplementary material*).

A phylogenetic analysis of all known fungal Gα proteins identified to date indicates that they fall into three major families (groups 1–3), each of which is represented by one of the three Gα proteins, Gpa1–3, from *P. brasiliensis* (Fig. S1). In contrast, only a single Gβ and Gγ have been identified in these fungi, raising the question as to whether they interact with more than one Gα. Consequently, we sought to test whether the Gβ protein Gpb1 interacts with

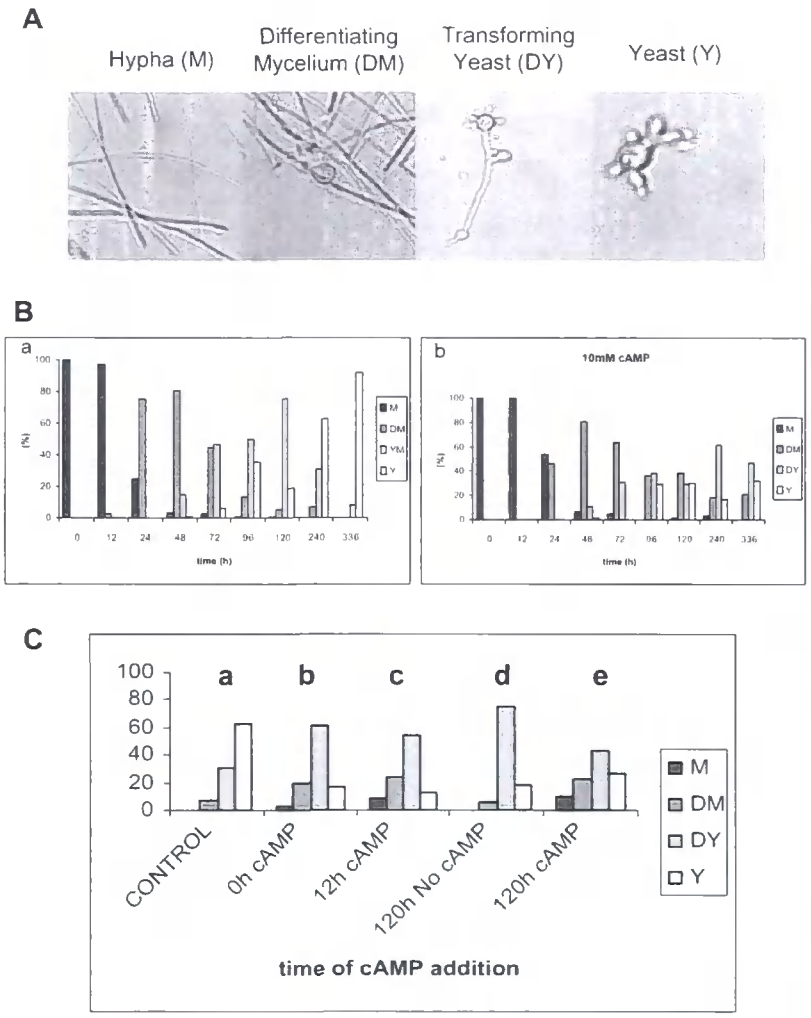

Fig. 1. The cAMP-signalling pathway regulates the transition from mycelium to yeast in *P. brasiliensis*.
A. The morphology of *P. brasiliensis* cells, growing in liquid culture, which had been induced to undergo the mycelium-to-yeast transition by increasing the temperature from 26°C to 37°C and was monitored to quantify the different morphotypes that are produced during this process. Cellular forms were classified into four different morphological states: (i) hyphae; (ii) differentiating hyphae, characterized by the development of chlamydospore-like cells, produced by intercalary or lateral swellings in the fertile hyphae; (iii) transforming yeast, characterized by the production of multiple buds by the chlamydospore; and (iv) mature, multibudding yeast. At the indicated times during the morphological switch, 300 morphological units were picked and the number of individual forms quantified.
B. The bar charts show the percentage of each morphological form at increasing times during the morphological transition from mycelium to yeast in the absence (a) and presence (b) of 10 mM dibutyryl-cAMP. The data indicate that exogenous dibutyryl-cAMP retards the mycelium-to-yeast morphological transition.
C. The bar charts show the percentage of each morphological form at 240 h after initiating the transition in the absence of cAMP (chart a) and for cells to which 10 mM dibutyryl-cAMP was added at the start of the transition (chart b), at 12 h (chart c) and 120 h (chart e) after initiating the transition; for comparison, the percentage of each morphological forms after 120 h is also shown (chart d). The data indicate that the addition of exogenous dibutyryl-cAMP late in the transition reverses the mycelium-to-yeast morphological transition. M-mycelium; DM-Differentiating mycelium; DY-Differentiating yeast; Y-Yeast.

Gpa1–3 from *P. brasiliensis* by two-hybrid screening in *S. cerevisiae*. Initially, no interactions between any of the Gα proteins and Gpb1 were detected (Fig. 2A). Although the Gβ protein Ste4 can interact independently, of its cognate Gγ protein Ste18, with the Gα protein Gpa1 in two-hybrid assays in *S. cerevisiae* (Ongay-Larios *et al.*, 2000), it is possible that the failure to detect any interaction between the *P. brasiliensis* Gβ and Gα proteins was attributable to the requirement for a Gγ protein to stabilize Gpb1 for interaction with the Gα proteins. However, we failed to identify an interaction between Gpa1–3 and a Gpb1-linker–Gpg1 fusion protein, nor was there an interaction between Gpb1 and Gpg1 (data not shown). Consequently, we decided to test whether any of the Gpa proteins would interact with discrete domains of Gpb1, which might only be available for interaction in the Gpb1–Gpg1 complex. These experiments revealed an interaction of Gpa1, but not Gpa2 or Gpa3, with C-terminal-truncated Gpb1, with a deletion analysis indicated that Gpa1 interacted with the first two WD domains at the N-terminus (Fig. 2A). Gpa1 also interacted with a fusion protein in which the first WD domain was fused to the third, but not the seventh, WD domain (Fig. 2A). In analogy, *S. cerevisiae* Gpa2 has been reported to interact with an N-terminal-truncated, consisting of residues 531–740 of the, but not with the full-size, kelch-repeat protein Gpb1 (Batlle *et al.*, 2003). We complemented this approach by constructing random mutagenesis libraries for Gpa1–3 and Gpb1 in the yeast two-hybrid vector pGADT7: screening the Gpa1–3 libraries with Gpb1 and the Gpb1 library with Gpa1–3. No point or frameshift mutations were detected that led to an interaction (data not shown). As a positive control we used the *GPR1* and *GPA2* genes that, respectively, encode a GPCR and its cognate Gα protein in *S. cerevisiae*: two-hybrid screens indicated that Gpa2 could interact with the C-terminal domain, encompassing residues 679–961, of Gpr1 (data not shown). When a random mutagenesis library of $GPR1^{679-7961}$ was screened with *GPA2*, at least 50 positive

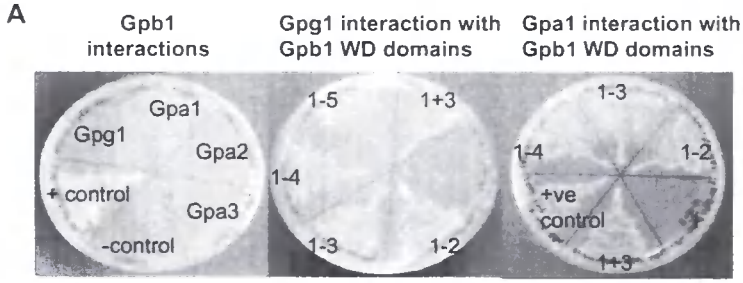

	WD1-7	WD1	WD1-2	WD1-3	WD1-4	WD1-5	WD1-6	WD2-7	WD6-7	WD1+3	WD1+7
GPG1	-	-	+	+	+	+	-	-	-	+	-
GPA1	-	-	+	+	+	-	-	-	-	+	-
GPA2	-	-	-	-	-	-	-	-	-	-	-
GPA3	-	-	-	-	-	-	-	-	-	-	-
CYR1	+	-	+	+	+	+	+	+	+	+	-

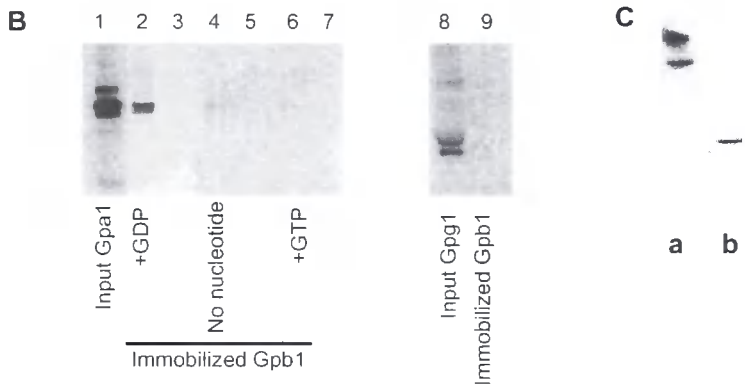

Fig. 2. A. *GPA1*, but not *GPA2* nor *GPA3*, and *GPG1* interact with *GPB1*. Each of the *P. brasiliensis* proteins Gpa1, Gpa2, Gpa3, Gpg1 and Cyr1 was tested by two-hybrid screening in *S. cerevisiae* for interactions with Gpb1 (e.g. WD1–7) and a series of truncates in which successive WD domains were deleted from the C-terminus (e.g. WD1–6 to WD1); a construct that lacked the N-terminal WD domain (e.g. WD2–7); a construct that comprised the two C-terminal WD domains (e.g. WD6–7); and a fusion of WD domains 1 and 3 (e.g. WD1+3), and 1 and 7 (e.g. WD1+7). *S. cerevisiae* strain AH109, harbouring pGADT7 plasmids bearing genes that encoded proteins to test for interactions with Gpb1 and truncates of this protein, expressed from pGBKT7, were identified by auxotrophic selection on SD/–Leu/–Trp/–His/–ADE plates and Xgal assays. As illustrated by the left-hand plate, full-length Gpb1 did not interact with Gpa1, Gpa2, Gpa3 nor Gpg1. However, full-length Gpb1 did interact with the positive control $Cyr^{1\text{-}678}$, consequently, establishing that the full-length protein is expressed. The middle- and right-hand plates show the interaction of Gpg1 and Gpa1 respectively with the WD domains of Gpb1. As a negative control, each pGBK protein vector was cotransformed, with pGADT7, into AH109 and screen for growth on SD/–Leu/–Trp/–His/–ADE plates. None of these control cells grew (data not shown). In the accompanying table, the (+) and (–) symbols are indicative of the presence and absence of protein–protein interactions respectively.

B. Pull-down assays to demonstrate that Gpa1 interacts with Gpb1. GST and GST-Gpb1 were purified from bacteria, loaded onto glutathione sepharose beads before incubation with *in vitro* translated ^{35}S-Gpa1and 10 mM nucleotide. After washing the beads, the proteins were eluted by the addition of 4× NuPAGE LDS sample buffer, followed by boiling at 90°C for 5 min, and separated on a 4–12% NuPAGE gel under denaturing conditions. Bound Gpa1 was detected as a gel band by autoradiography. Lanes 2, 4 and 6 establish that Gpa1 binds to immobilized Gpb1, but the apparent affinity decreases in order of incubation with GDP (lane 2), no nucleotide (lane 4) and GTP (lane 6). Negative controls, using immobilized GST, are shown in lanes 3, 5, 7 and 10. Using *in vitro* translated ^{35}S-Gpg1 (lane 8), there was no detectable interaction with Gpb1 (lane 9).

C. Gpb1 and Gpa1 used in pull-down assays cross-react with specific antibodies. (a) Gpb1 produced as a fusion protein with GST in *E. coli* and (b) Gpa1 synthesized using an *in vitro* transcription/translation system ran at the expected Mr on SDS-PAGE gels and cross-reacted with antibodies generated to specific sequences within these proteins.

colonies were detected. Screening the same library with *P. brasiliensis GPA1–3* did not yield any positive colonies, nor did a screen of the *P. brasiliensis GPA1–3* random mutagenesis libraries with *S. cerevisiae GPR1* (data not shown). These results establish that there is a high degree of stringency in the Gα–GPCR interaction because none of the Gα proteins from *P. brasiliensis* could interact with *S. cerevisiae* Gpr1. We conclude that of the three Gα proteins found in *P. brasiliensis*, only Gpa1 interacts with Gpb1, and that it binds to the same N-terminal region of Gpb1 to which Gpg1 binds. These results suggest that Gpa1, Gpb1 and Gpg1 form a Gαβγ trimer.

We used pull-down assays to confirm the interaction of Gpa1, produced by *in vitro* translation, with Gpb1, expressed and purified as a glutathione S-transferase (GST) fusion protein from bacteria. We found that Gpa1 could interact directly with Gpb1, but this interaction appeared to be strengthened by GDP and blocked by GTP (Fig. 2B). The apparent capability of Gpa1 to bind GTP and dissociate from Gpb1 provides strong evidence that both proteins are correctly folded and functional. Furthermore, we found that both Gpa1 and Gpb1 cross-reacted with specific antibodies to these proteins (Fig. 2C). Consistent with our yeast two-hybrid assays, no interaction between Gpb1 and Gpg1, produced by *in vitro* translation, was detected. This is perhaps not surprising because recent studies have revealed a role for phosducins as molecular chaperones required for Gβγ dimer assembly (Lukov *et al.*, 2005).

Adenylate cyclase interacts with Gpa1 and Gpb1

Although it has been known for some time that G proteins modulate the activity of mammalian AC by binding to the catalytic domain (Tesmer *et al.*, 1997), only recently has it been established that *S. pombe* Gpa2 and *S. cerevisiae* Gpa2 bind to the N-terminus of AC to cause its activation in *S. pombe* (Ogihara *et al.*, 2004; Ivey and Hoffman, 2005) and *S. cerevisiae* (Peeters *et al.*, 2006) respectively.

We used two-hybrid analyses to test whether any of the G proteins interact with AC from *P. brasiliensis*. The AC, when analysed with SMART (EMBL), contains four domains: a Ras association and Gα binding domain (RA. positions 1-678) domain (RA, positions); 14 leucine-rich repeats (LRR_TYR domains, positions 752–1244); a serine/threonine phosphatase family 2C catalytic domain (PP2Cc, positions 1341–1627); and an adenylyl/guanylyl cyclase catalytic domain (CYCc domain, positions 1574–1856). The AC cDNA was segmented into four parts with each containing an individual domain and cloned into yeast two-hybrid vectors to make constructions *PbCYR1*$^{1\text{-}678}$, *PbCYR1*$^{600\text{-}1316}$, *PbCYR1*$^{1301\text{-}1876}$ and *PbCYR1*$^{1347\text{-}2100}$ that were used to test for interactions with Gpa1–3 and Gpb1 from *P. brasiliensis*. We found that the N-terminus of AC, encoded by the pGBK-*PbCYR1*$^{1\text{-}678}$ construct, interacted with Gpa1 and Gpb1, but not with Gpa2 nor Gpa3 (Fig. 3A). Furthermore, a deletion analysis indicated that AC could interact with a pair of WD domains from the extremes of either the N- or C-terminus of Gpb1 (Fig. 2A). We also tested for interactions between the *PbCYR1*$^{1\text{-}678}$, *PbCYR1*$^{600\text{-}1316}$, *PbCYR1*$^{1301\text{-}1876}$ and *PbCYR1*$^{1347\text{-}2100}$ constructs, but none were found (data not shown).

To confirm these interactions, we used an N-terminal fragment of Cyr1, comprising residues 453–678, fused to GST, Cyr1$_{(453\text{-}678)}$-GST, produced and purified from bacteria, for pull-down assays with *in vitro* translated Gpa1; and an *in vitro* translated N-terminal fragment of Cyr1, comprising residues 1–678, for pull-down assays with the Gpb1–GST fusion protein (Fig. 3B). These assays establishing that both Gpa1 and Gpb1 could interact with the N-terminus of AC and specifically with a region that incorporates the putative Gα and Ras binding domains, between residues 453 and 678 (Fig. 3B). Gpa1 was able to bind Cyr1 in the presence of GTP or GDP or in the absence of nucleotides but, surprisingly, the relative intensities of the bands suggested a preference for Gpa1 in the absence of nucleotides. A similar comparison suggested that Gpa1-GDP had a stronger affinity for Gpb1 than for Cyr1 (Fig. 3B, lane 8). Indeed, in a pull-down assay using immobilized Gpb1-GST with *in vitro* translated, ^{35}S-labelled, Cyr1$^{1\text{-}678}$ and Gpa1, in the presence of excess Gpa1 and GDP, we did not detect a Cyr1 band, suggesting that Gpa1-GDP binds preferentially to Gpb1 (Fig. 3B, lane 9). However, the strength of these interactions will need to be confirmed by direct measurement when, and if, the proteins can be obtained in sufficient quantities for biophysical studies.

A transient increase in CYR1 *transcript and cellular cAMP levels correlates with the onset of the morphological switch*

Real-time reverse transcription polymerase chain reaction (RT-PCR) was used to evaluate the *CYR1* transcript levels, which revealed that it is differentially expressed at higher levels in yeast than in mycelium (Fig. 4A). However, monitoring the transcript levels during the morphological transition revealed a significant transient peak in *CYR1* transcripts after 24 h of the onset of the morphological transition, correlating with the peak in mycelial differentiation, and a further progressive increase in *CYR1* transcripts from about 72 h, as the fungus adopted the yeast form. Considering this behaviour, we sought to determine whether the increase in *CYR1* transcripts correlated with an increase in cellular cAMP levels. We found that the level of cellular cAMP peaked at about 12 h, and then progressively increased from a minimum at 72 h,

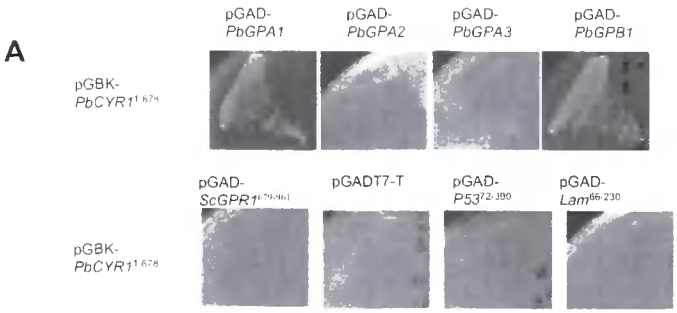

	pGBK-*PbCYR1*$^{1-678}$	pGBK-*PbCYR1*$^{600-1316}$	pGBK-*PbCYR1*$^{1302-1876}$	pGBK-*PbCYR1*$^{1638-2100}$
pGAD-*PbGPA1*	+	-	-	-
pGAD-*PbGPA2*	-	-	-	-
pGAD-*PbGPA3*	-	-	-	-
pGAD-*PbGPB1*	+	-	-	-
pGAD-*ScGPR1*$^{679-961}$	-	Not tested	Not tested	Not tested
pGADT7-T	-	Not tested	Not tested	Not tested
pGAD-*P53*$^{72-390}$	-	Not tested	Not tested	Not tested
pGAD-*Lam*$^{66-230}$	-	Not tested	Not tested	Not tested

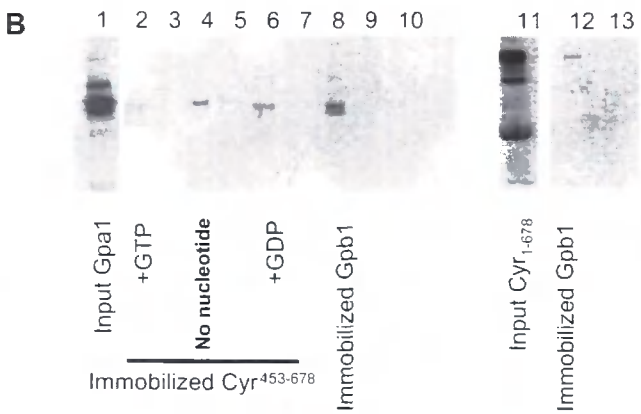

Fig. 3. A. Yeast two-hybrid assays indicate that full-length *GPA1* and *GPB1*, but not *GPA2* nor *GPA3*, directly interact with *CYR1*$^{1-678}$. Bait and prey vectors were simultaneously transformed into yeast strain AH109 and plated out on SD/–Leu/–Trp for 3 days. Yeast colonies that grew on SD/–Leu/Trp were restreaked on SD/–Ade/–His/–Leu/–Trp and incubated for a further 3 days. The results growths indicate that pGAD-*PbGPA1* and pGAD-*PbGPB1* could, but pGAD-*PbGPA2* and pGAD-*PbGPA3* could not, directly interact with pGBK-*PbCYR1*$^{1-678}$. In a series of negative controls, pGBK-*PbCYR1*$^{1-678}$ could not interact with pGAD-*ScGPR1*$^{679-961}$, pGADT7-T, pGAD-*P53*$^{72-390}$ and pGAD-*Lam*$^{66-230}$.
B. Pull-down assays to demonstrate that Gpa1 and Gpb1 both interact with Gpb1. GST and GST-Cyr$^{453-678}$ were purified from bacteria, loaded onto glutathione sepharose beads before incubation with *in vitro* translated ^{35}S-Gpa1 and 10 mM nucleotide. After washing the beads, the proteins were eluted by the addition of 4× NuPAGE LDS sample buffer, followed by boiling at 90°C for 5 min, and separated on a 4–12% NuPAGE gel under denaturing conditions. Bound Gpa1 was detected as a gel band by autoradiography. Lanes 2, 4 and 6 establish that Gpa1 binds to immobilized Cyr1, but there was little difference in apparent affinity after incubation with GTP (lane 2), no nucleotide (lane 4) or GDP (lane 6). Negative controls, using immobilized GST, are shown in lanes 3, 5, 7, 10 and 13. A control using immobilized GST-Gpb1 to pull-down ^{35}S-Gpa1, in the presence of 10 mM GDP, shows a more intense band, suggesting that Gpa1-GDP is bound with higher affinity to Gpb1 than to Cyr. Using *in vitro* translated ^{35}S-Cyr$^{1-678}$ (lane 11), an interaction with immobilized GST-Gpb1 (lane 12) was detected.

strongly suggesting that increasing cAMP levels regulate the morphological transition (Fig. 4B). We noted that the *CYR1* transcript levels increased at 24 and 240 h by about 3.2- and 7.5-fold respectively, while the cAMP levels were about 7.5- and 17-fold higher than in mycelium. This behaviour suggests that not only is the expression of AC upregulated, but it is also activated, presumably upon G protein binding.

Our results are intriguing because we previously found that the addition of exogenous dibutyryl-cAMP retarded the morphological transition. Perhaps the cells detect and respond to transient changes in cAMP levels rather than the absolute concentration of cAMP? Consistent with this proposal, we found that adding exogenous dibutyryl-cAMP 12 h after the onset of the morphological transition, when cellular cAMP levels would be maximal, had less effect in retarding the transition compared with its addition at the onset of the transition (i.e. compare charts b and c in Fig. 1C). However, the addition of dibutyryl-cAMP after 120 h, when the cAMP levels had dropped to a minimal level, similar to that in mycelium, induced a partial reversal of the transition (i.e. compare charts d and e in Fig. 1C): at this time, 0.5%, 5.5%, 75.5% and 18.5% of the morphology units were hyphae, differentiating hyphae, transforming yeast and yeast respectively (Fig. 1C, chart d); but after a further 120 h after the addition of the dibutyryl-cAMP, the proportion of these states was 9.3%, 22%, 43% and 25.7% respectively (Fig. 1C, chart e). Presumably because the cells are not synchronized in their development, some are committed to the transition and, accord-

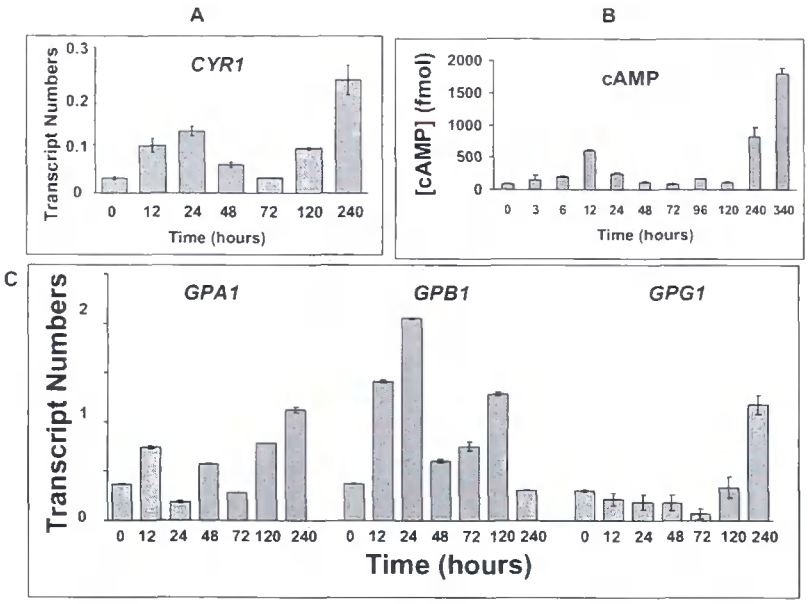

Fig. 4. The changes in intracellular cAMP levels correlate with the *CYR1*, *GPA1*, *GPB1* and *GPG1* transcript levels during the mycelium-to-yeast transition. The measured quantity of each *P. brasiliensis* gene mRNA in each of the treated samples was normalized by using the C_T values obtained for the *α-tubulin* RNA amplifications run on the same plate. The relative quantification of each *P. brasiliensis* gene and *α-tubulin* gene expression was determined by a standard curve (i.e. C_t values plotted against the logarithm of the DNA copy number). The values represent the number of copies of the cDNAs of each *P. brasiliensis* gene divided by the number of copies of the cDNAs of the *α-tubulin* gene.

A. A bar chart showing the *CYR1* transcript levels at the indicated times following an increase in temperature from 26°C to 37°C to induce the mycelium-to-yeast transformation. The data represent the average of three independent measurements.

B. The corresponding changes in the cellular cAMP levels during the morphological transition from mycelium to yeast are shown in chart B. Intracellular cAMP measurements were made using a non-acetylated EIA procedure (see *Experimental procedures*) and are the average of six assays.

C. A bar chart showing the *GPA1*, *GPB1* and *GPG1* transcript levels at the indicated times following an increase in temperature from 26°C to 37°C to induce the mycelium-to-yeast transformation. The data represent the average of three independent measurements.

ingly, transform into yeast, but a large proportion of the cells convert back to hyphae. Furthermore, the addition of dibutyryl-cAMP, at concentrations up to 20 mM, did not induce the transformation of yeast at 37°C, indicating that once the cells had passed a certain point in their development, increasing dibutyryl-cAMP was insufficient to reverse this process (data not shown). Indeed, this is consistent with our hypothesis because the cellular cAMP levels are relatively high in yeast, suggesting that the yeast-to-mycelium transition is triggered by decreasing cAMP levels. Consistent with this hypothesis, we could not prevent the temperature-induced yeast-to-mycelium interconversion (e.g. upon decreasing the temperature from 37°C to 26°C) with exogenous dibutyryl-cAMP (data not shown).

Evidence for a switch from G subunit-signalling during the morphological transition

As our studies indicated that both Gpa1 and Gpb1 could interact with AC, we sought to determine whether there was an imbalance in the concentrations of the G protein subunits during the morphological switch from mycelium to yeast in *P. brasiliensis*. RT-PCR experiments indicated that the *GPA1*, *GPB1* and *GPG1* transcript levels were equivalent in mycelium; but there was a 5.4-fold increase in *GPB1* transcript levels 24 h from the onset of the transition, while those for *GPA1* and *GPG1* declined 2-fold from that in mycelium, so that the *GPB1* transcript levels were more than 10-fold higher than those for *GPA1* and *GPG1*, which were still nearly equivalent (Fig. 5, left inset). Conversely, as the transition approached its endpoint, after 240 h, when most cells had adopted the yeast form, the *GPB1* transcript levels dropped to a level 3.7-fold lower than those for *GPA1* and *GPG1*. This behaviour contrasts with that for *RAS* transcript levels that were about 50-fold higher than those for the G protein subunits and fluctuated little during the transition, suggestive of a role in controlling basal cAMP levels (see Fig. S2). We sought to confirm the imbalance in Gpa1 and Gpb1 subunits by Western blotting: comparing the intensities of the bands for the Gpa1 and Gpb1 blots indicated that there was, as predicted, greater expression of Gpa1 than Gpb1 in yeast (Fig. 5, right inset). We did not extend such

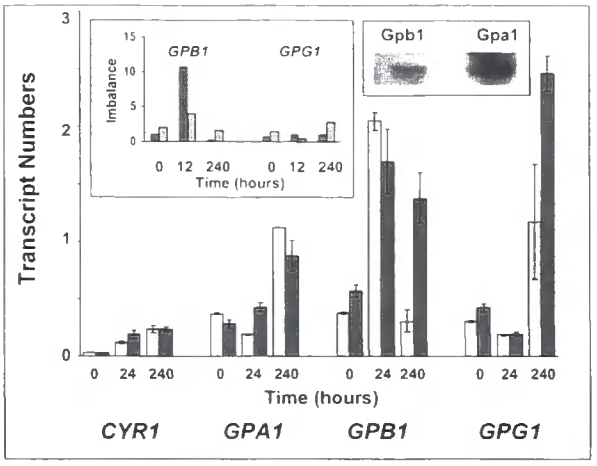

Fig. 5. The hindrance of the mycelium-to-yeast transition by dibutyryl-cAMP correlates with an imbalance in Gpa1 and Gpb1 expression. A set of bar charts for the transcript levels of the *CYR1*, *GPA1*, *GPB1* and *GPG1* genes at the indicated times following an increase in temperature from 26°C to 37°C to induce the mycelium-to-yeast transformation in the absence (black bars) and presence (grey bars) of 10 mM dibutyryl-cAMP. The right inset shows the ratio of the *GPB1* and *GPG1* transcripts respectively relative to the number of *GPA1* transcripts in mycelium, and at 12 and 240 h after the onset of the transition to the yeast form. The transcript numbers were determined in the absence (black bars) and presence (grey bars) of 10 mM dibutyryl-cAMP. Data are the average of three independent measurements. The right inset is a Western blot showing that Gpa1 is expressed at a higher level than Gpb1 in yeast.

analyses though, because they were complicated by the fact that the Gpa1 antibodies also cross-reacted with higher- and lower-molecular-weight proteins, which could be oligomers and degradation products respectively (data not shown). The presence of the latter would not be surprising if the concentration of Gpa1 needs to be finely controlled in order to modulate cAMP production. Indeed, it would be difficult to comprehend the functional significance of our finding that nucleotide-free Gpa1 and Gpb1 can bind to AC if these were always at equivalent concentrations and preferentially in complex with each other in the absence of GTP. However, we must be cautious in the interpretation of our transcript data because the imbalance in transcript levels may not reflect the difference in protein levels, especially if they are degraded at different rates, and there is a future need to ascertain whether, and how, Gpa1 and/or Gpb1 affect the catalytic activity of AC.

As our morphology studies indicated that the addition of exogenous dibutyryl-cAMP retarded the switch from mycelium to yeast, we sought to determine whether this reflected a change in transcription of AC and/or G proteins. Accordingly, we redetermined the transcript levels in mycelium, 24 h after the onset of the transition, and in yeast, in the presence of 10 mM dibutyryl-cAMP (Fig. 5). There was little change in the *CYR1* transcript levels at any stage in the morphological switch, which could have caused a reduction in cAMP levels to retard the transition. However, after 24 h, there was a notable reduction, from about 10- to 4-fold, in the imbalance in *GPB1* to *GPA1* transcripts. If Gpb1 has a lower affinity than Gpa1 for Cyr1, then this excess of Gpb1 might be insufficient to efficiently curtail the Gpa1 signal by displacing it from Cyr1, potentially retarding the transition. Furthermore, after 240 h there was still a 1.6-fold imbalance in *GPB1* to *GPA1* transcripts; whereas in the absence of exogenous dibutyryl-cAMP, the *GPB1* transcript levels were 3.7-fold lower than *GPA1*. All of the Gpa1 should be complexed in the trimer, and none would be freely available to interact with AC as normal.

Discussion

Our data are consistent with the morphological transition in *P. brasiliensis* being controlled by changing cAMP levels, with the onset of the transition correlating with a transient increase in cAMP, suggesting that the cAMP-signalling pathway is activated. Furthermore, there is a clear correlation with the changes in cAMP levels and the expression of AC during the transition. However, the fold-increase in *CYR1* transcripts (e.g. 3.2 and 7.5 at 24 and 240 h) was less than that in cAMP levels (e.g. 7.5 and 17 at 24 and 240 h), suggesting that increased cAMP was not simply due to more AC but because the protein is activated. We sought to identify the G proteins most likely responsible for the activation of AC. Most, if not all, filamentous fungi possess three or more Gα proteins, but, to date, only single Gβ and Gγ proteins have been identified. It has remained a mystery as to whether the Gβ and Gγ proteins can form trimeric complexes with the different Gα proteins. In this study, we have established for the first time that the Gβ and Gγ proteins, Gpb1 and Gpg1, interact with only a single Gα protein, Gpa1, in *P. brasiliensis*, presumably to form a Gpa1/Gpb1/Gpg1 trimeric complex. We did not find an interaction between Gpb1 and the other Gα proteins, Gpa2 and Gpa3, which work either independently or perhaps in association with other Gβ mimics (Harashima and Heitman, 2002; Palmer *et al.*, 2006; Slessareva *et al.*, 2006; reviewed by Hoffman, 2007). We then established that both the Gα and Gβ proteins, Gpa1 and Gpb1, could interact with the N-terminal domain of AC. Previous studies established that, in *S. Pombe*, Gpa2 interacts with the N-terminus of AC to cause its activation (Ogihara *et al.*, 2004; Ivey and Hoffman, 2005), while more recently, an interaction between Gpa2 and AC from *S. cerevisiae* was confirmed (Peeters *et al.*, 2006). Although there is genetic evidence for the Gβ protein Git5 interacting with and activating AC in *S. pombe* (Landry *et al.*, 2000), we have shown a direct interaction between Gβ and a fungal AC that has not previously been demonstrated.

Our studies demonstrate that both Gα and Gβ proteins Gpa1 and Gpb1 bind to a site that lies between residues 453 and 678 of *P. brasiliensis* AC. Similarly, the activity of mammalian ACs is regulated by the binding of Gα and Gβ proteins (Dessauer *et al.*, 2002; Diel *et al.*, 2006). However, mammalian ACs are integral membrane proteins that share little sequence homology with fungal ACs, which are only associated with the periphery of the membrane. Mammalian ACs have a common topology consisting of two transmembrane domains, M1 and M2, each followed by a cytosolic catalytic domain, C1 and C2 (Krupinski *et al.*, 1989). The catalytic activity of mammalian ACs is regulated by the binding of Gαs and Gαi proteins to the C2 and C1 cytoplasmic domains respectively, to increase or decrease the interactions of these domains (Dessauer *et al.*, 2002). The effect of binding the Gβγ subunits, apparently to C1, depends upon the AC subtype, for example, activating ACII but inhibiting ACIII (Diel *et al.*, 2006). Our data indicate that fungal ACs employ a different mechanism of modulation that involves the binding of G proteins to the N-terminus, but it is not clear how they modulate the activity of the catalytic domain, which is about 1000 residues away. We did not detect any interaction between the RA, LRR_TYR, PP2Cc and CYCc domains of AC, but these might only be induced by the binding of effectors, such as Gpa1 and Gpb1, to the N-terminal domain. The activity of AC in *S. cerevisiae* has been shown to be controlled by its interaction with Sgt1 that binds directly to the LRR domain (Dubacq *et al.*, 2002). Similarly, Git7, a homologue of Sgt1, has been shown to control cAMP levels and play a role in glucose-triggered cAMP signalling in *S. pombe* (Schadick *et al.*, 2002). Sequence analyses indicated that Sgt1 has features of a co-chaperone, and it has been proposed to act as a co-chaperone or factor in the assembly or the conformational activation of specific multiprotein complexes (Dubacq *et al.*, 2002). Consistent with such a role, recent studies have shown that Sgt1 interacts with Hsp90 (Bansal *et al.*, 2004; Lingelbach and Kaplan, 2004). Failure to detect interactions between the different domains of AC in the present investigation might be attributable to the involvement of Sgt1–Hsp90 in stabilizing inter-domain interactions and complex assembly. Considering the growing number of proteins identified as interacting with fungal ACs, this is an attractive hypothesis, as the interactions must occur in a controlled manner.

Our studies indicate that there is an imbalance in Gpa1, Gpb1 and Gpg1 G protein subunits as *P. brasiliensis* undergoes the morphological transition from mycelium to yeast. In mycelium the transcript levels for *GPA1*, *GPB1* and *GPG1* are nearly equivalent, but *GPB1* predominates during the transition, while *GPA1* predominates in yeast. It is notable that the *CYR1*, *GPA1*, *GPB1* and *GPG1* transcripts have extensive leader sequences that incorporate motifs likely to be targeted by RNA binding proteins that can be used to regulate the life times of these transcripts (see *Supplementary material* data). It seems plausible that signal progression is effected by regulating the longevity of these transcripts and of the translated proteins. Presumably, activation of the cAMP-signalling pathway in mycelium will depend upon GTP-induced dissociation of the Gpa1/Gpb1/Gpg1 trimer to release 'free' Gpa1 and Gpb1 that can interact with AC. However, remodelling of the cell, as it changes from mycelium to yeast, is a relatively lengthy process, requiring about 10 days for completion. A requirement for GTP to maintain the signal would constitute a metabolic waste over such a time period. An alternative strategy would be to increase the concentration of the protein that activates the signalling process, so that GTP-induced dissociation of the trimeric complex was not subsequently required. Early on in the transition Gpb1 is produced at higher levels than Gpa1 and, as we have established that it only interacts with the Gpa1, and not with Gpa2 or Gpa3, this excess will be 'free' to interact directly with AC. However, as we have found that Gpa1 can interact with AC in the absence of GTP, why does not the cell simply produce an excess of Gpa1 as it does in yeast? We note that the excess of Gpa1 in yeast correlates with an increase in the basal cAMP level, suggesting that nucleotide-free Gpa1 can activate AC. Consequently, if Gpa1 was produced in excess during the early stages of the transformation, it would be expected to maintain a high cAMP level, which we have shown, via the addition of dibutyryl-cAMP, actually retards the morphological transition. It seems plausible that Gpb1 serves a role in attenuating the cAMP signal by inactivating AC. Although we have not mapped the precise binding sites for Gpa1 and Gpb1, we have found that both G proteins bind to a domain of AC that incorporates residues 453–678, raising the possibility that they bind to the same site in a competitive manner. Considering the fact that the cAMP levels undergo cyclical changes during the morphological switch, and the effect of exogenous dibutyryl-cAMP in retarding the transition, particularly when cAMP levels are low, it seems likely that these changes in cAMP levels are needed to co-ordinate the activation of sequential steps in the morphological change.

Interestingly, while it is generally believed that it is the Gβγ dimer that is the functional unit, we have found that Gpb1 alone can interact with AC. This behaviour is, however, consistent with the expression of the Gpb1 exceeding that of Gpa1 and Gpg1 during the morphological switch. Gpg1 has a CCAAX box at its C-terminus (e.g. CCMIM) that is the site for prenylation, which is important in targeting the Gβγ dimer to the membrane (Whiteway and Thomas, 1994; Hirschman and Jenness, 1999;

Manahan *et al.*, 2000). A recent study indicated that there is considerable heterogeneity in the prenylation process, suggesting that this can affect the targeting of the Gβγ dimer, possibly as a means to switch between different signalling pathways (Cook *et al.*, 2006). Accordingly, it is worth considering whether the increased expression of Gpb1, above that of Gpg1 and Gpa1, during the morphological transition is not only used to differentially modulate the activity of AC, but could be used to alter the targeting of Gpb1. Recent studies have shown that Gα proteins are segregated into distinct pools that allow specific signalling pathways to be activated at the plasmamembrane and at intracellular membranes (Slessareva *et al.*, 2006; Slessareva and Dohlman, 2006).

Experimental procedures

Strain and culture

Paracoccidioides brasiliensis strain ATCC 90659 was grown as a mycelium form at 26°C and as a yeast form at 37°C in a modified liquid YPD medium (1% yeast extract, 2% neopeptone and 2% dextrose, pH 6.5) with shaking at 110 r.p.m. for up to 15 days. The primers and plasmids used in this investigation are described in Tables 1 and 2 respectively, and the primers used for gene cloning are shown in Table S1. Exogenous cAMP was added to cultures of *P. brasiliensis* as the non-metabolite cAMP analogue dibutyryl-adenosine 3′-5′-cyclic monophosphoric acid (Sigma).

Microscopy

For the microscopic assays, the different morphotypes were transferred to fixative solution (3.7% formaldehyde, 50 mM sodium phosphate buffer pH 7.0, 0.2% Triton X-100) for 120 min at room temperature. Then, they were briefly rinsed with PBS buffer (140 mM NaCl, 2 mM KCl, 10 mM $NaHPO_4$, 1.8 mM KH_2PO_4, pH 7.4) and mounted on the slides. The material was photographed using a Zeiss epifluorescence microscope.

RNA extraction

For the real-time RT-PCR experiments, yeast cells and mycelium were disrupted with glass beads and grinding in liquid nitrogen respectively, and immediately mixed with Trizol (Gibco-BRL) for RNA extraction following the supplier's recommendations. To verify the RNA integrity, 20 μg of RNA from each treatment was fractionated in 2.2 M formaldehyde, 1.2% agarose gel, stained with ethidium bromide, and visualized with UV light. The presence of intact 28S and 18S ribosomal RNA bands was used as a criterion to verify whether the RNA was intact. RNase-free DNase treatment was performed in a final volume of 100 μl containing 40 mM Tris-HCl pH 7.5 and 6 mM $MgCl_2$, 1 μl of RNasin (40 U μl^{-1}, Promega, USA), 10 μl of RNase-free DNase (1 U μl^{-1}, Promega or Life Technologies, USA), 2.5 μl of 200 mM DTT, and 10 μg of total RNA. The reaction was incubated at 37°C for 60 min and stopped by incubating at 70°C for 30 min. The absence of DNA contamination after the RNase-free DNase treatment was verified by PCR amplification of the *GP43* gene.

Construction of cDNA libraries

A *P. brasiliensis* yeast cDNA library was constructed in the vector pDNR-LIB using the Creator SMART cDNA Library (Clontech) according to the manufacturer's instructions. The *CYR1*, *GPA1*, *GPA2*, *GPA3*, *GPB1*, *GPG1* and *RAS* genes were cloned from the Creator pDNR Library as described in *Supplementary methods*.

Real-time PCR and RT-PCR reactions

All the real-time PCR and RT-PCR reactions were performed using an ABI Prism 7700 Sequence Detection System (Perkin-Elmer Applied Biosystems, USA). Taq-ManR EZ RT-PCR kits (Applied Biosystems, USA) were used for RT-PCR reactions. The thermocycling conditions comprised an initial step at 50°C for 2 min, followed by 30 min at 60°C for reverse transcription, 95°C for 5 min, and 40 cycles at 94°C for 20 s and 60°C for 1 min. Taq ManR PCR reagent kits were used for PCR reactions. As there is no ideal control for gene expression, we first compared several genes as normalizers for the expression experiments, such as those encoding α-tubulin, hexokinase and a translation factor. We have seen no difference by using any of these normalizers. Accordingly, the calibrator gene used for the expression experiments was the *α-tubulin* gene (data not shown). The reactions and calculations were performed according to Semighini *et al.* (2002). Primer and probe sequences are described in Table 1.

Subcloning of genes for yeast two-hybrid analysis

The *GPA1*, *GPA2*, *GPA3*, *GPB1* and *GPG1* genes, and fragments of the *CYR1* and *GPB1* gene, were subcloned into the vectors pGBKT7 and pGADT7 for use in yeast two-hybrid screens (Table 2).

Construction of random mutagenesis libraries for yeast two-hybrid screening

Random mutagenesis libraries for *GPA1*, *GPA2*, *GPA3* and *GPB1* from *P. brasiliensis*, *GPR1* from *S. cerevisiae*, and mammalian *P53* and *LAM* were constructed using the GeneMorph II Random Mutagenesis kit (Stratagene) and cloned into the prey vector pGADT7 to create the libraries pGAD-PbGPA1-RM-Lib, pGAD-PbGPA2-RM-Lib, pGAD-PbGPA3-RM-Lib, pGAD-PbGPB-RM-Lib, pGAD-ScGPR1-F5R1-RM-Lib, pGAD-P53-RM-Lib and pGAD-Lam-RM-Lib respectively for yeast two-hybrid screening.

Yeast two-hybrid analysis and screening

The Matchmaker Two-Hybrid System 3 (Clontech) was used to test for protein–protein interactions and to screen libraries

Table 1. Primers used for constructing yeast two-hybrid vectors, quantitative RT-PCR and expression constructs for pull-down assays.

Primer	Sequence (5′→3′; restriction sites underlined)	Description
PbAC-F26(KpnI)	GGTACCAAAATGTCTAGGAGACAGCGGGAGAAAGATAGG	Plasmid construction
PbAC-R34(NotI)	GCGGCCGCGCCGTGCTCGAAGAACTAGAACCAC	Plasmid construction
PbAC-GADF1(NcoI)	GGTACCACCATGGCAAGGAGACAGCGGGAGAAAG	Plasmid construction
PbAC-GADF2(NcoI)	TCGTCCATGGAAGATGAGCTGAATAACTAC	Plasmid construction
PbAC-GADR1(BamHI)	TGATTTGGATCCCGTTGATTCCCAAGTCAGC	Plasmid construction
PbAC-GADR2(BamHI)	CCCCAGGATCCTAAGATGTTTCAAAGAGTTG	Plasmid construction
PbAC-EF1(NdeI)	GGGATTCATATGGTTAATAGCACAGATCTG	Plasmid construction
PbAC-EF2(NdeI)	AGTATCCATATGGGACTGTCTCCATTAACTG	Plasmid construction
PbAC-ER1(XhoI)	CCATGGCTCGAGCGCCGTGCTCGAAGAACT	Plasmid construction
PbAC-ER2(XhoI)	CTCGCGCTCGAGATTGTGATTAAGATAGTC	Plasmid construction
PbGPA1-ExGPAF1	CATATGGGTTGTGGAATGAGC	Plasmid construction
PbGPA1-pYER3	GCCTAGGTCATATCAGTCCACAGAGGCGAAG	Plasmid construction
PbGPA2-F6	CATGGGTTGCGCAAGTTCTCAACCAGTGGA	Plasmid construction
PbGPA2-F7(EcoRI)	CTAGGAATTCATGGGTTGCGCAAGTTCTCA	Plasmid construction
PbGPA2-R6	CTGTTGGCACCTACAGAATCAGGTTGTTGA	Plasmid construction
PbGPA3-F5	TGGTATCAGATAGGATGGGTGGGTGTTGCA	Plasmid construction
PbGPA3-R5	CCCTTTCACAAAATACCAGAATCTTTCAGG	Plasmid construction
PbRAS-F1(NdeI)	CCGCGCTTCATATGCAGCTTTGTCTAAACC	Plasmid construction
PbRAS-R1(EcoRI)	GTGATACTGTAGAATTCCACGAAACCCTC	Plasmid construction
PbGPB-NdeI-F	ACGCTCATATGGCGGCCGATTTGAGCGG	Plasmid construction
PbGPB-BanHI-R	CGATGGATCCCTACCATGCCCAGACCTTGAG	Plasmid construction
PbGPG-NdeI-F	CATATGGCCCCTGCCTACGAGCTTCGAC	Plasmid construction
PbGPG-BamHI-R	GGATCCTTACATGATCATACAGCAGCCACCTGAT	Plasmid construction
pbgpb-NdeI-F	ACGCTCATATGGCGGCCGATTTGAGCGG	pAD-WD1
gpbWD-1R	GCTAGGATCCTAATCGGAGATGATTAGTTTCC	pAD-WD1
pbgpb-NdeI-F	ACGCTCATATGGCGGCCGATTTGAGCGG	pAD-WD2
gpbWD-2R	GCTAGGATCCTAATTATAGATGGAACAGATG	pAD-WD2
pbgpb-NdeI-F	ACGCTCATATGGCGGCCGATTTGAGCGG	pAD-WD3
gpbWD-3R	GCTAGGATCCTAATCCCATAGCATACAGGTC	pAD-WD3
pbgpb-NdeI-F	ACGCTCATATGGCGGCCGATTTGAGCGG	pAD-WD4
gpbWD-4R	GCTAGGATCCTAATCCCAGAGTTTAGCAAAGG	pAD-WD4
pbgpb-NdeI-F	ACGCTCATATGGCGGCCGATTTGAGCGG	pAD-WD5
gpbWD-5R	CGTAGGATCCTAATCGAATAGACGGCAGGTGG	pAD-WD5
pbgpb-NdeI-F	ACGCTCATATGGCGGCCGATTTGAGCGG	pAD-WD6
gpbWD-6R	GCTAGGATCCTAGTCCCAGACCTTGCACTCAT	pAD-WD6
pbgpb-NdeI-F	ACGCTCATATGGCGGCCGATTTGAGCGG	pAD-WD13
gpbWD-1R	GCTAGGATCCTAATCGGAGATGATTAGTTTCC	pAD-WD13
Gpb-WD3-F	GGATCCCTTTCCTCTCGAGAAGGTCC	pAD-WD13
gpbWD-3R	GCTAGGATCCTAATCCCATAGCATACAGGTC	pAD-WD13
Gpb-WD27-R	CATATGGCATACACAACAAACAAAGTGCAC	pAD-WD27
pbgpb-BanHI-R	CGATGGATCCCTACCATGCCCAGACCTTGAG	pAD-WD27
gpbWD-67-F	CATATG ATCCGCGCGGATAGAGAACTTAATAC	pAD-WD67
pbgpb-BanHI-R	CGATGGATCCCTACCATGCCCAGACCTTGAG	pAD-WD67
ScGPR1-F1	CGGGATCCGAAGTGTGACGAATAAAGC	Plasmid construction
ScGPR1-F3	CGGGATCCATATGATAACTGAGGGATTTCCCCCG	Plasmid construction
ScGPR1-F4	CCGGATCCGTGAAAGTAAAAGAATTAAAGCGC	Plasmid construction
ScGPR1-F5	CCGGATCCAGGAAAAACCTTGGAACTATTCATG	Plasmid construction
ScGPR1-R1	CGGGATCCATTTTCAAACATCGCGATAC	Plasmid construction
ScGPR1-R3	CCGGATCCTTAGATTCTTTTGAATTTGTGCC	Plasmid construction
ScGPA2-F1	CCGGATCCTGGGTCTCTGCGCATCTTCA	Plasmid construction
ScGPA2-R1	CCGGATCCGCTGTGCATTCATTGTAACAC	Plasmid construction
3′BD screening	TGGCTGCAAGCGCGCAAAAAACCCCTCAAGAC	Plasmid construction
5′BD screening	TCATCGGAAGAGAGTAGTAACAAAGGTCAAAGA	Plasmid construction
pGADT-linker-gamma-F1	CCGCTCCGGCCCTGACCCCGGCGGATGTGGCCCGCAGCAT GGCCCCTGCCTACGAGCTTCGACCCG	For construct of PbGpb-linker-PbGpgamma fusion gene
pGADT-linker-gamma-F2	GGATCCCGTATTAAAAACGGCAGCGGTGCGGCAGCCCCGAAA GCCGCTCCGGCCCTGACCCCGGCGGATG	For construct of PbGpb-linker-PbGpgamma fusion gene
pGADT-Gpb-R2(TAG)	GGATCCCCATGCCCAGACCTTGAGCAGAGAATC	For construct of PbGpb-linker-PbGpgamma fusion gene
Real-time PCR		
Alpha	CCAGAACCAGGCAGTCCAAA	Real-time PCR of α-tubulin
P-alpha	FAM-CACCTGCCTAACAAGATTGGACCAGG5G	

Table 1. *cont.*

Primer	Sequence (5'→3'; restriction sites underlined)	Description
P-gpa1_Pb	GTACCGCCACCTACGTCGAACATACGG5AC-FAM	Real-time PCR of *gpa1*
p-gpa1_Pb	ATGTCCTTCGCTCCCGTGTTA	
P-Gpb_Pb	CACGGCGAGAAGGTCCAACCCG5G-FAM	Real-time PCR of *gpb1*
p-Gpb_Pb	TCGCCGGAAGAAGTGATGATT	
P-Gpg_Pb	CGGTTGTCAATCTGTCCCCAAAC5G-FAM	Real-time PCR of *gpg1*
p-Gpg_Pb	CGGCCATGTCACTCATCAACT	
P-PbAden_cyc	CACATTCAAAGTTTCGTGGGAAGGAATG5G-FAM	Real-time PCR of *cyr1*
p-PbAden_cyc	AGAGGCCGATTCTCATGCAA	
Protein overexpression		
pGEX-6P-3 Cyr1453–678_Pb (BamHI and NotI)	AAGGATGGATCCGATAAAACCCATCAGGATAACTTTG CATATCGCGGCCGCTTAGTGGCTAAACTTTTGGTTCTCGTG	Plasmid construction
pGEX-6P-3 Gpb1 (BamHI and NotI)	ATACATGGATCCATGGCGGCCGATTTGAGCGGCG ATATCTGCGGCCGCCTACCATGCCCAGACCTTG	Plasmid construction

In most cases, the same primers were used to make constructs in both pGADT7 and pGBKT7 for yeast two-hybrid screens.

for potential interacting protein partners. For the former purpose, transformants were generated by introducing both bait and prey vectors into yeast strain AH109 simultaneously. For the latter, bait vectors were introduced into AH109 first, followed by sequential transformation with 20 µg of prey library plasmids. Experimental procedures were conducted in accord with the Matchmaker GAL4 Two-Hybrid System 3 manual and the Yeast Protocol Handbook (Clontech). Protein interactions were identified by observing the growth of transformants on SD-Ade/–His/–Leu/–Trp plates. After screening random mutagenesis libraries, candidate transformants were twice restreaked on SD-Ade/–His/–Leu/–Trp plates to allow loss of non-interacting prey vectors. Interacting prey vectors were purified using a Yeast Plasmid Isolation kit (Clontech) and subjected to DNA sequence analysis to confirm the identities of the interacting gene products.

Assays for cAMP production

Paracoccidioides brasiliensis mycelium growing in modified liquid YPD media at 26°C was subjected to an increase in temperature to 37°C to induce the morphological transition to the yeast form. Cells were harvested at different times during the transition and immediately stored at –80°C. To thawed cells, collected by centrifugation, 4% formic acid was added and agitated for 5 h to disrupt the cells. The cell debris was removed by centrifugation and the supernatant was lyophilized. Subsequently, the lyophilized pellet was made up in assay buffer, containing 2.5% dodecyl-trimethyl-ammonium-bromide, and was assayed using a Biotrak Enzyme Immuno Assay (EIA) kit from Amersham, according to the manufacturer's protocol 3. Measurements were normalized by using an equivalent wet weight of cells during the disruption procedure.

Expression of GST-Gpb1 and GST-Cyr1$^{453-678}$

GPB1 and *CYR1$^{453\ 5678}$* were cloned into pGEX6p-3, to enable expression of GST fusion proteins, and transformed into *Escherichia coli* codon plus cells, which were grown in 2YT, at 25°C with shaking at 200 r.p.m., before induction with 0.1 mM IPTG. Cells were harvested by centrifugation, resuspended and disrupted by passage through a Constant Systems cell disrupter; 0.1% Triton X-100 was added to the disrupted cells and the debris collected by ultracentrifugation. The supernatant was mixed with GST beads and incubated on a rotator for 30 min at 4°C, loaded into a glass column, and washed with PBS and finally with GST elution buffer (50 mM Tris/HCl pH 8.0, 10 mM glutothione). The elution fractions were run on 4–12% SDS-PAGE (NuPAGE precast) polyacrylamide gels. The protein concentrations were measured using a BCA™ protein assay kit (Pierce). These procedures typically yielded 7 mg ml^{-1} GST-Cyr1$^{453-678}$, 5 mg ml^{-1} GST-Gpb and 3 mg ml^{-1} GST.

In vitro *translation of Gpa1, Gpg1 and Cyr1$^{1-678}$*

Gpa1, Gpg1 and Cyr1$^{1-678}$ were synthesized by an *in vitro* coupled transcription and translation system (Promega), labelling the proteins with Redivue™ L-^{35}S-methionine (Amersham), using rabbit reticulocyte lysate. This was necessary because our attempts to overexpress these proteins, as well as full-length Cyr1, either as His-tagged or as GST-tagged proteins, always resulted in the production of inclusion bodies. The yeast two-hybrid pGBKT7 vectors, into which each gene or gene fragment had been cloned, were used as the template for the *in vitro* translation. The reaction was incubated at 30°C for 2 h, and 2.5 µl of the translated samples was loaded onto a gel to verify the translation. The translated proteins were stored at 4°C.

Pull-down assays

GST pull-down assays were performed with GST fusion proteins as bait and proteins labelled with ^{35}S, produced by TNT-coupled transcription/translation (Promega), as prey. The GST proteins were immobilized on 40 µl glutathione sepharose 4B beads (GE Healthcare), which had been preblocked with 200 µl of binding buffer (20 mM HEPES pH 7.9, 600 mM NaCl, 0.1% Tween 20, 5% glycerol, 1 mM DTT, 5% milk and 1% BSA) for 10–15 min at room temperature with 10 µl of EDTA-free protease inhibitor (1/4 tablet in 0.2 ml

Table 2. Plasmid used in this study.

Plasmid name	Vector	Insert and cloning description
pGEMTE-cPbAC-F26R34-1	pGEM T Easy (Promega)	The insert is the full-length *PbCYR1* cDNA amplified with PbAC-F26 and PbAC-R34
pGBK-PbCYR1$_{(1-678)}$	pGBKT7 (Clontech)	*PbCYR1* cDNA fragment (NcoI/BamHI) obtained by PCR with PbAC-GADF1 and PbAC-GADR1 cloned into pGBKT7 (NcoI/BamHI)
pGBK-PbCYR1$_{(600-1316)}$	pGBKT7 (Clontech)	*PbCYR1* cDNA fragment (NcoI/BamHI) obtained by PCR with PbAC-GADF2 and PbAC-GADR2 cloned into pGBKT7 (NcoI/BamHI)
pGBK-PbCYR1$_{(1302-1876)}$	pGBKT7 (Clontech)	*PbCYR1* cDNA fragment (NdeI/XhoI) obtained by PCR with PbAC-EF1 and PbAC-ER2 cloned into pGBKT7 (NdeI/SalI)
pGBK-PbCYR1$_{(1648-2100)}$	pGBKT7 (Clontech)	*PbCYR1* cDNA fragment (NdeI/XhoI) obtained by PCR with PbAC-EF2 and PbAC-ER1 cloned into pGBKT7 (NdeI/SalI)
pGAD-PbCYR1$_{(1-678)}$	pGADT7 (Clontech)	*PbCYR1*$^{1-678}$ fragment from pGBK-PbCYR1$_{(1-678)}$ (NdeI/BamHI) cloned into pGADT7 (NdeI/BamHI)
pGAD-PbCYR1$_{(600-1316)}$	pGADT7 (Clontech)	*PbCYR1*$^{600-1316}$ fragment from pGBK-PbCYR1$_{(600-1316)}$ (NdeI/BamHI) cloned into pGADT7 (NdeI/BamHI)
pGAD-PbCYR1$_{(1302-1876)}$	pGADT7 (Clontech)	*PbCYR1* cDNA fragment (NdeI/XhoI) obtained by PCR with PbAC-EF1 and PbAC-ER2 cloned into pGADT7 (NdeI/XhoI)
pGAD-PbCYR1$_{(1648-2100)}$	pGADT7 (Clontech)	*PbCYR1* cDNA fragment (NdeI/XhoI) obtained by PCR with PbAC-EF2 and PbAC-ER1 cloned into pGBKT7 (NdeI/XhoI)
pGEMTE-cPbGPA1-ExGPAF1pYER3-9(T7>SP6)	pGEM T Easy (Promega)	RT-PCR product with PbGPA1-ExGPAF1 and PbGPA1-pYER3 from *Pb* mRNA cloned into pGEM T Easy. The insert is the full-length *PbGPA1* cDNA
pGEMTE-cPbGPA2-F6R6-2(SP6>T7)	pGEM T Easy (Promega)	RT-PCR product with PbGPA2-F6 and PbGPA2-R6 from *Pb* mRNA cloned into pGEM T Easy. The insert is the full-length *PbGPA2* cDNA
pGEMTE-cPbGPA3-F5R5-2(T7>SP6)	pGEM T Easy (Promega)	RT-PCR product with PbGPA3-F5 and PbGPA3-R5 from *Pb* mRNA cloned into pGEM T Easy. The insert is the full-length *PbGPA3* cDNA
pGBK-PbGPA1	pGBKT7 (Clontech)	Insert (NdeI) from pGEMTE-cPbGPA1-ExGPAF1pYER3-9 cloned into pGBKT7 (NdeI)
pGAD-PbGPA1	pGADT7 (Clontech)	*PbGPA1* insert (NdeI digested) from pGBK-PbGPA1 cloned into pGADT7 (NdeI)
pGBK-PbGPA2	pGBKT7 (Clontech)	PCR product (EcoRI digested) with PbGPA2-F7 and T7 as primers and pGEMTE-cPbGPA2-F6R6-2 as template, cloned into pGBKT7 (EcoRI digested)
pGAD-PbGPA2	pGADT7 (Clontech)	*PbGPA2* insert (NdeI/SalI digested) from pGBK-PbGPA2 cloned into pGADT7 (NdeI/XhoI)
pGBK-PbGPA3	pGBKT7 (Clontech)	PCR product (EcoRI digested) with PbGPA3-F8 and SP6 as primers and pGEMTE-cPbGPA3-F5R5-2 as template, cloned into pGBKT7 (EcoRI digested)
pGAD-PbGPA3	pGADT7 (Clontech)	*PbGPA3* insert (NdeI/BamHI digested) from pGBK-PbGPA3 cloned into pGADT7 (NdeI/BamHI)
pGBK-PbGPB1	pGBKT7 (Clontech)	*PbGPB1* cDNA (NdeI/BamHI) cloned into pGBKT7 (NdeI/BamHI)
pGAD-PbGPB1	pGADT7 (Clontech)	*PbGPB1* cDNA (NdeI/BamHI) cloned into pGADT7 (NdeI/BamHI)
pGBK-PbRAS	pGBKT7 (Clontech)	*PbRAS* cDNA (NdeI/EcoRI) cloned into pGBKT7 (NdeI/EcoRII)
pGAD-PbRAS	pGADT7 (Clontech)	*PbRAS* insert (NdeI/EcoRI digested) from pGBK-PbRAS cloned into pGADT7 (NdeI/EcoRI)
pGBKT7-53	pGBKT7 (Clontech)	From Clontech
pGAD-P53$_{(72-390)}$	pGADT7 (Clontech)	*P53* insert (NdeI/BamHI digested) from pGBKT7-P53, cloned into pGADT7 (NdeI/BamHI)
pGBKT7-Lam	pGBKT7 (Clontech)	From Clontech
pGAD-Lam$_{(66-230)}$	pGADT7 (Clontech)	*Lam* insert (NdeI/BamHI) from pGBKT7-Lam cloned into pGADT7 (NdeI/BamHI)
pGADT7-T	pGADT7 (Clontech)	From Clontech
pGEMTE-ScGPR1-F1R1-17	pGEM T Easy (Promega)	The insert is the full-length *ScGPR1* amplified with Sc-GPR1-F1 and ScGPR1-R1
pGAD-ScGPR1$_{(679-961)}$-F5R1	pGADT7 (Clontech)	PCR product (BamHI digested) with ScGPR1-F5 and ScGPR1-R1 as primers, and pGEMTE-ScGPR1-F1R1-17 as template, cloned into pGADT7 (BamHI digested); corresponding to C-terminal cytoplasmic domain
pGAD-ScGPR1$_{(274-621)}$-F4R3	pGADT7 (Clontech)	PCR product (BamHI digested) with ScGPR1-F4 and ScGPR1-R3 as primers, and pGEMTE-ScGPR1-F1R1-17 as template, cloned into pGADT7 (BamHI digested); corresponding to the third cytoplasmic loop
pGAD-ScGPR1$_{(1-961)}$-F3R1	pGADT7 (Clontech)	PCR product (BamHI digested) with ScGPR1-F3 and ScGPR1-R1 as primers, and pGEMTE-ScGPR1-F1R1-17 as template, cloned into pGADT7 (BamHI digested); corresponding to full-length *ScGPR1*
pGBK-ScGPR1$_{(1-961)}$-F3R1	pGBKT7 (Clontech)	Insert (BamHI digested) from pGAD-ScGPR1$_{(1-961)}$-F3R1 cloned into pGBKT7

Table 2. *cont.*

Plasmid name	Vector	Insert and cloning description
pGBK-ScGPA2-F1R1	pGBKT7 (Clontech)	PCR product (BamHI digested) with ScGPA2-F1 and ScGPA2-R1 as primers, and Sc DNA as template, cloned into pGBKT7 (BamHI digested); corresponding to full-length ScGPA2
pAD-PbGPB1	pGADT7 (Clontech)	1062 bp *PbGPB1* gene linked into pGADT-7 at the sites of NdeI and BamHI
pBD-PbGPB1	pGBKT7 (Clontech)	1062 bp *PbGPB1* gene linked into pGBKT-7 at the sites of NdeI and BamHI
pAD-PbGPB1-TAG	pGADT7 (Clontech)	1059 bp *PbGPB1* gene without stop code was linked into pGADT-7 at the site of NdeI and BamHI
pBD-PbGPB1-TAG	pGBKT7 (Clontech)	1059 bp *PbGPB1* gene without stop code was linked into pGBDT-7 at the site of NdeI and BamHI
pAD-PbGPG1	pGADT7 (Clontech)	276 bp *PbGPG1* gene linked into pGADT-7 at the sites of NdeI and BamHI
pBD-PbGPG1	pGBKT7 (Clontech)	276 bp PbGpg gene linked into pGBKT-7 at the sites of NdeI and BamHI
pAD-PbGPB1-link-PbGPG1	pGADT7 (Clontech)	PbGpb-flexible linker-PbGpg was ligated into pGADT-7 at the site of NdeI and BamHI
pBD-PbGPB1-link-PbGPG1	pGBKT7 (Clontech)	PbGpb-flexible linker-PbGpb was ligated into pGBKT-7 at the site of NdeI and BamHI
pAD-WD1	pGBKT7 (Clontech)	The first WD domain of PbGpb1 with a stop codon linked into pGADT-7 at the sites of NdeI and BamHI
pAD-WD2	pGADT7 (Clontech)	The region encoding from the N-termini to the end of the second WD domain of PbGpb1 with a stop codon linked into pGADT-7 vector at the sites of NdeI and BamHI
pAD-WD3	pGADT7 (Clontech)	The region encoding from the N-termini to the end of the third WD domain of PbGpb1 with a stop codon linked into pGADT-7 vector at the sites of NdeI and BamHI
pAD-WD4	pGADT7 (Clontech)	The region encoding from the N-termini to the end of the fourth WD domain of PbGpb1 with a stop codon linked into pGADT-7 vector at the sites of NdeI and BamHI
pAD-WD5	pGADT7 (Clontech)	The region encoding from the N-termini to the end of the fifth WD domain of PbGpb1 with a stop codon linked into pGADT-7 vector at the sites of NdeI and BamHI
pAD-WD6	pGADT7 (Clontech)	The region encoding from the N-termini to the end of the sixth WD domain of PbGpb1 with a stop codon linked into pGADT-7 vector at the sites of NdeI and BamHI
pAD-WD13	pGADT7 (Clontech)	The region encoding a fragment containing the first and third WD domains of PbGpb1 with a start codon linked into pGADT-7 vector at the sites of NdeI and BamHI
pAD-WD27	pGADT7 (Clontech)	The region encoding a fragment from the second WD domain to the end of PgGpb1 with a start codon linked into pGADT-7 vector at the sites of NdeI and BamHI
pAD-WD67	pGADT7 (Clontech)	The region encoding a fragment from the sixth WD domain to the end of PgGpb1 with a start codon linked into pGADT-7 vector at the sites of NdeI and BamHI
pAD-WD17	pGADT7 (Clontech)	Deletion of a SalI fragment from the region encoding the fragment between the first and seventh WD domains of PbGpb1 in pAD-PbGPB1
pGEX-6P-3 $Cyr1_{(453-678)}$	pGEX-6P-3 (GE Healthcare)	The region encoding the cDNA fragment of *CYR1*, 225 bp (Gα binding domain and Ras association domain) linked to pGEX-6P-3 vector (GST fusion) at the sites of BamHI and NotI
pGEX-6P-3 Gpb1	pGEX-6P-3 (GE Healthcare)	1062 bp *PbGPB1* gene linked into pGEX-6P-3 (GST fusion) vector at the sites of BamHI and NotI

PBS) (Roche); to which was added 10 µl of *in vitro* translated protein and, in some assays, 10 mM GTP or GDP, and incubated on an end-over rotator at room temperature for 2 h. To facilitate comparisons between different pull-down experiments, we always utilized the same batch of *in vitro* translated product at an equivalent concentration. The beads were washed seven times with buffer (20 mM HEPES pH 7.9, 600 mM NaCl, 0.1% Tween 20, 5% glycerol, 1 mM DTT), and then proteins were eluted by the addition of 4× NuPAGE LDS sample buffer (Invitrogen), followed by boiling at 90°C for 5 min. The proteins were separated on 4–12% NuPAGE (precast Bis-Tris) gels. The gels were fixed with 20% ethanol and 10% acetic acid for 30 min, and then soaked in 5–10 ml of fluorographic reagent NAMP 100 (Amersham Biosciences) to amplify the signal. The gels were dried at 80°C for 35 min under vacuum and autoradiographed (2–3 days exposed at −80°C). Each assay was repeated three times with a different batch of *in vitro* translated product to confirm the results.

Western blots

Antibodies were to the GST tag (Novagen) or commercially produced polyclonal antibodies (Invitrogen) raised in rabbits to specific oligopeptides: Gpa1 – CFR RSR EYQ LND SAR and Gpb1 – CDI RAD REL NTY QSD.

Proteins were separated by SDS-PAGE (on 4–12% polyacrylamide gels) and electrotransferred to PVDF membranes. Blots were incubated with the respective antibodies (e.g. anti-GST at 1:12 500 dilution and specific antibodies at 1:2500 dilution). Alkaline-phosphatase-conjugated anti-mouse IgG (1:2500 dilution) and horseradish peroxidase-conjugated anti-rabbit IgG (1:2500 dilution) were used as secondary antibodies for GST and specific protein blots respectively.

Nucleotide sequence accession number

The GenBank accession numbers for the *P. brasiliensis* genes used in this study are: *CYR1* (AAS01025), *GPA1* (AAT40562), *GPA2* (AAT40564), *GPA3* (AAT40563), *GPB1* (AAT40565), *GPG1* (EF687895) and *RAS* (AY547438).

Acknowledgements

This work was supported by grants from the Wellcome Trust to M.I.B.W. and A.R.W., and from Fundacao de Amparo a Pesquisa do Estado de Sao Paulo (FAPESP) and Conselho Nacional de Desenvolvimento Científico e Tecnológico (CNPq), both from Brazil, to G.H.G. D.C. and G.C. were recipients of travelling fellowships from the Wellcome Trust. This collaboration was also supported by an international project grant from the Royal Society (UK).

References

Alspaugh, J.A., Pukkila-Worley, R., Harashima, T., Cavallo, L.M., Funnell, D., Cox, G.M., *et al.* (2002) Adenylyl cyclase functions downstream of the Galpha protein Gpa1 and controls mating and pathogenicity of *Cryptococcus neoformans*. *Eukaryot Cell* **1:** 75–84.

Bansal, P.K., Abdulle, R., and Kitagawa, K. (2004) Sgt1 associates with Hsp90: an initial step of assembly of the core kinetochore complex. *Mol Cell Biol* **24:** 8069–8079.

Batlle, M., Lu, A., Green, D.A., Xue, Y., and Hirsch, J.P. (2003) Krh1p and Krh2p act downstream of the Gpa2p G (alpha) subunit to negatively regulate haploid invasive growth. *J Cell Sci* **116:** 701–710.

Bennett, R.J., and Johnson, A.D. (2006) The role of nutrient regulation and the Gpa2 protein in the mating pheromone response of *C. albicans*. *Mol Microbiol* **62:** 100–119.

Borges-Walmsley, M.I., and Walmsley, A.R. (2000) cAMP signaling in pathogenic fungi: control of dimorphic switching and pathogenicity. *Trends Microbiol* **8:** 133–141.

Borges-Walmsley, M.I., Chen, D., Shu, X., and Walmsley, A.R. (2002) The pathobiology of *Paracoccidioides brasiliensis*. *Trends Microbiol* **10:** 80–87.

Bradsher, R.W., Chapman, S.W., and Pappas, P.G. (2003) Blastomycosis. *Infect Dis Clin North Am* **17:** 21–40, vii.

Chang, M.H., Chae, K.S., Han, D.M., and Jahng, K.Y. (2004) The GanB Galpha-protein negatively regulates asexual sporulation and plays a positive role in conidial germination in *Aspergillus nidulans*. *Genetics* **167:** 1305–1315.

Colombo, S., Ma, P., Cauwenberg, L., Winderickx, J., Crauwels, M., Teunissen, A., *et al.* (1998) Involvement of distinct G-proteins, Gpa2 and Ras, in glucose- and intracellular acidification-induced cAMP signalling in the yeast *Saccharomyces cerevisiae*. *EMBO J* **17:** 3326–3341.

Colombo, S., Ronchetti, D., Thevelein, J.M., Winderickx, J., and Martegani, E. (2004) Activation state of the Ras2 protein and glucose-induced signaling in *Saccharomyces cerevisiae*. *J Biol Chem* **279:** 46715–46722.

Cook, L.A., Schey, K.L., Wilcox, M.D., Dingus, J., Ettling, R., Nelson, T., *et al.* (2006) Proteomic analysis of bovine brain G protein γ subunit processing heterogeneity. *Mol Cell Proteomics* **5:** 671–685.

Delgado-Jarana, J., Martinez-Rocha, A.L., Roldan-Rodriguez, R., Roncero, M.I., and Di Pietro, A. (2005) *Fusarium oxysporum* G-protein beta subunit Fgb1 regulates hyphal growth, development, and virulence through multiple signalling pathways. *Fungal Genet Biol* **42:** 61–72.

Dessauer, C.W., Chen-Goodspeed, M., and Chen, J. (2002) Mechanism of Galpha i-mediated inhibition of type V adenylyl cyclase. *J Biol Chem* **277:** 28823–28829.

DiCaudo, D.J. (2006) Coccidioidomycosis: a review and update. *J Am Acad Dermatol* **55:** 929–942.

Diel, S., Klass, K., Wittig, B., and Kleuss, C. (2006) Gβγ activation site in adenylyl cyclase type II. Adenylyl cyclase type III is inhibited by Gβγ. *J Biol Chem* **281:** 288–294.

Dubacq, C., Guerois, R., Courbeyrette, R., Kitagawa, K., and Mann, C. (2002) Sgt1p contributes to cyclic AMP pathway activity and physically interacts with the adenylyl cyclase Cyr1p/Cdc35p in budding yeast. *Eukaryot Cell* **1:** 568–582.

Frank, M., Thumer, L., Lohse, M.J., and Bunemann, M. (2005) G-protein-activation without subunit dissociation depends on a Galpha i-specific region. *J Biol Chem* **280:** 24584–24590.

Ganem, S., Lu, S.W., Lee, B.N., Chou, D.Y., Hadar, R., Turgeon, B.G., and Horwitz, B.A. (2004) G-protein beta subunit of *Cochliobolus heterostrophus* involved in virulence, asexual and sexual reproductive ability, and morphogenesis. *Eukaryot Cell* **3:** 1653–1663.

Ghaemmaghami, S., Huh, W.K., Bower, K., Howson, R.W., Belle, A., Dephoure, N., *et al.* (2003) Global analysis of protein expression in yeast. *Nature* **425:** 737–741.

Hao, N., Yildirim, N., Wang, Y., Elston, T.C., and Dohlman, H.G. (2003) Regulators of G protein signaling and transient activation of signaling: experimental and computational analysis reveals negative and positive feedback controls on G protein activity. *J Biol Chem* **278:** 46506–46515.

Harashima, T., and Heitman, J. (2002) The Galpha protein Gpa2 controls yeast differentiation by interacting with kelch repeat proteins that mimic Gbeta subunits. *Mol Cell* **10:** 163–173.

Hirschman, J.E., and Jenness, D.D. (1999) Dual lipid modification of the yeast Gγ subunit Ste18p determines membrane localization of Gβγ. *Mol Cell Biol* **19:** 7705–7711.

Hoffman, C.S. (2005) Except in every detail: comparing and contrasting G-protein signaling in *Saccharomyces cerevi-*

siae and Schizosaccharomyces pombe. Eukaryot Cell **4:** 495–503.

Hoffman, C.S. (2007) Propping up our knowledge of G protein signaling pathways: diverse functions of putative noncanonical Gβ subunits in fungi. *Sci STKE* **370:** pe3.

Ivey, F.D., and Hoffman, C.S. (2005) Direct activation of fission yeast adenylate cyclase by the Gpa2 Galpha of the glucose signaling pathway. *Proc Natl Acad Sci USA* **102:** 6108–6113.

Jain, S., Akiyama, K., Kan, T., Ohguchi, T., and Takata, R. (2003) The G protein beta subunit FGB1 regulates development and pathogenicity in *Fusarium oxysporum*. *Curr Genet* **43:** 79–86.

Kasahara, S., and Nuss, D.L. (1997) Targeted disruption of a fungal G-protein beta subunit gene results in increased vegetative growth but reduced virulence. *Mol Plant Microbe Interact* **10:** 984–993.

Kauffman, C.A. (2007) Histoplasmosis: a clinical and laboratory update. *Clin Microbiol Rev* **20:** 115–132.

Kraakman, L., Lemaire, K., Ma, P., Teunissen, A.W., Donaton, M.C., Van Dijck, P., *et al.* (1999) A *Saccharomyces cerevisiae* G-protein coupled receptor, Gpr1, is specifically required for glucose activation of the cAMP pathway during the transition to growth on glucose. *Mol Microbiol* **32:** 1002–1012.

Krupinski, J., Coussen, F., Bakalyar, H.A., Tang, W.J., Feinstein, P.G., Orth, K., *et al.* (1989) Adenylyl cyclase amino acid sequence: possible channel- or transporter-like structure. *Science* **244:** 1558–1564.

Krystofova, S., and Borkovich, K.A. (2005) The heterotrimeric G-protein subunits GNG-1 and GNB-1 form a Gbetagamma dimer required for normal female fertility, asexual development, and galpha protein levels in *Neurospora crassa*. *Eukaryot Cell* **4:** 365–378.

Ladds, G., Davis, K., Das, A., and Davey, J. (2005) A constitutively active GPCR retains its G protein specificity and the ability to form dimers. *Mol Microbiol* **55:** 482–497.

Lafon, A., Seo, J.A., Han, K.H., Yu, J.H., and d'Enfert, C. (2005) The heterotrimeric G-protein GanB ({alpha})-SfaD ({beta})-GpgA ({gamma}) is a carbon source sensor involved in early cAMP-dependent germination in *Aspergillus nidulans*. *Genetics* **171:** 71–80.

Lafon, A., Han, K.H., Seo, J.A., Yu, J.H., and d'Enfert, C. (2006) G-protein and cAMP-mediated signaling in aspergilli: a genomic perspective. *Fungal Genet Biol* **43:** 490–502.

Landry, S., and Hoffman, C.S. (2001) The *git5* Gbeta and *git11* Ggamma form an atypical Gbetagamma dimer acting in the fission yeast glucose/cAMP pathway. *Genetics* **157:** 1159–1168.

Landry, S., Pettit, M.T., Apolinario, E., and Hoffman, C.S. (2000) The fission yeast *git5* gene encodes a Gbeta subunit required for glucose-triggered adenylate cyclase activation. *Genetics* **154:** 1463–1471.

Leeuw, T., Wu, C., Schrag, J.D., Whiteway, M., Thomas, D.Y., and Leberer, E. (1998) Interaction of a G-protein beta-subunit with a conserved sequence in Ste20/PAK family protein kinases. *Nature* **391:** 191–195.

Liebmann, B., Gattung, S., Jahn, B., and Brakhage, A.A. (2003) cAMP signaling in *Aspergillus fumigatus* is involved in the regulation of the virulence gene *pksP* and in defense against killing by macrophages. *Mol Genet Genomics* **269:** 420–435.

Lingelbach, L.B., and Kaplan, K.B. (2004) The interaction between Sgt1p and Skp1p is regulated by HSP90 chaperones and is required for proper CBF3 assembly. *Mol Cell Biol* **24:** 8938–8950.

Lorenz, M.C., and Heitman, J. (1997) Yeast pseudohyphal growth is regulated by GPA2, a G protein alpha homolog. *EMBO J* **16:** 7008–7018.

Lorenz, M.C., Pan, X., Harashima, T., Cardenas, M.E., Xue, Y., Hirsch, J.P., and Heitman, J. (2000) The G protein-coupled receptor gpr1 is a nutrient sensor that regulates pseudohyphal differentiation in *Saccharomyces cerevisiae*. *Genetics* **154:** 609–622.

Lukov, G.L., Hu, T., McLaughlin, J.N., Hamm, H.E., and Willardson, B.M. (2005) Phosducin-like protein acts as a molecular chaperone for G protein betagamma dimer assembly. *EMBO J* **24:** 1965–1975.

Maidan, M.M., De Rop, L., Serneels, J., Exler, S., Rupp, S., Tournu, H., *et al.* (2005) The G protein-coupled receptor Gpr1 and the Galpha protein Gpa2 act through the cAMP-protein kinase A pathway to induce morphogenesis in *Candida albicans*. *Mol Biol Cell* **16:** 1971–1986.

Manahan, C.L., Patnana, M., Blumer, K.J., and Linder, M.E. (2000) Dual lipid modification motifs in G(alpha) and G(gamma) subunits are required for full activity of the pheromone response pathway in *Saccharomyces cerevisiae*. *Mol Biol Cell* **11:** 957–968.

Medoff, G., Painter, A., and Kobayashi, G.S. (1987) Mycelial-to-yeast-phase transitions of the dimorphic fungi *Blastomyces dermatitidis* and *Paracoccidioides brasiliensis*. *J Bacteriol* **169:** 4055–4060.

Miwa, T., Takagi, Y., Shinozaki, M., Yun, C.W., Schell, W.A., Perfect, J.R., *et al.* (2004) Gpr1, a putative G-protein-coupled receptor, regulates morphogenesis and hypha formation in the pathogenic fungus *Candida albicans*. *Eukaryot Cell* **3:** 919–931.

Morris-Jones, R. (2002) Sporotrichosis. *Clin Exp Dermatol* **27:** 427–431.

Muller, P., Leibbrandt, A., Teunissen, H., Cubasch, S., Aichinger, C., and Kahmann, R. (2004) The Gbeta-subunit-encoding gene bpp1 controls cyclic-AMP signaling in *Ustilago maydis*. *Eukaryot Cell* **3:** 806–814.

Nemecek, J.C., Wuthrich, M., and Klein, B.S. (2006) Global control of dimorphism and virulence in fungi. *Science* **312:** 583–588.

Nishimura, M., Park, G., and Xu, J.R. (2003) The G-beta subunit MGB1 is involved in regulating multiple steps of infection-related morphogenesis in *Magnaporthe grisea*. *Mol Microbiol* **50:** 231–243.

Obara, T., Nakafuku, M., Yamamoto, M., and Kaziro, Y. (1991) Isolation and characterization of a gene encoding a G-protein alpha subunit from *Schizosaccharomyces pombe*: involvement in mating and sporulation pathways. *Proc Natl Acad Sci USA* **88:** 5877–5881.

Ogihara, H., Shima, F., Naito, K., Asato, T., Kariya, K., and Kataoka, T. (2004) Direct activation of fission yeast adenylyl cyclase by heterotrimeric G protein gpa2. *Kobe J Med Sci* **50:** 111–121.

Ongay-Larios, L., Savinon-Tejeda, A.L., Williamson, M.J. Jr,

Duran-Avelar, M., and Coria, R. (2000) The Leu-132 of the Ste4(Gbeta) subunit is essential for proper coupling of the G protein with the Ste2 alpha factor receptor during the mating pheromone response in yeast. *FEBS Lett* **467:** 22–26.

Palmer, D.A., Thompson, J.K., Li, L., Prat, A., and Wang, P. (2006) Gib2, a novel Gβ-like/RACK1 homolog, functions as a Gβ subunit in cAMP signaling and is essential in *Cryptococcus neoformans*. *J Biol Chem* **281:** 32596–32605.

Paris, S., and Duran, S. (1985) Cyclic adenosine 3′,5′ monophosphate (cAMP) and dimorphism in the pathogenic fungus *Paracoccidioides brasiliensis*. *Mycopathologia* **92:** 115–120.

Peeters, T., Louwet, W., Gelade, R., Nauwelaers, D., Thevelein, J.M., and Versele, M. (2006) Kelch-repeat proteins interacting with the Gα protein Gpa2 bypass adenylate cyclase for direct regulation of protein kinase A in yeast. *Proc Natl Acad Sci USA* **103:** 13034–11309.

Pryciak, P.M., and Huntress, F.A. (1998) Membrane recruitment of the kinase cascade scaffold protein Ste5 by the Gbetagamma complex underlies activation of the yeast pheromone response pathway. *Genes Dev* **12:** 2684–2697.

Regenfelder, E., Spellig, T., Hartmann, A., Lauenstein, S., Bolker, M., and Kahmann, R. (1997) G proteins in *Ustilago maydis*: transmission of multiple signals? *EMBO J* **16:** 1934–1942.

Restrepo, A., McEwen, J.G., and Castañeda, E. (2001) The habitat of *Paracoccidioides brasiliensis*: how far from solving the riddle? *Med Mycol* **39:** 233–241.

Rocha, C.R., Schroppel, K., Harcus, D., Marcil, A., Dignard, D., Taylor, B.N., *et al.* (2001) Signaling through adenylyl cyclase is essential for hyphal growth and virulence in the pathogenic fungus *Candida albicans*. *Mol Biol Cell* **12:** 3631–3643.

Rosen, S., Yu, J.H., and Adams, T.H. (1999) The *Aspergillus nidulans sfaD* gene encodes a G protein beta subunit that is required for normal growth and repression of sporulation. *EMBO J* **18:** 5592–5600.

San-Blas, G., and Niño-Veja, G. (2001) *Paracoccidioides brasiliensis*: virulence and host response. In *Fungal Pathogenesis: Principles and Clinical Applications*. Cihlar, R.L., and Calderone, R.A. (eds). New York, N.Y.: Marcel Dekker Inc., pp. 205–226.

San-Blas, G., Niño-Veja, G., and Iturriaga, T. (2002) *Paracoccidioides brasiliensis* and paracoccidioidomycosis: molecular approaches to morphogenesis, diagnosis, epidemiology, taxonomy and genetics. *Med Mycol* **40:** 225–242.

Sanchez-Martinez, C., and Perez-Martin, J. (2002) Gpa2, a G-protein alpha subunit required for hyphal development in *Candida albicans*. *Eukaryot Cell* **1:** 865–874.

Schadick, K., Fourcade, H.M., Boumenot, P., Seitz, J.J., Morrell, J.L., Chang, L., *et al.* (2002) *Schizosaccharomyces pombe* Git7p, a member of the *Saccharomyces cerevisiae* Sgtlp family, is required for glucose and cyclic AMP signaling, cell wall integrity, and septation. *Eukaryot Cell* **1:** 558–567.

Semighini, C.P., Marins, M., Goldman, M.H., and Goldman, G.H. (2002) Quantitative analysis of the relative transcript levels of ABC transporter Atr genes in *Aspergillus nidulans* by real-time reverse transcription-PCR assay. *Appl Environ Microbiol* **68:** 1351–1357.

Seo, J.A., Han, K.H., and Yu, J.H. (2005) Multiple roles of a heterotrimeric G protein {gamma} subunit in governing growth and development of *Aspergillus nidulans*. *Genetics* **171:** 81–89.

Slessareva, J.E., and Dohlman, H.G. (2006) G protein signaling in yeast: new components, new connections, new compartments. *Science* **314:** 1412–1413.

Slessareva, J.E., Routt, S.M., Temple, B., Bankaitis, V.A., and Dohlman, H.G. (2006) Activation of the phosphatidylinositol 3-kinase Vps34 by a G protein α subunit at the endosome. *Cell* **126:** 191–203.

Sprang, S.R. (1997) G protein mechanisms: insights from structural analyses. *Annu Rev Biochem* **66:** 639–678.

Tesmer, J.J., Sunahara, R.K., Gilman, A.G., and Sprang, S.R. (1997) Crystal structure of the catalytic domains of adenylyl cyclase in a complex with Gsalpha.GTPgammaS. *Science* **278:** 1907–1916.

Vallim, M.A., Nichols, C.B., Fernandes, L., Gramer, K.L., and Alspaugh, J.A. (2005) A Rac homolog functions downstream of Ras1 to control hyphal differentiation and high temperature growth in the pathogenic fungus cryptococcus neoformans. *Eukaryot Cell* **4:** 1066–1078.

Vanittanakom, N., Cooper, C.R. Jr, Fisher, M.C., and Sirisanthana, T. (2006) *Penicillium marneffei* infection and recent advances in the epidemiology and molecular biology aspects. *Clin Microbiol Rev* **19:** 95–110.

Wang, P., Perfect, J.R., and Heitman, J. (2000) The G-protein beta subunit GPB1 is required for mating and haploid fruiting in *Cryptococcus neoformans*. *Mol Cell Biol* **20:** 352–362.

Whiteway, M.S., and Thomas, D.Y. (1994) Site-directed mutations altering the CAAX box of Ste18, the yeast pheromone-response pathway Gγ subunit. *Genetics* **137:** 967–976.

Whiteway, M.S., Wu, C., Leeuw, T., Clark, K., Fourest-Lieuvin, A., Thomas, D.Y., and Leberer, E. (1995) Association of the yeast pheromone response G protein beta gamma subunits with the MAP kinase scaffold Ste5p. *Science* **269:** 1572–1575.

Xue, Y., Batlle, M., and Hirsch, J.P. (1998) GPR1 encodes a putative G protein-coupled receptor that associates with the Gpa2p Galpha subunit and functions in a Ras-independent pathway. *EMBO J* **17:** 1996–2007.

Yu, J.H. (2006) Heterotrimeric G protein signaling and RGSs in *Aspergillus nidulans*. *J Microbiol* **44:** 145–154.

Yu, J.H., Wieser, J., and Adams, T.H. (1996) The Aspergillus FlbA RGS domain protein antagonizes G protein signaling to block proliferation and allow development. *EMBO J* **15:** 5184–5190.

Supplementary material

The following supplementary material is available for this article:

Fig. S1. The phylogenetic relationship between *Paracoccidioides brasiliensis* and other fungal cAMP-signalling proteins – a neighbour-joining bootstrap tree is derived from the amino-acid sequence alignments of fungal (A) adenylate

cyclase (AC) (B) Gβ, (C) Gγ and (D) Gα proteins, using the VectorNTi 6.0 align program (Informax).
Fig. S2. The RAS transcript levels during the mycelium-to-yeast transition.
Table S1. Primers used for gene cloning.

This material is available as part of the online article from: http://www.blackwell-synergy.com/doi/abs/10.1111/j.1365-2958.2007.05824.x
(This link will take you to the article abstract).

Please note: Blackwell Publishing is not responsible for the content or functionality of any supplementary materials supplied by the authors. Any queries (other than missing material) should be directed to the corresponding author for the article.

